ANALYSIS OF FRAMED-TUBE STRUCTURES FOR HIGH-RISE BUILDINGS

by

BISHWANATH BOSE

A thesis presented for the degree of

Doctor of Philosophy

of the

University of Strathclyde, Glasgow

in the

Department of Civil Engineering

1976

SYNOPSIS

All the previous works on Framed-tube structures required the services of a digital computer of reasonable size to obtain a solution. There appears to be a distinct need to develop a simple method which will enable hand-calculations to be carried out rapidly in the early stage of design to give a reasonable assessment of the structural behaviour and to make preliminary estimates of the main structural element sizes.

In the simple approximate analysis presented in this thesis, the rigidly-jointed perimeter frame panels are replaced by equivalent orthotropic plates, whose properties are chosen to represent both the axial and shearing deformation characteristics of the frames. The use of an artificially low shear modulus G enables the racking deformations of the frame to be simulated. The stress distributions in the panels are assumed to be represented with sufficient accuracy by polynomial series in the horizontal coordinates, the coefficients of the series being functions of the height coordinate only. After satisfying the equations of equilibrium, the unknown functions are determined from the principle of least work by means of the calculus of variations.

Two methods of analysis are suggested. In the first very simple method the stress distributions represented by the basic beam theory are modified to include the effects of shear lag. Closed form solutions are presented for three standard load cases, a uniformly

and a triangularly distributed load, and a point load at the top. Design curves are developed to enable solutions to be obtained rapidly. A limited study is carried out to examine the effects of variable corner column stiffness and the ratio of column width to spandrel beam depth on the optimisation of the Framed-tube structure.

A more general analysis of the Framed-tube structure yields simultaneous differential equations for the two unknown functions which are solved for the three standard load cases.

The effects of an elastic base on the boundary conditions of the Framed-tube structure are considered. Framed-tube structures with different stiffness regions are also examined.

An analogous simplified method is presented for the analysis of Framed-tube structure subjected to torsion. Closed form solutions, and associated design curves, are presented for the three standard load cases.

The behaviour of Bundled-tube structures is more complex and a number of simplifying assumptions are made to reduce the number of unknown functions to a manageable size. Both simple and more general methods are presented for the analyses of such structures with two and nine modular tubes.

A method is presented to consider the likely effects of the flexibility of the spandrel beams on the stress distribution in a Framed-tube structure subjected to vertical forces.

A number of numerical examples are given which illustrate the various aspects of the theories developed and enable the best disposition of the materials to be made.

The results from a series of tests carried out on Perspex models are compared with the theoretical values in order to assess the validity of the approximations.

ACKNOWLEDGEMENTS

The author wishes to express his deep appreciation and gratitude to Professor A. Coull, B.Sc., Ph.D., F.I. Struct. E., F.I.C.E., F.R.S.E., F.A.S.C.E., Professor of Structural Engineering and Chairman of the Civil Engineering Department for the supervision, guidance and encouragement during the course of the research work and in the preparation of the thesis.

In the fabrication of the models for the experimental investigation, the author was assisted by Mr. J. Morrin and the staff of the Structures Laboratory. He is grateful for their assistance and cooperation.

The author is greatly indebted to the Science Research Council and The British Council for the financial assistance, which made this research work possible. The help of the authorities of Patna University, India in granting him study leave is gratefully acknowledged.

Sincere thanks are expressed to Mrs. G. Stewart for the neat typing of the manuscript.

The author fondly remembers all the encouragement he received from and the sacrifices made by his mother, Mrs. Lilabati Bose, which greatly contributed towards the successful completion of the work.

CONTENTS

CHAPTER 1

INTRODUCTION

1.1 BACKGROUND

The shear wall type of construction was first introduced in the early fifties and was immediately used in the construction of apartment and office buildings. This type of construction has been found to be efficient for buildings up to about 30 storeys in height, but for taller buildings the lateral sway as well as the wind stresses begin to control the design. As a result, the structural elements designed only for gravity loads need to be increased in order to increase the stiffness and strength of the building. For buildings over 30 storeys in height the framed-tube type of construction has been found to be more efficient. In its basic form, the system consists of closely spaced exterior columns tied at each floor level by deep spandrel beams to form a rectangular tube perforated by holes for the windows. Alternatively it may be regarded as a system of four orthogonal rigidly jointed frame panels forming a closed rectangular system as shown in Fig. 1.1. Both steel and concrete have been used in the construction of such structures. This system was first used in 1963 for the 43-storey De Witt Chestnut Apartment Building in Chicago, U.S.A. Since then the concept has been widely used by designers all over the world, the most significant of which are the 110-storey twin towers for the World Trade Centre in New York, U.S.A.

From the point of view of construction economy, the framed-tube compares favourably with the usual shear wall type of construction for medium rise buildings, but possesses definite advantage for taller buildings. The closely spaced column system also serves as the window wall system, thus replacing the vertical mullions for the support of glass windows.

In the framed-tube system the exterior columns are usually spaced from 1.2 m to a maximum of 4.5 m, centre to centre. The size of the spandrel beams varies from 600 mm to 1.2 m in depth and from 250 mm to 1 m in width. In the De Witt Chestnut Apartment Building the columns were spaced at 1.68 m centres and the spandrel beams were 600 mm deep.(1)

The framed-tube type of structure is suitable for buildings up to about 50 storeys. Beyond this the premium, in terms of increased member sizes, increases rapidly. The main reason for this is that, although the system looks like a tube, the two faces parallel to the direction of wind act like multi-bay rigidly-jointed frames when subjected to wind load. Consequently the bending moments in the columns and edge beams due to wind load become the controlling factors for very tall buildings. Furthermore, of the total lateral sway under wind load about 75 per cent is caused by frame racking and only 25 per cent is due to column shortening caused by the cantilever action of the framed-tube. For taller buildings, it is generally more efficient to use the Hull-core or

Tube-in-tube structure as illustrated in Fig. 1.2. It consists of an outer framed-tube connected by floor slabs to a central core which houses all the services. This system provides large column-free space, and is very suitable for office buildings. The 52-storey One Shell Plaza Building in Houston, U.S.A. with a height of 218 m was designed as a tube-in-tube structure. The tube-in-tube system is a refined version of the frame-shear wall interaction type of structure and combines the advantages of both framed-tube and shear wall types of structure. The shear wall inner core reduces the shear deflection of the columns in the outer framed-tube and greatly increases the efficiency of the structure.

For still taller structures, especially where a large plan area is involved, the modular tube or bundled-tube system may be used. This system consists basically of a bundling of smaller size tubes which reduces the shear lag effect and thereby induces more effective participation of the interior columns in resisting the wind load. The Sears Tower, Chicago, the world's tallest building, with 109 storeys for a height of 442 m above ground was designed as a bundled-tube structure[2,3,4] and is illustrated in Fig. 1.3. The basic shape consists of nine 22.86 m x 22.86 m modular tubes for an overall square floor size of 68.58 m x 68.58 m which continues up to the 50th floor. Step Backs, in the form of a termination of megamodular areas, then occur at floors 50, 66 and 90, creating a variety of floor configuration as shown in Fig. 1.3.

It is obvious that better cantilever efficiency can be achieved by replacing the vertical columns altogether and substituting closely spaced diagonals in either direction, as illustrated in Fig. 1.4. This "Diagonal truss tube" system is an extremely efficient system and was used in the not too high 13-storey IBM Building in Pittsburgh, U.S.A. A large number of joints have to be handled as in the framed-tube system, but as the diagonal truss system is much more rigid, any adjustment during construction becomes extremely difficult.(5)

The problems of large shear lag and a large number of joints in the framed-tube structure, and excessive rigidity and number of joints in the diagonal truss tube system can be largely overcome by the use of an optimum combination of columns, spandrels and diagonals to form an effective tube, as shown in Fig. 1.5. In this system, known as the Column diagonal truss tube(5), the exterior columns can be spaced between 6 m and 18 m, connected by widely spaced diagonals at an inclination of about 45^{o}. The spandrels designed for floor loads are normally sufficient to resist the internal force distribution between the columns and the diagonals except at levels where the diagonals from both planes meet at the corner. At these levels heavier tie spandrels are provided to limit the horizontal stretching of the floors and also to make the diagonals more efficient as inclined columns and as primary load distribution members.

1.2 PAST WORK

It is theoretically possible to analyse framed-tube structure by matrix techniques using standard three-dimensional computer programs. But small computers are not generally equipped with such programs, and even if they are, the storage requirements for such an analysis may overtax their capacity. It is, therefore, necessary to develop simplified methods of analysis, which reduce the number of degrees of freedom to a manageable size.

By recognising the dominant modes of deformation in the orthogonal planes Coull and Subedi[6] have produced a method to reduce the three-dimensional system to an equivalent plane frame with a consequent large reduction in the amount of computation required. This simplified method recognises that the lateral loads are resisted by two primary actions, the rigidly jointed side frames parallel to the direction of loads undergo shearing deformations, whilst the normal frame panels undergo axial deformations of the columns, the uniformity of which will depend on the stiffness of the connecting spandrel beams. The interactions between the side and normal panels consist mainly of vertical shear forces, and fictitious elements have been introduced to effect the vertical shear transfer which occurs.

Rutenberg[7] investigated the out-of-plane deformation of the frames by an alteration to the equivalent plane frame used in the analysis by Coull and Subedi. These out-of-plane deformations will always occur, but

these will be restricted by the high in-plane stiffness of the floor slabs, and are usually assumed insignificant in relation to the primary actions.

Khan and Amin[8] used the equivalent plane frame technique for developing a series of 'influence curves' for the preliminary analysis of framed-tube structures. These curves are used to compute the column axial force coefficients for both the side and normal frames and shear force coefficients for the spandrels in the side frames. These curves have been plotted against non-dimensional parameters representing the basic properties of the column and beam elements and aspect ratios (length of normal frame/length of side frame). Although developed for ten-storey structures, these design curves can be used for framed-tubes of any number of storeys by the use of reduction model techniques.

Schwaighofer and Ast[9,10] suggest complete separation of the frames to reduce the computer storage requirement. The interaction forces between the frames are determined and their effect combined with the effect of horizontal load for the side frames. The normal frames are subjected to interaction forces only. Using the above technique they carried out a series of analyses on a wide range of framed-tube structures with different geometrical characteristics, and tabulated the results for the side frames only. The effects of joint stiffnesses were taken into account in the analysis.

The design of a 37-storey building, built in Caracas, Venezuela, was described by Mazzeo and De Fries.[11]

A frame-tube structure is used to resist all of the seismic effects and to limit the side sway. Columns are purposely omitted at the corners, so that the beams near the building corners transfer vertical shears. The equivalent plane frame technique is applied to analyse the structure.

The effect of torsional action on framed-tube structures was investigated by Coull and Subedi.[12] Two forms of deformation are produced in the framed-tube structure under torsional moments, a pure rotation and an out-of-plane warping displacement of the cross-section. The structure is reduced to an equivalent plane frame system and the flexibility matrices in the two directions are derived by the standard plane frame programs. For the complete solution of the structure a special program is needed.

Rutenberg[13] has presented two methods of analysing tube structures under torsion, using the equivalent plane frame approach. In the first method of successive approximations, the spatial behaviour is represented by two plane frames. In one, the fictitious corner supports are constrained vertically at every floor level and the frame analysed. In the other, which is horizontally constrained at every floor level, the frame is subjected to vertical forces found acting on the fictitious corner supports. By the process of iteration satisfactory results are obtained. The second method of Rutenberg is very similar to the one proposed by Coull and Subedi,[12] except that the frame is analysed directly

without first deriving the flexibility matrices.

As a result of the work carried out in this thesis a paper[14] was published in which the simple approximate method for the rapid evaluation of the stresses in the framed-tube structures, subjected to lateral forces was presented. Design curves were given for different loading conditions.

1.3 REASONS FOR STUDY

All the previous works on framed-tube structures, mentioned earlier, require the services of a digital computer of reasonable size to obtain a solution. There appears to be a distinct need for a simple method which can be used in the early stages of design to give a reasonable assessment of the structural behaviour, and allow preliminary evaluation of the main structural element sizes to be made. The simplified analysis of framed-tube structures under bending has been presented in a paper[14] and will form part of this thesis.

1.4 SCOPE OF THE THESIS

This thesis is concerned with the investigation of high-rise buildings essentially comprising framed-tube or bundled-tube structures, under the action of lateral wind load. Particular attention is paid to the assessment of sway caused by lateral forces, since this may control the design of the structural system.

A very simple method of analysing a framed-tube structure is presented, and design curves are given for

three standard load cases, a uniformly distributed load, a triangularly distributed load, and a point load at the top. The design curves enable hand-calculations to be carried out rapidly in a design office. In many cases, the four corner columns are considerably stiffer than the other columns, and provision is made in the analysis for the inclusion of stiff individual corner elements. In the particular case of a uniformly distributed load a formula is presented to assess the maximum drift at the top of the structure. The effects of variable corner column stiffness and variable column width to spandrel beam thickness ratio on the optimisation of a framed-tube structure are investigated.

The assumption of a rigid base for the framed-tube structure is not strictly true and a simple method is presented for the bending analysis of the structure supported on an elastic base.

The structural properties of the framed-tube structure may not be uniform over the entire height, but may be constant over specified levels. Such cases are also treated in this thesis.

The vertical forces acting on a framed-tube structure consist of (a) a uniform component due to the self weight of the structure itself, and (b) a variable component induced due to the dead and live load acting on the floor areas. A simple procedure is described to consider the effects of vertical forces on the structure, with a view to examine any redistribution which may take place.

The effect of torsion on framed-tube structure is considered and simple equations are derived to analyse the structure. A method is presented to determine the maximum rotation at the top of the structure, when subjected to a uniformly distributed torque and a point torque at the top. Most of the design curves used for bending analysis may also be used for torsion.

The effect of lateral load on bundled-tube structure is also considered. The same design curves used for framed-tube structures can also be used for bundled-tube structures.

A description is given of an experimental investigation carried out to study the effect of lateral load on perspex models of framed-tube and bundled-tube structures. The results of the tests are compared with the relevant analytical solutions in order to assess the validity of the latter.

In the thesis figures and tables are referred to by the chapter number and are included at the end of the relevant chapter.

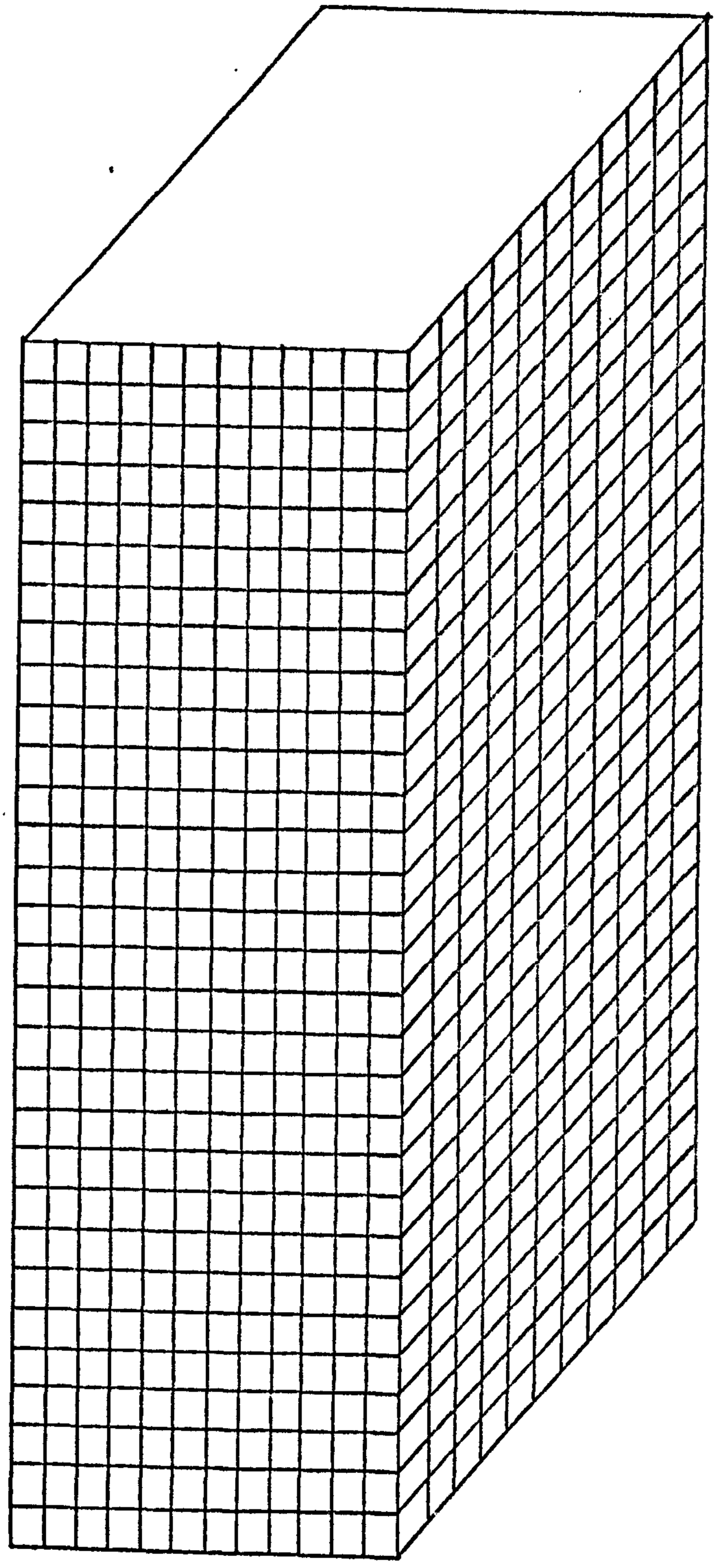

Fig. 1.1 Framed-tube building

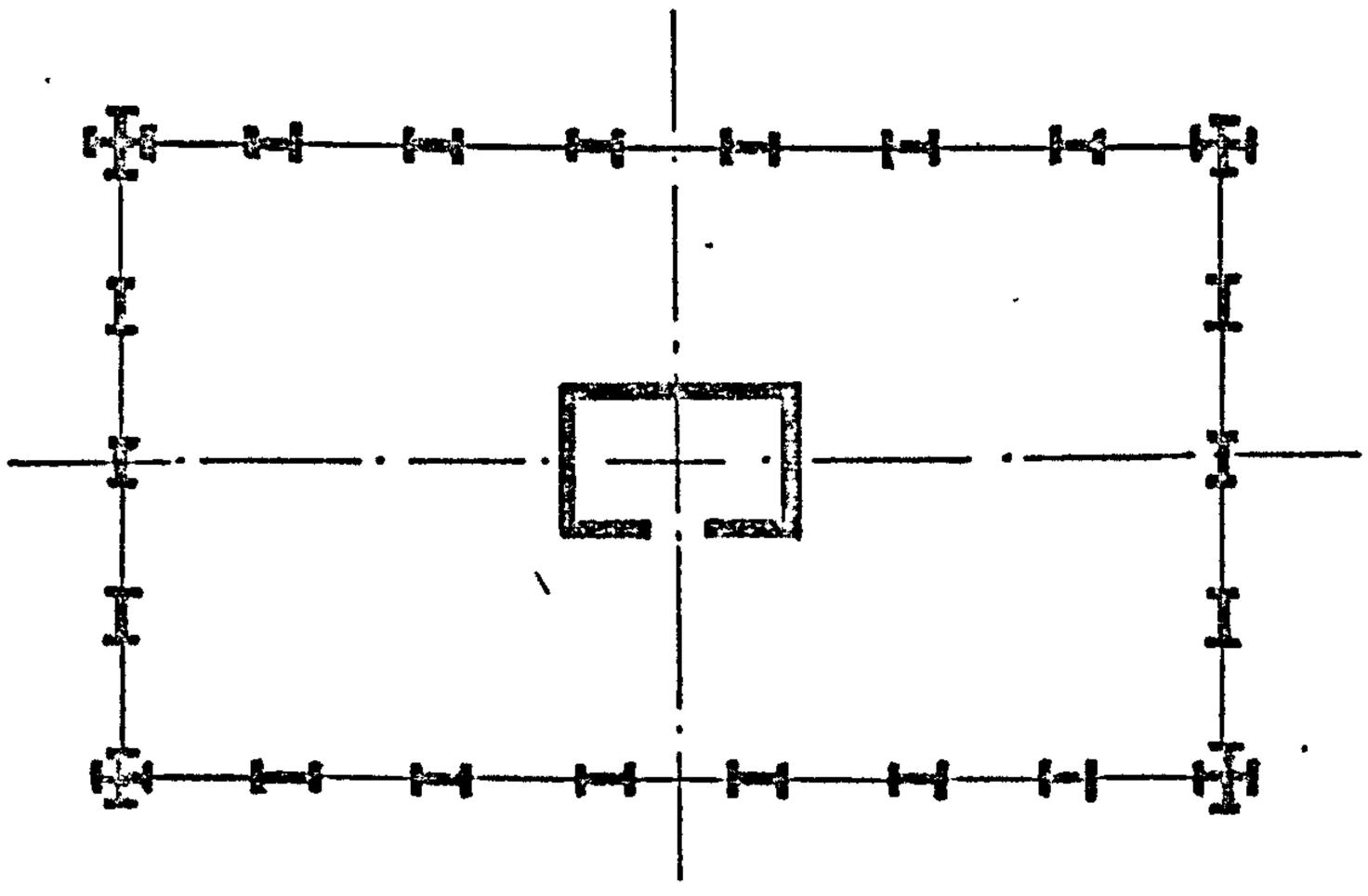

Fig. 1.2 Hull-core structure

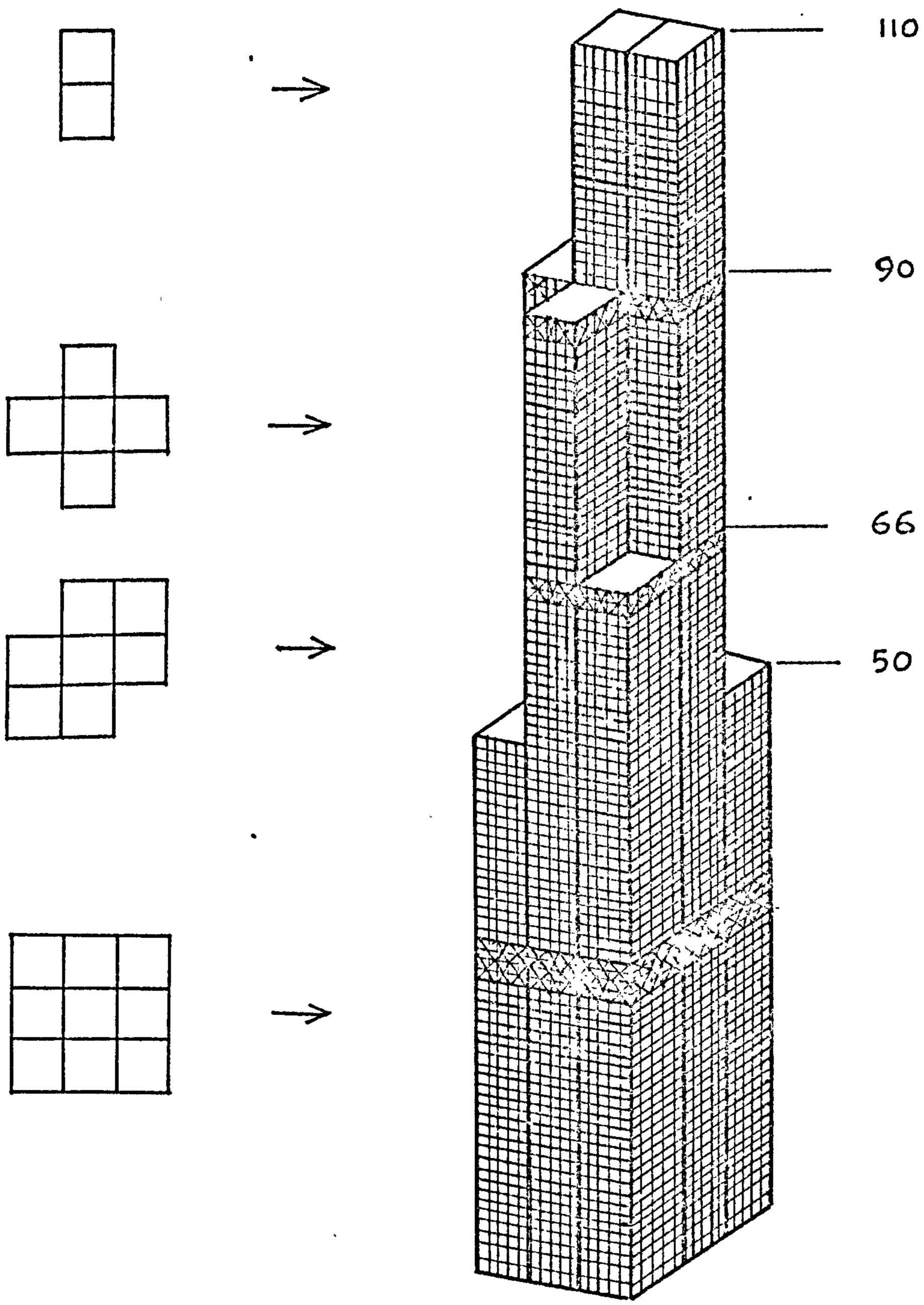

Fig. 1.3 Bundled-tube structure

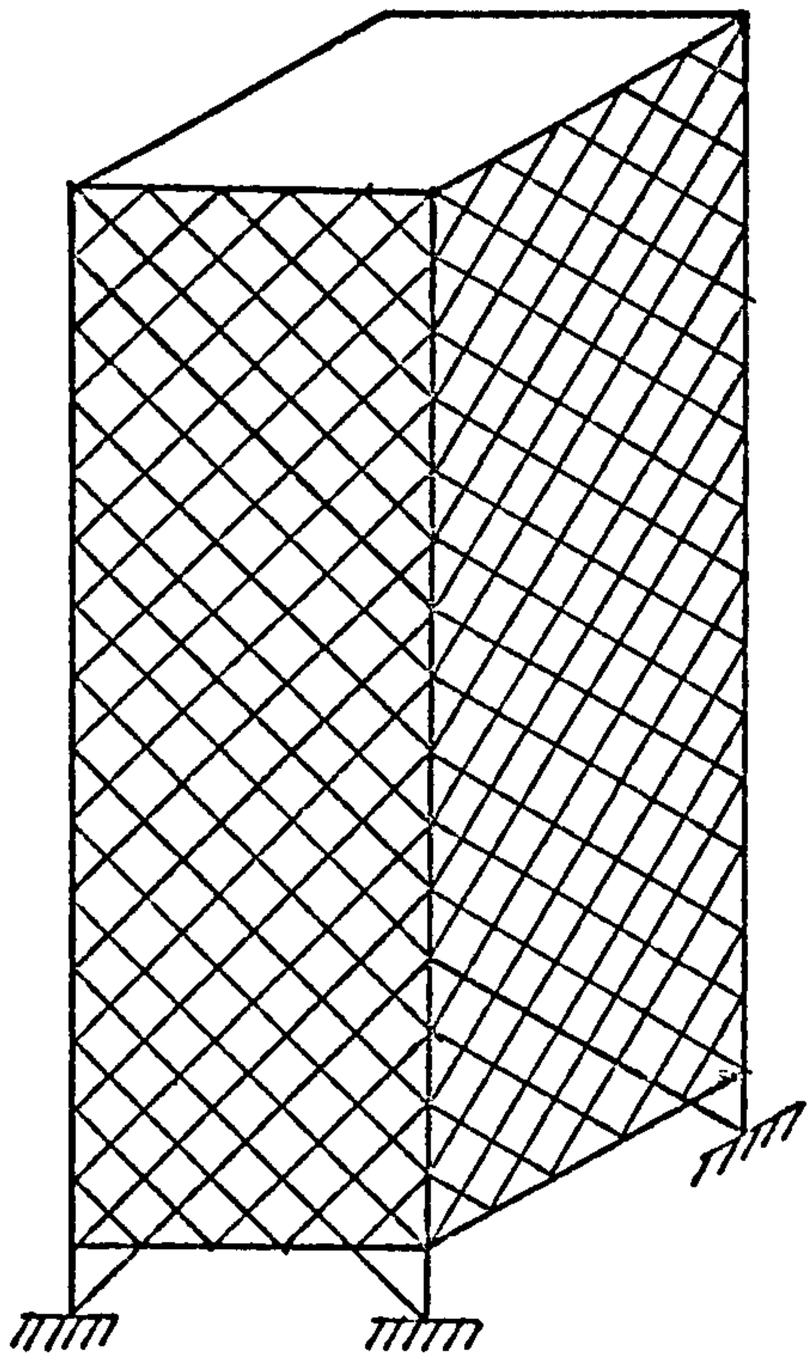

Fig. 1.4 Diagonal truss-tube system

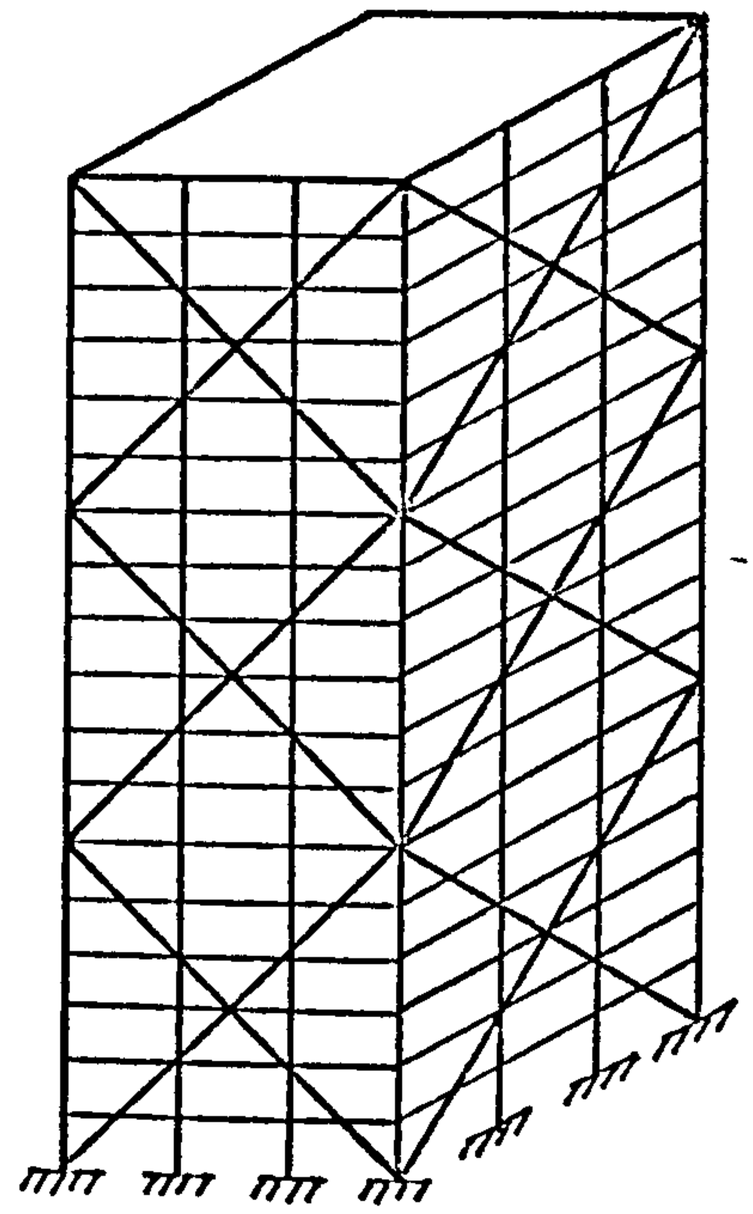

Fig. 1.5 Column diagonal truss-tube system

CHAPTER 2

ANALYSIS OF FRAMED-TUBE STRUCTURES SUBJECTED TO BENDING

NOTATION

The following symbols are used in this chapter:

A_c	area of corner column;
a	aspect ratio (b/c);
b	half breadth of framed-tube;
c	half depth of framed-tube;
d, d_1, d_2	bay widths;
E	elastic modulus;
E_x, E'_z, E_{xz} E_y, E_z, E_{yz}	elastic moduli of equivalent orthotropic plate;
e	clear distance between spandrel beams;
e_x, e'_z e_y, e_z	direct strains;
F	total shearing force at any level;
F_1, F_2, F_3	design functions;
f_1, f_2, f_3, f_4	stress functions;
G	shear modulus;
G_{xz}, G_{yz}	shear moduli of equivalent orthotropic plate;
H	total height of building;
h	storey height;
I	second moment of area of framed-tube;
I_d, I_{d_1}, I_{d_2}	second moments of area of beams;
I_h	second moment of area of column;

k, k_1, k_2 structural parameters;

l, l_1, l_2 clear distance between columns;

M applied moment at any level;

m geometrical ratio;

N axial force in column;

n ratio $\frac{A_c}{ct}$;

P concentrated load at top;

p intensity of lateral loading per unit height;

S, S_0, S_1 stress functions;

S_b, S_c shearing forces in beams and columns respectively;

t thickness of equivalent plate;

t_1 width of column;

t_2 depth of spandrel beam;

U strain energy;

x horizontal coordinate;

y horizontal coordinate;

z, z' vertical coordinates;

α_1, α_2 geometrical ratios;

β_1, β_2 structural parameters;

γ shear strain;

γ_{xz}, γ_{yz} shear strains in the equivalent orthotropic plate;

δ lateral deflection at the top of structure;

ϵ direct strain;

$\lambda, \lambda_1, \lambda_2$ geometrical ratios;

ξ non-dimensional height coordinate $(\frac{z}{H})$;

σ direct stress;

σ_b direct stress according to engineer's beam theory;

τ shear stress.

2.1 INTRODUCTION

The behaviour of a framed-tube is more complex than that of a simple closed tube, and the stiffness is less. In addition to the cantilever bending action, which produces tensile and compressive stresses on opposite faces of the tube, the side frames undergo the usual plane-frame shearing action in each storey under the action of lateral forces. This primary action is complicated by the fact that the flexibility of the spandrel beams produces a shear lag which has the effect of increasing the axial stresses in the corner columns, and of reducing them in the inner columns of the normal panels as illustrated in Fig. 2.1. The latter effects will produce warping of the floor slabs, and consequent deformations of the interior partitions and secondary structure which must be considered in the design.

Problems of shear lag occur in aircraft wing structure which consists mainly of a cantilevered tapered box beam in which thin sheets are reinforced by corner booms and intermediate stringers.[15,16] Due to shearing deformations of the sheets the load distribution in the booms and stringers is not uniform. Theoretical and experimental investigations of the problem have been carried out to determine the magnitude of the effect of shear lag and many methods have been suggested for its

solution.

Reissner has presented simple solutions for a thin-walled box beam type of structure using the principle of least work[17] and minimum potential energy.[18] In the least work solution, Reissner has assumed a parabolic stress distribution in the flanges and derived a simple differential equation for the stress function and boundary conditions for it. A parabolic variation of sheet displacements is assumed in his minimum potential energy solution and an ordinary differential equation for the beam deflection and boundary conditions for it are obtained.

In the present analysis, a parabolic distribution of stress in the flanges will be assumed and the principle of least work applied.

The magnitude of lateral displacement of the building is a measure of the stiffness of the structure and its maximum allowable limit is based on the consideration of the effects of lateral sway on (a) the stability of the individual columns and the structure as a whole, (b) the integrity of nonstructural partitions and glazing, and (c) the comfort of the occupants of the building. In designing for wind load, a deflection index ranging from $\frac{1}{300}$ to $\frac{1}{600}$ has been used in practice. The higher value of about $\frac{1}{300}$ appears to be more appropriate for the building types of several decades ago where the heavy so-called non-structural masonry partitions and exterior cladding considerably increased the lateral stiffness of such structures. The recent trend of using

lightweight elements and glass for interior partitions and exterior cladding would suggest the use of a relatively lower limit. The ACI committee 435 on "Allowable deflections"[19] recommends a deflection limit of $\frac{1}{500}$. Under earthquake forces the allowable drift may be increased to twice that allowed for wind.

2.2 ASSUMPTIONS

The analysis of the framed-tube structure is based on the following assumptions:

(i) The material for all the members of the tube is the same; it is homogeneous, isotropic and stressed within the linear elastic limit.

(ii) The floor system is very stiff in its own plane which will restrict any tendency for the exterior frame panels to deform out of plane. Thus only in-plane effects will be considered in each panel.

(iii) Spacing of columns and beams are uniform throughout the height.

(iv) Both beams and columns are of uniform section or the axial stiffness EA and the shearing rigidity GA remain constant throughout the height.

2.3 REPLACEMENT OF FRAMED PANELS BY EQUIVALENT ORTHOTROPIC PLATES

In the framed-tube structure shown in Fig. 2.2(a), the lateral load is resisted primarily by the following actions: (a) the rigidly-jointed frame actions of the shear-resisting panels parallel to the load (AB and DC), (b) the axial deformations of the frame panels normal to

the direction of the load (AD and BC) and (c) the axial forces in the discrete corner columns. The interactions between the normal and side panels consist mainly of vertical interactive forces along corners A, B, C and D. As a result of these interactive forces, panels AD and BC undergo axial deformations, the uniformity of which across each panel will depend on the relative stiffness of the spandrel beams.

Certain plane stress problems which cannot readily be solved by mathematical methods have been solved by substituting the solid plate by an equivalent grid to reproduce the physical deformation characteristics of the plate.[20] In the present analysis it is assumed conversely that each framework panel of columns and spandrel beams may be replaced by an equivalent orthotropic plate, to form a substitute closed tube structure as illustrated in Fig. 2.2(b). The properties of the orthotropic plate must be chosen so that the two elastic moduli in the horizontal and vertical directions represent the axial stiffnesses of the beams and columns respectively, and the shear modulus represents the shear stiffness of the frame work. That is, under the actions of identical axial or shear forces, the axial or shear deformations of both framework and equivalent orthotropic plate will be the same.

In the case of axial forces, (Fig. 2.3), the load deformation relationships for both frame and plate will be equal if, for each bay,

$$AE = d\ t\ E_Z \qquad \ldots\ldots\ (2.1)$$

where A is the cross-sectional area of a column in a bay of span d, E is the elastic modulus, t is the thickness of the equivalent plate, and E_z is the equivalent elastic modulus. It is then most convenient to fix the value of t for the structure, by making the area of the plate of width d equal to the cross-sectional area of the column in each panel, and vary the elastic moduli for different panels. In the normal case of a square or rectangular tube with identical column cross sectional areas on all four faces, the orthotropic plates will have identical properties in all faces. In the particular case where the normal and side panels have different equivalent elastic moduli these could be included in the analysis.

A similar relationship to equation (2.1) may be written for horizontal axial deformations also.

The shear modulus of the equivalent plate must be chosen so that the horizontal displacement of both frame panel and plate must be the same when both are subjected to the same shearing forces Q (Fig. 2.3).

Consider the single storey segment of a frame panel shown in Fig. 2.3. Since the columns may be closely spaced, and the spandrel beams relatively deep, the finite size of the joint relative to the free column height and beam span must be taken into account. This may be done by assuming that short rigid arms exist at each node, of width equal to the width of the column, and of height equal to the depth of the beams. This gives an upper bound to the equivalent shear modulus. The lower bound may also be determined by neglecting the finite

size of the joint.

It is assumed that the columns are constrained to deflect equally at each floor level due to the high in-plane rigidity of the floor slabs, and that the beams deflect with a point of contraflexure at their mid-span position. It is further assumed that the columns bend with points of contraflexure at their mid-height positions. The forces on the frame segment, and effective boundary conditions, are then as shown in Fig. 2.3.

If a horizontal shear force of magnitude Q is applied at the node D, the resulting horizontal displacement is Δ .

The slope-deflection method will be applied to analyse the different members of the frame segment, shown isolated in Fig. 2.4.

For the member AE (Fig. 2.4(a)), the end reactions may be computed by statics to be,

$$R_A = \frac{2M_{EA}}{d_1} \qquad \ldots\ldots (2.2)$$

The slope-deflection equations applied to the elastic ends of the member will give,

$$M_{AE} = 0 = \frac{4EI_{d_1}\,\theta_A}{\frac{l_1}{2}} - \frac{2EI_{d_1}\,\theta_E}{\frac{l_1}{2}} - \frac{6EI_{d_1}\frac{t_1}{2}\,\theta_E}{(\frac{l_1}{2})^2}$$

$$= \frac{8EI_{d_1}\,\theta_A}{l_1} - \frac{4E\,I_{d_1}}{l_1}\left(1 + \frac{3t_1}{l_1}\right)\theta_E \qquad \ldots\ldots (2.3)$$

$$M_{EA} - R_A \cdot \frac{t_1}{2} = \frac{2EI_{d_1}\,\theta_A}{(\frac{l_1}{2})} - \frac{4EI_{d_1}\,\theta_E}{(\frac{l_1}{2})} - \frac{6EI_{d_1}\,\frac{t_1}{2}\,\theta_E}{(\frac{l_1}{2})^2}$$

$$= \frac{4EI_{d_1}\theta_A}{l_1} - \frac{4EI_{d_1}}{l_1}\left(2 + \frac{3t_1}{l_1}\right)\theta_E \quad \ldots\ldots \quad (2.4)$$

On substituting equation (2.2) into equation (2.4) it is found that,

$$M_{EA} = \frac{4EI_{d_1}d_1}{l_1^2}\theta_A - \frac{4EI_{d_1}d_1}{l_1^2}\left(2 + \frac{3t_1}{l_1}\right)\theta_E \quad \ldots\ldots \quad (2.5)$$

Eliminating θ_A from the equations (2.3) and (2.5) M_{EA} becomes,

$$M_{EA} = -\frac{6EI_{d_1}d_1^2}{l_1^3}\theta_E \quad \ldots\ldots \quad (2.6)$$

The same procedure when followed for the member EC will give,

$$M_{EC} = -\frac{6EI_{d_2}d_2^2}{l_2^3}\theta_E \quad \ldots\ldots \quad (2.7)$$

If the equilibrium of the complete frame panel (Fig. 2.3) is considered, it is found that the horizontal reaction at the hinge B is equal in magnitude to the applied shearing force Q.

For the member BE, the slope-deflection equations yield

$$M_{BE} = 0 = \frac{-4EI_{h_1}\theta_B}{\left(\frac{e}{2}\right)} - \frac{2EI_{h_1}\theta_E}{\left(\frac{e}{2}\right)} + \frac{6EI_{h_1}\left(\Delta_1 - \frac{t_2}{2}\theta_E\right)}{\left(\frac{e}{2}\right)^2}$$

$$= -\frac{8EI_{h_1}\theta_B}{e} - \frac{4EI_{h_1}}{e}\left(1 + \frac{3t_2}{e}\right)\theta_E + \frac{24EI_{h_1}\Delta_1}{e^2}$$

$$\ldots\ldots \quad (2.8)$$

$$M_{EB} - Q \cdot \frac{t_2}{2} = - \frac{2EI_{h_1}\,\theta_B}{(\frac{e}{2})} - \frac{4EI_{h_1}\,\theta_E}{(\frac{e}{2})} + \frac{6EI_{h_1}(\Delta_1 - \frac{t_2}{2}\,\theta_E)}{(\frac{e}{2})^2}$$

$$= - \frac{4EI_{h_1}\,\theta_B}{e} - \frac{4EI_{h_1}}{e}(2 + 3\,\frac{t_2}{e})\,\theta_E + \frac{24EI_{h_1}\,\Delta_1}{e^2}$$

..... (2.9)

Also $$Q = \frac{M_{EB}}{(\frac{h}{2})}$$ ..... (2.10)

Substituting equation (2.10) into equation (2.9) yields,

$$M_{EB} = - \frac{4EI_{h_1}\,h\,\theta_B}{e^2} - \frac{4EI_{h_1}\,h}{e^2}(2 + \frac{3t_2}{e})\,\theta_E + \frac{24EI_{h_1}\,h\,\Delta_1}{e^3}$$

..... (2.11)

The slope θ_B is eliminated from the equations (2.8) and (2.11) giving,

$$M_{EB} = - \frac{6EI_{h_1}\,h^2}{e^3}\,\theta_E + \frac{12EI_{h_1}\,h}{e^3}\,\Delta_1$$ ..... (2.12)

Similarly for the member ED, the slope-deflection equations yield,

$$M_{ED} = - \frac{6EI_{h_2}\,h^2}{e^3}\,\theta_E + \frac{12EI_{h_2}\,h}{e^3}\,(\Delta - \Delta_1)$$ ..... (2.13)

In the above equations, h = storey height, I_{h_1} and I_{h_2} are the second moments of area of columns of two consecutive storeys, I_{d_1} and I_{d_2} are the second moments of area of the adjacent beams of total lengths d_1 and d_2 respectively, t_1 and t_2 are the length and height of the rigid arms, and

$$e = h - t_2$$

$$l_1 = d_1 - t_1$$

$$l_2 = d_2 - t_1$$

The resultant moment at E must be zero, so that

$$M_{EA} + M_{EC} + M_{EB} + M_{ED} = 0 \qquad \ldots\ldots \quad (2.14)$$

The moments M_{EB} and M_{ED} are equal, each being equal to $Q.\frac{h}{2}$. From the equations (2.12) and (2.13) it follows that,

$$\Delta_1 = \frac{I_{h_2}}{I_{h_1} + I_{h_2}} \Delta + \frac{I_{h_1} - I_{h_2}}{I_{h_1} + I_{h_2}} \frac{h}{2} \theta_E \qquad \ldots\ldots \quad (2.15)$$

On substituting equations (2.6), (2.7), (2.12), (2.13) and (2.15) into equation (2.14), the slope θ_E at E may be expressed as,

$$\theta_E = \frac{\frac{4\, I_{h_1}\, I_{h_2}}{I_{h_1} + I_{h_2}} \frac{h}{e^3} \Delta}{\frac{I_{d_1} \cdot d_1^2}{l_1^3} + \frac{I_{d_2} \cdot d_2^2}{l_2^3} + \frac{4\, I_{h_1}\, I_{h_2}}{I_{h_1} + I_{h_2}} \frac{h^2}{e^3}} \qquad (2.16)$$

Consideration of the equation $M_{EB} = M_{ED} = Q.\frac{h}{2}$ shows that the load-displacement relationship is

$$\frac{Q}{2}h = \frac{12Eh}{e^3} \frac{I_{h_1}\, I_{h_2}}{I_{h_1} + I_{h_2}} \frac{\Delta}{1 + \frac{\frac{4h^2}{e^3} \frac{I_{h_1}\, I_{h_2}}{I_{h_1} + I_{h_2}}}{\frac{I_{d_1} \cdot d_1^2}{l_1^3} + \frac{I_{d_2} \cdot d_2^2}{l_2^3}}} \qquad (2.17)$$

For an equivalent plate of the same width, subjected to the same shearing force Q (Fig. 2.3), the

load-displacement relationship is,

$$\Delta = \frac{Q}{GA} h \qquad \ldots\ldots \qquad (2.18)$$

where G is the effective shear modulus and A is the plate area.

From the two relationships (2.17) and (2.18), the shearing rigidity GA of the equivalent plate becomes,

$$GA = \frac{24Eh}{e^3} \frac{I_{h_1} I_{h_2}}{I_{h_1} + I_{h_2}} \frac{1}{1 + \dfrac{\dfrac{4h^2}{e^3} \dfrac{I_{h_1} I_{h_2}}{I_{h_1} + I_{h_2}}}{\dfrac{I_{d_1} d_1^2}{l_1^3} + \dfrac{I_{d_2} d_2^2}{l_2^3}}} \qquad (2.19)$$

This relationship is applicable also to an exterior column if the second moment of area of one of the beams is taken to be zero.

If, as is normally the case with this kind of structure, $I_{h_1} = I_{h_2} = I_h$, $I_{d_1} = I_{d_2} = I_d$, and $d_1 = d_2 = d$ or $l_1 = l_2 = l = d - t_1$

$$GA = \frac{12E\, I_h\, h}{e^3} \frac{1}{1 + \dfrac{I_h}{I_d} \dfrac{h^2}{d^2} \dfrac{l^3}{e^3}} \qquad \ldots\ldots \qquad (2.20)$$

If the finite size of the joint is neglected, that is, $t_1 = t_2 = 0$, the equation (2.19) for the effective shearing rigidity reduces to,

$$GA = \frac{24E}{h^2} \frac{I_{h_1} I_{h_2}}{I_{h_1} + I_{h_2}} \frac{1}{1 + \dfrac{\dfrac{4I_{h_1} I_{h_2}}{I_{h_1} + I_{h_2}}}{h\left(\dfrac{I_{d_1}}{d_1} + \dfrac{I_{d_2}}{d_2}\right)}} \qquad (2.21)$$

If a stiffer corner column is included in the analysis, part of the corner column area may be distributed to the adjacent end half bays to produce the equivalent uniform smeared plate area. The rest constitutes the area A_c, concentrated at the corner of the structure. When the analysis has been completed, the stresses, and the corresponding forces in these end half bays must be allocated as additional forces to the corner columns.

2.4 METHOD OF ANALYSIS OF THE EQUIVALENT TUBE

The equivalent tube composed of orthotropic plate panels is shown in Fig. 2.5, in which the stress system on a small element on each face is given.

The equations of equilibrium for the normal panel 1 are, in the absence of any body forces,

$$\frac{\partial \sigma_y}{\partial y} + \frac{\partial \tau_{yz}}{\partial z} = 0 \qquad \ldots\ldots(2.22)$$

$$\frac{\partial \sigma_z}{\partial z} + \frac{\partial \tau_{yz}}{\partial y} = 0$$

The corresponding equilibrium conditions for the side panel 2 are,

$$\frac{\partial \sigma_x}{\partial x} + \frac{\partial \tau_{xz}}{\partial z} = 0 \qquad \ldots\ldots(2.23)$$

$$\frac{\partial \sigma_z'}{\partial z} + \frac{\partial \tau_{xz}}{\partial x} = 0$$

It is assumed that the structure possesses two horizontal axes of symmetry, passing through the vertical central axis, so that the stress systems in the side

panels are identical, and those in the normal panels are equal and opposite.

The orthotropic stress-strain relations for the two panels may be expressed as,[21]

$$\sigma_y = E_y e_y + E_{yz} e_z$$
$$\sigma_z = E_z e_z + E_{yz} e_y \qquad \ldots\ldots \quad (2.24)$$
$$\tau_{yz} = G_{yz}\ \gamma_{yz}$$

and

$$\sigma_x = E_x e_x + E_{xz} e'_z$$
$$\sigma'_z = E'_z e'_z + E_{xz} e_x \qquad \ldots\ldots \quad (2.25)$$
$$\tau_{xz} = G_{xz}\ \gamma_{xz}$$

where the two sets of equations refer to the normal and side panels respectively. In structures of this nature, the cross-elasticity terms E_{yz} and E_{xz} may be assumed negligible. In addition, since the spacings and properties of both beams and columns are assumed uniform throughout the height,

$$E_z = E'_z = E$$
$$G_{yz} = G_{xz} = G \qquad \ldots\ldots \quad (2.26)$$

This latter assumption is not essential, but it does accord with the common practice which requires as great a level of uniformity as possible for simplifying the construction, and enables the complexity of the formulae to be reduced to a minimum.

The assumption is now made that the stresses may be expressed with sufficient accuracy as a power series

in the horizontal coordinate x or y, the coefficients of the series being arbitrary functions of the height coordinate z.

In order to model the anticipated distribution of vertical stresses σ_z in the normal panel, caused by the shear lag effect, the simplest approximation which may be used is a parabolic distribution. The stress distribution σ_z may thus be expressed in the form, (cf. Fig. 2.6),

$$\sigma_z = \frac{M}{I} c + S_o(z) + \left(\frac{y}{b}\right)^2 S(z) \qquad \ldots\ldots (2.27)$$

where $S_o(z)$ and $S(z)$ are functions of the height coordinate z only and M is the bending moment at any level.

The second and third terms are thus perturbations on the basic beam theory stress given by the first term. Because of symmetry, only even powers of the normal coordinate y may be used.

In equation (2.27) I is the second moment of area of the equivalent tube cross-section, given by

$$I = \frac{4}{3} tc^2(3b + c) + 4A_c.c^2$$

where 2b and 2c are the lengths of the normal and side panels, t is the effective thickness of the orthotropic tube, and A_c is the cross-sectional area of the corner column. The value of I is equal to that of the individual column areas in the real structure.

In the same way, the distribution of vertical stresses σ'_z in the side panels may be expressed in the form,

$$\sigma'_z = \frac{M}{I} x + \left(\frac{x}{c}\right)^3 S_1(z) \qquad \ldots\ldots (2.28)$$

In this case, because of the skew-symmetry of the stress distribution, only odd powers of the polynomial may be used.

The condition of vertical strain compatibility at the corners requires that

$$\frac{\sigma_z}{E}(\pm b, z) = \frac{\sigma'_z}{E}(c, z) = \frac{\sigma_c(z)}{E} \qquad (2.29)$$

where σ_c is the axial stress in the corner column given by, on using equation (2.27),

$$\sigma_c = (\sigma_z)_{y=b} = \frac{M}{I} c + S_o + S \qquad (2.30)$$

In equation (2.29) the elastic moduli of the corner columns and the plates are assumed to be equal; as will generally be the case in practice.

If the stiffnesses of the normal and side panels were not the same, and the corner columns were of a different material, different values of the effective elastic modulus E would be required in equation (2.29).

Substitution of equations (2.27) and (2.28) into (2.29) gives,

$$S_1 = S_o + S \qquad \ldots\ldots \qquad (2.31)$$

The condition of overall moment equilibrium at any height is,

$$2\int_{-b}^{b} \sigma_z \, tc \, dy + 2\int_{-c}^{c} \sigma'_z \, t \, x \, d\,x + 4A_c \, c \, \sigma_c = M(z) \qquad \ldots\ldots \qquad (2.32)$$

where M(z) is the total bending moment at any level due to the applied lateral loading.

On substituting equations (2.27), (2.28), (2.30)

and (2.31) into (2.32) and integrating, it is found that,

$$S_o = -\frac{1}{3} mS \qquad \ldots\ldots \quad (2.33)$$

where

$$m = \frac{5b + 3c + 15 \frac{A_c}{t}}{5b + c + 5 \frac{A_c}{t}}$$

which is always greater than unity.

The vertical stresses σ_z and σ_z' may thus be expressed in terms of the single unknown function S(z) as,

$$\sigma_z = \frac{M}{I} c - \left[\frac{1}{3} m - \left(\frac{y}{b}\right)^2 \right] S \qquad \ldots\ldots \quad (2.34)$$

$$\sigma_z' = \frac{M}{I} x + \left(1 - \frac{1}{3}m\right)\left(\frac{x}{c}\right)^3 S \qquad \ldots\ldots \quad (2.35)$$

The stress in the corner column then becomes,

$$\sigma_c = \left(\sigma_z\right)_{y=b} = \frac{M}{I} c + \left(1 - \frac{1}{3}m\right)S \qquad \ldots\ldots \quad (2.36)$$

On substituting equations (2.34) and (2.35) into the equilibrium conditions (2.22) and (2.23), and integrating, the remaining stress components become,

$$\sigma_y = -\frac{b^2 c}{2I} \left[1 - \left(\frac{y}{b}\right)^2\right] \frac{d^2M}{dz^2} + \frac{b^2}{12} \cdot$$

$$\left[(2m - 1) - 2m \left(\frac{y}{b}\right)^2 + \left(\frac{y}{b}\right)^4\right] \frac{d^2S}{dz^2}$$

$$\tau_{yz} = -y \left\{\frac{c}{I}\frac{dM}{dz} - \frac{1}{3}\left[m - \left(\frac{y}{b}\right)^2\right] \frac{dS}{dz}\right\} \qquad (2.37)$$

$$\sigma_x = -\frac{c^3}{2I}\left[2\left(\frac{1}{3} + \frac{b}{c} + \frac{A_c}{ct}\right) + \left(1 + 2\frac{b}{c} + \frac{2A_c}{ct}\right)\left(\frac{x}{c}\right) - \frac{1}{3}\left(\frac{x}{c}\right)^3\right] \frac{d^2M}{dz^2}$$

$$- \left(1 - \frac{1}{3}m\right) \frac{c^2}{20} \left[\left(\frac{x}{c}\right) - \left(\frac{x}{c}\right)^5\right] \frac{d^2S}{dz^2}$$

$$\tau_{xz} = \frac{c^2}{2I}\left[1 + 2\frac{b}{c} + \frac{2A_c}{ct} - \left(\frac{x}{c}\right)^2\right] \frac{dM}{dz} + \left(1 - \frac{1}{3}m\right) \frac{c}{4}\left[\frac{1}{5} - \left(\frac{x}{c}\right)^4\right] \frac{dS}{dz}$$

The integration constants were evaluated from the following boundary conditions,

$$\text{At } x = -c, \quad \sigma_x = 0$$

$$\text{At } y = \pm b, \quad \sigma_y = 0$$

The equation of equilibrium at the corner column is,

$$(\tau_{xz})_{x=c} + (\tau_{yz})_{y=b} = \frac{A_c}{t} \frac{\partial \sigma_c}{\partial z}$$

τ_{yz} is skew-symmetric with respect to the axis $y = 0$.

The following conditions are satisfied automatically as a result of the earlier equilibrium conditions that have been used.

$$\text{At } x = +c, \quad \sigma_x = \frac{p}{2t} = -\frac{1}{2t} \frac{d^2M}{dz^2}$$

Because of symmetry, each side frame will carry half of the total applied shear, so that,

$$t \int_{-c}^{+c} \tau_{xz} \, dx = \tfrac{1}{2}F = \tfrac{1}{2} \int_{o}^{z} p \, dz = \tfrac{1}{2} \frac{dM}{dz}$$

where p is the total applied load per unit height of building, and F is the total shear force.

The total strain energy U stored in the structure is given by,

$$U = t \int_{o}^{H} \left\{ \int_{-b}^{+b} \left(\frac{\sigma_z^2}{E} + \frac{\tau_{yz}^2}{G}\right) dy + \int_{-c}^{+c} \left(\frac{\sigma_z'^2}{E} + \frac{\tau_{xz}^2}{G}\right) dx \right\} dz$$

$$+ 2 \frac{A_c}{E} \int_{o}^{H} \sigma_c^2 \, dz \qquad \ldots\ldots \quad (2.38)$$

It is assumed that, because of the high in-plane

stiffness of the floor slabs, the horizontal strains are negligible, and the strain energy due to the horizontal direct stresses σ_x and σ_y may be neglected.

On substituting equations (2.34), (2.35), (2.36) and (2.37) into equation (2.38), the strain energy U may be expressed as,

$$U = t \int_o^H \Big(\frac{1}{E} \int_{-b}^{+b} \Big\{ \frac{M}{I} c - \Big[\tfrac{1}{3}m - \big(\tfrac{y}{b}\big)^2 \Big] S \Big\}^2 dy$$

$$+ \frac{1}{G} \int_{-b}^{+b} y^2 \Big\{ \frac{c}{I} \frac{dM}{dz} - \tfrac{1}{3} \Big[m - \big(\tfrac{y}{b}\big)^2 \Big] \frac{dS}{dz} \Big\}^2 dy$$

$$+ \frac{1}{E} \int_{-c}^{+c} \Big\{ \frac{M}{I} x + (1 - \tfrac{1}{3}m)\big(\tfrac{x}{c}\big)^3 S \Big\}^2 dx$$

$$+ \frac{1}{G} \int_{-c}^{+c} \Big\{ \frac{c^2}{2I} \Big[1 + 2\frac{b}{c} + \frac{2A_c}{ct} - \big(\tfrac{x}{c}\big)^2 \Big] \frac{dM}{dz}$$

$$+ (1 - \tfrac{1}{3}m) \frac{c}{4} \Big[\frac{1}{5} - \big(\tfrac{x}{c}\big)^4 \Big] \frac{dS}{dz} \Big\}^2 dx$$

$$+ 2 \frac{A_c}{tE} \Big\{ \frac{M}{I} c + (1 - \tfrac{1}{3}m) S \Big\}^2 \Big) dz \qquad \ldots\ldots (2.39)$$

The strain energy integral must be a minimum, by virtue of the principle of least work. According to the rules of the calculus of variations,[22] the condition for a minimum of U is that the variation of U, δU, vanishes.

From equation (2.39) the variation of U is expressed as,

$$\delta U = 2t \int_o^H \Big(\frac{1}{E} \int_{-b}^{+b} \Big\{ \frac{M}{I} c - \Big[\tfrac{1}{3}m - \big(\tfrac{y}{b}\big)^2 \Big] S \Big\} \Big\{ - \Big[\tfrac{1}{3}m - \big(\tfrac{y}{b}\big)^2 \Big] \delta S \Big\} dy$$

$$+ \frac{1}{G}\int_{-b}^{+b} y^2 \left\{ \frac{c}{I}\frac{dM}{dz} - \tfrac{1}{3}\left[m - \left(\frac{y}{b}\right)^2 \right]\frac{dS}{dz} \right\} \left\{ - \tfrac{1}{3}\left[m - \left(\frac{y}{b}\right)^2 \right] \delta\left(\frac{dS}{dz}\right) \right\} dy$$

$$+ \frac{1}{E}\int_{-c}^{+c} \left\{ \frac{M}{I}x + (1 - \tfrac{1}{3}m)\left(\frac{x}{c}\right)^3 S \right\} \left\{ (1 - \tfrac{1}{3}m)\left(\frac{x}{c}\right)^3 \delta S \right\} dx$$

$$+ \frac{1}{G}\int_{-c}^{+c} \left\{ \frac{c^2}{2I}\left[1 + 2\frac{b}{c} + 2\frac{A_c}{ct} - \left(\frac{x}{c}\right)^2 \right]\frac{dM}{dz} + (1-\tfrac{1}{3}m)\frac{c}{4} \cdot \right.$$

$$\left. \left[\frac{1}{5} - \left(\frac{x}{c}\right)^4 \right]\frac{dS}{dz} \right\} \cdot \left\{ (1-\tfrac{1}{3}m)\frac{c}{4}\left[\frac{1}{5} - \left(\frac{x}{c}\right)^4 \right] \delta\left(\frac{dS}{dz}\right) \right\} dx$$

$$+ \frac{2A_c}{tE}\left\{ \frac{M}{I}c + (1 - \tfrac{1}{3}m)S \right\} (1 - \tfrac{1}{3}m)\ \delta S)dz$$

and since $\delta(dS) = d(\delta S)$

there follows, on integrating by parts,

$$\delta U = 2t \int_0^H \left\{ -\frac{1}{G}\left[\frac{2b^3}{945}(35m^2 - 42m + 15) + \frac{2c^3}{225}(1-\tfrac{1}{3}m)^2 \right]\frac{d^2S}{dz^2} \right.$$

$$+ \frac{1}{E}\left[\frac{2b}{45}(5m^2 - 10m + 9) + \frac{2c}{7}(1-\tfrac{1}{3}m)^2 + \frac{2A_c}{t}(1-\tfrac{1}{3}m)^2 \right] S$$

$$\left. + \frac{1}{G}\left[\frac{2b^3c}{45I}(5m - 3) - \frac{2c^4}{105I}(1-\tfrac{1}{3}m) \right]\frac{d^2M}{dz^2} \right\} dz\ \delta S$$

$$+ \frac{2t}{G}\left[\left(\left\{ \frac{2b^3}{945}(35m^2 - 42m + 15) + \frac{2c^3}{225}(1-\tfrac{1}{3}m)^2 \right\}\frac{dS}{dz} \right.\right.$$

$$\left.\left. + \left\{ - \frac{2b^3c}{45I}(5m - 3) + \frac{2c^4}{105I}(1-\tfrac{1}{3}m) \right\}\frac{dM}{dz} \right) \delta S \right]_0^H$$

$$= 0 \qquad \ldots\ldots (2.40)$$

Since the structure is free at the top the direct stresses σ_z and σ_z' become zero at $z = 0$. It, therefore, follows from equations (2.34) and (2.35) that

At $z = 0$, $S = 0$

Hence at $z = 0$, $\delta S = 0$ ..... (2.41)

Also since $\delta S(z)$ is arbitrary throughout the height, including the base, the integrand of the first term and the second term of equation (2.40) must vanish separately, resulting, together with equation (2.41), in the following differential equation and boundary conditions for $S(z)$:

$$\frac{d^2S}{dz^2} - 45\,\frac{G}{E}\left(\frac{H}{b}\right)^2 \frac{7(5m^2 - 10m + 9) + 5(3 - m)^2\,\frac{c}{b}\left(1+7\frac{A_c}{ct}\right)}{15(35m^2 - 42m + 15) + 7\left(\frac{c}{b}\right)^3(3 - m)^2} \cdot \frac{S}{H^2}$$

$$= 45\,\frac{7(5m - 3) - \left(\frac{c}{b}\right)^3(3 - m)}{15(35m^2 - 42m + 15) + 7\left(\frac{c}{b}\right)^3(3 - m)^2}\,\frac{d^2\sigma_b}{dz^2} \qquad (2.42)$$

At $z = 0$, $S = 0$

$$\text{At } z = H,\ \frac{dS}{dz} - 45\,\frac{7(5m - 3) - \left(\frac{c}{b}\right)^3(3-m)}{15(35m^2 - 42m + 15) + 7\left(\frac{c}{b}\right)^3(3-m)^2}\,\frac{d\sigma_b}{dz}$$

..... (2.43)

For convenience, and in order to indicate the relationship between the perforated tube stresses and those derived from ordinary beam theory, the right hand side of equation (2.42) has been expressed in terms of the stress σ_b, given by

$$\sigma_b = \frac{M}{I}\,c \qquad \text{..... (2.44)}$$

that is, σ_b is the stress in the normal faces assuming that the framed tube behaves as a simple cantilevered tubular beam. Since the function $S(z)$ is a measure of the degree of shear lag in the normal panels, its relative

magnitude compared to the beam theory stresses is immediately apparent.

The differential equation (2.42) and the boundary condition (2.43) may be written in simpler forms as,

$$\frac{d^2S}{dz^2} - \left(\frac{k}{H}\right)^2 S = \lambda^2 \frac{d^2 \sigma_b}{dz^2} \quad \ldots\ldots \quad (2.45)$$

$$\text{At } z = H, \quad \frac{dS}{dz} - \lambda^2 \frac{d\,\sigma_b}{dz} = 0 \quad \ldots\ldots \quad (2.46)$$

where the parameters k and λ are defined as

$$k^2 = 45 \frac{G}{E} \left(\frac{H}{b}\right)^2 \frac{7(5m^2-10m+9) + 5(3-m)^2 \frac{c}{b}(1 + 7 \frac{A_c}{ct})}{15(35m^2-42m+15) + 7\left(\frac{c}{b}\right)^3 (3-m)^2}$$

$\ldots\ldots$ (2.47)

$$\lambda^2 = 45 \frac{7(5m - 3) - \left(\frac{c}{b}\right)^3 (3 - m)}{15(35m^2 - 42m + 15) + 7\left(\frac{c}{b}\right)^3 (3 - m)^2}$$

In the particular case where the corner columns are of the same stiffness as the others, so that they can be included as a segment of the equivalent orthotropic plates, the concentrated area A_c is zero, and the parameters k^2 and λ^2 reduce to,

$$k^2 = 9 \frac{G}{E} \left(\frac{H}{b}\right)^2 \frac{(5m^2 + 15m - 6)(3 - m)}{(35m^3 - 42m^2 + 51m - 20)}$$

$$\lambda^2 = -9 \frac{45m^3 - 72m^2 - 33m + 32}{(3 - m)(35m^3 - 42m^2 + 51m - 20)}$$

and the cross-sectional shape of the structure is described by the ratio m, given by

$$m = \frac{5b + 3c}{5b + c}$$

In the common practical case of a building with

square section of sides 2b and corner column area A_c, the parameters reduce to

$$k^2 = 45 \frac{G}{E} \left(\frac{H}{b}\right)^2 \frac{10m^2 - 25m + 27 + \frac{35}{4}(3 - m)^2 \frac{A_c}{bt}}{133m^2 - 168m + 72}$$

$$\lambda^2 = \frac{135(3m - 2)}{133m^2 - 168m + 72}$$

and the geometrical ratio m is expressed as

$$m = \frac{8b + 15 \frac{A_c}{t}}{6b + 5\frac{A_c}{t}}$$

In the case of a square section, where the corner columns are of the same stiffness as the other columns, m is equal to 1.33. Assuming that the extreme ranges of shape would be given by the cases b = 2c, and 2b = c, the values of m range from 1.18 to 1.57.

For practical structures, the value of k^2 as given by equation (2.47) is positive for all values of $(\frac{b}{c})$ and $(\frac{A_c}{ct})$.

Consequently, the homogeneous part of the solution of equation (2.45) may always be expressed in the form,

$$S = A \cosh \frac{k}{H} z + B \sinh \frac{k}{H} z \qquad \ldots\ldots (2.48)$$

The particular integral part of the solution will depend on the form of applied loading and the resultant stress σ_b.

Solutions are derived for three standard load cases, a point load P at the top, a uniformly distributed load of intensity p per unit height, and a triangularly distributed load whose intensity varies linearly from

zero at the base to a value p at the top. Any trapezoidal form of applied loading may be obtained by the superposition of uniform and triangular load forms. A uniformly distributed or trapezoidal form of loading may be used to simulate wind effects, whereas a combination of point loads and triangularly distributed loads may be used to simulate seismic effects.

Case 1 Concentrated load P at z = 0

In this case, the applied moment M at any level z is given by,

$$M = Pz$$

and the datum stress of σ_b becomes,

$$\sigma_b = \frac{P.c}{I} z \quad ,$$

The complete solution of equation (2.45), subject to the boundary conditions (2.41) and (2.46), then becomes,

$$S(\xi) = \frac{\lambda^2}{k} \sigma_b(H) \frac{\sinh k\xi}{\cosh k} \qquad \ldots\ldots (2.49)$$

where the base stress $\sigma_b(H) = \frac{PcH}{I}$ and,

for convenience, the solution has been expressed in terms of a non-dimensional height coordinate ξ given by

$$\xi = \frac{z}{H}$$

Case 2 Uniformly distributed load p throughout the height

In this case,

$$M = \frac{pz^2}{2} \quad \text{and} \quad \sigma_b = \frac{pc}{2I} z^2$$

The complete solution becomes,

$$S(\xi) = \frac{2\lambda^2}{k^2} \sigma_b(H) \left[\frac{\cosh k(1 - \xi) + k \sinh k\xi}{\cosh k} - 1 \right] \qquad \ldots\ldots (2.50)$$

where $\sigma_b(H) = \frac{pcH^2}{2I}$

Case 3 Triangularly distributed load

For a load intensity which varies linearly from 0 at z = H to p at z = 0,

$$M = \frac{p}{2}\left(z^2 - \frac{z^3}{3H}\right)$$

and $\sigma_b = \frac{pc}{2I}\left(z^2 - \frac{z^3}{3H}\right)$

The complete solution is found to be,

$$S(\xi) = \frac{3\lambda^2}{k^2}\sigma_b(H)\left[\frac{2k\cosh k(1-\xi) + (k^2-2)\sinh k\xi}{2k\cosh k} - (1-\xi)\right] \quad \ldots\ldots (2.51)$$

where

$$\sigma_b(H) = \frac{pcH^2}{3I}$$

Once the indeterminate stress function S has been determined, the other stress components follow from the formulae derived earlier (equations (2.34), (2.35) and (2.37)).

In the above analysis the strain energy due to the horizontal direct stresses σ_x and σ_y were neglected and the simple second order differential equation (2.45) was obtained for the stress function S. If, however, the strain energy due to σ_x and σ_y are also included in the total strain energy equation (2.38) the analysis will yield a fourth order differential equation. Such an equation will be more difficult to solve. For distributed load another boundary condition, which was neglected in the present analysis, becomes

At $z = 0$, $\frac{dS}{dz} = 0$

The above boundary condition ensures that the shear stresses τ_{yz} and τ_{xz} are zero at $z = 0$.

2.5 DESIGN CURVES

The four important design stress components σ_z, σ_z', τ_{yz} and τ_{xz} may be expressed in terms of the stress functions S and $\frac{dS}{dz}$ as indicated in equations (2.34), (2.35) and (2.37).

In order to produce simple design curves, it is convenient to express the stresses in the following forms,

$$\sigma_z = \sigma_b - \left[\tfrac{1}{3}m - \left(\tfrac{y}{b}\right)^2 \right] \sigma_b(H)\ F_1F_2$$

$$\sigma_z' = \sigma_b\left(\tfrac{x}{c}\right) + \left(1 - \tfrac{1}{3}m\right)\left(\tfrac{x}{c}\right)^3\ \sigma_b(H)\ F_1F_2$$

$$\tau_{yz} = -\frac{y}{H}\left\{ \frac{d\sigma_b}{d\xi} - \tfrac{1}{3}\left[m - \left(\tfrac{y}{b}\right)^2 \right] \sigma_b(H)\ F_1F_3 \right\} \qquad (2.52)$$

$$\tau_{xz} = \frac{c}{2H}\left[1 + 2\frac{b}{c} + \frac{2A_c}{ct} - \left(\tfrac{x}{c}\right)^2 \right] \frac{d\sigma_b}{d\xi}$$

$$+ \left(1 - \tfrac{1}{3}m\right)\frac{c}{4H}\left[\frac{1}{5} - \left(\tfrac{x}{c}\right)^4 \right] \sigma_b(H)\ F_1F_3$$

in which the parameters and functions σ_b, $\frac{d\sigma_b}{d\xi}$, F_1, F_2 and F_3 for the three standard load cases are shown in Table 2.1.

σ_b and $\frac{d\sigma_b}{d\xi}$ are functions of the load form only.

The function F_1, equal to λ^2, is a function only of the cross-sectional shape and relative size of corner columns, defined by the parameter m of equation (2.33).

The functions F_2 and F_3 depend on the parameter k

and the height ordinate ξ . As shown in equation (2.47), the parameter k is in turn a function of the parameters $\frac{G}{E}$, $\frac{H}{b}$ and m.

A set of curves showing the variations of the functions F_1, F_2 and F_3 for all three standard load cases, for the range of parameters likely to be met in practice, are given in Figs. 2.7 to 2.13.

2.6 USE OF DESIGN CURVES

For a given structure, the values of the effective elastic and shear moduli E and G may be determined from the formulae given in Article 2.3. A knowledge of the cross-sectional dimensions b and c, and the area of the corner columns A_c, yields the value of the ratio m from equation (2.33), and the value of k follows from equation (2.47). The value of function F_1, (i.e., λ^2), may be determined directly from Fig. 2.7, or may be calculated from the formula of equation (2.47). For the standard load conditions specified, the values of the functions F_2 and F_3 follow from the appropriate curves in Figs. 2.8 to 2.13, for the known value of k, for the level to be investigated. Knowing the values of σ_b and $\frac{d\sigma_b}{d\xi}$ at the required level, the stress components follow from equations(2.52).

Design curves have not been presented for the horizontal axial stresses σ_x and σ_y since they are generally small. However, if necessary, they may be obtained directly from equations(2.37).

2.7 CALCULATION OF COLUMN AND BEAM FORCES

The results from the equivalent continuous system must be transformed into the real discrete structure. The axial force in any particular column, for example, will be obtained by integrating, graphically, numerically or analytically, the direct stresses σ_z or σ'_z over half a bay width on either side of the column concerned. The axial forces in the corner columns will be obtained from contributions from the stresses in the end bays on both normal and side panels, and from the stresses in the corner column. The shear force in any column or beam will be obtained by integrating the appropriate shear stress over half a bay or storey height on either side of the column or beam respectively.

The axial forces in columns and the shear forces in columns and beams for the normal and side panels are given below. The axial force in the corner area A_c is also given.

NORMAL PANELS

(i) The axial force in a column at position y_i and level z is given by

$$N_i = t \int_{y_i - \frac{d}{2}}^{y_i + \frac{d}{2}} \sigma_z \, dy$$

On substituting the value of σ_z from equation (2.34) and integrating, the axial force becomes

$$N_i = t\, d \left\{ \sigma_b - \tfrac{1}{3} \left[m - \frac{1}{b^2}\left(3y_i^2 + \frac{d^2}{4}\right) \right] s \right\} \qquad (2.53)$$

where $S = \sigma_b(H)F_1F_2$ and may be evaluated at that level directly from the design curves.

(ii) The axial force in the corner column is given by

$$N_1 = t \int_{b-\frac{d}{2}}^{b} \sigma_z \, dy$$

$$= \frac{td}{2} \left\{ \sigma_b - \tfrac{1}{3} \left[m - \frac{1}{b^2} \left(3b^2 - \frac{3}{2} bd + \frac{d^2}{4} \right) \right] \sigma_b(H)F_1F_2 \right\}$$

(2.54)

(iii) The shear force in a column at position y_i is given by

$$S_{c_i} = t \int_{y_i - \frac{d}{2}}^{y_i + \frac{d}{2}} \tau_{yz} \, dy$$

The value of τ_{yz} may be substituted from equation (2.37) and then integrated, giving,

$$S_{c_i} = - \frac{tdy_i}{H} \left\{ \frac{d\sigma_b}{d\xi} - \tfrac{1}{3} \left[m - \frac{1}{b^2} \left(y_i^2 + \frac{d^2}{4} \right) \right] \frac{dS}{d\xi} \right\} \qquad (2.55)$$

where $\frac{dS}{d\xi} = \sigma_b(H)F_1F_3$.

(iv) The shear force in the corner column becomes

$$S_{c_1} = t \int_{b-\frac{d}{2}}^{b} \tau_{yz} \, dy$$

$$= - \frac{td}{2H} \left(b - \frac{d}{4} \right) \left\{ \frac{d\sigma_b}{d\xi} - \tfrac{1}{3} \left[m - \frac{1}{2b^2} \left(2b^2 - bd + \frac{d^2}{4} \right) \right] \cdot \sigma_b(H)F_1F_3 \right\} \qquad (2.56)$$

(v) The shear force in spandrel beam at position y_i and level $\xi_j(z_j)$ is given by

$$S_{b_{ij}} = t \int_{z_j - \frac{h}{2}}^{z_j + \frac{h}{2}} \tau_{yz}\, dz$$

$$= -ty_i \left\{ \left[\sigma_b(z_j + \tfrac{h}{2}) - \sigma_b(z_j - \tfrac{h}{2}) \right] - \tfrac{1}{3} \left[m - \left(\frac{y_i}{b}\right)^2 \right] \right.$$

$$\left. \sigma_b(H) F_1 \left[F_2(z_j + \tfrac{h}{2}) - F_2(z_j - \tfrac{h}{2}) \right] \right\} \qquad (2.57)$$

SIDE PANELS

(i) The axial force in a column at position x_i is

$$N_i = t \int_{x_i - \frac{d}{2}}^{x_i + \frac{d}{2}} \sigma'_z\, dx$$

$$= \frac{t dx_i}{c} \left\{ \sigma_b + (1 - \tfrac{1}{3}m) \frac{1}{c^2} (x_i^2 + \frac{d^2}{4}) \quad \sigma_b(H) F_1 F_2 \right\} \qquad (2.58)$$

(ii) The axial force in the corner column becomes,

$$N_1 = t \int_{c - \frac{d}{2}}^{c} \sigma'_z\, dx$$

$$= \frac{td(c - \frac{d}{4})}{2c} \left\{ \sigma_b + (1 - \tfrac{1}{3}m) \frac{1}{c^2} (c^2 - \frac{cd}{2} + \frac{d^2}{8}) \ \sigma_b(H) F_1 F_2 \right\} \qquad (2.59)$$

(iii) The shear force in column at position x_i may be expressed as

$$S_{c_i} = t \int_{x_i - \frac{d}{2}}^{x_i + \frac{d}{2}} \tau_{xz}\, dx$$

$$= \frac{tcd}{2H}\left\{\left[1 + 2\frac{b}{c} + 2\frac{A_c}{ct} - \frac{1}{3c^2}\left(3x_i^2 + \frac{d^2}{4}\right)\right]\frac{d\sigma_b}{d\xi}\right.$$

$$\left. + \frac{1}{10}\left(1 - \tfrac{1}{3}m\right)\left[1 - \frac{1}{c^4}\left(5x_i^4 + \frac{5}{2}d^2x_i^2 + \frac{d^4}{16}\right)\right]\sigma_b(H)F_1F_3\right\} \quad (2.60)$$

(iv) The shear force in the corner column is

$$S_{c_1} = t\int_{c-\frac{d}{2}}^{c}\tau_{xz}\,dx$$

$$= \frac{tcd}{4H}\left\{\left[2\frac{b}{c} + \frac{2A_c}{ct} + \frac{d}{2c^2}\left(c - \frac{d}{6}\right)\right]\frac{d\sigma_b}{d\xi}\right.$$

$$- \frac{2}{5}\left(1-\tfrac{1}{3}m\right)\left[1 - \frac{d}{4c^4}\left(5c^3 - \frac{5}{2}c^2d + \frac{5}{8}cd^2 - \frac{d^3}{16}\right)\right]\cdot$$

$$\left.\sigma_b(H)F_1F_3\right\} \quad (2.61)$$

(v) The shear force in spandrel beam at position x_i and level $z_j(\xi_j)$ is

$$S_{b_{ij}} = t\int_{z_j-\frac{h}{2}}^{z_j+\frac{h}{2}}\tau_{xz}\,dz$$

$$= \frac{tc}{2}\left\{\left[1 + 2\frac{b}{c} + \frac{2A_c}{ct} - \left(\frac{x_i}{c}\right)^{-2}\right]\cdot\right.$$

$$\left[\sigma_b\left(z_j + \frac{h}{2}\right) - \sigma_b\left(z_j - \frac{h}{2}\right)\right] + \frac{1}{2}\left(1 - \frac{1}{3}m\right)\cdot$$

$$\left.\left[\frac{1}{5} - \left(\frac{x_i}{c}\right)^4\right]\sigma_b(H)F_1\left[F_2\left(z_j + \frac{h}{2}\right) - F_2\left(z_j - \frac{h}{2}\right)\right]\right\} \quad (2.62)$$

CORNER AREA A_c

The axial force in the concentrated area A_c at the corner is given by,

$$N_c = A_c \sigma_c$$

On substituting the value of σ_c from equation (2.36), N_c is obtained as,

$$N_c = A_c \left\{ \sigma_b + (1 - \tfrac{1}{3}m) \sigma_b(H)F_1F_2 \right\} \qquad (2.63)$$

The total axial force in the corner column is the sum of the three values obtained by equations (2.54), (2.59) and (2.63).

2.8 ASSESSMENT OF LATERAL DRIFT

Once the stress distribution is known throughout the structure, it is a relatively straightforward although tedious procedure to determine the deflection at any position by means of the principle of virtual work.

In particular, the lateral deflection δ at the top of the building is given by,

$$\delta = 2 \int_0^H \int_{-b}^{b} \sigma \epsilon \, t \, dy \, dz + 2 \int_0^H \int_{-c}^{c} \sigma \epsilon \, t \, dx \, dz + 4 \int_0^H (\sigma \epsilon)_c A_c \, dz \qquad (2.64)$$

where ϵ is the true (direct or shear) strain, σ is the virtual (direct or shear) stress in equilibrium with a unit lateral load applied at the top of the structure, and the suffix c denotes the corner column position.

The stresses under a uniformly distributed load p may be evaluated from equations (2.34), (2.35), (2.36)

and (2.37) and are expressed as,

$$\sigma_z = \frac{pc}{2I}\left\{ z^2 - \frac{2\lambda^2}{k^2} H^2 \left[\tfrac{1}{3}m - \left(\frac{y}{b}\right)^2 \right] \cdot \left[\frac{\cosh k\,(1 - \frac{z}{H}) + k\sinh \frac{kz}{H}}{\cosh k} - 1 \right] \right\}$$

$$\sigma'_z = \frac{pc}{2I}\left\{ \left(\frac{x}{c}\right) z^2 + \frac{2\lambda^2}{k^2} H^2 (1 - \tfrac{1}{3}m)\left(\frac{x}{c}\right)^3 \cdot \left[\frac{\cosh k(1 - \frac{z}{H}) + k \sinh \frac{kz}{H}}{\cosh k} - 1 \right] \right\}$$

$$\sigma_c = \frac{pc}{2I}\left\{ z^2 + \frac{2\lambda^2}{k^2} H^2 (1 - \tfrac{1}{3}m) \cdot \left[\frac{\cosh k(1 - \frac{z}{H}) + k \sinh \frac{kz}{H}}{\cosh k} - 1 \right] \right\}$$

$$\tau_{yz} = -\frac{pc}{I} y \left\{ z - \frac{\lambda^2}{3k \cosh k} H \left[m - \left(\frac{y}{b}\right)^2 \right] \cdot \left[-\sinh k\,(1 - \frac{z}{H}) + k \cosh \frac{kz}{H} \right] \right\}$$

$$\tau_{xz} = \frac{pc^2}{2I}\left\{ \left[1 + 2\,\frac{b}{c} + \frac{2A_c}{ct} - \left(\frac{x}{c}\right)^2 \right] z + \frac{\lambda^2}{2k \cosh k} H(1 - \tfrac{1}{3}m) \cdot \left[\tfrac{1}{5} - \left(\frac{x}{c}\right)^4 \right] \left[-\sinh k(1 - \frac{z}{H}) + k \cosh \frac{kz}{H} \right] \right\} \qquad (2.65)$$

The stresses due to a unit load applied at the top are given by,

$$\sigma_z = \frac{c}{I}\left\{ z - \frac{\lambda^2}{k \cosh k} H \left[\tfrac{1}{3}m - \left(\frac{y}{b}\right)^2 \right] \sinh \frac{kz}{H} \right\}$$

$$\sigma'_z = \frac{c}{I}\left\{ \left(\frac{x}{c}\right) z + \frac{\lambda^2}{k \cosh k} H(1 - \tfrac{1}{3}m)\left(\frac{x}{c}\right)^3 \sinh \frac{kz}{H} \right\}$$

$$\sigma_c = \frac{c}{I} \left\{ z + \frac{\lambda^2}{k \cosh k} H(1 - \tfrac{1}{3}m) \sinh \frac{kz}{H} \right\} \qquad (2.66)$$

$$\tau_{yz} = - \frac{c}{I} y \left\{ 1 - \frac{\lambda^2}{3 \cosh k} \left[m - \left(\frac{y}{b}\right)^2 \right] \cosh \frac{kz}{H} \right\}$$

$$\tau_{xz} = \frac{c^2}{2I} \left\{ \left[1 + 2 \frac{b}{c} + \frac{2A_c}{ct} - \left(\frac{x}{c}\right)^2 \right] + \frac{\lambda^2}{2 \cosh k} (1 - \tfrac{1}{3}m) \cdot \right.$$

$$\left. \left[\frac{1}{5} - \left(\frac{x}{c}\right)^4 \right] \cdot \cosh \frac{kz}{H} \right\}$$

From the stresses given in equation (2.65) the true strains can be evaluated by the stress-strain relationships

$$\epsilon = \frac{\sigma}{E} \; ; \quad \gamma = \frac{\tau}{G}$$

Substituting the values of virtual stress σ_z and true strain ϵ_z it is found that

$$2 \int_0^H \int_{-b}^{b} \sigma_z \; \epsilon_z \; t \; dy \; dz$$

$$= \frac{pc^2t}{E \; I^2} \int_0^H \int_{-b}^{b} \left\{ z - \frac{\lambda^2 H}{k \cosh k} \left[\tfrac{1}{3}m - \left(\frac{y}{b}\right)^2 \right] \sinh \frac{kz}{H} \right\} \cdot$$

$$\left\{ z^2 - \frac{2 \lambda^2 H^2}{k^2} \left[\tfrac{1}{3}m - \left(\frac{y}{b}\right)^2 \right] \left[\frac{\cosh k(1 - \frac{z}{H}) + k \sinh \frac{kz}{H}}{\cosh k} - 1 \right] \right\}$$

$$dy \; dz$$

Integrating first with respect to y and then with respect to z it is found that

$$2 \int_0^H \int_{-b}^{b} \sigma_z \; \epsilon_z \; t \; dy \; dz = \frac{2pbc^2H^4t}{E \; I^2} \left\{ \frac{1}{4} - \frac{2 \lambda^2 (m - 1)}{3k^4 \cosh k} \cdot \right.$$

$$\left. (k^2 \cosh k - 2k \sinh k + 2 \cosh k - 2) + \frac{\lambda^4}{k^4 \cosh^2 k} \cdot \right.$$

$$(\frac{m^2}{9} - \frac{2m}{9} + \frac{1}{5}).(2\cosh k - 2\cosh^2 k - k^2 + k\sinh k + k\sinh k\cosh k)\Big\} \quad (2.67)$$

Similarly the other virtual work components due to axial stresses become

$$2\int_0^H \int_{-c}^{c} \sigma_z' \epsilon_z' t\, dx\, dz = \frac{2pc^3H^4t}{E I^2}\left\{\frac{1}{12} + \frac{2\lambda^2}{5k^4\cosh k}\cdot\right.$$

$$(1 - \tfrac{1}{3}m).(k^2\cosh k - 2k\sinh k + 2\cosh k - 2)$$

$$+ \frac{\lambda^4}{7k^4\cosh^2 k}(1 - \tfrac{1}{3}m)^2\cdot$$

$$\left.(2\cosh k - 2\cosh^2 k - k^2 + k\sinh k + k\sinh k\cosh k)\right\} \quad (2.68)$$

$$4\int_0^H \sigma_c \epsilon_c \Lambda_c\, dz = \frac{2pc^2H^4\Lambda_c}{E I^2}\left\{\tfrac{1}{4} + \frac{2\lambda^2}{k^4\cosh k}(1 - \tfrac{1}{3}m)\cdot\right.$$

$$(k^2\cosh k - 2k\sinh k + 2\cosh k - 2) + \frac{\lambda^4}{k^4\cosh^2 k}(1 - \tfrac{1}{3}m)^2\cdot$$

$$\left.(2\cosh k - 2\cosh^2 k - k^2 + k\sinh k + k\sinh k\cosh k)\right\} \quad (2.69)$$

The equations (2.67), (2.68) and (2.69) are added to give

$$\delta_1 = \frac{2pc^3H^4t}{E I^2}\left\{\frac{I}{16c^3t} + \frac{1}{9}\left[\frac{1}{5}(5m^2 - 10m + 9)\frac{b}{c} + (3 - m)^2\cdot\right.\right.$$

$$\left.\left.(\frac{1}{7} + \frac{A_c}{ct})\right]\frac{\lambda^4}{k^4\cosh^2 k}(2\cosh k - 2\cosh^2 k - k^2 + k\sinh k + k\sinh k\cosh k)\right\} \quad (2.70)$$

The deflection δ_1 is caused by the cantilever action of the framed-tube. If the second term inside the bracket, which represents the effect of shear lag, is

neglected, δ_1 becomes

$$\delta_1 = \frac{pH^4}{8EI} .$$

The above expression is identical to the one obtained in basic beam theory.

The virtual work components due to shear stresses are

$$2\int_0^H \int_{-b}^{b} \tau_{yz}\gamma_{yz}\, t\, dy\, dz$$

$$= \frac{4}{3}\frac{pb^3c^2H^2t}{G\,I^2}\left\{\tfrac{1}{2} - \frac{2\lambda^2}{k\cosh k}\left(\tfrac{1}{3}m - \tfrac{1}{5}\right)\left[\sinh k - \tfrac{1}{k}(\cosh k - 1)\right]\right.$$

$$\left. + \frac{\lambda^4}{6k\cosh^2 k}\left(\frac{m^2}{3} - \frac{2m}{5} + \frac{1}{7}\right)(k - \sinh k + \sinh k\cosh k)\right\} \qquad (2.71)$$

$$2\int_0^H \int_{-c}^{c} \tau_{xz}\gamma_{xz}\, t\, dx\, dz$$

$$= \frac{2pc^5H^2t}{G\,I^2}\left\{\left[\frac{2}{15} + \tfrac{2}{3}\frac{b}{c} + \tfrac{2}{3}\frac{A_c}{ct} + 2\frac{b}{c}\frac{A_c}{ct} + \left(\frac{b}{c}\right)^2 + \left(\frac{A_c}{ct}\right)^2\right]\right.$$

$$+ \frac{4\lambda^2}{105k\cosh k}\left(1 - \tfrac{1}{3}m\right)\left[\sinh k - \frac{1}{k}(\cosh k - 1)\right]$$

$$\left. + \frac{\lambda^4}{225k\cosh^2 k}\left(1 - \tfrac{1}{3}m\right)^2(k - \sinh k + \sinh k\cosh k)\right\} \qquad (2.72)$$

The equations (2.71) and (2.72) are added giving

$$\delta_2 = \frac{2pc^5H^2t}{G\,I^2}\left\{\left[\frac{2}{15} + \tfrac{2}{3}\frac{b}{c} + \tfrac{2}{3}\frac{A_c}{ct} + \left(\frac{b}{c}\right)^2 + 2\frac{b}{c}\frac{A_c}{ct} + \left(\frac{A_c}{ct}\right)^2\right.\right.$$

$$\left.\left. + \tfrac{1}{3}\left(\frac{b}{c}\right)^3\right] + \frac{4}{45}\left[\frac{1}{7}(3-m) - (5m-3)\left(\frac{b}{c}\right)^3\right]\frac{\lambda^2}{k^2\cosh k}\right. .$$

$$(k \sinh k - \cosh k + 1) + \frac{1}{135}\left[\frac{1}{15}(3-m)^2 + \frac{1}{7}(35m^2 - 42m + 15)\left(\frac{b}{c}\right)^3\right] \frac{\lambda^4}{k \cosh^2 k} (k - \sinh k + \sinh k \cosh k)\Bigg\} \quad (2.73)$$

The deflection δ_2 includes the racking of the side frames.

The top lateral deflection for a uniformly distributed load is the sum of the two equations (2.70) and (2.73) and is given by,

$$\delta = \delta_1 + \delta_2 \quad (2.74)$$

In the particular case of a square section of side 2b the deflection equation is reduced to

$$\delta = \frac{2pb^3H^4t}{E\,I^2}\left\{\frac{I}{16b^3t} + \frac{1}{9}\left[\frac{1}{5}(5m^2 - 10m + 9) + (3 - m)^2 \cdot \left(\frac{1}{7} + \frac{A_c}{bt}\right)\right] \frac{\lambda^4}{k^4 \cosh^2 k} (2 \cosh k - 2 \cosh^2 k - k^2 + k \sinh k + k \sinh k \cosh k)\right\}$$

$$+ \frac{2pb^5H^2t}{G\,I^2}\left\{\left[\frac{32}{15} + \frac{8}{3}\frac{A_c}{bt} + \left(\frac{A_c}{bt}\right)^2\right] - \frac{16}{105}(3m - 2) \cdot \frac{\lambda^2}{k^2 \cosh k}(k \sinh k - \cosh k + 1) + \frac{4}{14175}(133m^2 - 168m + 72) \cdot \frac{\lambda^4}{k \cosh^2 k} (k - \sinh k + \sinh k \cosh k)\right\}$$

Similar expressions may be derived for the other standard load cases.

2.9 NUMERICAL EXAMPLE

A 50-storey concrete high-rise building, shown in plan in Fig. 2.14, is considered with the following

dimensions:

h = storey height = 3.6 m,

d = bay width = 3.0 m,

$2b$ = total width of framed tube = 24 m,

$2c$ = total depth of the framed tube = 12 m,

t_1 = width of the columns = 1.0 m,

t_2 = depth of the spandrel beams = 0.6 m,

t_w = thickness of columns and beams = 0.3m.

The corner columns are twice the area of other columns. The building is subjected to a uniform lateral load of 1 kN/m height.

For concrete, $E = 22.24 \times 10^6$ kN/m^2.

The thickness t of the equivalent orthotropic plate is given by

dt = area of a column = 1×0.3 m^2

$$\therefore t = \frac{0.3}{3.0} = 0.1 \text{ m}$$

$$\frac{b}{c} = \frac{12}{6} = 2$$

$$H = 50 \times 3.6 = 180 \text{ m}$$

$$A_c = 1 \times 0.3 = 0.3 \text{ m}^2$$

$$\frac{A_c}{ct} = \frac{0.3}{6 \times 0.1} = 0.5$$

$$m = \frac{5 \times 12 + 3 \times 6 + 15 \times \frac{0.3}{0.1}}{5 \times 12 + 6 + 5 \times \frac{0.3}{0.1}} = 1.5185$$

$$I = \frac{4}{3} \times 0.1 \times 6^2(3 \times 12 + 6) + 4 \times 0.3 \times 6^2 = 244.8 \text{ m}^4$$

$$\sigma_b(H) = \frac{1 \times 180^2}{2 \times 244.8} \times 6 = 397.06 \text{ kN/m}^2$$

$$\lambda^2 = 45 \times \frac{32.1475 - 0.1852}{478.912 + 1.9205} = 2.9913$$

$$I_h = \frac{0.3 \times 1^3}{12} = 0.025 \text{ m}^4$$

$$I_d = \frac{0.3 \times 0.6^3}{12} = 0.0054 \text{ m}^4$$

$$l = d - t_1 = 2.0 \text{ m}$$

$$e = h - t_2 = 3.0 \text{ m}$$

$$\frac{G}{E} = \frac{12 \times 0.025 \times 3.6}{1 \times 0.3 \times 27} \times \frac{1}{1 + 1.9753} = 0.044813$$

$$k^2 = 45 \times 0.044813 \times \left(\frac{180}{12}\right)^2 \frac{37.4095 + 24.6920}{478.9122 + 1.9205}$$

$$= 58.6013$$

$$k = 7.655$$

$$\sinh k = \cosh k = 1055.6$$

The columns and beams are numbered as shown in Fig. 2.14.

Axial forces in columns

The axial forces in columns at the second floor level are evaluated as follows

$$\xi = \frac{48}{50} = 0.96$$

$$\sigma_b = \xi^2 \ \sigma_b(H) = 0.9216 \ \sigma_b(H)$$

$$k\xi = 7.349$$

$$k(1 - \xi) = 0.306$$

$$\sinh k\xi = 777.32$$

$$\cosh k(1 - \xi) = 1.0472$$

$$\frac{S(\xi)}{\sigma_b(H)} = \frac{2 \times 2.9913}{58.6013} (5.6380 - 1) = 0.4735$$

Normal Panel

The axial forces in the columns of the normal panel

are evaluated from equations (2.53) and (2.54) as

$$N_1 = \frac{0.1 \times 3}{2} \times 397.06 \left\{ 0.9216 - \tfrac{1}{3}(1.5185 - 2.6406)0.4735 \right\}$$
$$= 65.4378 \text{ kN}$$

$$N_2 = 0.1 \times 3 \times 397.06 \left\{ 0.9216 - \tfrac{1}{3}(1.5185 - 1.7031)0.4735 \right\}$$
$$= 113.2498 \text{ kN}$$

$$N_3 = 0.1 \times 3 \times 397.06 \left\{ 0.9216 - \tfrac{1}{3}(1.5185 - 0.7656)0.4735 \right\}$$
$$= 95.6240 \text{ kN}$$

$$N_4 = 0.1 \times 3 \times 397.06 \left\{ 0.9216 - \tfrac{1}{3}(1.5185 - 0.2031)0.4735 \right\}$$
$$= 85.0486 \text{ kN}$$

$$N_5 = 0.1 \times 3 \times 397.06 \left\{ 0.9216 - \tfrac{1}{3}(1.5185 - 0.01563)0.4735 \right\}$$
$$= 81.5240 \text{ kN}$$

Side Panel

The axial forces in the side panel are determined with the help of equations (2.58) and (2.59) as

$$N_1 = \frac{0.1 \times 3 \times 5.25}{12} \times 397.06(0.9216 + 0.49383 \times 0.78125 \times 0.4735) = 57.5485 \text{ kN}$$

$$N_2 = \frac{0.1 \times 3 \times 3}{6} \times 397.06(0.9216 + 0.49383 \times 0.3125 \times 0.4735) = 59.2416 \text{ kN}$$

$$N_3 = 0$$

Corner area A_c

The axial force in the corner area is obtained from equation (2.63) as

$$N_1 = 0.3 \times 397.06(0.9216 + 0.49383 \times 0.4735) = 137.6323 \text{ kN}$$

$\therefore$ Total axial force in the corner column

$$= 65.4378 + 57.5485 + 137.6323$$

$$= 260.6186 \text{ kN}$$

Shear forces in columns

The shear forces in the columns are determined at the middle of the third storey.

$$\xi = \frac{47.5}{50} = 0.95$$

$$\frac{d\sigma_b}{d\xi} = 2\xi\ \sigma_b(H) = 1.90\ \sigma_b(H)$$

$$k\xi = 7.272$$

$$k(1 - \xi) = 0.383$$

$$\sinh k(1 - \xi) = 0.3924$$

$$\cosh k\xi = 719.72$$

$$\frac{dS}{d\xi} = \frac{2 \times 2.9913}{7.655} \times 5.2189\ \sigma_b(II) = 4.0787\ \sigma_b(II)$$

Normal Panel

The shear forces in the columns of the normal panel are (cf equations (2.55) and (2.56))

$$S_{c_1} = -\frac{0.1 \times 3}{360} \times 11.25 \times 397.06 \left\{ 1.90 - \tfrac{1}{3}(1.5185 - 0.8828) \cdot 4.0787 \right\} = -3.8554 \text{ kN}$$

$$S_{c_2} = -\frac{0.1 \times 3 \times 9}{180} \times 397.06 \left\{ 1.90 - \tfrac{1}{3}(1.5185 - 0.5781) \cdot 4.0787 \right\} = -3.7014 \text{ kN}$$

$$S_{c_3} = -\frac{0.1 \times 3 \times 6}{180} \times 397.06 \left\{ 1.90 - \tfrac{1}{3}(1.5185 - 0.2656) \cdot 4.0787 \right\} = -0.7806 \text{ kN}$$

$$S_{c_4} = -\frac{0.1 \times 3 \times 3}{180} \times 397.06 \left\{ 1.90 - \tfrac{1}{3}(1.5185 - 0.078125) \cdot 4.0787 \right\} = 0.1157 \text{ kN}$$

$$S_{c_5} = 0$$

Side Panel

The shear forces in the columns of the side panel are (equations 2.60 and 2.61)

$$S_{c_1} = \frac{0.1 \times 6 \times 3}{720} \times 397.06 \left\{ 5.2292 \times 1.90 - \frac{2}{5} \times 0.49383 \times (1 - 0.4873) 4.0787 \right\} = 9.4524 \text{ kN}$$

$$S_{c_2} = \frac{0.1 \times 6 \times 3}{360} \times 397.06 \left\{ 5.7292 \times 1.90 + \frac{1}{10} \times 0.49383 \times (1 - 0.4727) 4.0787 \right\} = 21.8218 \text{ kN}$$

$$S_{c_3} = \frac{0.1 \times 6 \times 3}{360} \times 397.06 \left\{ 5.9792 \times 1.90 + \frac{1}{10} \times 0.49383 \times (1 - 0.003906) 4.0787 \right\} = 22.9523 \text{ kN}$$

Shear forces in spandrel beams

The shear forces in the spandrel beams are determined at the second floor level.

$z_j + \frac{h}{2} = 174.6$ m

corresponding $\xi_1 = \frac{174.6}{180} = 0.97$

$z_j - \frac{h}{2} = 171.0$ m

corresponding $\xi_2 = \frac{171.0}{180} = 0.95$

$$\sigma_b(z_j + \frac{h}{2}) - \sigma_b(z_j - \frac{h}{2}) = (\xi_1^2 - \xi_2^2)\, \sigma_b(H) = 0.0384\, \sigma_b(H)$$

$k\xi_1 = 7.425$

$k(1 - \xi_1) = 0.230$

$\sinh k\xi_1 = 838.71$

$\cosh k(1 - \xi_1) = 1.0266$

$$S(z_j + \frac{h}{2}) = \frac{2 \times 2.9913}{58.6013} \times (6.0831 - 1)\ \sigma_b(H) = 0.51893\ \sigma_b(H)$$

$k\xi_2 = 7.272$

$k(1 - \xi_2) = 0.383$

$\sinh k\xi_2 = 719.72$

$\cosh k(1 - \xi_2) = 1.0742$

$$S(z_j - \frac{h}{2}) = \frac{2 \times 2.9913}{58.6013} \times (5.2203 - 1)\ \sigma_b(H)$$

$$= 0.43085\ \sigma_b(H)$$

$$S(z_j + \frac{h}{2}) - S(z_j - \frac{h}{2}) = 0.08808\ \sigma_b(H)$$

Normal Panel

For the normal panel the shear forces in the spandrel beams are evaluated as (equation 2.57)

$$S_{b_1} = -0.1 \times 10.5 \times 397.06 \left\{ 0.0384 - \tfrac{1}{3}(1.5185 - 0.7656) \cdot 0.08808 \right\} = -6.7936 \text{ kN}$$

$$S_{b_2} = -0.1 \times 7.5 \times 397.06 \left\{ 0.0384 - \tfrac{1}{3}(1.5185 - 0.3906) \cdot 0.08808 \right\} = -1.5738 \text{ kN}$$

$$S_{b_3} = -0.1 \times 4.5 \times 397.06 \left\{ 0.0384 - \tfrac{1}{3}(1.5185 - 0.1406) \cdot 0.08808 \right\} = +0.3672 \text{ kN}$$

$$S_{b_4} = -0.1 \times 1.5 \times 397.06 \left\{ 0.0384 - \tfrac{1}{3}(1.5185 - 0.015625) \cdot 0.08808 \right\} = +0.3409 \text{ kN}$$

Side Panel

The shear forces in the side panels are calculated as (equation 2.62)

$$S_{b_1} = \frac{0.1 \times 6}{2} \times 397.06\ (5.4375 \times 0.0384 - \tfrac{1}{2} \times 0.49383 \times 0.11641 \times 0.08808) = 24.5703 \text{ kN}$$

$$S_{b_2} = \frac{0.1 \times 6}{2} \times 397.06\ (5.9375 \times 0.0384 + \tfrac{1}{2} \times 0.49383 \times 0.19609 \times 0.08808) = 27.6669 \text{ kN}$$

Deflection at the top

The deflection at the top of the structure is

$$\delta = \frac{2 \times 1 \times 6^3 \times 180^4 \times 0.1 \times 1000}{22.24 \times 10^6 \times (244.8)^2} \left\{ 0.70833 + \tfrac{1}{9}(2.1377 + 1.4110) 0.014758 \right\}$$

$$+ \frac{2 \times 1 \times 6^5 \times 180^2 \times 0.1 \times 1000}{0.044813 \times 22.24 \times 10^6 \times (244.8)^2} \left\{ 10.7167 + \right.$$

$$\tfrac{4}{45} \cdot (0.21164 - 36.740)\ 0.33975 +$$

$$\left.\frac{1}{135}(0.14632 + 36.4885)1.1678\right\} \text{ mm}$$

$$= 24.30 + 8.378$$

$$= 32.678 \text{ mm}$$

2.10 COMPARISON BETWEEN APPROXIMATE SOLUTION AND MORE ACCURATE ANALYSIS

Using the equivalent plane frame technique described in Chapter 1, Schwaighofer and Ast[9] carried out a series of analyses on a range of framed-tube structures with different geometrical characteristics, and tabulated the results for the side frames only.

All structures considered were square in plan, with a constant storey height of 12 ft., thickness of columns and beams 1 ft., and with 12 columns in each frame. Three different heights, three different ratios of bay width to storey height, three different column width and three different spandrel beam depth were considered. The analyses refer to the lateral wind load specified by the National Building Code of Canada, which allows for a uniform suction on the leeward side, and a variable pressure on the windward side of the building.

The results obtained from the present simplified procedure are compared with the column axial forces given by Schwaighofer and Ast, for nine different representative 50-storey buildings, in Table 2.2. The present results are based on a uniform pressure loading which gives the same total moment at the section considered, at second storey level, 24 ft. above the base. Similar results have been obtained for the range of structures examined by

Schwaighofer and Ast.

It is seen that the maximum forces in the corner columns are generally predicted to a good degree of accuracy, although the errors are greater in the interior less highly stressed columns. In most cases, the values are conservative, and are sufficiently accurate for initial design studies.

Unfortunately, Schwaighofer and Ast did not tabulate the forces in the normal panels, and so it is not possible to compare results other than in the corner columns.

2.11 OPTIMISATION OF FRAMED-TUBE STRUCTURE

2.11.1 INTRODUCTION

Optimisation of a Framed-tube structure consists of proportioning the individual members of the structure to develop maximum strength and minimum lateral drift with minimum materials and cost. The level of optimisation depends on the number of design variables considered.

One such variable is the stiffness of the corner columns. The corner columns may be of the same stiffness as the other interior columns or, as is usually the case in practice, they may be considerably stiffer than the interior columns. The effect of variable corner column stiffness on the optimisation of the structure is investigated.

Another variable which is considered is the ratio of column width to spandrel beam depth. For the same total quantity of materials this ratio is varied and the effect on the distribution of stresses in the structure

and horizontal deflection at the top is investigated.

2.11.2 EFFECT OF VARIABLE CORNER COLUMN STIFFNESS

Due to the shear lag effect, corner columns are stressed more heavily than other columns in the normal panels of the structure. It may, therefore, seem logical to concentrate more of the total column areas at the corners and less in the interior of the structure. But the effect of this unequal distribution of column areas on the stress distribution in the interior columns and spandrel beams and also on the lateral drift should be investigated. The stress in any single column is the sum of the stresses due to the axial force and due to the bending moment caused by the shear force in that column. For a spandrel beam the axial force has been neglected and the only stress is that due to bending moment caused by the shear force.

In order to examine the effect of variable corner column stiffness, a typical concrete building of square section is considered, with constant storey height 12 ft. (3.66 m), total height 600 ft. (183 m), thickness of columns and beams 1 ft. (0.3 m), total area of columns 154.0 ft.^{2} (14.31 m^2), and with 12 columns in each frame. Three different ratios of bay width to storey height (β = 0.8, 1.0 and 1.2), three different spandrel beam depth (t_2 = 2.5 ft. (0.76 m), 3.5 ft. (1.07 m) and 4.5 ft. (1.37 m)) and six different corner column area ($\frac{A_c}{ct}$ = 0, 0.2, 0.4, 0.6, 1.0 and 2.0) are considered. The value of E for concrete is assumed to be 464,500 kips/ft^2

(22.24×10^6 kN/m^2). The structure is analysed for the same lateral wind load as in Article 2.10. The stresses in the columns and beams at the second floor level and the maximum deflection at the top of the building are determined.

The results of the analysis are shown in Figs.(2.16) to (2.24). The columns and beams are numbered from the corner to the centre of the side frame, as illustrated in Fig. 2.15. They indicate that the increase in the corner column areas has the beneficial effect of reducing the stresses in these columns. But it has the adverse effect of rapidly increasing the stresses in the interior columns of the side panels and the horizontal deflection at the top of the building. The stresses in the spandrel beams also increase gradually.

A large corner column area is, therefore, discouraged. An area of corner columns roughly twice those of interior columns appears to yield the optimum solution based on these limited criterion.

2.11.3 EFFECT OF VARIABLE RATIO OF COLUMN WIDTH TO SPANDREL BEAM DEPTH

The amount of shear lag encountered in framed-tube structures depends largely on the flexibility of the spandrel beams. With the columns remaining the same, any increase in the depth of the spandrel beams tends to reduce the shear lag effect. The horizontal deflection at the top of the structure is also reduced. It was, therefore, decided to examine the effect of a variable

ratio of column width to spandrel beam depth on the strength and lateral sway characteristics of the structure.

The same typical concrete high-rise building of square cross-sectional area is considered, with constant storey height 12 ft. (3.66 m), total height 600 ft. (183 m), thickness of columns and beams 1 ft. (0.3m), volume of the sub-system consisting of a column and a spandrel beam (Fig. 2.25) 65.0 ft.^{3} (1.84 m^3), and with 12 columns in each frame. Three different ratios of bay width to storey height (β = 0.8, 1.0 and 1.2), three different corner column areas ($\frac{A_c}{ct}$ = 0, 0.2 and 0.4) and seven different ratios of column width to spandrel beam depth ($\frac{t_1}{t_2}$ = 0.50, 0.75, 1.00, 1.25, 1.50, 1.75 and 2.00) are considered. The structure is subjected to the same wind load as described earlier in Article 2.10. The results of the analysis of the structure are shown in Figs. (2.26) to (2.34).

On examining the figures it appears that the optimum solution is obtained for a ratio of column width to spandrel beam depth ranging from 1.0 to 1.5. The ratio to produce optimum solution seems to increase with the decrease of β (ratio of bay width to storey height) and also with the decrease of corner column area.

2.12 MORE GENERAL ANALYSIS OF THE EQUIVALENT TUBE

In Article 2.4 the vertical stresses in the normal and side panels were given by equations (2.34) and (2.35), where the first term in each equation represented the basic beam theory stress. For the side panels the

perturbation on the linear basic beam theory stress distribution was a cubic term in coordinate x. It seems more appropriate that the perturbation consists of linear and cubic terms to represent more accurately the stress distribution in the side panels. To achieve this the vertical stresses in the two panels may be expressed in general terms as, (c.f. Fig. 2.35)

$$\sigma_z = f_1 + \left(\frac{y}{b}\right)^2 f_2 \qquad \ldots\ldots (2.75)$$

$$\sigma'_z = \left(\frac{x}{c}\right) f_3 + \left(\frac{x}{c}\right)^3 f_4 \qquad \ldots\ldots (2.76)$$

where f_1, f_2, f_3 and f_4 are functions of the coordinate z only.

The condition of vertical strain compatibility at the corner yields,

$$f_1 + f_2 = f_3 + f_4 \qquad \ldots\ldots (2.77)$$

The condition of moment equilibrium at any height was expressed by equation (2.32). On substituting equations (2.75), (2.76) and (2.77) into equation (2.32) and integrating, it is found that

$$f_1 = \frac{M}{I} c - \frac{a + 3n + 1}{3a + 3n + 1} f_2 + \frac{2}{5(3a + 3n + 1)} f_4 \qquad (2.78)$$

where $a = \frac{b}{c}$, $n = \frac{A_c}{ct}$ and

$$I = \frac{4}{3} tc^2(3b + c) + 4A_c c^2$$

From equation (2.77) it follows that

$$f_3 = \frac{M}{I} c + \frac{2a}{3a + 3n + 1} f_2 - \frac{3(5a + 5n + 1)}{5(3a + 3n + 1)} f_4 \qquad (2.79)$$

The vertical stresses σ_z and σ'_z may, therefore, be expressed in terms of two unknown functions f_2 and f_4 as,

$$\sigma_z = \frac{M}{I} c - \left[\frac{a + 3n + 1}{3a + 3n + 1} - \left(\frac{y}{b}\right)^2 \right] f_2 + \frac{2}{5(3a + 3n + 1)} f_4 \quad \ldots\ldots \quad (2.80)$$

$$\sigma'_z = \frac{M}{I} x + \frac{2a}{3a + 3n + 1} \left(\frac{x}{c}\right) f_2 - \left[\frac{3(5a + 5n + 1)}{5(3a + 3n + 1)} \left(\frac{x}{c}\right) - \left(\frac{x}{c}\right)^3 \right] f_4 \quad \ldots\ldots \quad (2.81)$$

The second and third terms in equations (2.80) and (2.81) represent the perturbations on the basic beam theory stress expressed by the first term.

The stress σ_c in the corner column then becomes,

$$\sigma_c = (\sigma_z)_{y=b} = \frac{M}{I} c + \frac{2a}{3a + 3n + 1} f_2 + \frac{2}{5(3a + 3n + 1)} f_4 \quad \ldots\ldots \quad (2.82)$$

The equilibrium conditions for the normal and side panels were given by equations (2.22) and (2.23) respectively. On substituting equations (2.80) and (2.81) into the equilibrium conditions, and integrating, the shear stress components τ_{yz} and τ_{xz} are found to be,

$$\tau_{yz} = -y \left\{ \frac{c}{I} \frac{dM}{dz} - \left[\frac{a + 3n + 1}{3a + 3n + 1} - \tfrac{1}{3}\left(\frac{y}{b}\right)^2 \right] \frac{df_2}{dz} + \frac{2}{5(3a + 3n + 1)} \frac{df_4}{dz} \right\} \quad \ldots\ldots \quad (2.83)$$

$$\tau_{xz} = \frac{c^2}{2I} \left[(2a + 2n + 1) - \left(\frac{x}{c}\right)^2 \right] \frac{dM}{dz} + \frac{ca}{3a + 3n + 1} \cdot \left[\tfrac{1}{3} - \left(\frac{x}{c}\right)^2 \right] \frac{df_2}{dz} - \frac{c}{20} \left[\frac{7a + 7n + 1}{3a + 3n + 1} - \frac{6(5a + 5n + 1)}{3a + 3n + 1} \cdot \left(\frac{x}{c}\right)^2 + 5\left(\frac{x}{c}\right)^4 \right] \frac{df_4}{dz}$$

The conditions for evaluating the integration constants are identifal to those of the simplified analysis of Article 2.4.

The total strain energy stored in the structure was given by equation (2.38). On substituting equations (2.80), (2.81), (2.82), and (2.83) into equation (2.38), the total strain energy U is expressed as,

$$U = t \int_0^H \left[\frac{1}{E} \int_{-b}^{b} \left\{ \frac{M}{I} c - \left[\frac{a+3n+1}{3a+3n+1} - \left(\frac{y}{b}\right)^2 \right] f_2 + \frac{2}{5(3a+3n+1)} f_4 \right\}^2 dy \right.$$

$$+ \frac{1}{G} \int_{-b}^{b} y^2 \left\{ \frac{c}{I} \frac{dM}{dz} - \left[\frac{a+3n+1}{3a+3n+1} - \tfrac{1}{3}\left(\frac{y}{b}\right)^2 \right] \frac{df_2}{dz} + \frac{2}{5(3a+3n+1)} \frac{df_4}{dz} \right\}^2 dy$$

$$+ \frac{1}{E} \int_{-c}^{c} \left\{ \frac{M}{I} x + \frac{2a}{3a+3n+1} \left(\frac{x}{c}\right) f_2 - \left[\frac{3(5a+5n+1)}{5(3a+3n+1)} \left(\frac{x}{c}\right) - \left(\frac{x}{c}\right)^3 \right] f_4 \right\}^2 dx$$

$$+ \frac{1}{G} \int_{-c}^{c} \left\{ \frac{c^2}{2I} \left[(2a+2n+1) - \left(\frac{x}{c}\right)^2 \right] \frac{dM}{dz} + \frac{ca}{3a+3n+1} \left[\tfrac{1}{3} - \left(\frac{x}{c}\right)^2 \right] \cdot \right.$$

$$\left. \frac{df_2}{dz} - \frac{c}{20} \left[\frac{7a+7n+1}{3a+3n+1} - \frac{6(5a+5n+1)}{3a+3n+1} \left(\frac{x}{c}\right)^2 + 5\left(\frac{x}{c}\right)^4 \right] \frac{df_4}{dz} \right\}^2 dx$$

$$\left. + \frac{2A_c}{tE} \left\{ \frac{M}{I} c + \frac{2a}{3a+3n+1} f_2 + \frac{2}{5(3a+3n+1)} f_4 \right\}^2 \right] dz$$

..... (2.84)

The variation of U, δU, vanishes giving,

$$\int_0^H \left[\frac{1}{E} \int_{-b}^{b} \left\{ \frac{M}{I} c - \left[\frac{a+3n+1}{3a+3n+1} - \left(\frac{y}{b}\right)^2 \right] f_2 + \frac{2}{5(3a+3n+1)} f_4 \right\} \cdot \right.$$

$$\left. \left\{ - \left[\frac{a+3n+1}{3a+3n+1} - \left(\frac{y}{b}\right)^2 \right] \delta f_2 + \frac{2}{5(3a+3n+1)} \delta f_4 \right\} dy \right.$$

$$+\frac{1}{G}\int_{-b}^{b} y^2\left\{\frac{c}{I}\frac{dM}{dz}-\left[\frac{a+3n+1}{3a+3n+1}-\tfrac{1}{3}\left(\frac{y}{b}\right)^2\right]\frac{df_2}{dz}+\frac{2}{5(3a+3n+1)}\frac{df_4}{dz}\right\}\cdot$$

$$\left\{-\left[\frac{a+3n+1}{3a+3n+1}-\tfrac{1}{3}\left(\frac{y}{b}\right)^2\right]\delta\left(\frac{df_2}{dz}\right)+\frac{2}{5(3a+3n+1)}\delta\left(\frac{df_4}{dz}\right)\right\}dy$$

$$+\frac{1}{E}\int_{-c}^{c}\left\{\frac{M}{I}x+\frac{2a}{3a+3n+1}\left(\frac{x}{c}\right)f_2-\left[\frac{3(5a+5n+1)}{5(3a+3n+1)}\left(\frac{x}{c}\right)-\left(\frac{x}{x}\right)^3\right]f_4\right\}\cdot$$

$$\left\{\frac{2a}{3a+3n+1}\left(\frac{x}{c}\right)\delta f_2-\left[\frac{3(5a+5n+1)}{5(3a+3n+1)}\left(\frac{x}{c}\right)-\left(\frac{x}{c}\right)^3\right]\delta f_4\right\}dx$$

$$+\frac{1}{G}\int_{-c}^{c}\left\{\frac{c^2}{2I}\left[(2a+2n+1)-\left(\frac{x}{c}\right)^2\right]\frac{dM}{dz}+\frac{ca}{3a+3n+1}\left[\tfrac{1}{3}-\left(\frac{x}{c}\right)^2\right]\frac{df_2}{dz}-\right.$$

$$\left.\frac{c}{20}\left[\frac{7a+7n+1}{3a+3n+1}-\frac{6(5a+5n+1)}{3a+3n+1}\left(\frac{x}{c}\right)^2+5\left(\frac{x}{c}\right)^4\right]\frac{df_4}{dz}\right\}\cdot$$

$$\left\{\frac{ca}{3a+3n+1}\left[\tfrac{1}{3}-\left(\frac{x}{c}\right)^2\right]\delta\left(\frac{df_2}{dz}\right)-\frac{c}{20}\left[\frac{7a+7n+1}{3a+3n+1}-\right.\right.$$

$$\left.\left.\frac{6(5a+5n+1)}{3a+3n+1}\left(\frac{x}{c}\right)^2+5\left(\frac{x}{c}\right)^4\right]\delta\left(\frac{df_4}{dz}\right)\right\}dx$$

$$+\frac{2A_c}{tE}\left\{\frac{M}{I}c+\frac{2a}{3a+3n+1}f_2+\frac{2}{5(3a+3n+1)}f_4\right\}\cdot$$

$$\left.\left\{\frac{2a}{3a+3n+1}\delta f_2+\frac{2}{5(3a+3n+1)}\delta f_4\right\}\right]dz=0$$

According to the theory of variations

$$\delta(df_2)=d(\delta f_2);\quad \delta(df_4)=d(\delta f_4)$$

Integrating and rearranging the above equation yields,

$$\int_0^H\left[-\frac{1}{G}\frac{10}{21}c^3a^2(6a^3+54a^2n+153an^2+18a^2+102an+17a+7)\frac{d^2f_2}{dz^2}\right.$$

$$\left.+\frac{1}{E}\cdot 10ca(3a^2+18n^2+21an+7a+12n+2)f_2\right.$$

$$+ \frac{1}{G} \frac{2c^3}{7} a(7a^3 + 42a^2n + 14a^2 + 10a + 10n + 1) \frac{d^2f_4}{dz^2}$$

$$- \frac{1}{E} 10ca(3a + 3n + 1)f_4$$

$$+ \frac{1}{G} \frac{5c^4}{3I} a(3a + 3n + 1)(3a^3+18a^2n+6a^2-1) \frac{d^2M}{dz^2} \Bigg] dz \ \delta f_2$$

$$+ \int_0^H \Bigg[\frac{1}{G} \frac{2c^3}{7} a(7a^3 + 42a^2n + 14a^2 + 10a + 10n + 1) \frac{d^2f_2}{dz^2}$$

$$- \frac{1}{E} 10ca(3a + 3n + 1) f_2$$

$$- \frac{1}{G} \frac{2c^3}{105} (105a^3+135a^2+135n^2+270an+30a+30n+2) \frac{d^2f_4}{dz^2}$$

$$+ \frac{1}{E} \frac{6c}{7} (30a^2 + 30n^2 + 60an + 13a + 13n + 1)\tilde{f}_4$$

$$- \frac{1}{G} \frac{c^4}{7I}(3a + 3n + 1)(35a^3-10a-10n-1) \frac{d^2M}{dz^2} \Bigg] dz \ \delta f_4$$

$$+ \frac{1}{G} \Bigg[\Bigg\{ \frac{10}{21} c^3a^2(6a^3+54a^2n+153an^2+18a^2+102an+17a+7) \frac{df_2}{dz}$$

$$- \frac{2c^3}{7} a(7a^3 + 42a^2n + 14a^2 + 10a + 10n + 1) \frac{df_4}{dz}$$

$$- \frac{5c^4}{3I} a(3a + 3n + 1)(3a^3 + 18a^2n + 6a^2 - 1)\frac{dM}{dz} \Bigg\} \delta f_2 \Bigg]_0^H$$

$$+ \frac{1}{G} \Bigg[\Bigg\{ - \frac{2c^3}{7} a(7a^3+42a^2n+14a^2+10a+10n+1) \frac{df_2}{dz}$$

$$+ \frac{2c^3}{105} (105a^3+135a^2+135n^2+270an+30a+30n+2) \frac{df_4}{dz}$$

$$+ \frac{c^4}{7I} (3a + 3n + 1)(35a^3 - 10a - 10n - 1) \frac{dM}{dz} \Bigg\} \delta f_4 \Bigg]_0^H = 0$$

..... (2.85)

The structure is free at the top and the vertical stresses σ_z and σ'_z are, therefore, zero at $z = 0$. It follows from equations (2.80) and (2.81) that

$$\text{At } z = 0, \quad f_2 = 0 \qquad \ldots\ldots \quad (2.86)$$

$$\text{Hence} \quad \delta f_2 = 0$$

$$\text{At } z = 0, \quad f_4 = 0 \qquad \ldots\ldots \quad (2.87)$$

$$\text{Hence} \quad \delta f_4 = 0$$

Since f_2 and f_4 are arbitrary throughout the height, including the base, the integrands of the first and second term of equation (2.85) have to vanish separately. The third and fourth term of the same equation must also vanish. This will give the differential equations for the functions f_2 and f_4 as,

$$\frac{d^2 f_2}{dz^2} - \left(\frac{k_1}{H}\right)^2 f_2 - \alpha_1^2 \frac{d^2 f_4}{dz^2} + \left(\frac{\beta_1}{H}\right)^2 f_4 = \lambda_1^2 \frac{d^2 \sigma_b}{dz^2} \qquad (2.88)$$

$$\frac{d^2 f_2}{dz^2} - \left(\frac{k_2}{H}\right)^2 f_2 - \alpha_2^2 \frac{d^2 f_4}{dz^2} + \left(\frac{\beta_2}{H}\right)^2 f_4 = \lambda_2^2 \frac{d^2 \sigma_b}{dz^2} \qquad (2.89)$$

where the parameters k_1, α_1, β_1, λ_1, k_2, α_2, β_2 and λ_2 are defined as

$$k_1^2 = 21 \frac{G}{E}\left(\frac{H}{b}\right)^2 \frac{a(3a + 3n + 1)(a + 6n + 2)}{6a^3+54a^2n+153an^2+18a^2+102an+17a+7}$$

$$\alpha_1^2 = \frac{3}{5} \frac{7a^3 + 42a^2n + 14a^2 + 10a + 10n + 1}{a(6a^3 + 54a^2n + 153an^2 + 18a^2 + 102an + 17a + 7)}$$

$$\beta_1^2 = 21 \frac{G}{E}\left(\frac{H}{b}\right)^2 \frac{a(3a + 3n + 1)}{6a^3+54a^2n+153an^2+18a^2+102an+17a+7}$$

$$\lambda_1^2 = \frac{7}{2} \frac{(3a + 3n + 1)(3a^3 + 18a^2n + 6a^2 - 1)}{a(6a^3+54a^2n+153an^2+18a^2+102an+17a+7)}$$

$$k_2^2 = 35 \frac{G}{E}\left(\frac{H}{b}\right)^2 \frac{a^2(3a + 3n + 1)}{7a^3 + 42a^2n + 14a^2 + 10a + 10n + 1}$$

$$\alpha_2^2 = \frac{1}{15} \frac{105a^3 + 135a^2 + 135n^2 + 270an + 30a + 30n + 2}{a(7a^3 + 42a^2n + 14a^2 + 10a + 10n + 1)}$$

$$\beta_2^2 = 3 \frac{G}{E}\left(\frac{H}{b}\right)^2 \frac{a(3a + 3n + 1)(10a + 10n + 1)}{7a^3 + 42a^2n + 14a^2 + 10a + 10n + 1}$$

$$\lambda_2^2 = \frac{1}{2} \frac{(3a + 3n + 1)(35a^3 - 10a - 10n - 1)}{a(7a^3 + 42a^2n + 14a^2 + 10a + 10n + 1)}$$

The boundary conditions for f_2 and f_4 may then be expressed as

At $z = 0$, $f_2 = 0$ (equation 2.86)

At $z = 0$, $f_4 = 0$ (equation 2.87)

$$\text{At } z = H, \quad \frac{df_2}{dz} - \alpha_1^2 \frac{df_4}{dz} - \lambda_1^2 \frac{d\sigma_b}{dz} = 0 \qquad (2.90)$$

$$\text{At } z = H, \quad \frac{df_2}{dz} - \alpha_2^2 \frac{df_4}{dz} - \lambda_2^2 \frac{d\sigma_b}{dz} = 0 \qquad (2.91)$$

Using the operator D, the homogeneous equations corresponding to equations (2.88) and (2.89) may be written as

$$(D^2 - \frac{k_1^2}{H^2})f_2 - (\alpha_1^2 D^2 - \frac{\beta_1^2}{H^2})f_4 = 0 \qquad (2.92)$$

$$(D^2 - \frac{k_2^2}{H^2})f_2 - (\alpha_2^2 D^2 - \frac{\beta_2^2}{H^2})f_4 = 0 \qquad (2.93)$$

In order to satisfy the differential equation (2.92) the variables f_2 and f_4 may be expressed in terms of a new variable w as

$$f_2 = (\alpha_1^2 D^2 - \frac{\beta_1^2}{H^2})w \qquad \ldots\ldots (2.94)$$

$$f_4 = (D^2 - \frac{k_1^2}{H^2})w \qquad \ldots\ldots (2.95)$$

where w is a function of the coordinate z only.

On substituting equations (2.94) and (2.95) into equation (2.93) it is found that,

$$\left\{(\alpha_1^2 - \alpha_2^2)D^4 - \frac{1}{H^2}(\alpha_1^2 k_2^2 - \alpha_2^2 k_1^2 + \beta_1^2 - \beta_2^2)D^2 + \frac{1}{H^4}(\beta_1^2 k_2^2 - \beta_2^2 k_1^2)\right\} w = 0 \qquad \ldots\ldots (2.96)$$

The characteristic equation for the differential equation (2.96) is,

$$(\alpha_1^2 - \alpha_2^2)m_o^4 - \frac{1}{H^2}(\alpha_1^2 k_2^2 - \alpha_2^2 k_1^2 + \beta_1^2 - \beta_2^2)m_o^2 + \frac{1}{H^4} \cdot (\beta_1^2 k_2^2 - \beta_2^2 k_1^2) = 0$$

The above equation may be solved to give,

$$m_o^2 = \frac{1}{2H^2(\alpha_1^2 - \alpha_2^2)} \left\{ (\alpha_1^2 k_2^2 - \alpha_2^2 k_1^2 + \beta_1^2 - \beta_2^2) \pm \sqrt{(\alpha_1^2 k_2^2 - \alpha_2^2 k_1^2 + \beta_1^2 - \beta_2^2)^2 - 4(\alpha_1^2 - \alpha_2^2)(\beta_1^2 k_2^2 - \beta_2^2 k_1^2)} \right\}$$

$\ldots\ldots$ (2.97)

For practical structures, the value of aspect ratio $m (= \frac{b}{c})$ should range from 0.5 to 2 and n $(= \frac{A_c}{ct})$ from 0 to 2. The values of m_o^2, as given by equation (2.97), are positive for all values of m and n within the above range.

The constant m_o has four values which may be expressed as $\pm m_1$ and $\pm m_2$. The solution of equation

(2.96) then becomes

$$w = A_1 \cosh m_1 z + A_2 \sinh m_1 z + A_3 \cosh m_2 z + A_4 \sinh m_2 z \qquad \ldots\ldots \text{(2.98)}$$

On substituting equation (2.98) into equations (2.94) and (2.95), f_2 and f_4 are found as

$$f_2 = (\alpha_1^2 m_1^2 - \frac{\beta_1^2}{H^2})(A_1 \cosh m_1 z + A_2 \sinh m_1 z) +$$

$$(\alpha_1^2 m_2^2 - \frac{\beta_1^2}{H^2})(A_3 \cosh m_2 z + A_4 \sinh m_2 z) \qquad \text{(2.99)}$$

$$f_4 = (m_1^2 - \frac{k_1^2}{H^2})(A_1 \cosh m_1 z + A_2 \sinh m_1 z) +$$

$$(m_2^2 - \frac{k_1^2}{H^2})(A_3 \cosh m_2 z + A_4 \sinh m_2 z) \qquad \text{(2.100)}$$

The particular integral part of the solution will depend on the stress σ_b, which in turn depends on the form of applied loading.

<u>Uniformly distributed load p throughout the height</u>

In this case,

$$\sigma_b = \frac{pc}{2I} z^2 , \quad \frac{d^2 \sigma_b}{dz^2} = \frac{pc}{I}$$

Let the particular integrals for the differential equations (2.88) and (2.89) be given by

$$f_2 = A_5 ; \quad f_4 = A_6$$

Substituting the values of f_2 and f_4 into equations (2.88) and (2.89) yields

$$- \frac{k_1^2}{H^2} A_5 + \frac{\beta_1^2}{H^2} A_6 = \lambda_1^2 \frac{pc}{I}$$

$$-\frac{k_2^2}{H^2} A_5 + \frac{\beta_2^2}{H^2} A_6 = \lambda_2^2 \frac{pc}{I}$$

The particular integrals A_5 and A_6 are, therefore, evaluated as

$$A_5 = \frac{\lambda_1^2 \beta_2^2 - \lambda_2^2 \beta_1^2}{\beta_1^2 k_2^2 - \beta_2^2 k_1^2} \frac{pc}{I} H^2$$

$$A_6 = \frac{\lambda_1^2 k_2^2 - \lambda_2^2 k_1^2}{\beta_1^2 k_2^2 - \beta_2^2 k_1^2} \frac{pc}{I} H^2$$

The constants A_1, A_2, A_3 and A_4 are determined from the boundary conditions (2.86), (2.87), (2.90) and (2.91) and are expressed as

$$A_1 = \frac{-pcH^2}{I(m_1^2-m_2^2)(\alpha_1^2 k_1^2-\beta_1^2)} \left\{ \frac{\lambda_1^2(\alpha_1^2 k_2^2-\beta_2^2) - \lambda_2^2(\alpha_1^2 k_1^2 - \beta_1^2)}{m_1^2 H^2 (\alpha_1^2 - \alpha_2^2)} - \lambda_1^2 \right\}$$

$$A_2 = \frac{pcH^2(\sinh m_1 H - m_1 H)}{I(m_1^2 - m_2^2)(\alpha_1^2 k_1^2 - \beta_1^2) \cosh m_1 H} \cdot$$

$$\left\{ \frac{\lambda_1^2(\alpha_1^2 k_2^2 - \beta_2^2) - \lambda_2^2(\alpha_1^2 k_1^2 - \beta_1^2)}{m_1^2 H^2(\alpha_1^2 - \alpha_2^2)} - \lambda_1^2 \right\}$$

$$A_3 = \frac{pcH^2}{I(m_1^2 - m_2^2)(\alpha_1^2 k_1^2 - \beta_1^2)} \cdot$$

$$\left\{ \frac{\lambda_1^2(\alpha_1^2 k_2^2 - \beta_2^2) - \lambda_2^2(\alpha_1^2 k_1^2 - \beta_1^2)}{m_2^2 H^2(\alpha_1^2 - \alpha_2^2)} - \lambda_1^2 \right\}$$

$$A_4 = \frac{-pcH^2(\sinh m_2 H - m_2 H)}{I(m_1^2-m_2^2)(\alpha_1^2 k_1^2 - \beta_1^2) \cosh m_2 H} \cdot$$

$$\left\{ \frac{\lambda_1^2(\alpha_1^2 k_2^2 - \beta_2^2) - \lambda_2^2(\alpha_1^2 k_1^2 - \beta_1^2)}{m_2^2 H^2(\alpha_1^2 - \alpha_2^2)} - \lambda_1^2 \right\}$$

The complete solution then becomes,

$$f_2 = 2\sigma_b(H)\left\{ - \frac{(\alpha_1^2 m_1^2 H^2 - \beta_1^2)}{H^2(m_1^2 - m_2^2)(\alpha_1^2 k_1^2 - \beta_1^2)} \cdot \right.$$

$$\left[\frac{\lambda_1^2(\alpha_1^2 k_2^2 - \beta_2^2) - \lambda_2^2(\alpha_1^2 k_1^2 - \beta_1^2)}{m_1^2 H^2(\alpha_1^2 - \alpha_2^2)} - \lambda_1^2 \right] \cdot$$

$$\left[\frac{\cosh m_1 H(1 - \xi) + m_1 H \sinh m_1 H\xi}{\cosh m_1 H} \right]$$

$$+ \frac{(\alpha_1^2 m_2^2 H^2 - \beta_1^2)}{H^2(m_1^2 - m_2^2)(\alpha_1^2 k_1^2 - \beta_1^2)} \cdot$$

$$\left[\frac{\lambda_1^2(\alpha_1^2 k_2^2 - \beta_2^2) - \lambda_2^2(\alpha_1^2 k_1^2 - \beta_1^2)}{m_2^2 H^2(\alpha_1^2 - \alpha_2^2)} - \lambda_1^2 \right] \cdot$$

$$\left[\frac{\cosh m_2 H(1 - \xi) + m_2 H \sinh m_2 H\xi}{\cosh m_2 H} \right]$$

$$\left. + \frac{\lambda_1^2 \beta_2^2 - \lambda_2^2 \beta_1^2}{\beta_1^2 k_2^2 - \beta_2^2 k_1^2} \right\} \qquad \ldots\ldots (2.101)$$

$$f_4 = 2\sigma_b(H)\left\{ - \frac{(m_1^2 H^2 - k_1^2)}{H^2(m_1^2 - m_2^2)(\alpha_1^2 k_1^2 - \beta_1^2)} \cdot \right.$$

$$\left[\frac{\lambda_1^2(\alpha_1^2 k_2^2 - \beta_2^2) - \lambda_2^2(\alpha_1^2 k_1^2 - \beta_1^2)}{m_1^2 H^2(\alpha_1^2 - \alpha_2^2)} - \lambda_1^2 \right] \cdot$$

$$\left[\frac{\cosh m_1 H(1 - \xi) + m_1 H \sinh m_1 H\xi}{\cosh m_1 H} \right]$$

$$+ \frac{(m_2^2H^2 - k_1^2)}{H^2(m_1^2 - m_2^2)(\alpha_1^2 k_1^2 - \beta_1^2)} \cdot$$

$$\left[\frac{\lambda_1^2(\alpha_1^2 k_2^2 - \beta_2^2) - \lambda_2^2(\alpha_1^2 k_1^2 - \beta_1^2)}{m_2^2 H^2(\alpha_1^2 - \alpha_2^2)} - \lambda_1^2 \right] \cdot$$

$$\left[\frac{\cosh m_2 H(1 - \xi) + m_2 H \sinh m_2 H \xi}{\cosh m_2 H} \right]$$

$$+ \left. \frac{\lambda_1^2 k_2^2 - \lambda_2^2 k_1^2}{\beta_1^2 k_2^2 - \beta_2^2 k_1^2} \right\} \qquad \ldots\ldots (2.102)$$

Concentrated Load P at the top

In this case,

$$M = Pz ,$$

$$\sigma_b = \frac{Pc}{I} z ,$$

$$\frac{d\sigma_b}{dz} = \frac{Pc}{I} , \quad \frac{d^2\sigma_b}{dz^2} = 0$$

The equations (2.88) and (2.89) become homogeneous and the solutions of the equations were given by (2.99) and (2.100). The constants of integration A_1, A_2, A_3 and A_4 are determined to satisfy the boundary conditions (2.86), (2.87), (2.90) and (2.91). They are

$$A_1 = A_3 = 0$$

$$A_2 = \frac{\frac{P_c}{I}}{(\alpha_1^2 - \alpha_2^2)(m_1^2 - m_2^2)\, m_1 \cosh m_1 H}$$

$$\left[\lambda_2^2 - \frac{\lambda_1^2}{\alpha_1^2 k_1^2 - \beta_1^2} \left\{ (\alpha_1^2 - \alpha_2^2) m_2^2 H^2 + (\alpha_2^2 k_1^2 - \beta_1^2) \right\} \right]$$

$$A_4 = \frac{-\frac{Pc}{I}}{(\alpha_1^2 - \alpha_2^2)(m_1^2 - m_2^2)m_2 \cosh m_2 H} \cdot$$

$$\left[\lambda_2^2 - \frac{\lambda_1^2}{\alpha_1^2 k_1^2 - \beta_1^2}\left\{(\alpha_1^2 - \alpha_2^2)m_1^2 H^2 + (\alpha_2^2 k_1^2 - \beta_1^2)\right\}\right]$$

On substituting the value of the constants into the equations (2.99) and (2.100) the variables f_2 and f_4 are expressed as

$$f_2 = \frac{\sigma_b(H)}{(\alpha_1^2 - \alpha_2^2)(m_1^2 - m_2^2)H^2}\left\{\left[\lambda_2^2 - \frac{\lambda_1^2}{\alpha_1^2 k_1^2 - \beta_1^2} \cdot \left\{(\alpha_1^2 - \alpha_2^2)m_2^2 H^2 + (\alpha_2^2 k_1^2 - \beta_1^2)\right\}\right] \cdot \frac{(\alpha_1^2 m_1^2 H^2 - \beta_1^2) \sinh m_1 H\xi}{m_1 H \cosh m_1 H}\right.$$

$$\left. - \left[\lambda_2^2 - \frac{\lambda_1^2}{\alpha_1^2 k_1^2 - \beta_1^2}\left\{(\alpha_1^2 - \alpha_2^2)m_1^2 H^2 + (\alpha_2^2 k_1^2 - \beta_1^2)\right\}\right] \cdot \frac{(\alpha_1^2 m_2^2 H^2 - \beta_1^2) \sinh m_2 H\xi}{m_2 H \cosh m_2 H}\right\} \quad \ldots\ldots (2.103)$$

$$f_4 = \frac{\sigma_b(H)}{(\alpha_1^2 - \alpha_2^2)(m_1^2 - m_2^2)H^2}\left\{\left[\lambda_2^2 - \frac{\lambda_1^2}{\alpha_1^2 k_1^2 - \beta_1^2} \cdot \left\{(\alpha_1^2 - \alpha_2^2)m_2^2 H^2 + (\alpha_2^2 k_1^2 - \beta_1^2)\right\}\right] \cdot \frac{(m_1^2 H^2 - k_1^2) \sinh m_1 H\xi}{m_1 H \cosh m_1 H}\right.$$

$$- \left[\lambda_2^2 - \frac{\lambda_1^2}{\alpha_1^2 k_1^2 - \beta_1^2} \left\{ (\alpha_1^2 - \alpha_2^2) m_1^2 H^2 + (\alpha_2^2 k_1^2 - \beta_1^2) \right\} \right] \cdot$$

$$\left. \frac{(m_2^2 H^2 - k_1^2) \sinh m_2 H \xi}{m_2 H \cosh m_2 H} \right\} \qquad \ldots\ldots (2.104)$$

Triangularly distributed load

For triangularly distributed load which varies linearly from 0 at $z = H$ to p at $z = 0$,

$$M = \frac{p}{2} \left(z^2 - \frac{z^3}{3H} \right) ,$$

$$\sigma_b = \frac{pc}{2I} \left(z^2 - \frac{z^3}{3H} \right) ,$$

$$\frac{d\sigma_b}{dz} = \frac{pc}{2I} \left(2z - \frac{z^2}{H} \right) , \quad \frac{d^2\sigma_b}{dz^2} = \frac{pc}{I} \left(1 - \frac{z}{H} \right)$$

The particular integrals of the equations (2.88) and (2.89) are evaluated as

$$f_2 = - \frac{pcH^2}{I} \frac{\beta_1^2 \lambda_2^2 - \beta_2^2 \lambda_1^2}{\beta_1^2 k_2^2 - \beta_2^2 k_1^2} \left(1 - \frac{z}{H} \right)$$

$$f_4 = - \frac{pcH^2}{I} \frac{\lambda_2^2 k_1^2 - \lambda_1^2 k_2^2}{\beta_1^2 k_2^2 - \beta_2^2 k_1^2} \left(1 - \frac{z}{H} \right)$$

The complete solutions of the equations (2.88) and (2.89) are

$$f_2 = \left(\alpha_1^2 m_1^2 - \frac{\beta_1^2}{H^2} \right) (A_1 \cosh m_1 z + A_2 \sinh m_1 z)$$

$$+ \left(\alpha_1^2 m_2^2 - \frac{\beta_1^2}{H^2} \right) (A_3 \cosh m_2 z + A_4 \sinh m_2 z)$$

$$- \frac{\beta_1^2 \lambda_2^2 - \beta_2^2 \lambda_1^2}{\beta_1^2 k_2^2 - \beta_2^2 k_1^2} \frac{pcH^2}{I}(1 - \frac{z}{H}) \quad \ldots\ldots\ldots \quad (2.105)$$

$$f_4 = (m_1^2 - \frac{k_1^2}{H^2})(A_1 \cosh m_1 z + A_2 \sinh m_1 z)$$

$$+ (m_2^2 - \frac{k_1^2}{H^2})(A_3 \cosh m_2 z + A_4 \sinh m_2 z)$$

$$- \frac{\lambda_2^2 k_1^2 - \lambda_1^2 k_2^2}{\beta_1^2 k_2^2 - \beta_2^2 k_1^2} \frac{pcH^2}{I}(1 - \frac{z}{H}) \quad \ldots\ldots\ldots \quad (2.106)$$

The constants of integration A_1, A_2, A_3 and A_4 are determined from the boundary conditions (2.86), (2.87), (2.90) and (2.91) as

$$A_1 = \frac{-pcH^2}{I(\alpha_1^2 k_1^2 - \beta_1^2)(m_1^2 - m_2^2)} \cdot$$

$$\left[\frac{\lambda_1^2(\alpha_1^2 k_2^2 - \beta_2^2) - \lambda_2^2(\alpha_1^2 k_1^2 - \beta_1^2)}{(\alpha_1^2 - \alpha_2^2) m_1^2 H^2} - \lambda_1^2 \right]$$

$$A_2 = \frac{pcH}{2I(\alpha_1^2 k_1^2 - \beta_1^2)(\alpha_1^2 - \alpha_2^2)(m_1^2 - m_2^2) m_1 \cosh m_1 H} \cdot$$

$$\left\{ 2(\alpha_1^2 - \alpha_2^2) m_1 H \sinh m_1 H \cdot \right.$$

$$\left[\frac{\lambda_1^2(\alpha_1^2 k_2^2 - \beta_2^2) - \lambda_2^2(\alpha_1^2 k_1^2 - \beta_1^2)}{(\alpha_1^2 - \alpha_2^2) m_1^2 H^2} - \lambda_1^2 \right]$$

$$+ \left[\frac{\lambda_1^2(2\alpha_1^2 k_2^2 - 2\beta_2^2 - \beta_1^2 k_2^2 + \beta_2^2 k_1^2) - 2\lambda_2^2(\alpha_1^2 k_1^2 - \beta_1^2)}{m_1^2 H^2} \right.$$

$$\left. \left. - \lambda_1^2(\alpha_2^2 k_1^2 - \beta_1^2 + 2\alpha_1^2 - 2\alpha_2^2) + \lambda_2^2(\alpha_1^2 k_1^2 - \beta_1^2) \right] \right\}$$

$$A_3 = \frac{pcH^2}{I(\alpha_1^2 k_1^2 - \beta_1^2)(m_1^2 - m_2^2)} \cdot$$

$$\left[\frac{\lambda_1^2(\alpha_1^2 k_2^2 - \beta_2^2) - \lambda_2^2(\alpha_1^2 k_1^2 - \beta_1^2)}{(\alpha_1^2 - \alpha_2^2) m_2^2 H^2} - \lambda_1^2 \right]$$

$$A_4 = \frac{- pcH}{2I(\alpha_1^2 k_1^2 - \beta_1^2)(\alpha_1^2 - \alpha_2^2)(m_1^2 - m_2^2) m_2 \cosh m_2 H} \cdot$$

$$\left\{ 2(\alpha_1^2 - \alpha_2^2)\, m_2 H \sinh m_2 H \cdot \right.$$

$$\left[\frac{\lambda_1^2(\alpha_1^2 k_2^2 - \beta_2^2) - \lambda_2^2(\alpha_1^2 k_1^2 - \beta_1^2)}{(\alpha_1^2 - \alpha_2^2) m_2^2 H^2} - \lambda_1^2 \right]$$

$$+ \left[\frac{\lambda_1^2(2\alpha_1^2 k_2^2 - 2\beta_2^2 - \beta_1^2 k_2^2 + \beta_2^2 k_1^2) - 2\lambda_2^2(\alpha_1^2 k_1^2 - \beta_1^2)}{m_2^2 H^2} \right.$$

$$\left. \left. - \lambda_1^2(\alpha_2^2 k_1^2 - \beta_1^2 + 2\alpha_1^2 - 2\alpha_2^2) + \lambda_2^2(\alpha_1^2 k_1^2 - \beta_1^2) \right] \right\}$$

The values of the constants A_1, A_2, A_3 and A_4 may be substituted in the equations (2.105) and (2.106) to determine the variables f_2 and f_4.

2.13 NUMERICAL EXAMPLE

The problem considered earlier in Article 2.9 is solved here applying the general analysis of Article 2.12.

$$a = \frac{b}{c} = 2$$

$$n = \frac{A_c}{ct} = 0.5$$

$$k_1^2 = 21 \frac{G}{E}\left(\frac{H}{b}\right)^2 \quad \frac{2 \times 8.5 \times 7}{447.5} = 5.584358 \frac{G}{E} \frac{H^2}{b^2}$$

$$\alpha_1^2 = \frac{3}{5} \quad \frac{222}{2 \times 447.5} = 0.148827$$

$$\beta_1^2 = 21 \times \frac{G}{E} \left(\frac{H}{b}\right)^2 \quad \frac{2 \times 8.5}{447.5} = 0.797765 \frac{G}{E} \frac{H^2}{b^2}$$

$$\lambda_1^2 = \frac{7}{2} \quad \frac{8.5 \times 83}{2 \times 447.5} = 2.758939$$

$$k_2^2 = 35 \frac{G}{E}\left(\frac{H}{b}\right)^2 \quad \frac{4 \times 8.5}{222} = 5.360360 \frac{G}{E} \frac{H^2}{b^2}$$

$$\alpha_2^2 = \frac{1}{15} \quad \frac{1760.75}{2 \times 222} = 0.264377$$

$$\beta_2^2 = 3 \frac{G}{E}\left(\frac{H}{b}\right)^2 \quad \frac{2 \times 8.5 \times 26}{222} = 5.972973 \frac{G}{E} \frac{H^2}{b^2}$$

$$\lambda_2^2 = \frac{1}{2} \frac{8.5 \times 254}{2 \times 222} = 2.431306$$

$$m_o^2 = \frac{1}{-2H^2 \times 0.11555} \frac{G}{E} \frac{H^2}{b^2} \left\{ -5.853818 \pm \sqrt{34.267180 - 13.440272} \right\}$$

$$= 45.077754 \quad \frac{G}{E} \frac{1}{b^2} \quad \text{or} \quad 5.582722 \quad \frac{G}{E} \quad \frac{1}{b^2}$$

$$\therefore m_o = \pm 6.713997 \sqrt{\frac{G}{E}} \frac{1}{b} \quad \text{or} \quad \pm 2.362778 \sqrt{\frac{G}{E}} \frac{1}{b}$$

$$\alpha_1^2 m_1^2 H^2 - \beta_1^2 = 5.911022 \quad \frac{G}{E} \frac{H^2}{b^2}$$

$$\alpha_1^2 m_2^2 H^2 - \beta_1^2 = 0.0330947 \frac{G}{E} \frac{H^2}{b^2}$$

$$(m_1^2 - m_2^2)H^2 = 39.495032 \quad \frac{G}{E} \frac{H^2}{b^2}$$

$$\alpha_1^2 k_1^2 - \beta_1^2 = 0.0333382 \frac{G}{E} \frac{H^2}{b^2}$$

$$m_1^2 H^2 - k_1^2 = 39.493396 \quad \frac{G}{E} \frac{H^2}{b^2}$$

$$m_2^2 H^2 - k_1^2 = - 0.001636 \frac{G}{E} \frac{H^2}{b^2}$$

$$\beta_1^2 k_2^2 - \beta_2^2 k_1^2 = - 29.078912 \frac{G^2}{E^2} \frac{H^4}{b^4}$$

$$\lambda_1^2 \beta_2^2 - \lambda_2^2 \beta_1^2 = 14.539458 \frac{G}{E} \frac{H^2}{b^2}$$

$$\lambda_1^2 k_2^2 - \lambda_2^2 k_1^2 = 1.211623 \frac{G}{E} \frac{H^2}{b^2}$$

$$\frac{\lambda_1^2(\alpha_1^2 k_2^2 - \beta_2^2) - \lambda_2^2(\alpha_1^2 k_1^2 - \beta_1^2)}{m_1^2 H^2(\alpha_1^2 - \alpha_2^2)} - \lambda_1^2 = - 0.002197$$

$$\frac{\lambda_1^2(\alpha_1^2 k_2^2 - \beta_2^2) - \lambda_2^2(\alpha_1^2 k_1^2 - \beta_1^2)}{m_2^2 H^2(\alpha_1^2 - \alpha_2^2)} - \lambda_1^2 = 19.500385$$

The variables f_2 and f_4 are evaluated from equations (2.101) and (2.102) as

$$f_2 = 2 \sigma_b(H) \frac{E}{G} \frac{b^2}{H^2} \left\{ \frac{5.911022 \times 0.002197}{39.495032 \times 0.0333382} \cdot \right.$$

$$\left[\frac{\cosh m_1 H(1 - \xi) + m_1 H \sinh m_1 H \xi}{\cosh m_1 H} \right]$$

$$+ \frac{0.0330947 \times 19.500385}{39.495032 \times 0.0333382} \left[\frac{\cosh m_2 H(1 - \xi) + m_2 H \sinh m_2 H \xi}{\cosh m_2 H} \right]$$

$$\left. - \frac{14.539458}{29.078912} \right\}$$

$$= \frac{E}{G} \frac{b^2}{H^2} \sigma_b(H) \left\{ 0.019726 \left[\frac{\cosh m_1 H(1 - \xi) + m_1 H \sinh m_1 H \xi}{\cosh m_1 H} \right] \right.$$

$$\left. + 0.9803 \left[\frac{\cosh m_2 H(1 - \xi) + m_2 H \sinh m_2 H \xi}{\cosh m_2 H} \right] - 1.0 \right\}$$

$$f_4 = 2 \sigma_b(H) \frac{E}{G} \frac{b^2}{H^2} \left\{ \frac{39.493396 \times 0.002197}{39.495032 \times 0.0333382} \cdot \right.$$

$$\left[\frac{\cosh m_1H(1-\xi) + m_1H \sinh m_1H\xi}{\cosh m_1H} \right]$$

$$- \frac{0.001636 \times 19.500385}{39.495032 \times 0.0333382} \cdot$$

$$\left[\frac{\cosh m_2H(1-\xi) + m_2H \sinh m_2H\xi}{\cosh m_2H} \right] - \frac{1.211623}{29.078912} \Bigg\}$$

$$= \frac{E}{G} \frac{b^2}{H^2} \sigma_b(H) \Bigg\{ 0.13180 \left[\frac{\cosh m_1H(1-\xi) + m_1H \sinh m_1H\xi}{\cosh m_1H} \right]$$

$$-0.04846 \left[\frac{\cosh m_2H(1-\xi) + m_2H \sinh m_2H\xi}{\cosh m_2H} \right] -0.08333 \Bigg\}$$

$$\frac{G}{E} = 0.044813$$

$$\sqrt{\frac{G}{E}} = 0.2117$$

$$m_1H = 6.713997 \times 0.2117 \times \frac{180}{12} = 21.32$$

$$m_2H = 2.362778 \times 0.2117 \times \frac{180}{12} = 7.503$$

$$\cosh m_1H = 9.088 \times 10^8$$

$$\cosh m_2H = 906.75$$

The column axial forces are evaluated at the second floor level, where

$$\xi = 0.96$$

$$m_1H\xi = 20.47$$

$$m_1H(1-\xi) = 0.8528$$

$$\sinh m_1H\xi = 3.8853 \times 10^8$$

$$\cosh m_1H(1-\xi) = 1.3862$$

$$m_2H\xi = 7.203$$

$$m_2H(1-\xi) = 0.3001$$

$$\sinh m_2H\xi = 671.73$$

$$\cosh m_2H(1-\xi) = 1.0454$$

$$f_2 = \frac{1}{0.044813}\left(\frac{12}{180}\right)^2(0.019726 \times 9.1147 + 0.9803 \times 5.5595 - 1.0)\ \sigma_b(H)$$

$$= 0.4592\ \sigma_b(H)$$

$$f_4 = \frac{1}{0.044813}\left(\frac{12}{180}\right)^2(0.13180 \times 9.1147 - 0.04846 \times 5.5595 - 0.08333)\ \sigma_b(H)$$

$$= 0.08416\ \sigma_b(H)$$

$$\sigma_b(z) = \xi^2\ \sigma_b(H) = 0.9216\ \sigma_b(H)$$

$$\sigma_z = \frac{M}{I}\,c - \left[\frac{9}{17} - \left(\frac{y}{b}\right)^2\right] f_2 + \frac{4}{85} f_4$$

$$\sigma'_z = \frac{M}{I}\,x + \frac{8}{17}\left(\frac{x}{c}\right) f_2 - \left[\frac{81}{85}\left(\frac{x}{c}\right) - \left(\frac{x}{c}\right)^3\right] f_4$$

The columns are numbered as shown in Fig. 2.14.

Normal Panel

(i) The axial force in column at position y_i may be expressed as

$$N_i = t \int_{y_i-\frac{d}{2}}^{y_i+\frac{d}{2}} \sigma_z\, dy$$

$$= td\left\{\sigma_b - \left[\frac{9}{17} - \frac{1}{3b^2}\left(3y_i^2 + \frac{d^2}{4}\right)\right] f_2 + \frac{4}{85}\ f_4\right\}$$

(ii) The axial force in the corner column becomes

$$N_1 = t \int_{b-\frac{d}{2}}^{b} \sigma_z\ dy$$

$$= \frac{td}{2}\left\{\sigma_b - \left[\frac{9}{17} - \frac{1}{3b^2}\left(3b^2 - \frac{3}{2}\,bd + \frac{d^2}{4}\right)\right] f_2 + \frac{4}{85}\ f_4\right\}.$$

The axial forces in columns are,

$$N_1 = \frac{0.1 \times 3}{2} \times 397.06 \left\{ 0.9216 - \left(\frac{9}{17} - 0.8802\right) 0.4592 + \frac{4}{85} \times 0.08416 \right\} = 64.7192 \text{ kN}$$

$$N_2 = 0.1 \times 3 \times 397.06 \left\{ 0.9216 - \left(\frac{9}{17} - 0.5677\right) 0.4592 + \frac{4}{85} \times 0.08416 \right\} = 112.3452 \text{ kN}$$

$$N_3 = 0.1 \times 3 \times 397.06 \left\{ 0.9216 - \left(\frac{9}{17} - 0.2552\right) 0.4592 + \frac{4}{85} \times 0.08416 \right\} = 95.2516 \text{ kN}$$

$$N_4 = 0.1 \times 3 \times 397.06 \left\{ 0.9216 - \left(\frac{9}{17} - 0.06771\right) 0.4592 + \frac{4}{85} \times 0.08416 \right\} = 84.9979 \text{ kN}$$

$$N_5 = 0.1 \times 3 \times 397.06 \left\{ 0.9216 - \left(\frac{9}{17} - 0.005208\right) 0.4592 + \frac{4}{85} \times 0.08416 \right\} = 81.5792 \text{ kN}$$

<u>Side Panel</u>

(i) The axial force in column at position x_i is given by

$$N_i = t \int_{x_i - \frac{d}{2}}^{x_i + \frac{d}{2}} \sigma_z' \, dx$$

$$= \frac{t dx_i}{c} \left\{ \sigma_b + \frac{8}{17} f_2 - \left[\frac{81}{85} - \frac{1}{c^2} \left(x_i^2 + \frac{d^2}{4}\right) \right] f_4 \right\}$$

(ii) The axial force in corner column is expressed as

$$N_1 = t \int_{c - \frac{d}{2}}^{c} \sigma_z' \, dx$$

$$= \frac{td\left(c - \frac{d}{4}\right)}{2c} \left\{ \sigma_b + \frac{8}{17} f_2 - \left[\frac{81}{85} - \frac{1}{c^2}\left(c^2 - \frac{cd}{2} + \frac{d^2}{8}\right) \right] f_4 \right\}$$

The axial forces in columns are evaluated as,

$$N_1 = \frac{0.1 \times 3 \times 5.25}{12} \times 397.06 \left\{ 0.9216 + \frac{8}{17} \times 0.4592 - \left(\frac{81}{85} - 0.78125\right)0.08416 \right\} = 58.5369 \text{ kN}$$

$$N_2 = \frac{0.1 \times 3 \times 3}{6} \times 397.06 \left\{ 0.9216 + \frac{8}{17} \times 0.4592 - \left(\frac{81}{85} - 0.3125\right)0.08416 \right\} = 64.5497 \text{ kN}$$

$N_3 = 0$

Corner area A_c

The axial force in the concentrated corner area A_c is

$$N_1 = A_c\left(\sigma_b + \frac{8}{17} f_2 + \frac{4}{85} f_4\right)$$

$$= 0.3 \times 397.06\left(0.9216 + \frac{8}{17} \times 0.4592 + \frac{4}{85} \times 0.08416\right)$$

$$= 135.9916 \text{ kN}$$

Total axial force in the corner column is

$N_1 = 64.7192 + 58.5369 + 135.9916 = 259.2477$ kN

If necessary, the shear forces in columns and spandrel beams may also be evaluated.

The results obtained by the more general analysis are compared with the column axial forces at the second floor level given by Schwaighofer and Ast, for nine different frame combinations, in Table 2.3.

The results of the more general analysis are also compared with the approximate analysis of Article 2.4 for the same frame combinations, in Table 2.4.

Function	Point load at top	Uniformly distributed load	Triangularly distributed load
σ_b	$\frac{PcH}{I}\xi$	$\frac{pcH^2}{2I} \cdot \xi^2$	$\frac{pcH^2}{2I}\left(\xi^2 - \frac{1}{3}\xi^3\right)$
$\frac{d\sigma_b}{d\xi}$	$\frac{PcH}{I}$	$\frac{pcH^2}{I}\xi$	$\frac{pcH^2}{2I}(2\xi - \xi^2)$
F_1	λ^2	λ^2	λ^2
F_2	$\frac{\sinh k\xi}{k \cosh k}$	$\frac{2}{k^2}\left[\frac{\cosh k(1-\xi) + k \sinh k\xi}{\cosh k} - 1\right]$	$\frac{3}{k^2}\left[\frac{2k \cosh k(1-\xi) + (k^2-2)\sinh k\xi}{2k \cosh k} - (1-\xi)\right]$
F_3	$\frac{\cosh k\xi}{\cosh k}$	$\frac{2}{k}\frac{k \cosh k\xi - \sinh k(1-\xi)}{\cosh k}$	$\frac{3}{k^2}\left[\frac{(k^2-2)\cosh k\xi - 2k \sinh k(1-\xi)}{2 \cosh k} + 1\right]$

Table 2.1 Design Functions

Framed-tube Geometry		Column 1	Column 2	Column 3	Column 4	Column 5	Column 6
B1.0/600/20-20	$\frac{N_a}{N_s}$	1.00	1.38	1.49	1.53	1.53	1.54
B1.0/600/20-33	$\frac{N_a}{N_s}$	0.96	1.17	1.25	1.28	1.30	1.30
B1.0/600/20-45	$\frac{N_a}{N_s}$	0.95	1.08	1.15	1.17	1.18	1.17
B1.0/600/30-20	$\frac{N_a}{N_s}$	1.00	1.24	1.35	1.35	1.36	1.37
B1.0/600/30-33	$\frac{N_a}{N_s}$	0.97	1.06	1.12	1.14	1.15	1.15
B1.0/600/30-45	$\frac{N_a}{N_s}$	0.96	1.00	1.05	1.06	1.07	1.09
B1.0/600/40-20	$\frac{N_a}{N_s}$	0.99	1.14	1.24	1.25	1.26	1.24
B1.0/600/40-33	$\frac{N_a}{N_s}$	0.96	1.00	1.05	1.07	1.08	1.11
B1.0/600/40-45	$\frac{N_a}{N_s}$	0.97	0.97	1.01	1.03	1.04	1.05

Table 2.2 Comparison between Results of Schwaighofer and Ast and Present Approximate Solution.

Note - In the above table,

(1) N_a and N_s are the column axial forces due to the present method and Schwaighofer's results respectively.

(2) The columns are numbered from the corner to the centre of the side frame.

(3) The notation used to describe the geometry of the framed-tube is that given by Schwaighofer and Ast. The four figures mean, respectively, the ratio of bay width d to storey height h; the building height (in ft.); $100 \frac{t_2}{h}$, where t_2 is the depth of the spandrel beams; $1200 \frac{t_1}{B}$, where t_1 and B are the column width and total width of building (B = 2b = 11d) respectively.

Framed-tube Geometry		Column 1	Column 2	Column 3	Column 4	Column 5	Column 6
B1.0/600/20-20	$\frac{N_g}{N_s}$	1.04	1.34	1.33	1.26	1.20	1.17
B1.0/600/20-33	$\frac{N_g}{N_s}$	0.99	1.15	1.16	1.14	1.10	1.08
B1.0/600/20-45	$\frac{N_g}{N_s}$	0.96	1.06	1.08	1.07	1.05	1.03
B1.0/600/30-20	$\frac{N_g}{N_s}$	1.02	1.22	1.27	1.24	1.21	1.19
B1.0/600/30-33	$\frac{N_g}{N_s}$	0.98	1.05	1.09	1.09	1.08	1.08
B1.0/600/30-45	$\frac{N_g}{N_s}$	0.96	1.00	1.03	1.04	1.05	1.05
B1.0/600/40-20	$\frac{N_g}{N_s}$	1.00	1.13	1.20	1.20	1.19	1.16
B1.0/600/40-33	$\frac{N_g}{N_s}$	0.97	1.00	1.05	1.05	1.06	1.09
B1.0/600/40-45	$\frac{N_g}{N_s}$	0.97	0.97	1.01	1.03	1.04	1.05

Table 2.3 Comparison between Results of Schwaighofer and Ast and the Present more General Solution.

Note: N_g and N_s are the column axial forces due to the present method and the Schwaighofer's results respectively.

Framed-tube Geometry		Column 1	Column 2	Column 3	Column 4	Column 5	Column 6
B1.0/600/20-20	$\frac{N_g}{N_a}$	1.04	0.97	0.90	0.83	0.79	0.76
B1.0/600/20-33	$\frac{N_g}{N_a}$	1.03	0.98	0.93	0.88	0.85	0.83
B1.0/600/20-45	$\frac{N_g}{N_a}$	1.02	0.98	0.95	0.91	0.89	0.88
B1.0/600/30-20	$\frac{N_g}{N_a}$	1.02	0.98	0.94	0.91	0.89	0.87
B1.0/600/30-33	$\frac{N_g}{N_a}$	1.01	0.99	0.97	0.96	0.95	0.94
B1.0/600/30-45	$\frac{N_g}{N_a}$	1.01	1.00	0.99	0.98	0.97	0.97
B1.0/600/40-20	$\frac{N_g}{N_a}$	1.01	0.99	0.97	0.95	0.94	0.94
B1.0/600/40-33	$\frac{N_g}{N_a}$	1.00	1.00	0.99	0.99	0.98	0.98
B1.0/600/40-45	$\frac{N_g}{N_a}$	1.00	1.00	1.00	1.00	1.00	1.00

Table 2.4 Comparison between Results of Approximate Solution and the more General Solution.

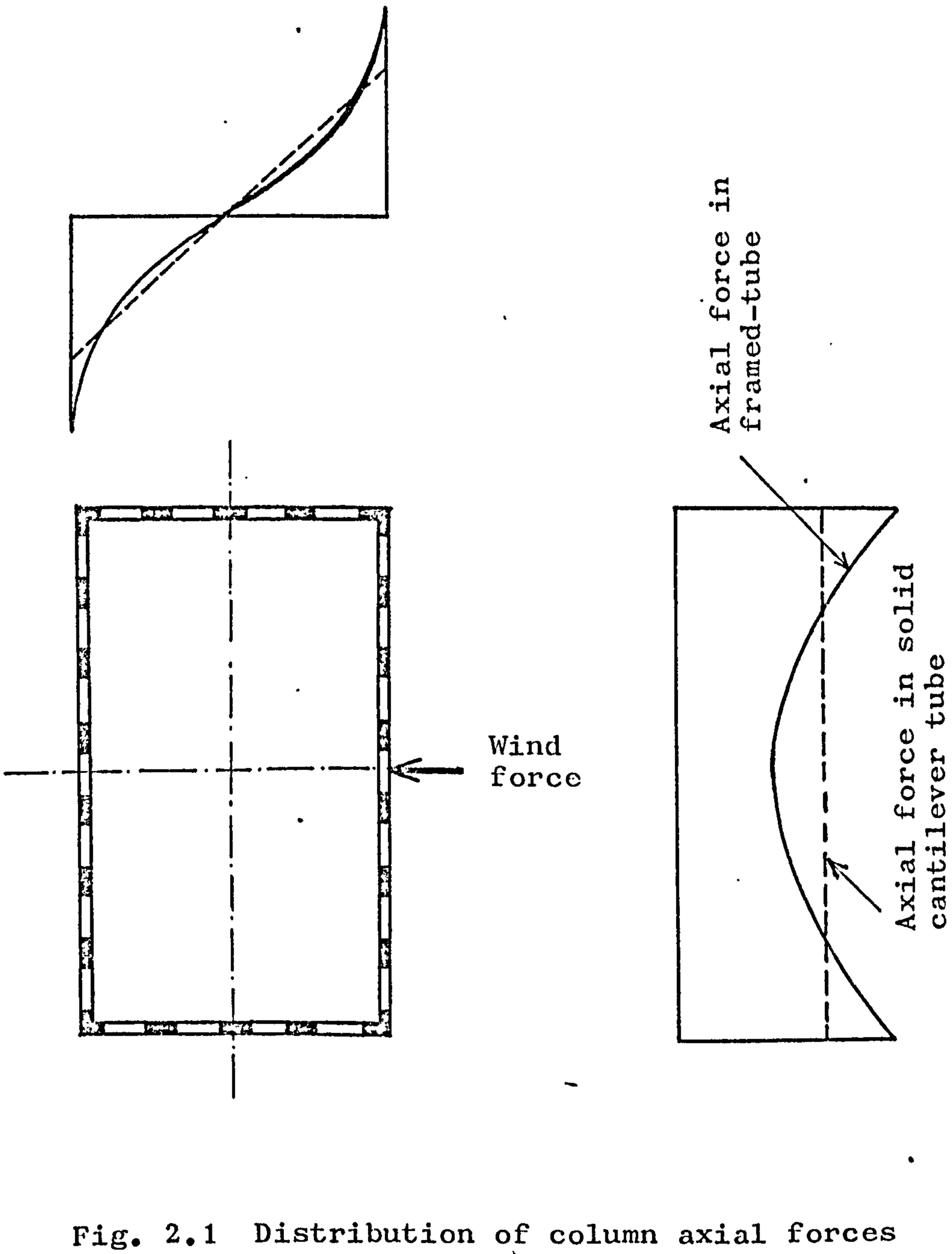

Fig. 2.1 Distribution of column axial forces in solid and framed-tube

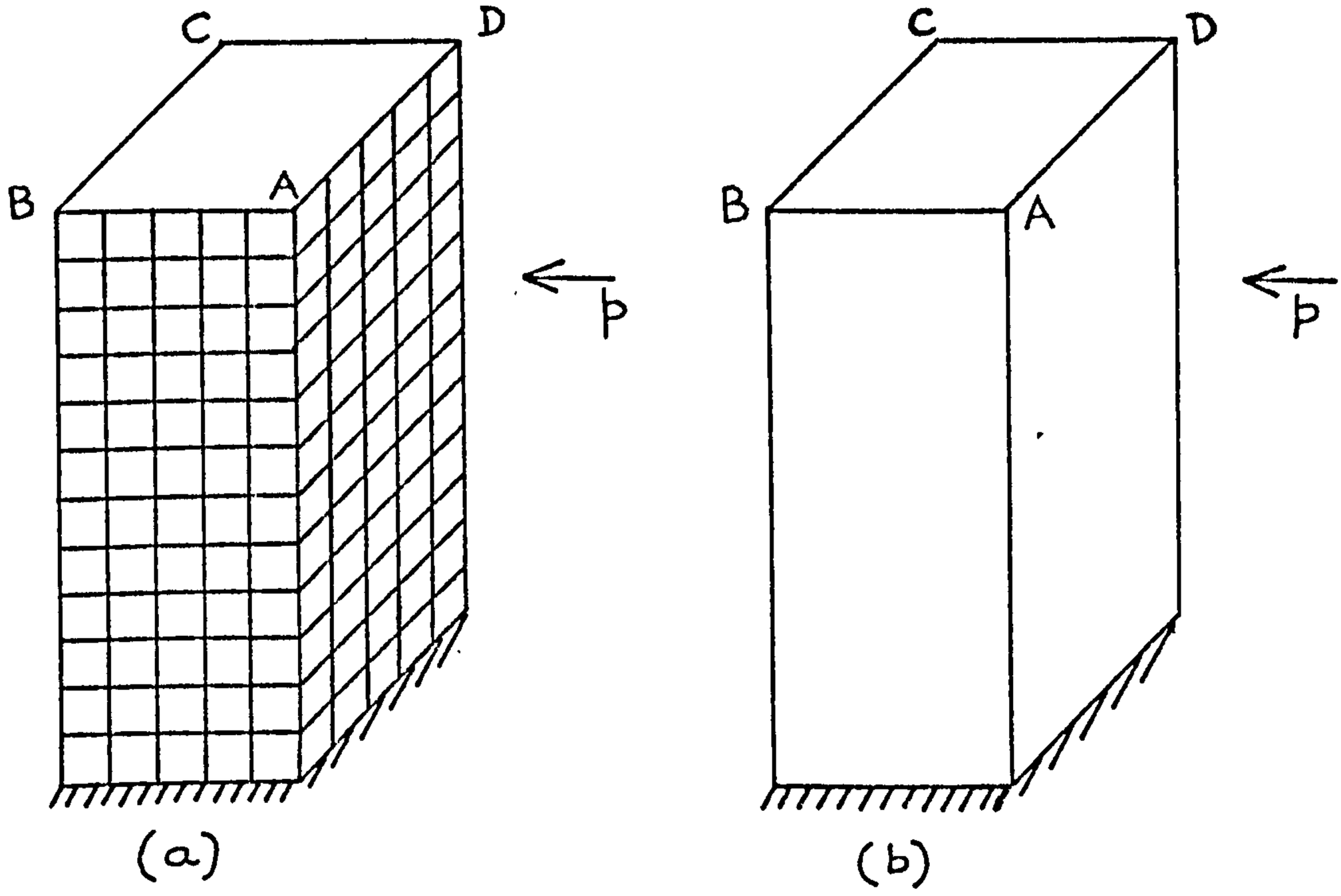

(a) (b)

Fig. 2.2 Framed tube - Real and substitute structure

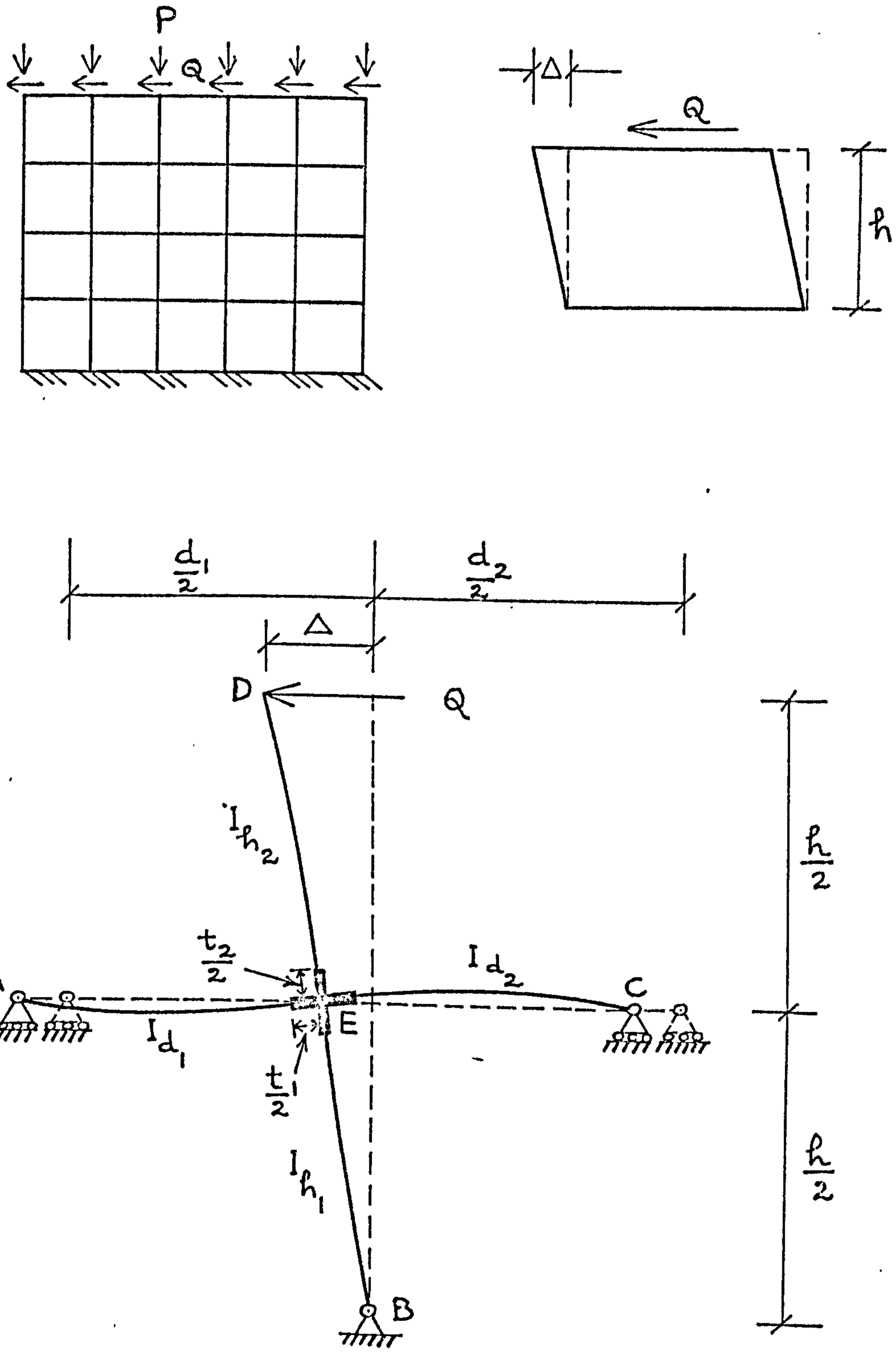

Fig. 2.3 Replacement of Frame Panel by
Equivalent Shear Cantilever element

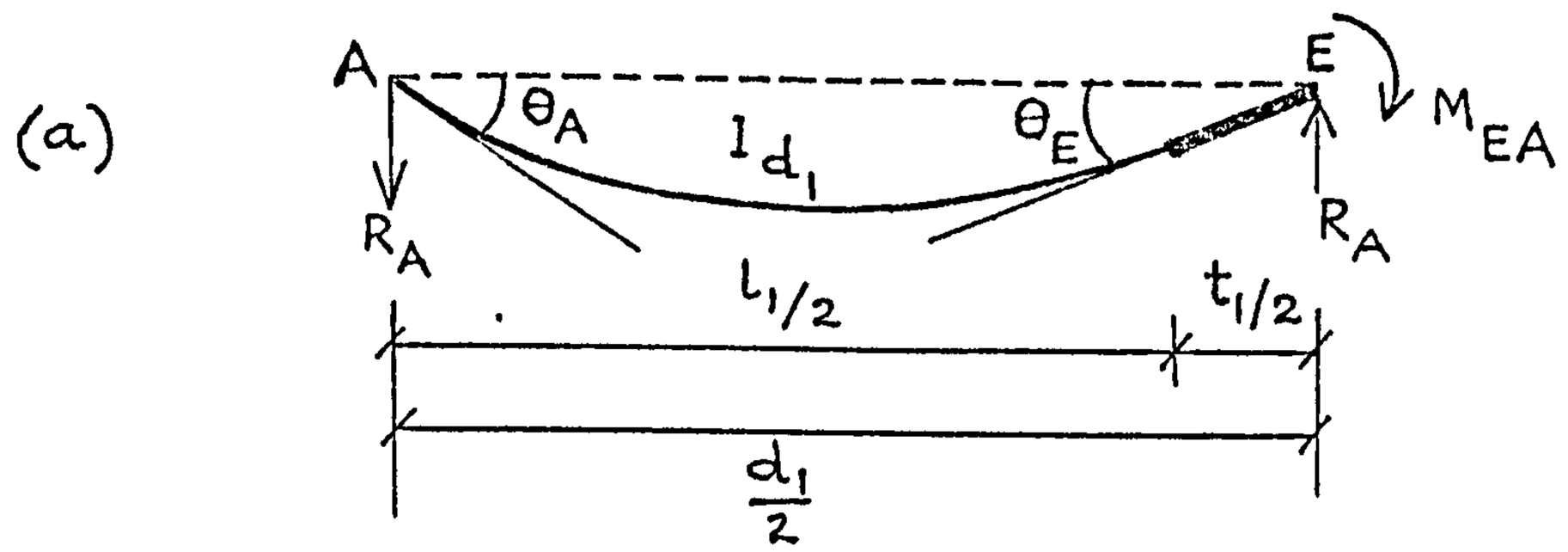

Fig. 2.4 Isolation of Members of Frame Panel

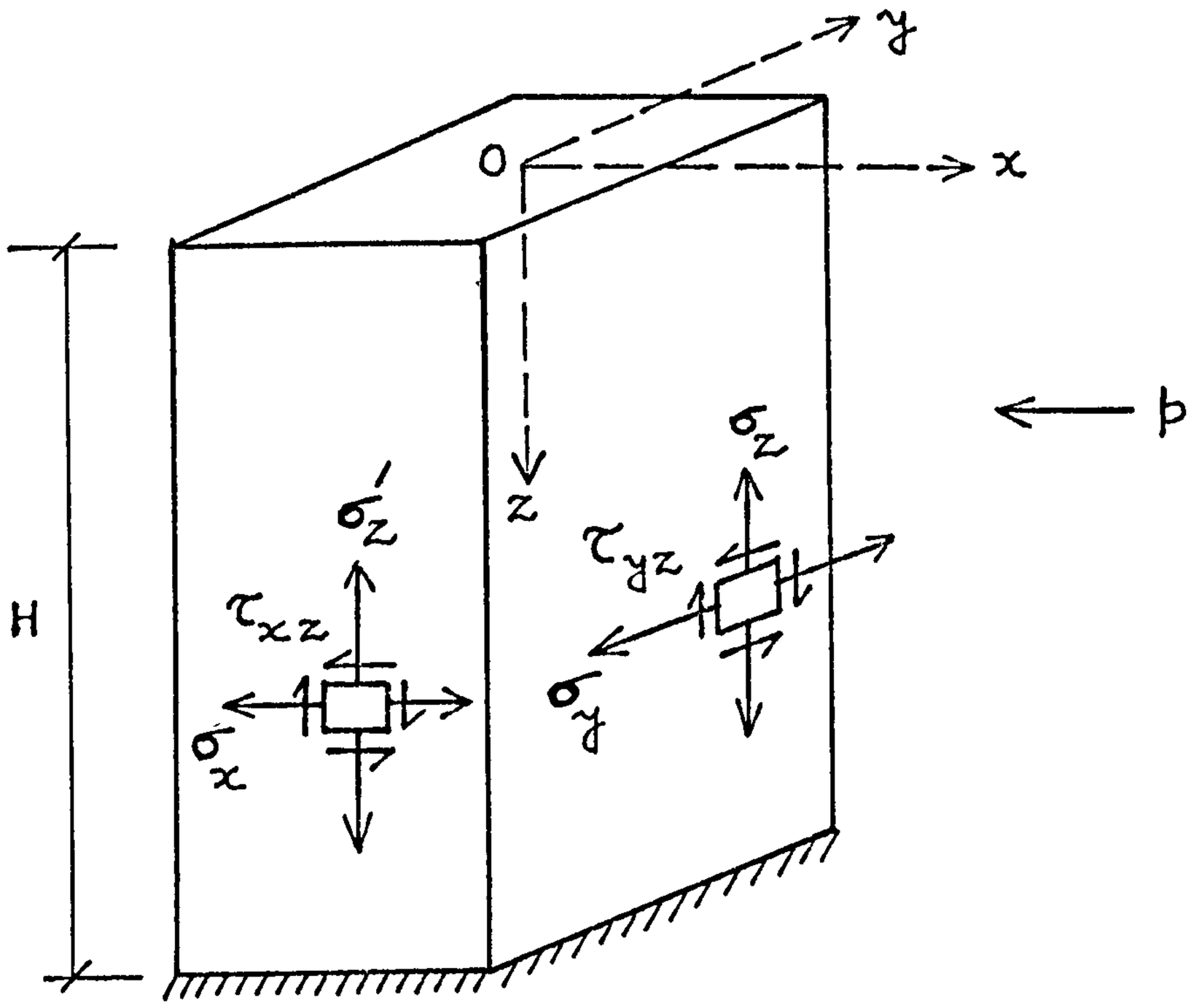

Fig. 2.5 Notation for stresses

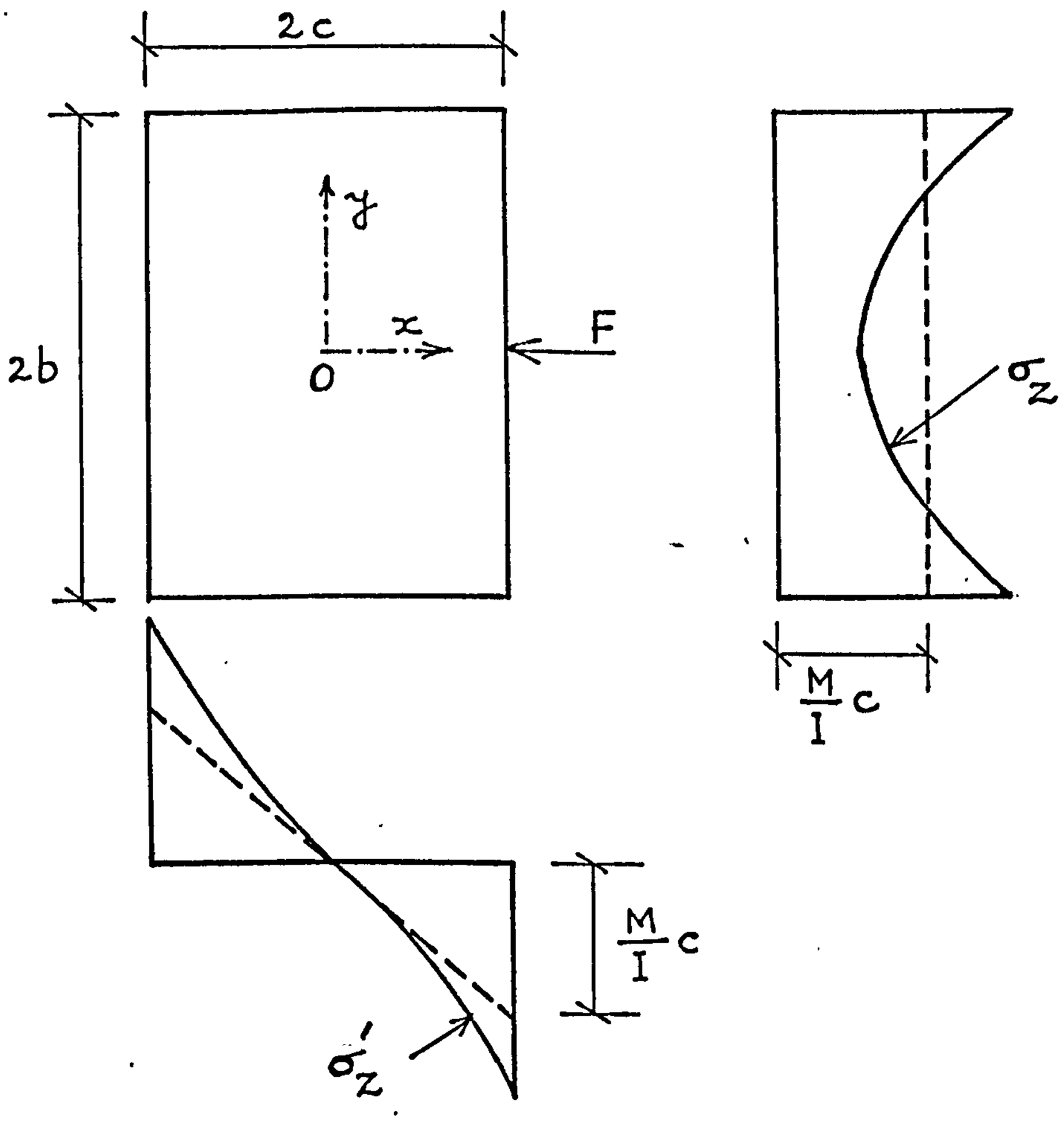

Fig. 2.6 Shear lag in Framed-tube

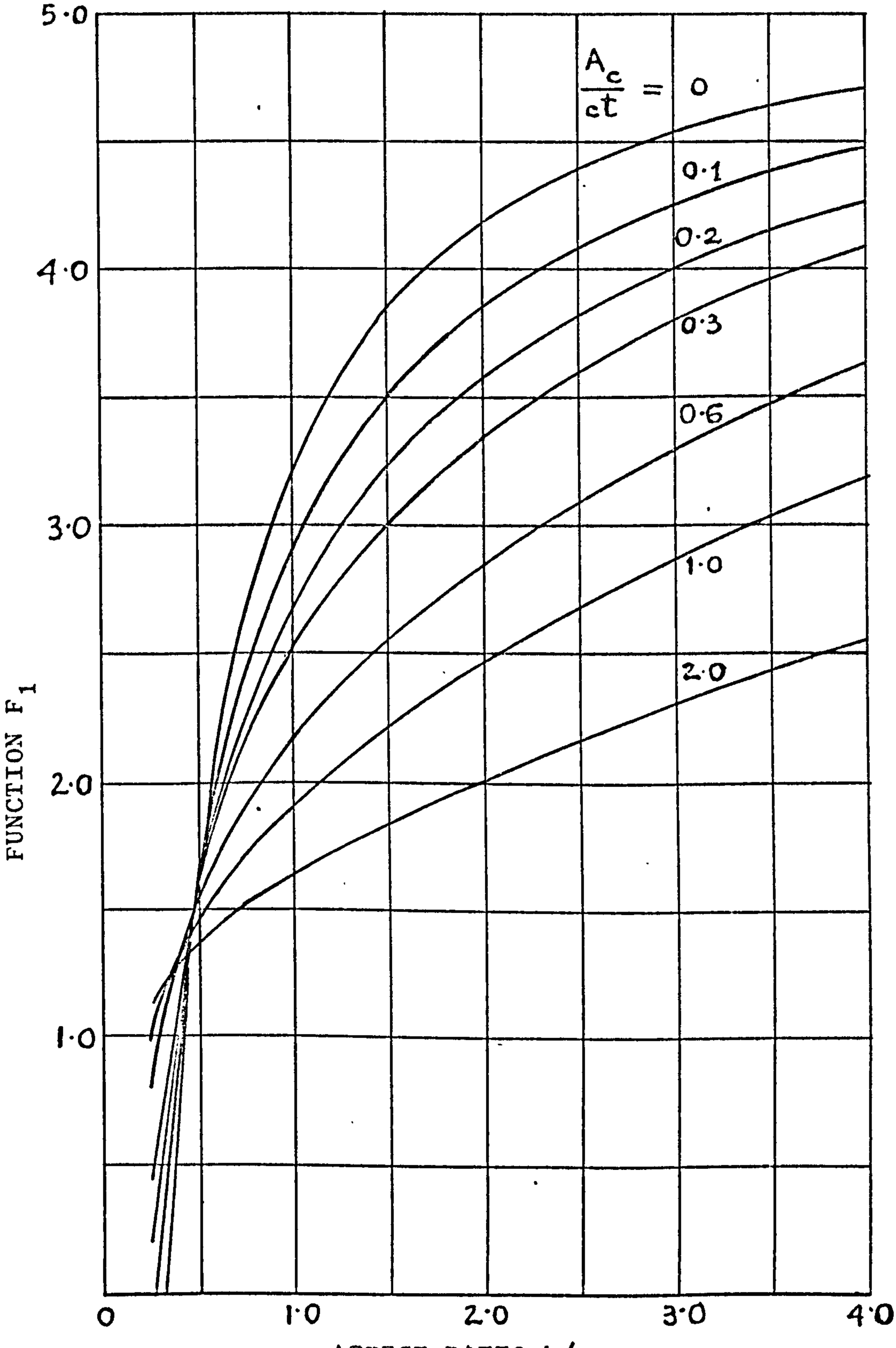

Fig. 2.7 Variation of Geometrical Function with Aspect ratio for various ratios of stiff corner column area

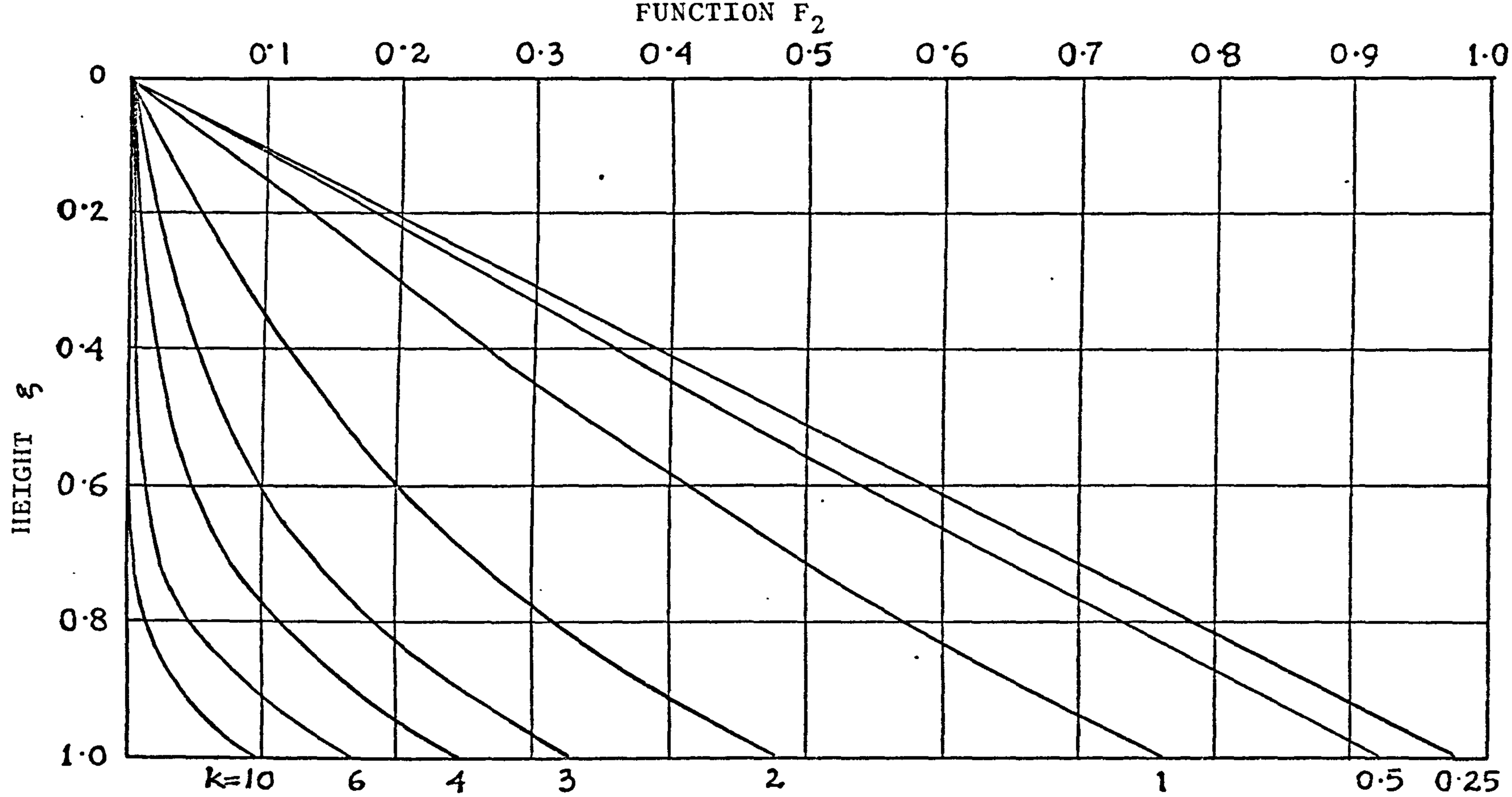

Fig. 2.8 Stress Function F_2 for Point load at top

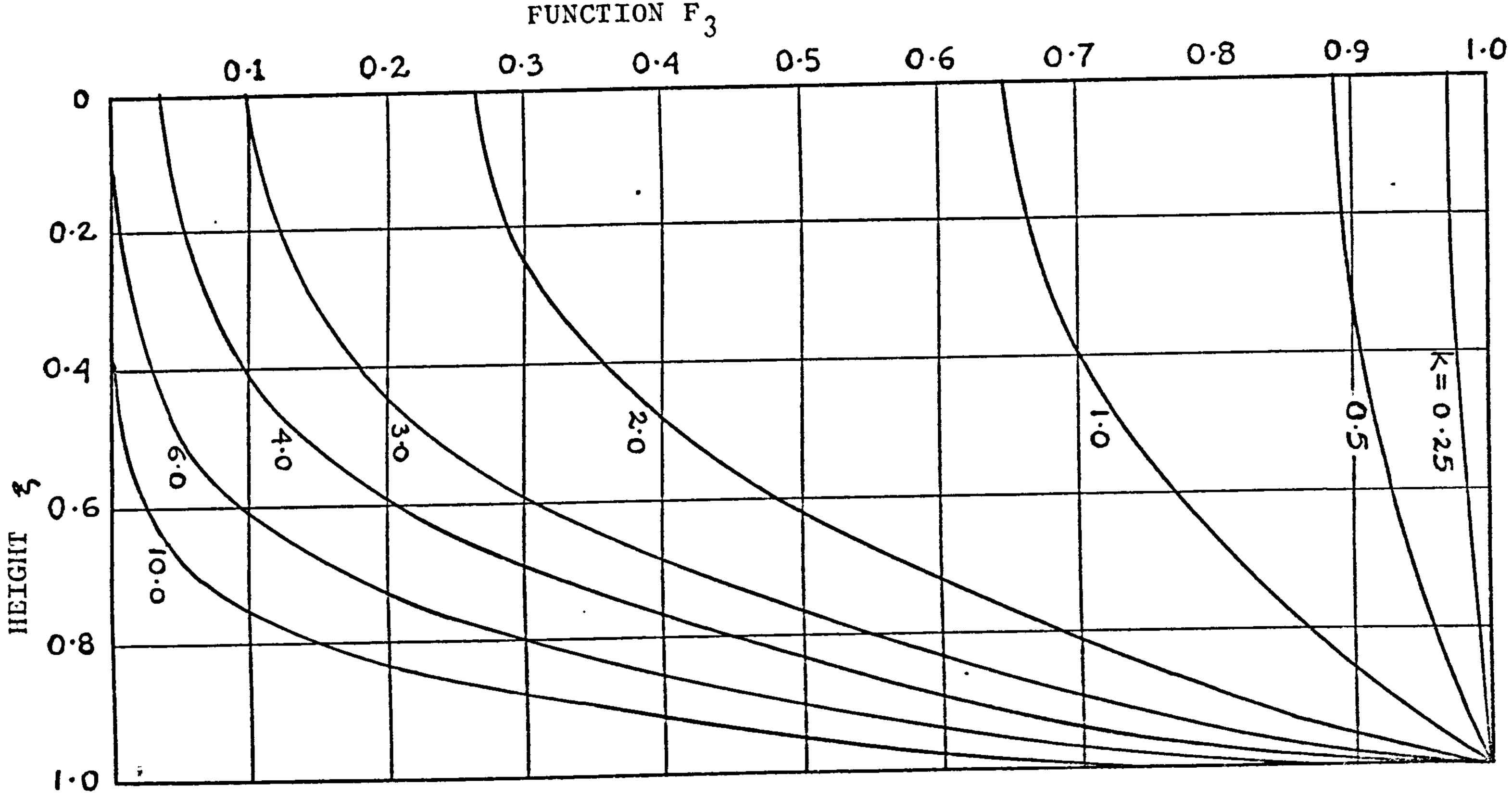

Fig. 2.9 Stress Function F_3 for Point Load at Top

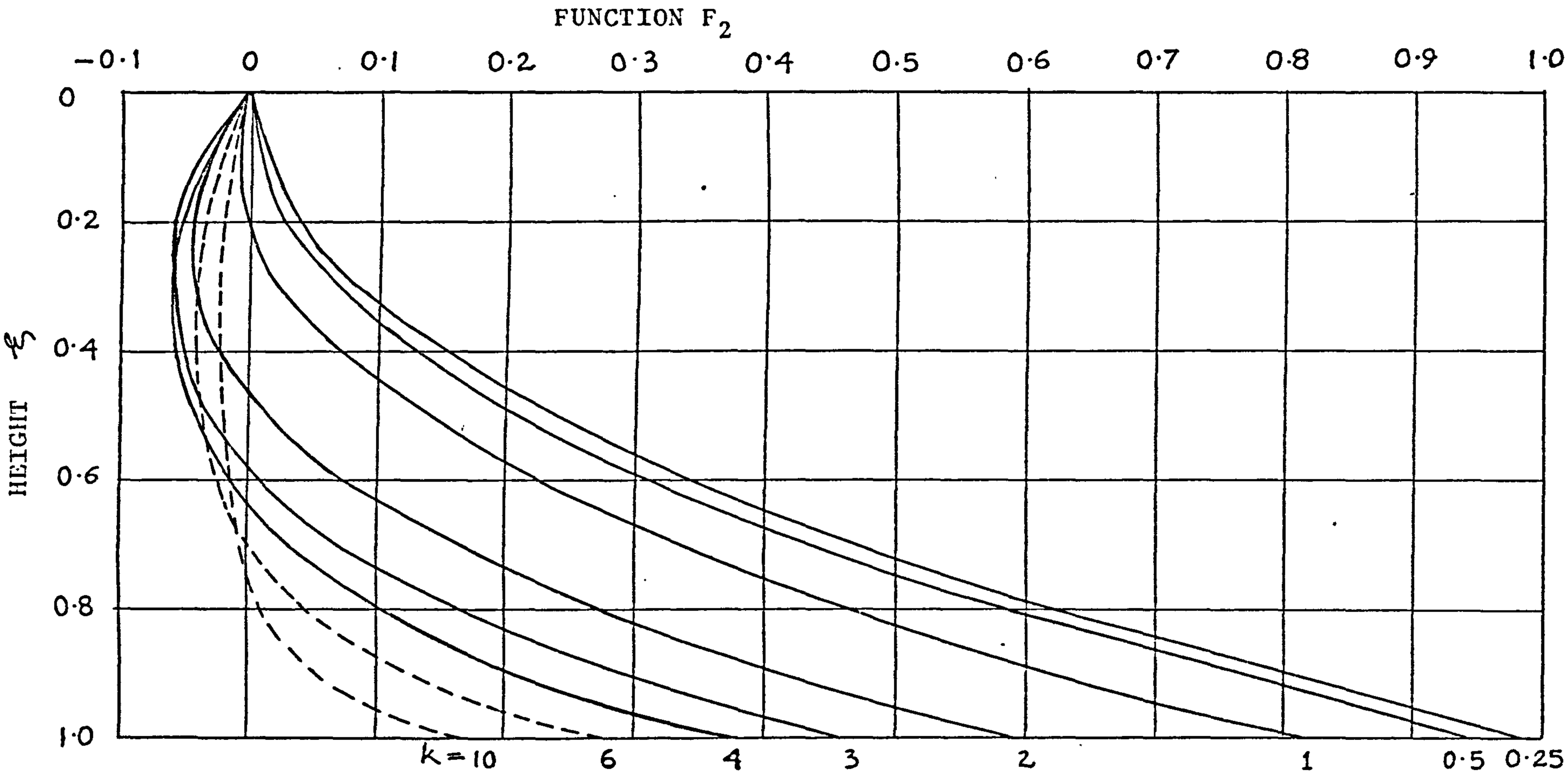

Fig. 2.10 Stress Function F_2 for Uniformly Distributed Load

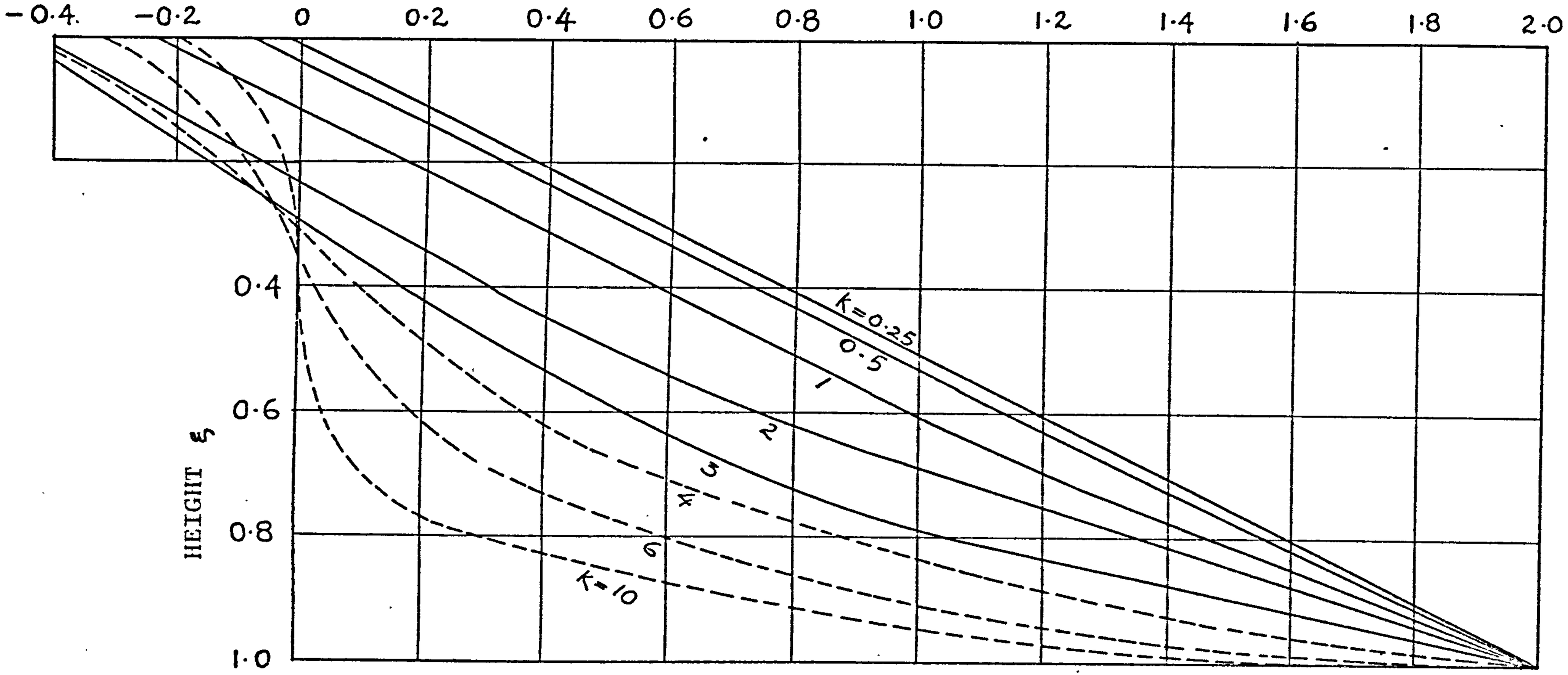

Fig. 2.11 Stress Function F_3 for Uniformly Distributed Load

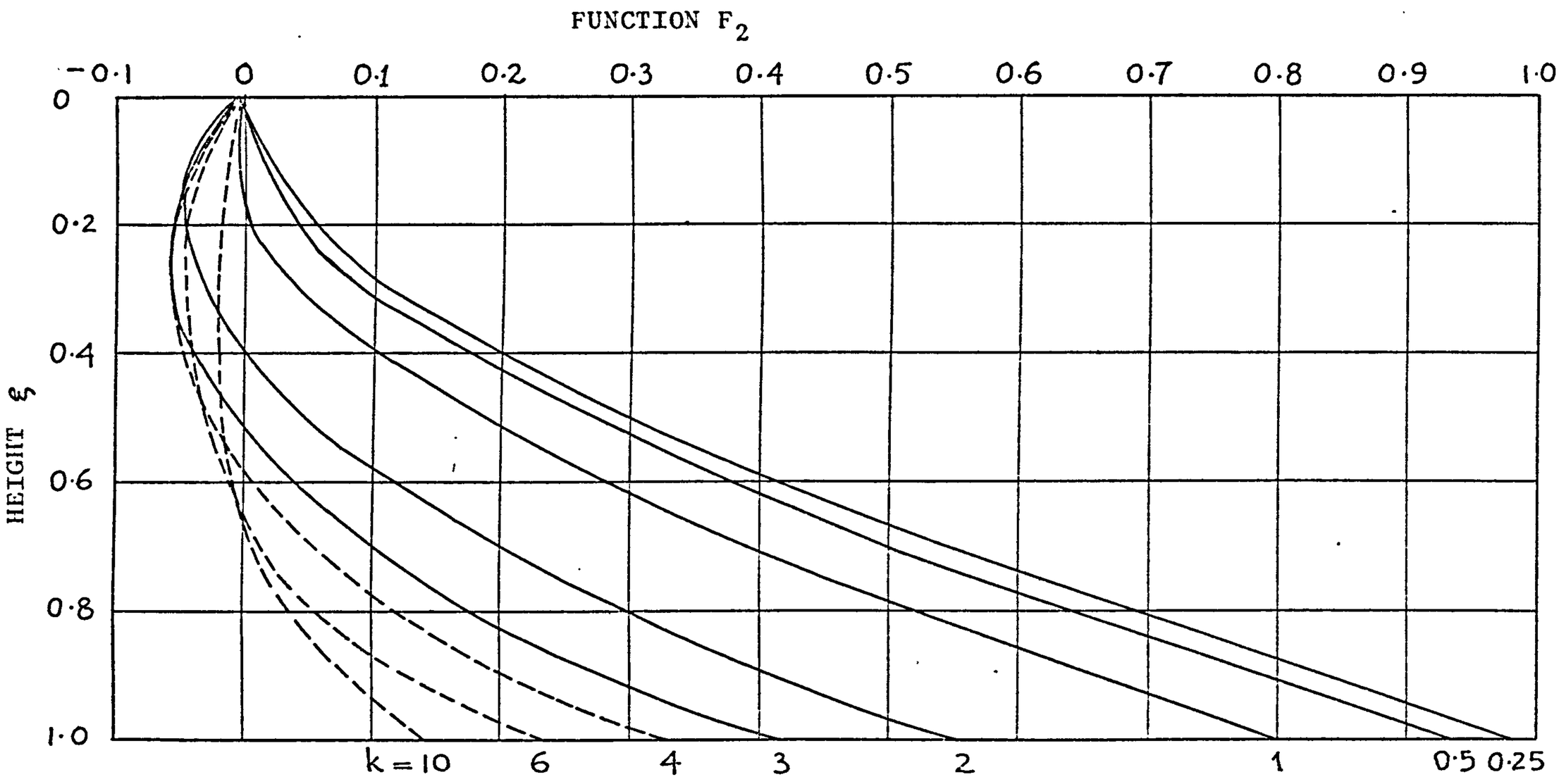

Fig. 2.12 Stress Function F_2 for Triangularly Distributed Load

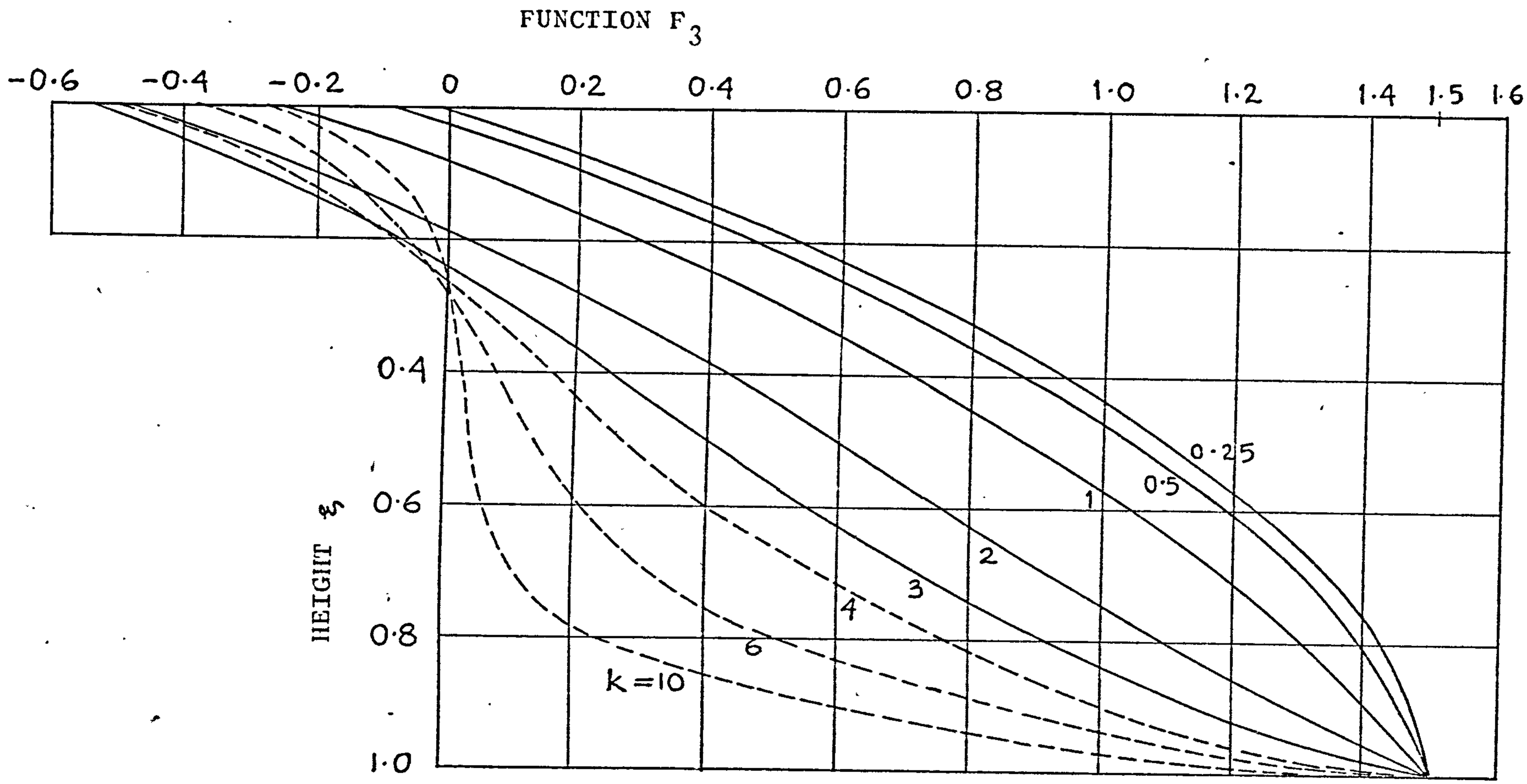

Fig. 2.13 Stress Function F_3 for Triangularly Distributed Load

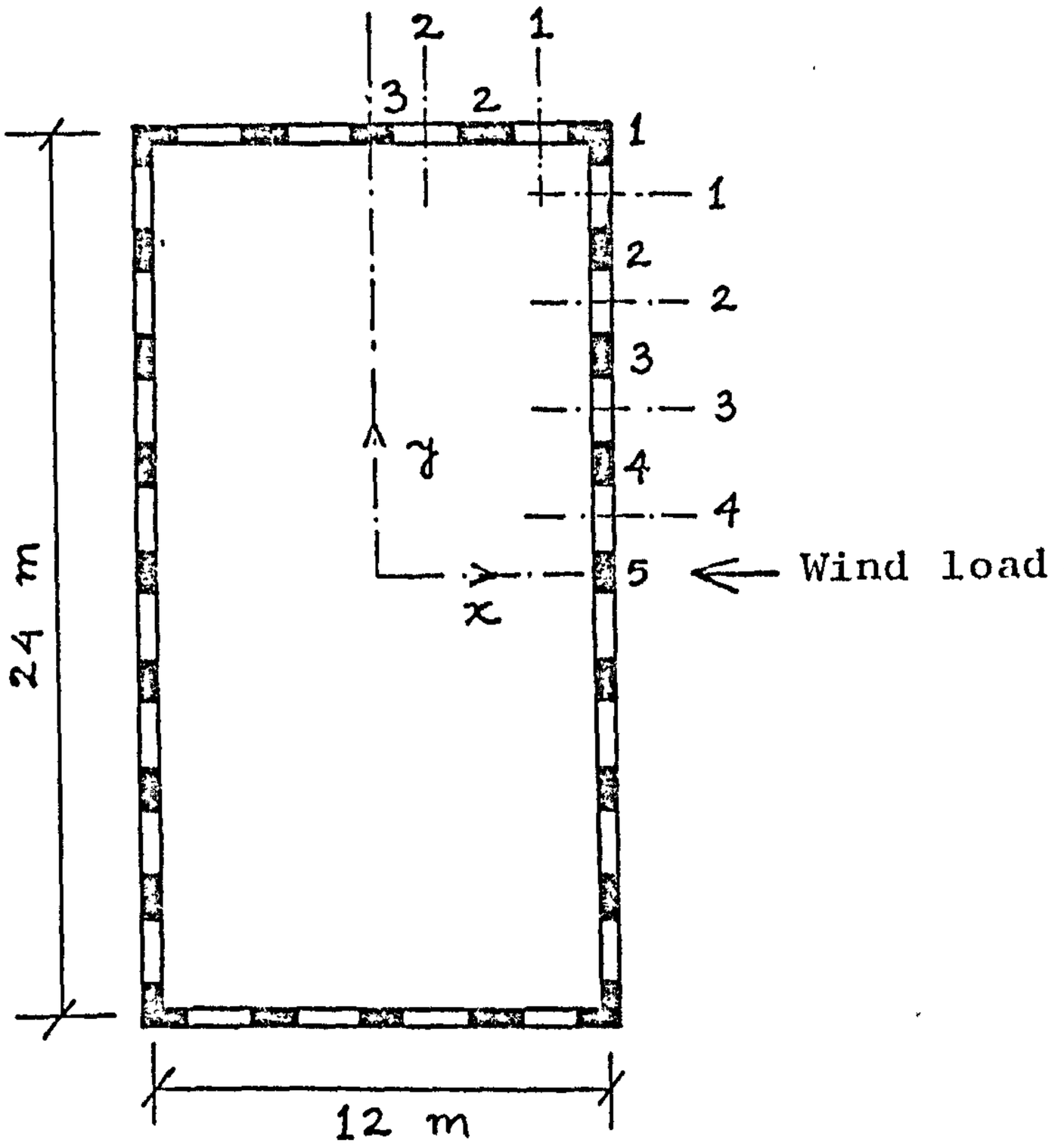

Fig. 2.14 Building Plan

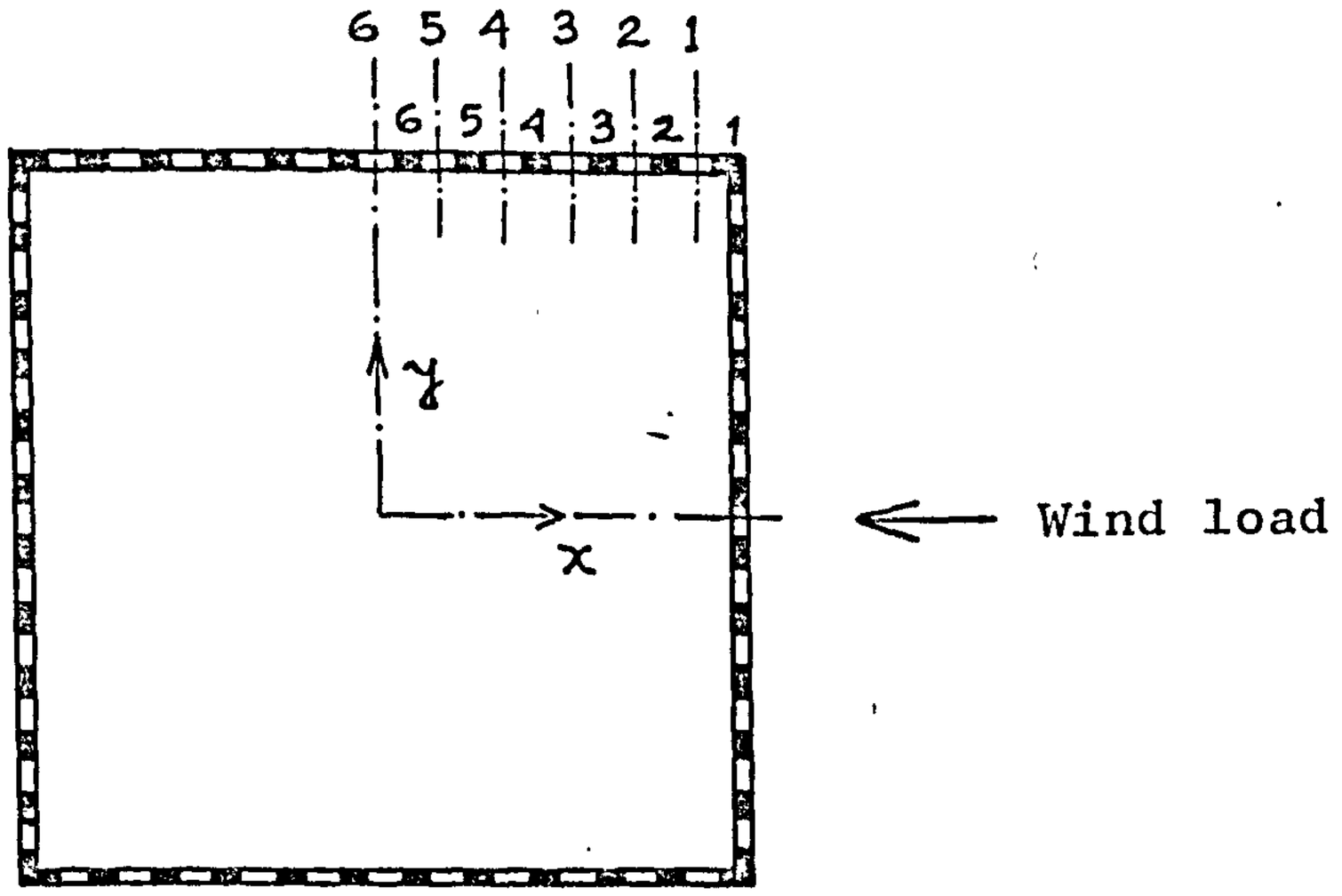

Fig. 2.15 Typical building square in plan

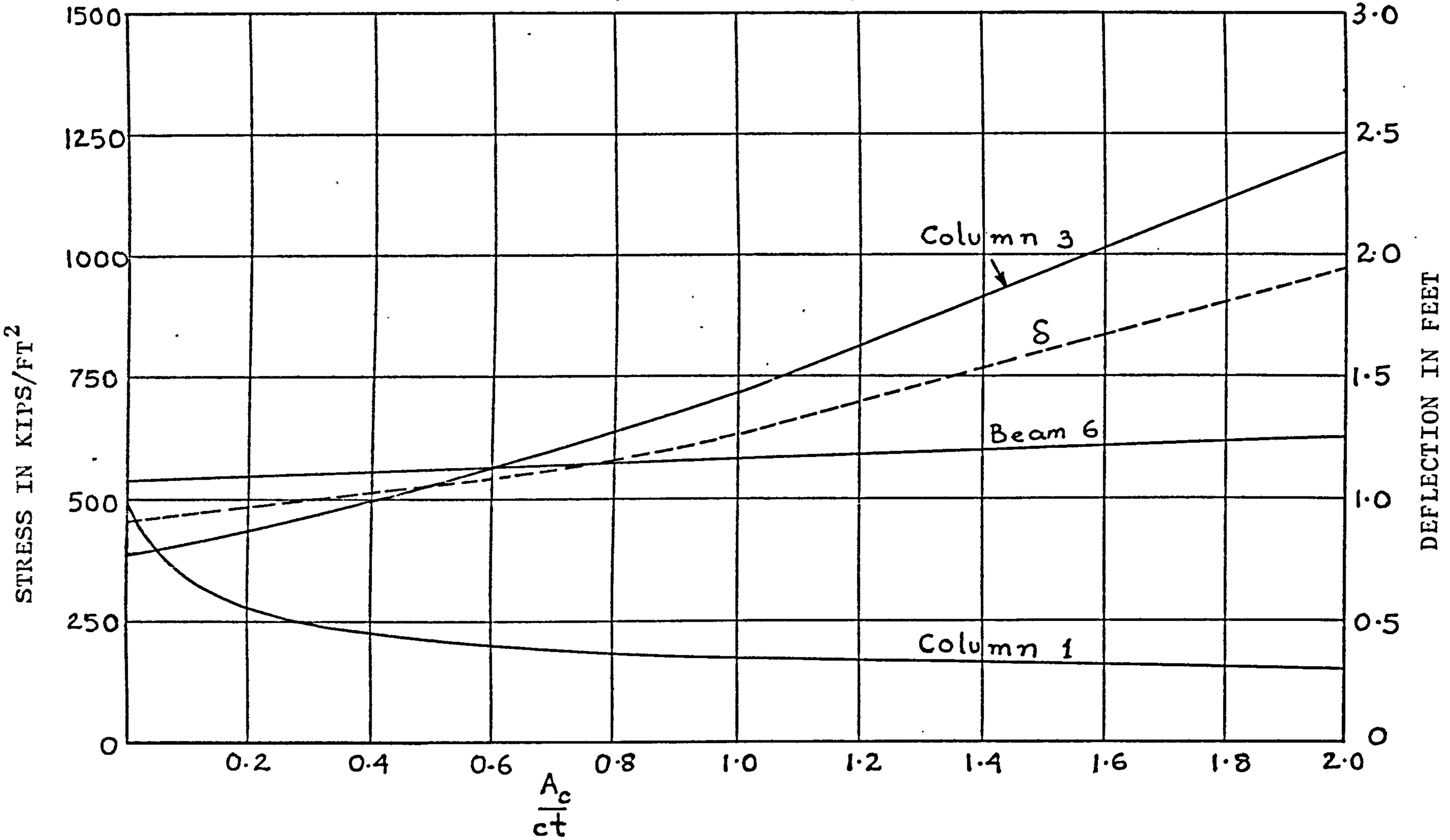

Fig.(2.16) Stresses and Deflections for β = 0.8, t_2 = 2.5 ft.

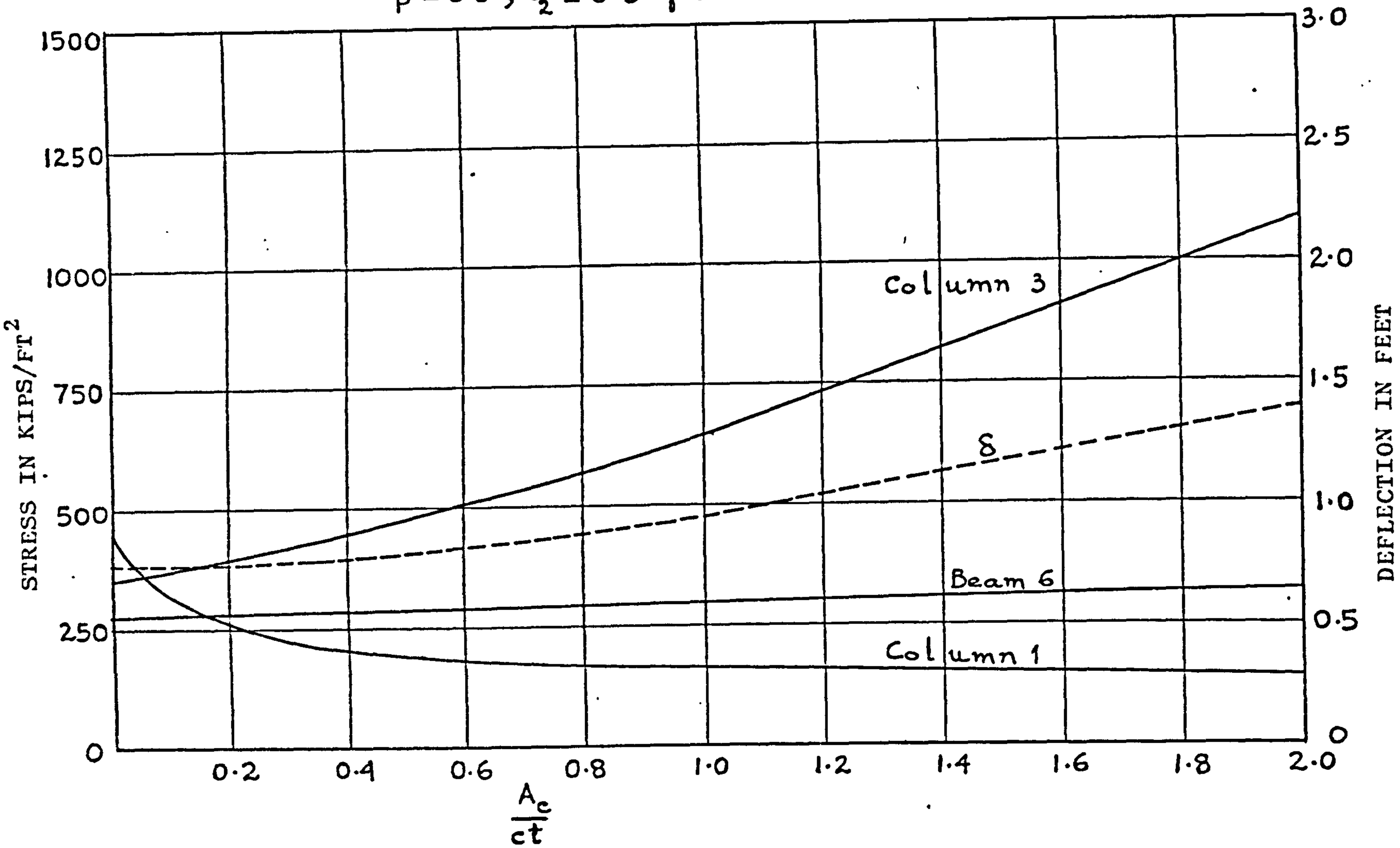

Fig. (2.17) Stresses and deflections for $\beta = 0.8$, $t_2 = 3.5$ ft.

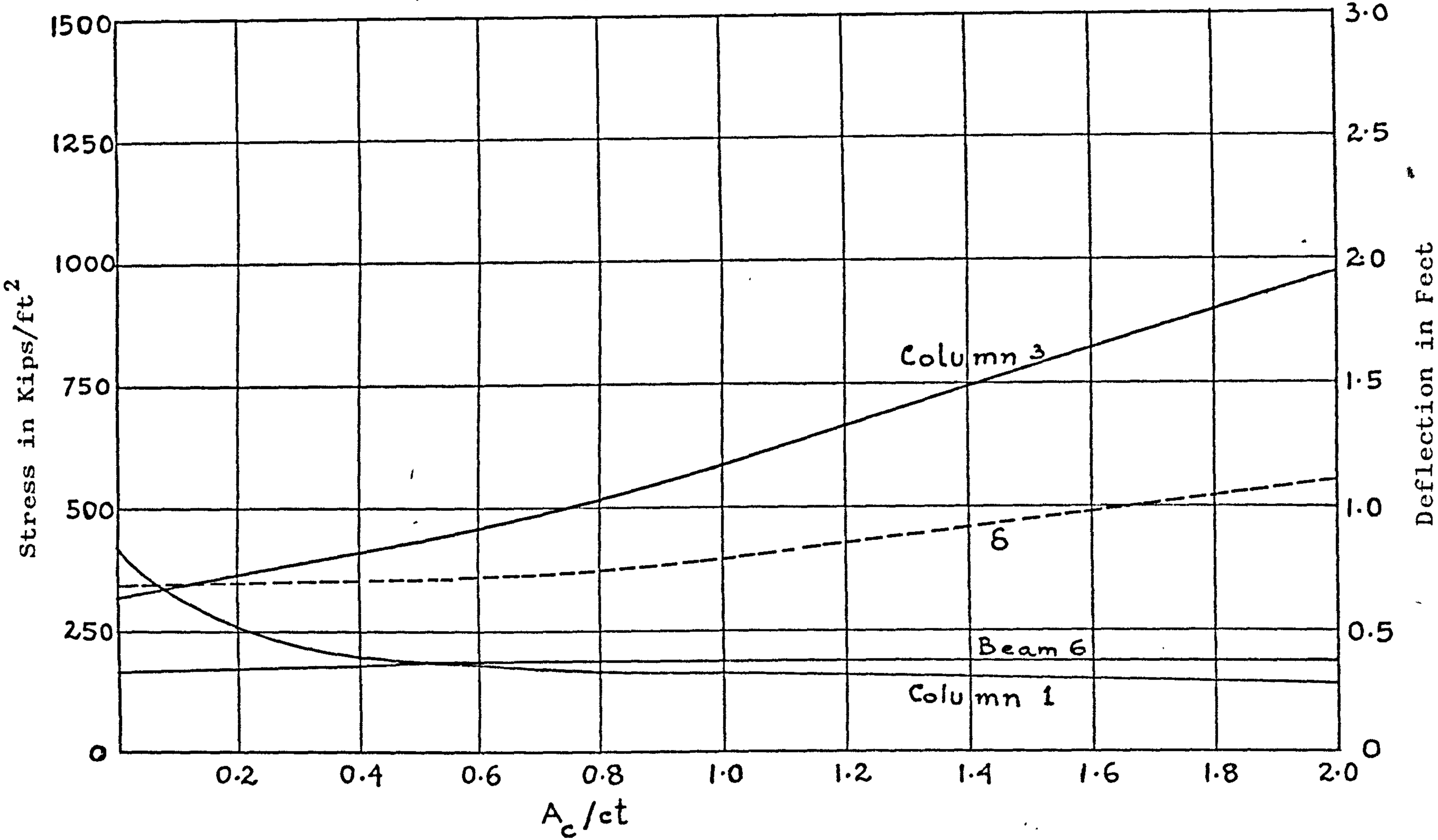

Fig.(2.18) Stresses and Deflections for $\beta = 0.8$, $t_2 = 4.5$ ft.

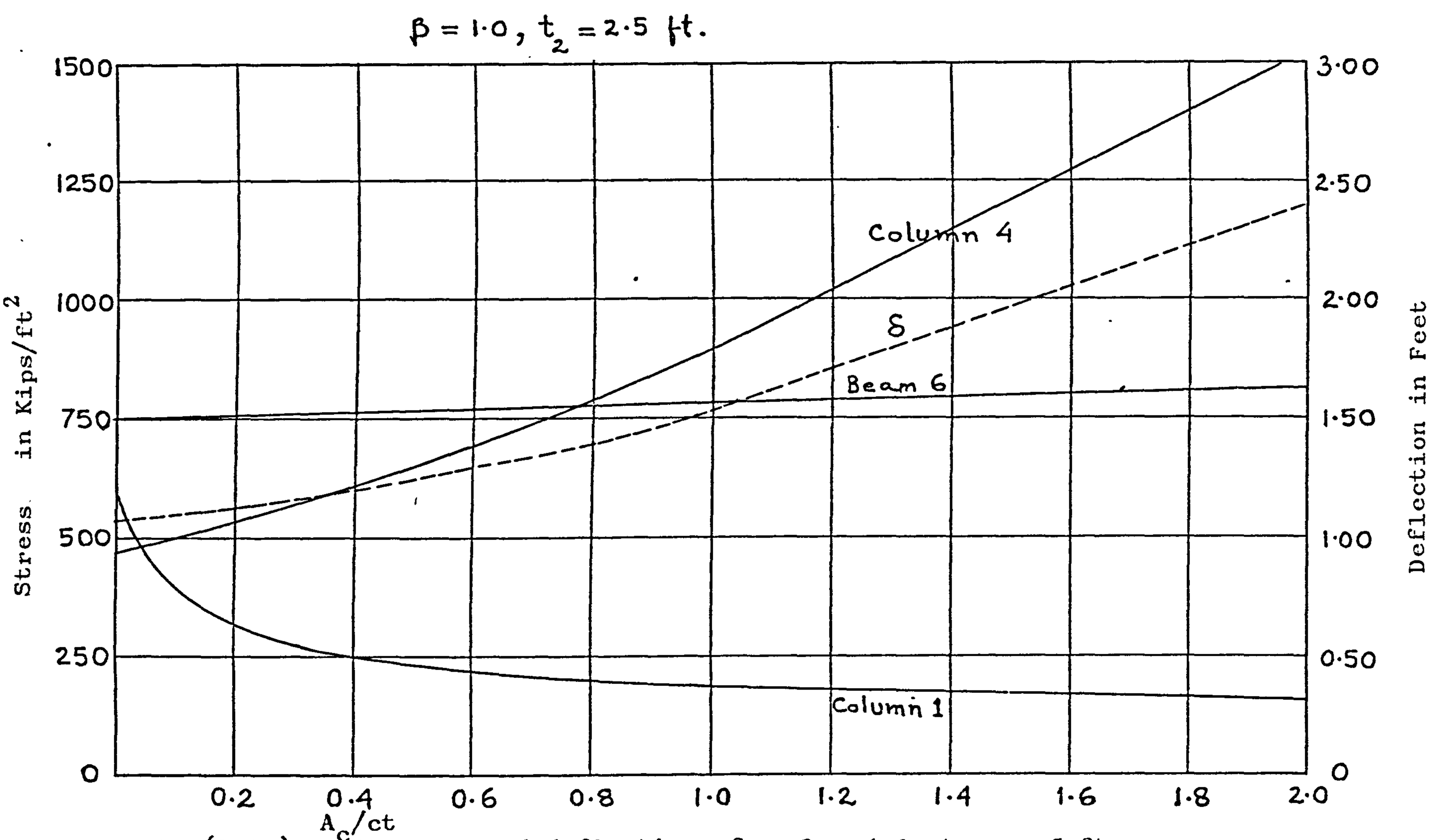

Fig. (2.19) Stresses and deflections for $\beta = 1.0$, $t_2 = 2.5$ ft.

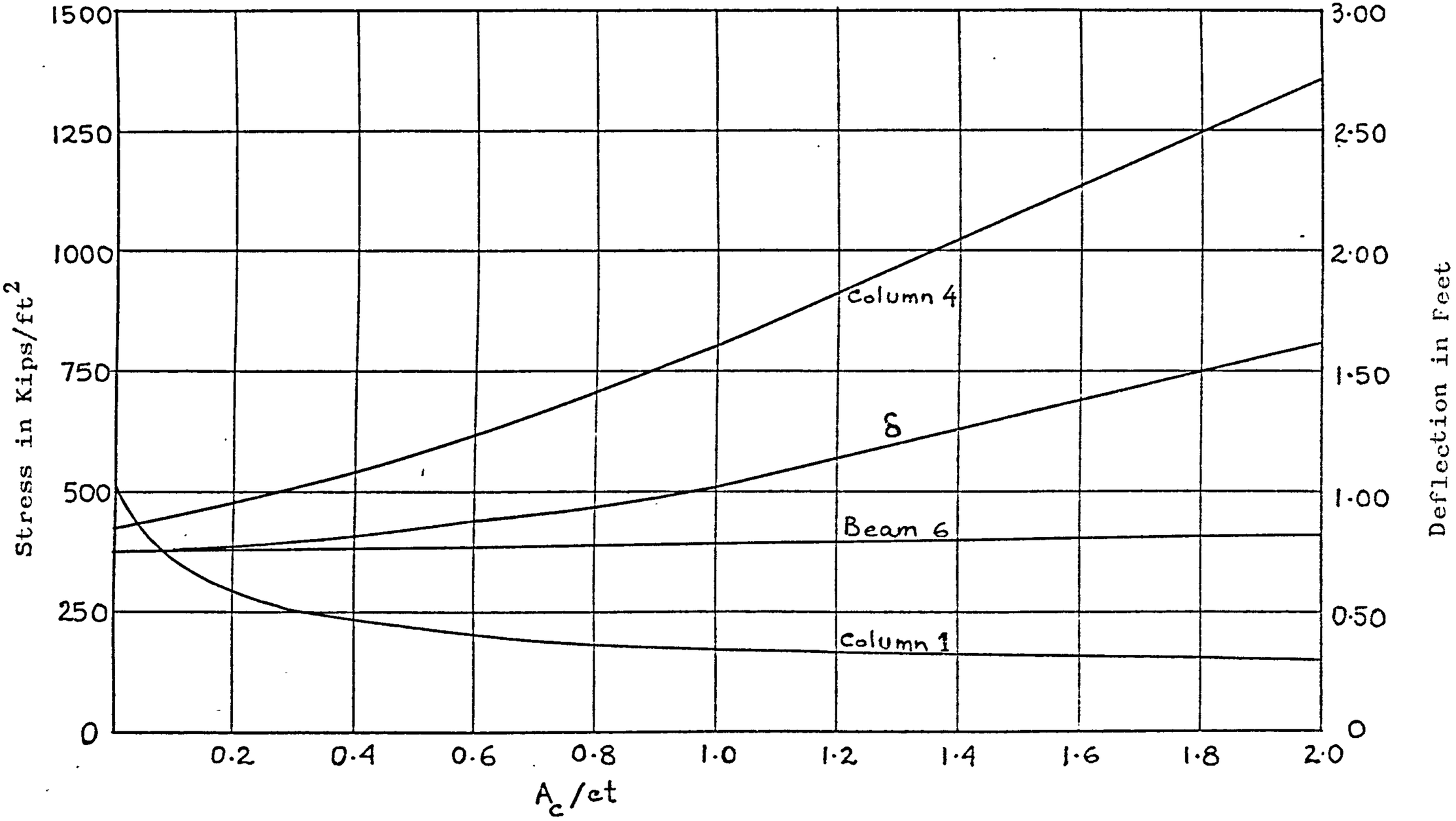

Fig.(2.20) Stresses and deflections for $\beta = 1.0$, $t_2 = 3.5$ ft.

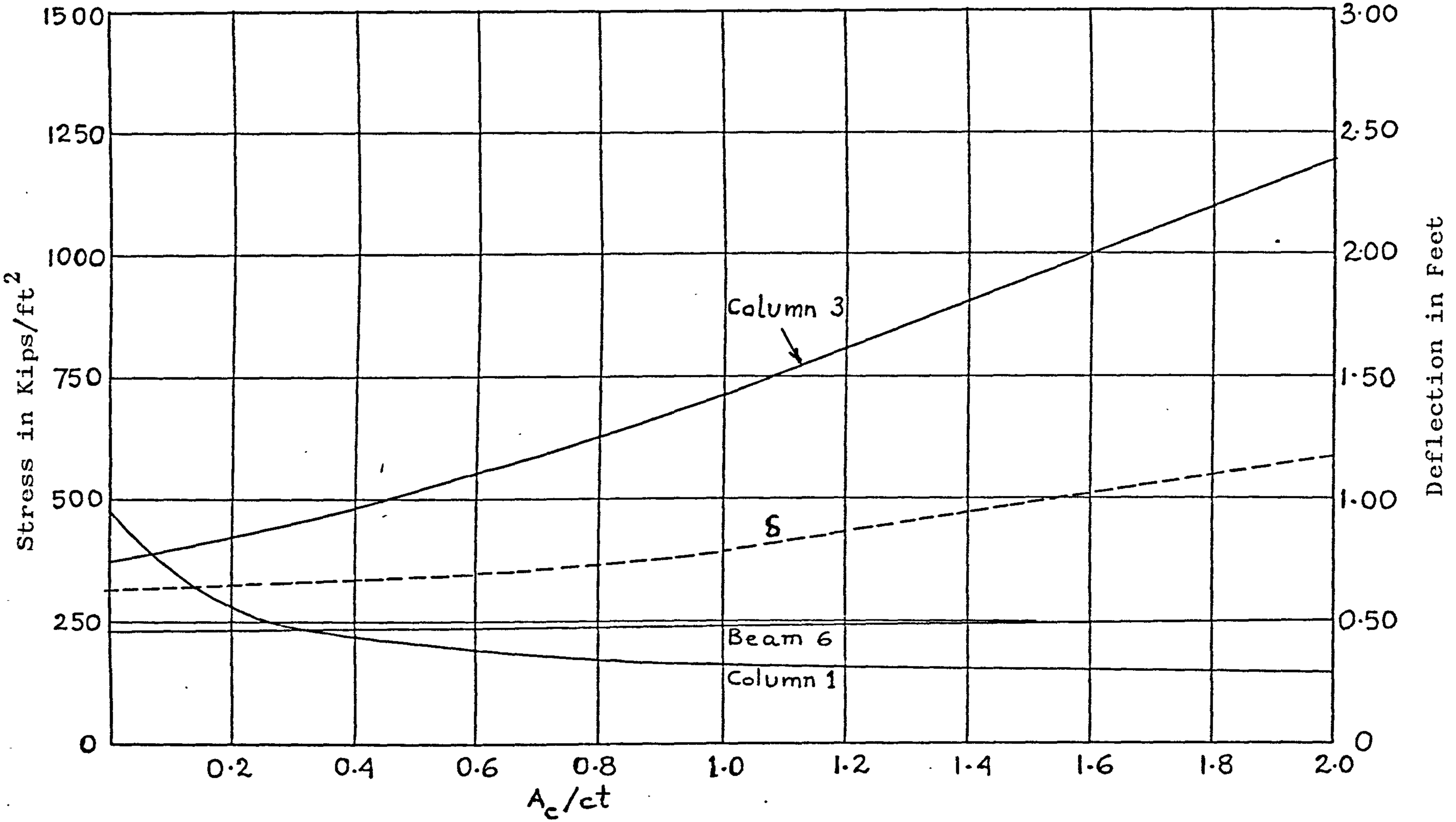

Fig.(2.21) Stresses and deflections for $\beta = 1.0$, $t_2 = 4.5$ ft.

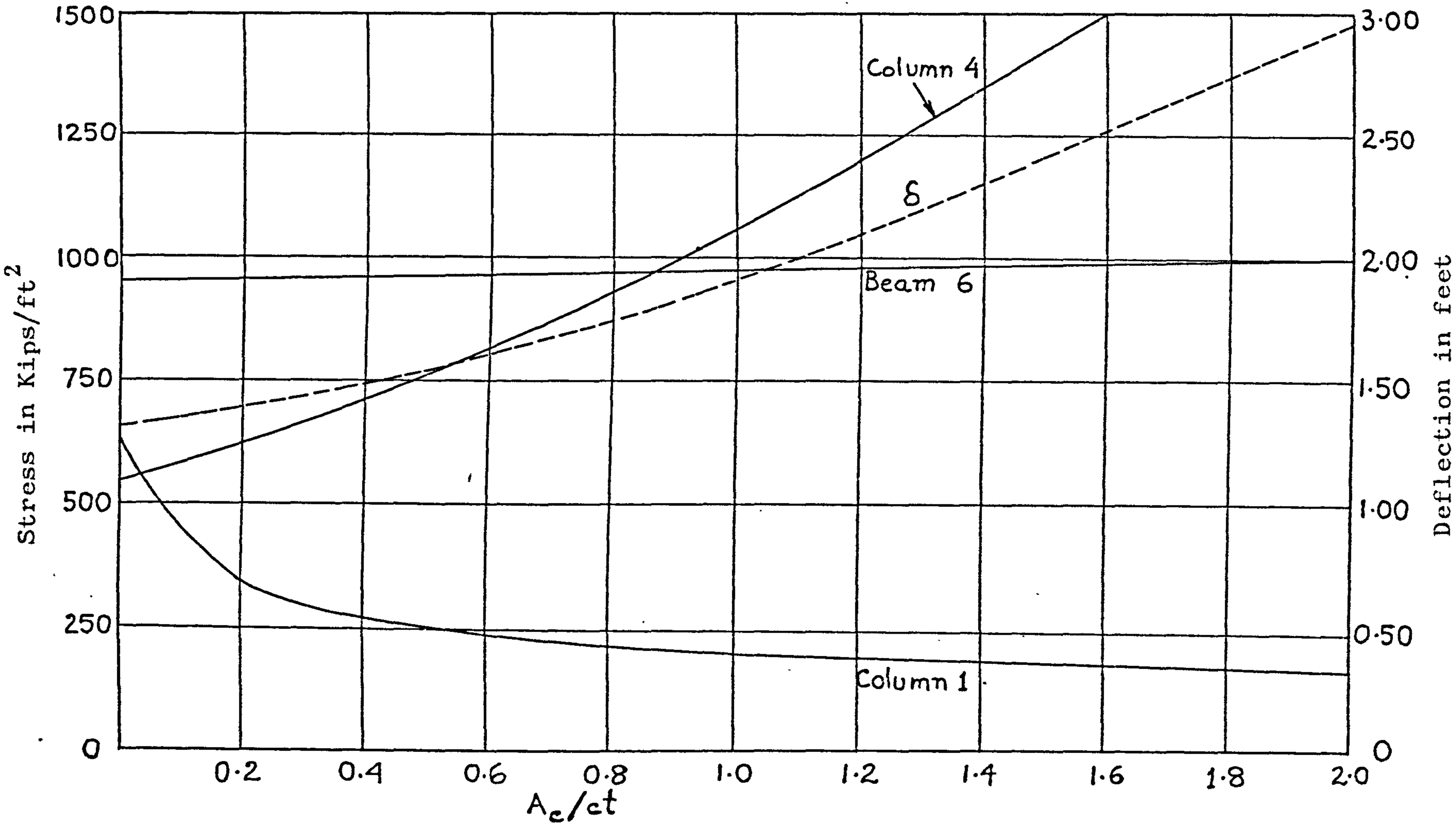

Fig. (2.22) Stresses and deflections for $\beta = 1.2$, $t_2 = 2.5$ ft.

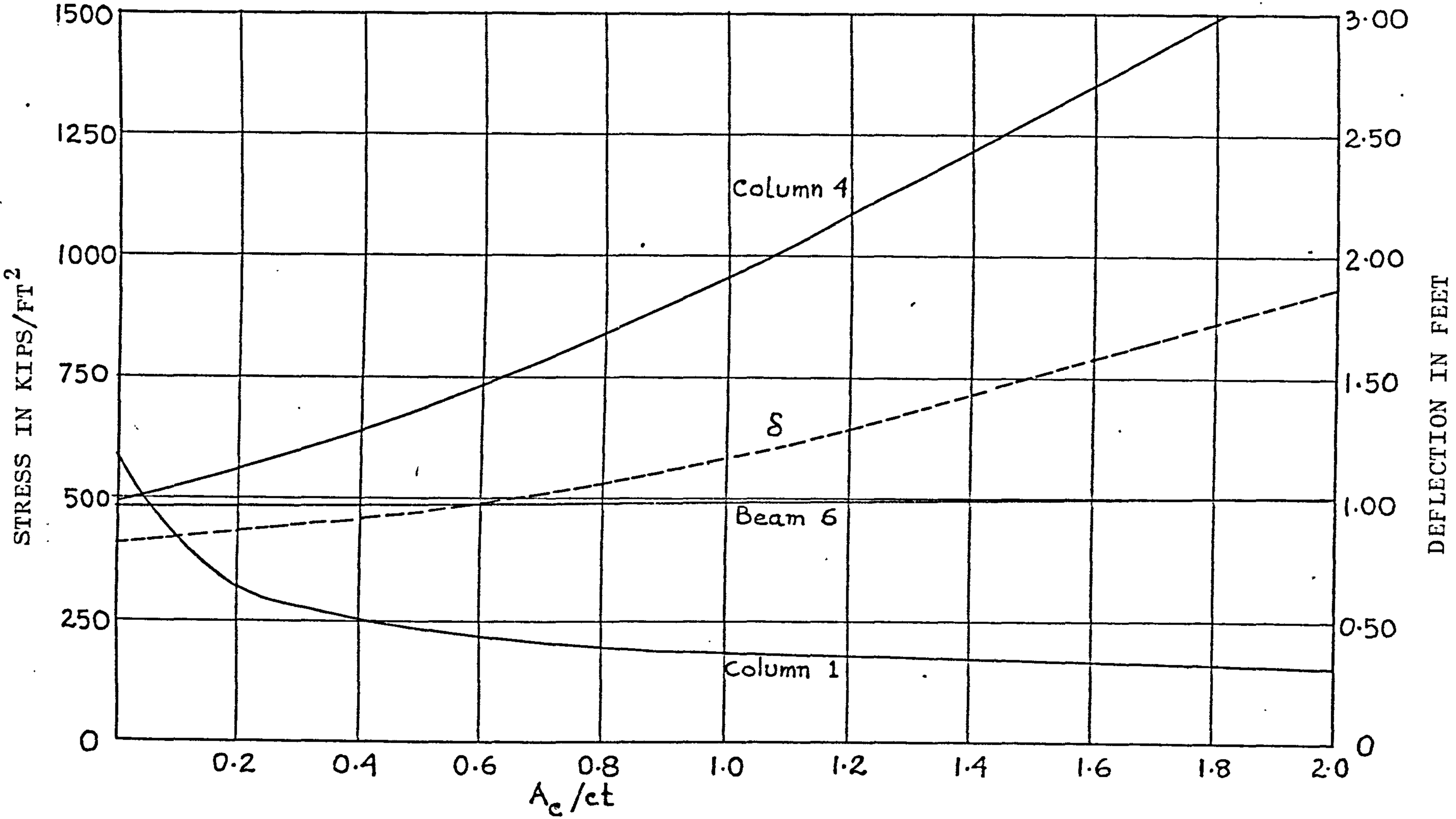

Fig.(2.23) Stresses and Deflections for $\beta = 1.2$, $t_2 = 3.5$ ft.

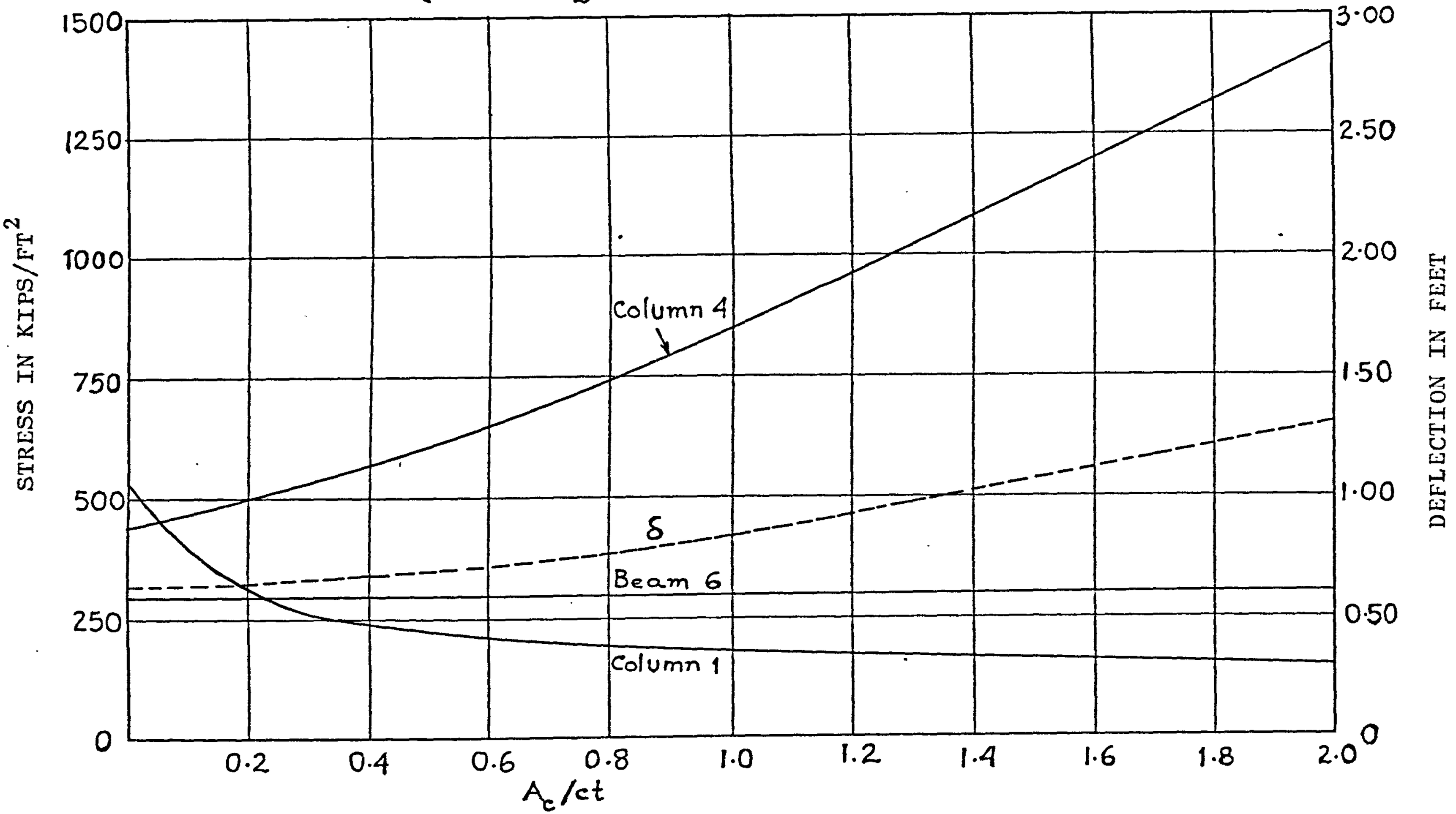

Fig. (2.24) Stresses and deflections for $\beta = 1.2$, $t_2 = 4.5$ ft.

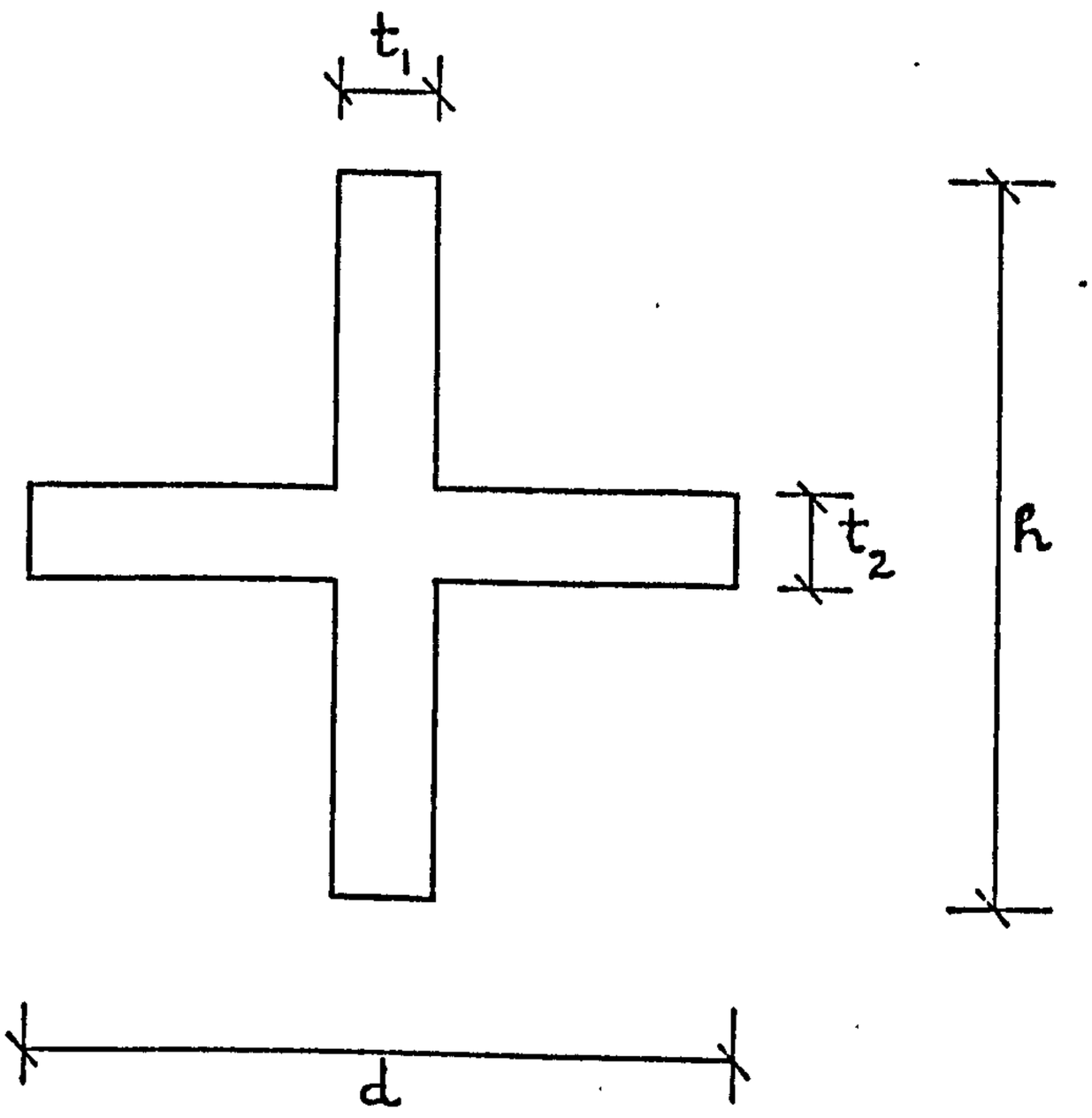

Fig. 2.25 Column-beam subsystem

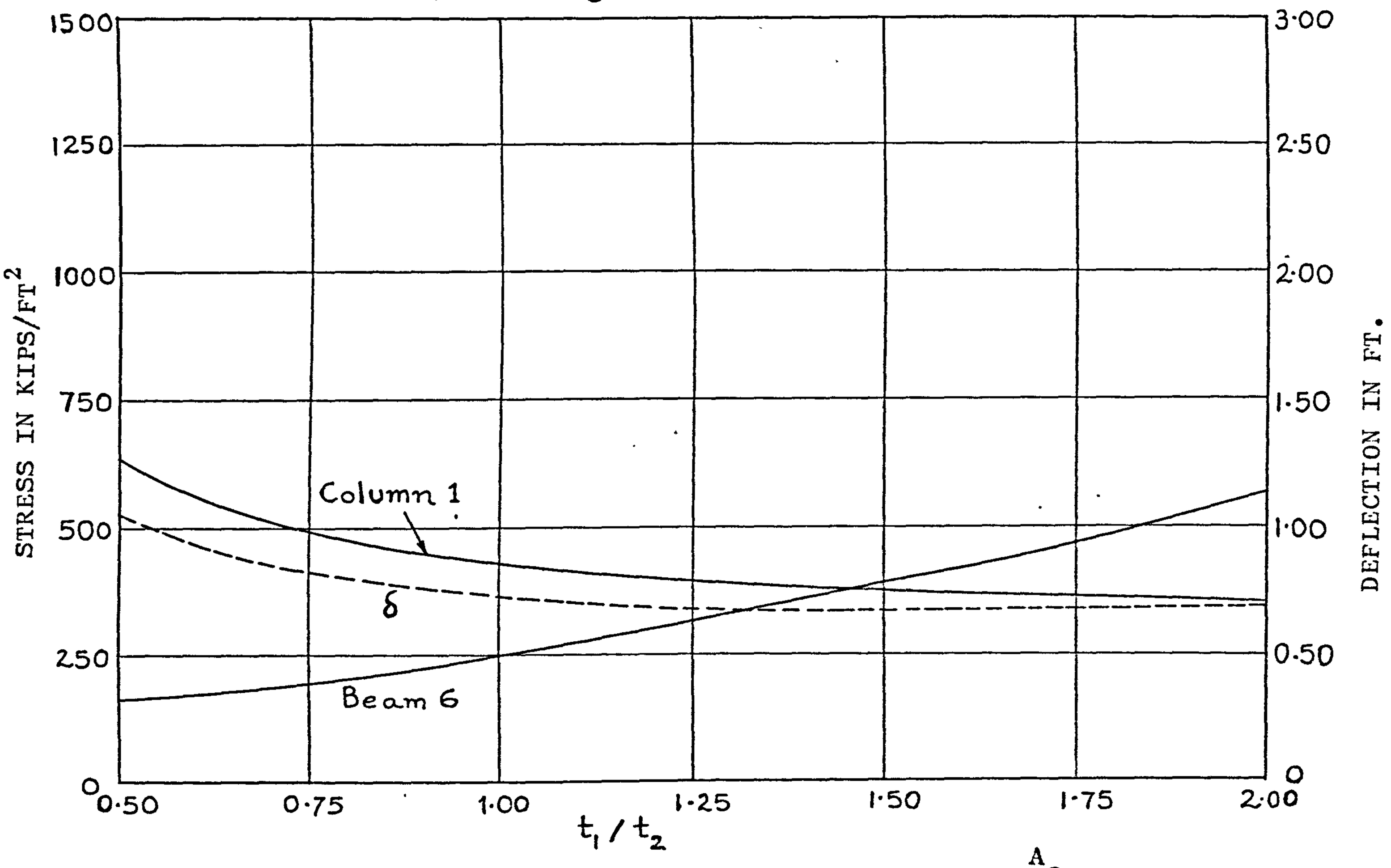

Fig. (2.26) Stresses and deflections for $\beta = 0.8$, $\frac{A_c}{ct} = 0$

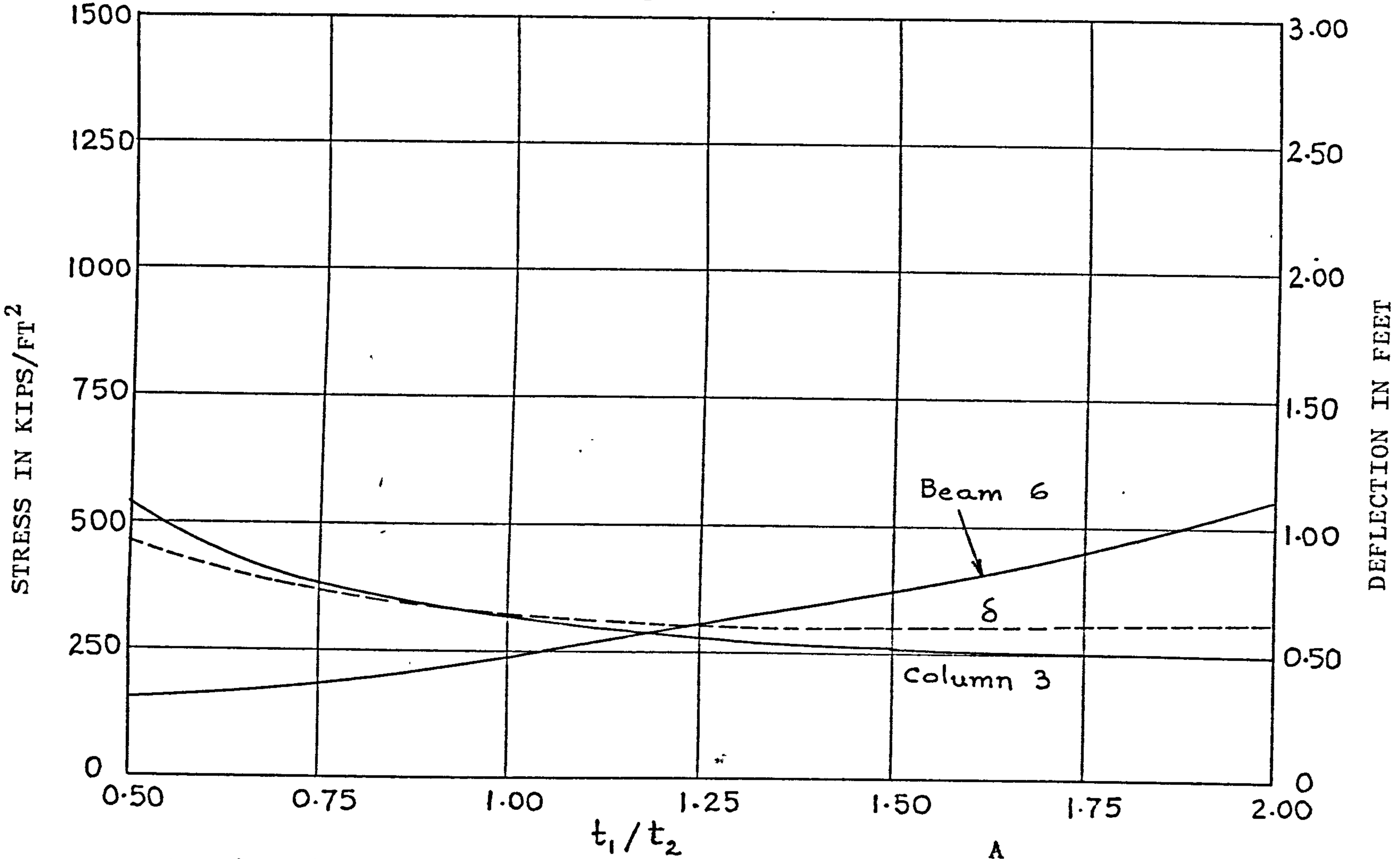

Fig. (2.27) Stresses and deflections for $\beta = 0.8$, $\frac{A_c}{ct} = 0.2$

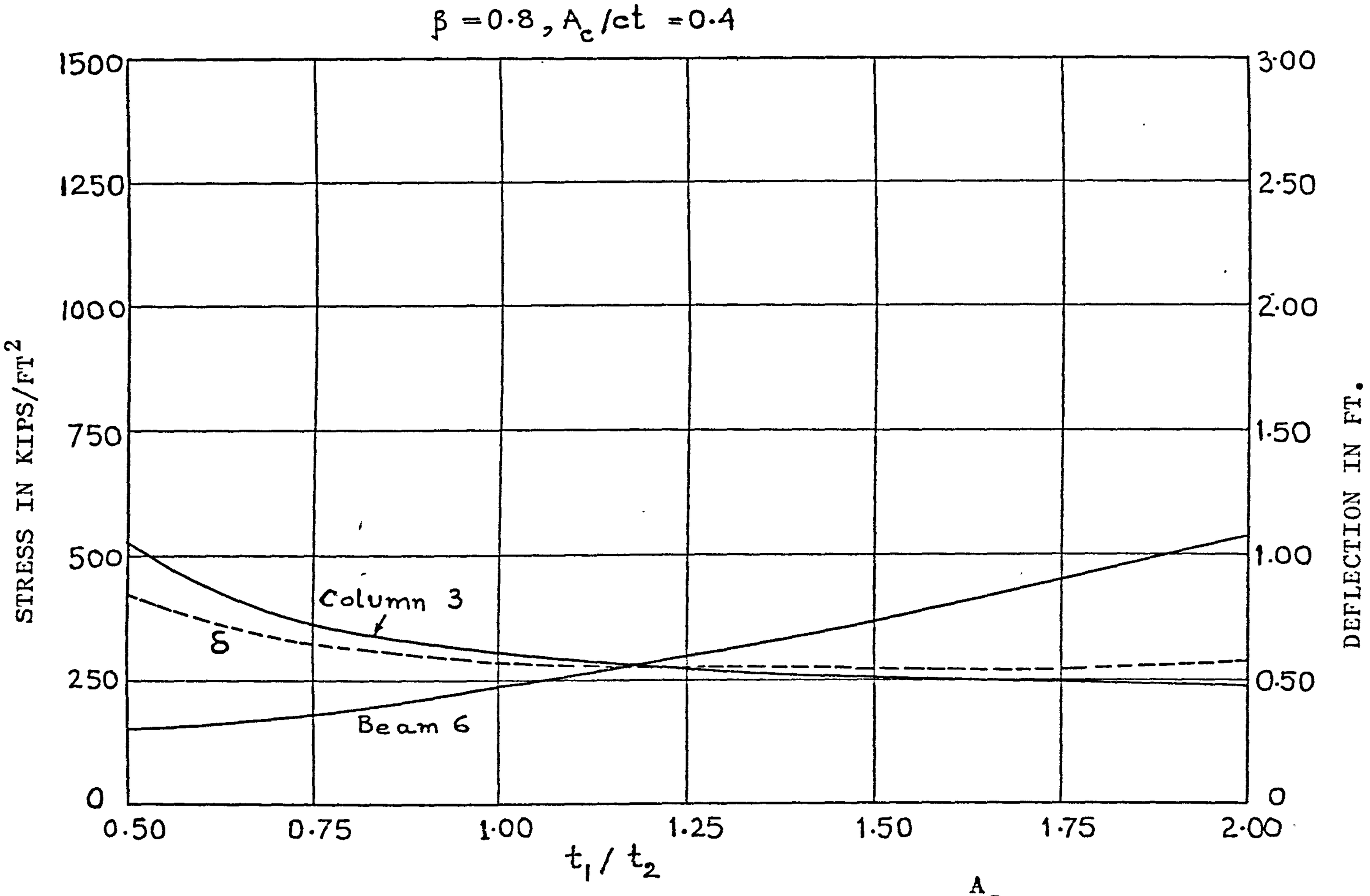

Fig. (2.28) Stresses and deflections for $\beta = 0.8$, $\frac{A_c}{ct} = 0.4$

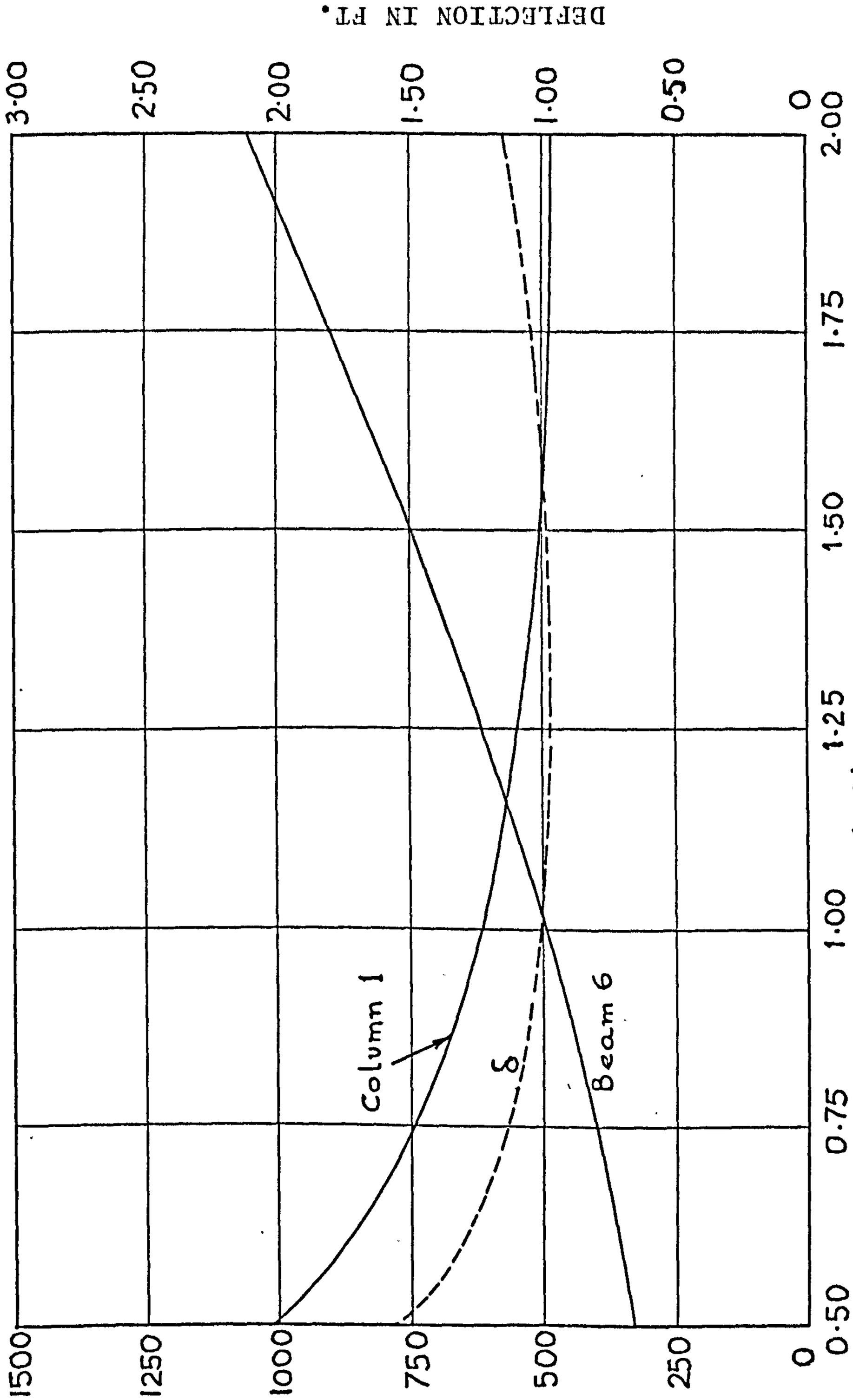

Fig. (2.29) Stresses and deflections for $\beta = 1.0$, $\frac{A_c}{ct} = 0$

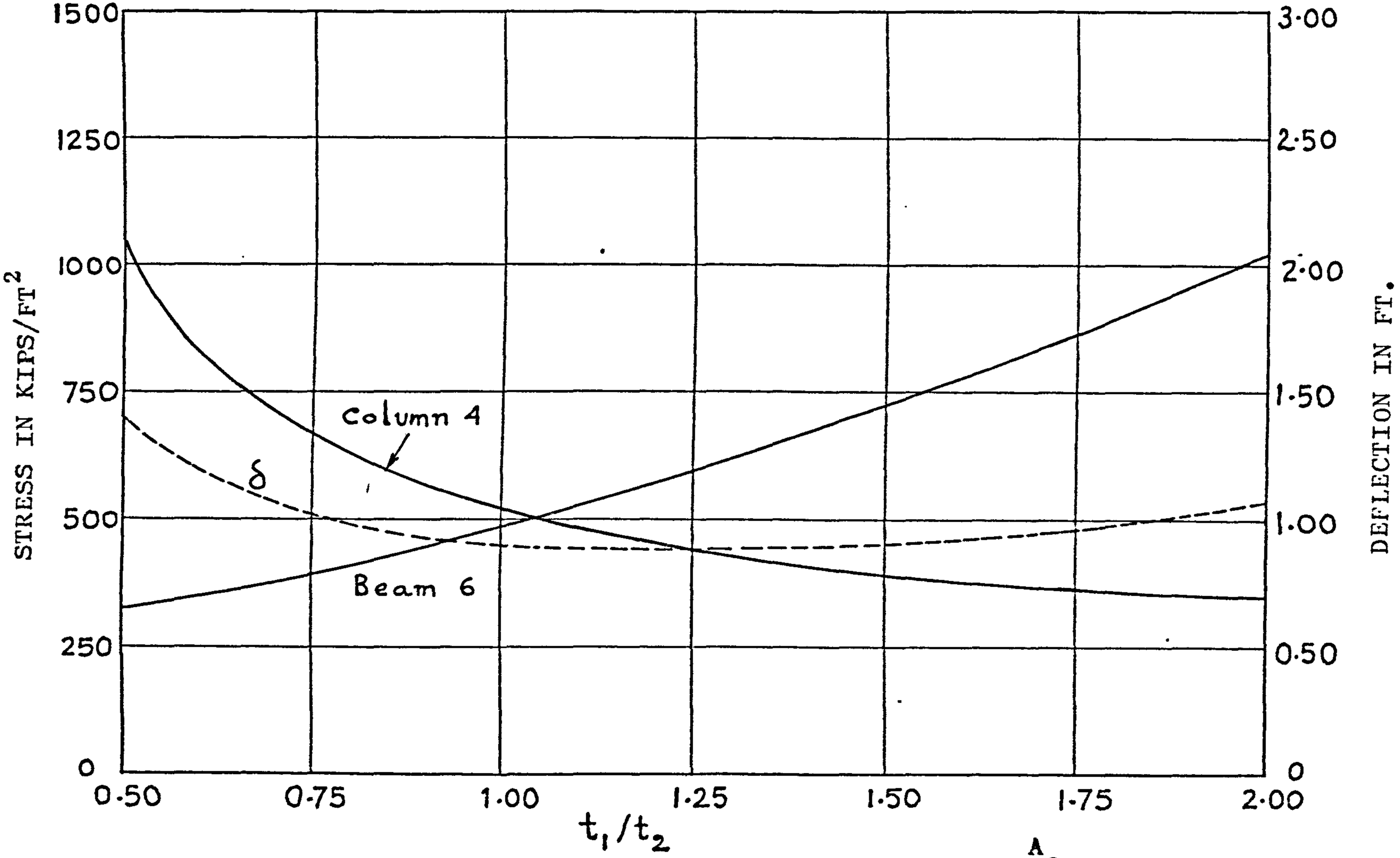

Fig. (2.30) Stresses and deflections for $\beta = 1.0$, $\frac{A_c}{ct} = 0.2$

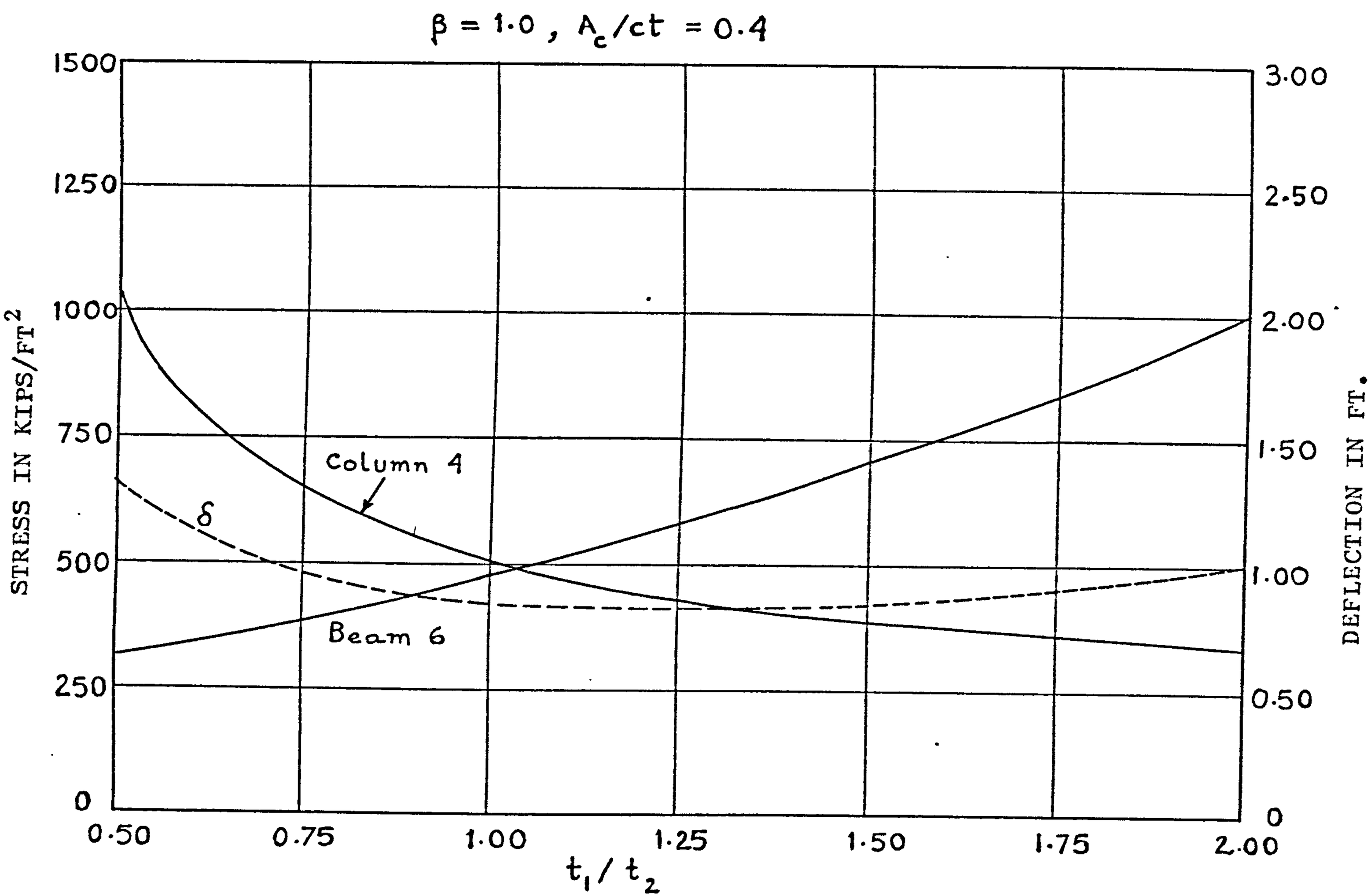

Fig. (2.31) Stresses and deflections for $\beta = 1.0$, $\frac{A_c}{ct} = 0.4$

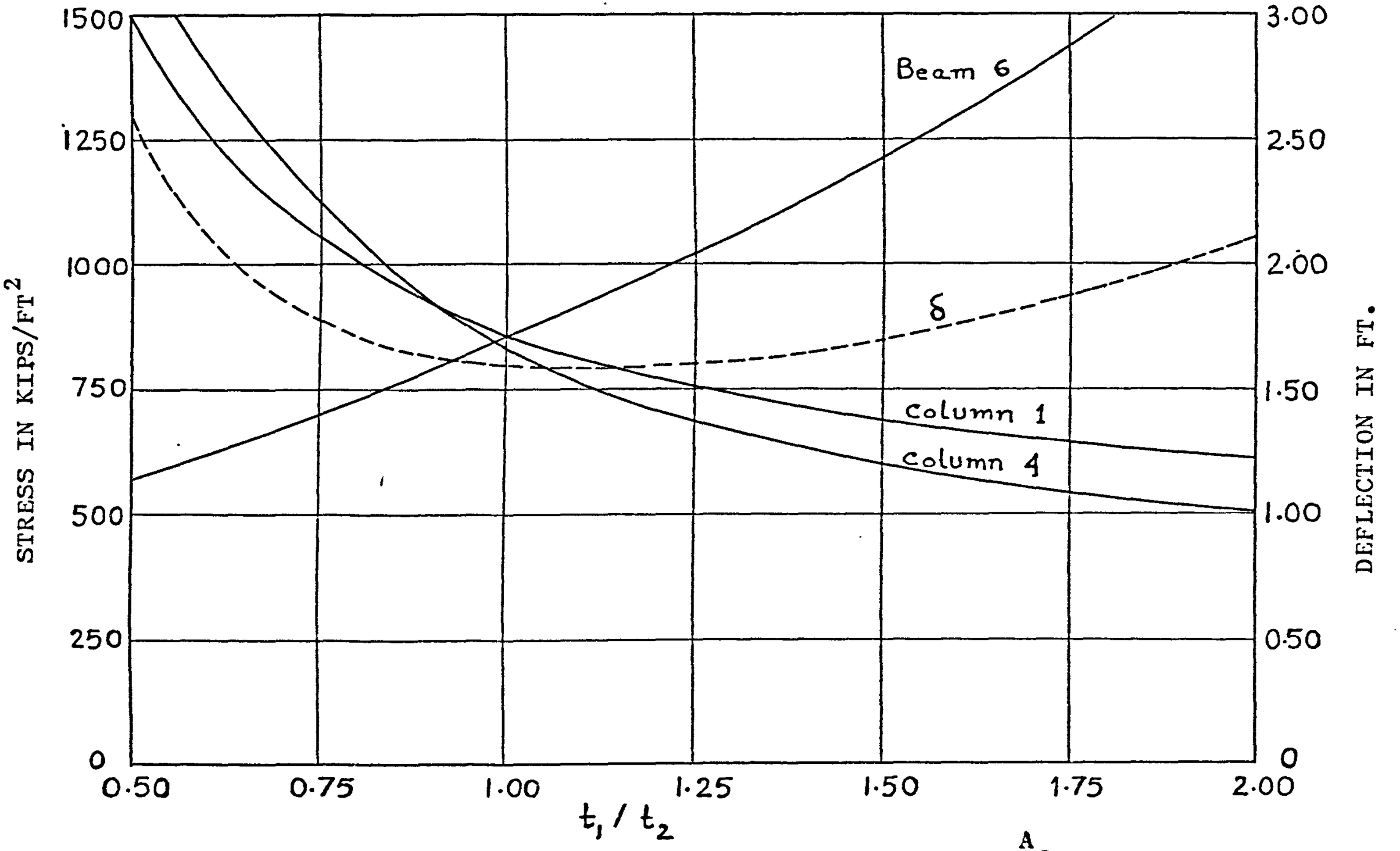

Fig. (2.32) Stresses and deflections for $\beta = 1.2$, $\frac{A_c}{ct} = 0$

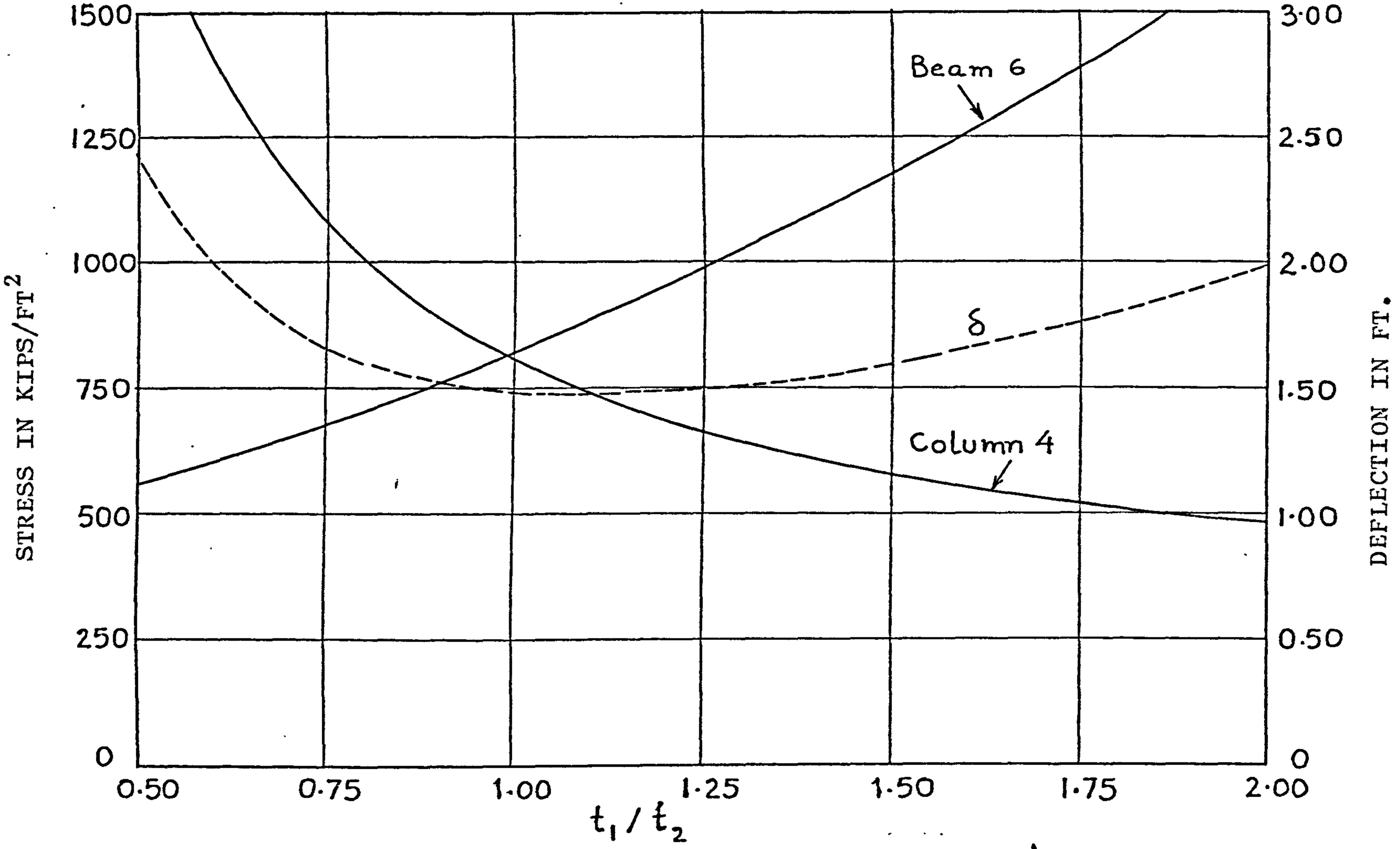

Fig. (2.33) Stresses and deflections for $\beta = 1.2$, $\frac{A_c}{ct} = 0.2$

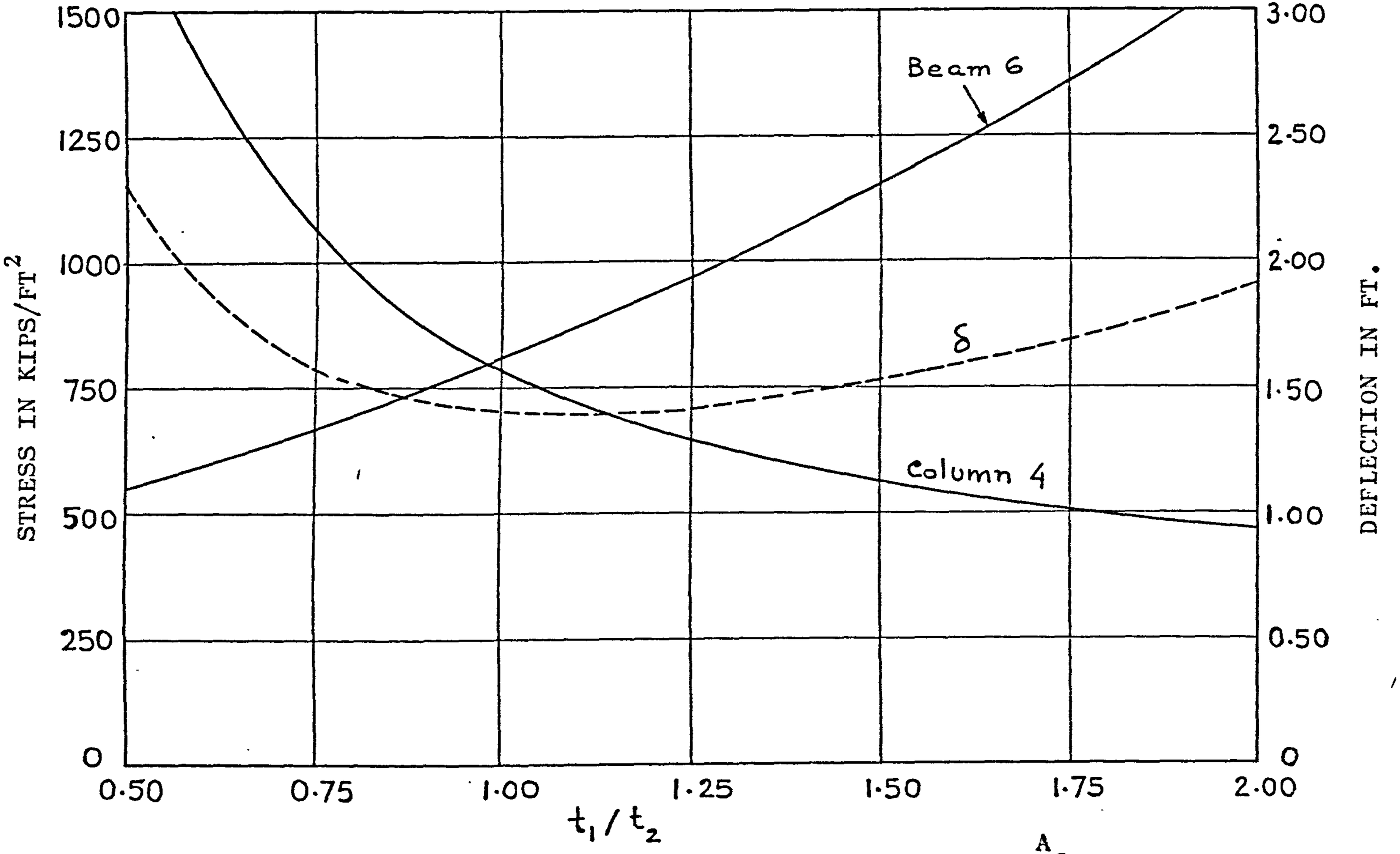

Fig. (2.34) Stresses and deflections for $\beta = 1.2$, $\frac{A_c}{ct} = 0.4$

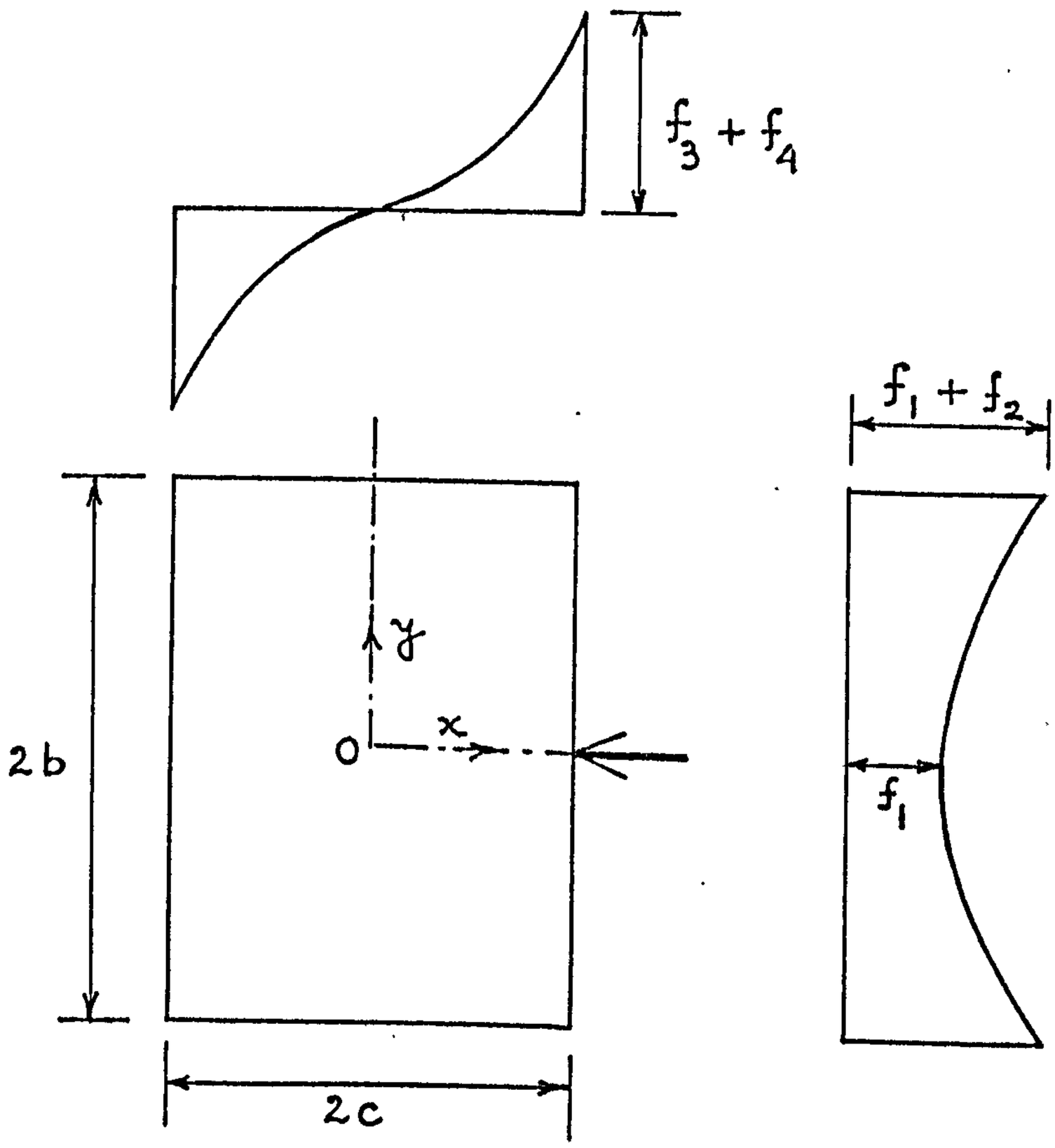

Fig. 2.35 Stresses in Framed-tube

CHAPTER 3

ANALYSIS OF FRAMED-TUBE STRUCTURES SUBJECTED TO TORSION

NOTATION

The following symbols are used in this chapter:

A_c	area of corner column;
a	aspect ratio (b/c);
b	half breadth of framed-tube;
c	half depth of framed-tube;
d	bay width;
E	elastic modulus;
F_2, F_3	Design functions for bending action corresponding to functions R_2 and R_3 for torsional action ;
G	equivalent shear modulus;
H	total height of building;
h	storey height;
k	structural parameter;
N	axial force in column;
n	ratio $\frac{A_c}{ct}$;
R_1, R_2, R_3	design functions;
r_0, r , r_1, r_2	stress functions;
S_b, S_c	shear forces in beam and column respectively;
T	torsional moment at any level;
T_o	concentrated torque applied at the top;
t	thickness of the equivalent orthotropic plate;

t_o torsional moment per unit height;

U total strain energy;

x, y horizontal coordinates;

z', z vertical coordinates;

β design factor ($\frac{R_2}{F_2}$ or $\frac{R_3}{F_3}$);

θ rotation at top of structure;

λ geometrical ratio;

ξ non-dimensional height coordinate ($\frac{z}{H}$);

σ direct stress;

τ shear stress;

τ_s St. Venant shear stress.

3.1 INTRODUCTION

In Chapter 2 a method was presented for the simplified analysis of framed-tube structures under bending actions. By replacing the discrete structure by an equivalent orthotropic tube, whose elastic properties were chosen to model both the axial and shearing or racking deformations of the framed panels, and making simplifying assumptions regarding the stress distributions in the structure, a simple second-order governing differential equation was obtained. Closed form solutions were obtained for three standard load cases, which enabled design curves to be derived for rapid approximate analyses of the dominant behaviour, suitable for design office use.

Provision was made in the analysis for the inclusion of stiffer individual corner elements, since in many practical situations the four corner columns are designed to be considerably stiffer than the others.

A similar simple analysis, based on the same basic assumptions regarding the structural behaviour, is presented in this chapter for the torsional analysis of framed-tube structures. Closed form solutions are obtained, and design curves are developed for three standard torsional loading cases, corresponding to those considered in the bending analyses, namely a point torque at the top, and uniformly and triangularly distributed twisting moments. It is shown that the design curves are identical in form to those derived for the bending case.

3.2 METHOD OF ANALYSIS

The application of a torsional moment to a framed-tube structure produces two forms of deformation, a pure rotation and an out-of-plane warping displacement of the cross-section. The combined action may be considered as a combination of plane frame actions of the four panels and the effects of the interactions between the orthogonal panels. It is again assumed that the floor slabs act as rigid diaphragms so that all structural elements at any cross-section rotate equally under torque. Twisting moments will be resisted primarily by shearing actions, giving rise to shear forces S_1 and S_2 in the frame panels, as illustrated in Fig. 3.1. The interactions between the orthogonal panels consist mainly of vertical interactive forces along the corners A, B, C and D. Torsional moments resisted by individual beam and column elements are assumed negligible in comparison with the primary action. If the rotations are small, the frame panels may be

assumed to deform in their own planes.

The spacings of the beams and columns are assumed uniform throughout the height, as is usually the case in practice. In addition, in order to simplify the analysis, it is assumed that both beams and columns are uniform throughout the height. This is not strictly necessary, and it is straightforward to extend the analysis to include a number of regions in which the beams and columns have constant stiffnesses. The framed-tube structure with different stiffness regions has been analysed for bending in Chapter 5 and a similar procedure may be followed for torsion as well.

It is then assumed that each framework panel of columns and spandrel beams may be replaced by an equivalent uniform orthotropic plate, to form a substitute closed tube structure. The substitute tube is assumed to have a uniform thickness t, with vertical elastic modulus E and shear modulus G. The use of an artificially low shear modulus G enables the racking deformations of the frame to be simulated in a way that the usual elastic moduli would not. The derivation of the properties of the orthotropic plate to model the vertical, horizontal and shearing stiffnesses of the frame panels was given in Chapter 2.

The stress system on a small element of each face of the equivalent tube is shown in Fig. 3.2.

The equations of equilibrium for the two mutually perpendicular panels are, in the absence of any body forces,

$$\left.\begin{aligned} \frac{\partial \sigma_x}{\partial x} + \frac{\partial \tau_{xz}}{\partial z} &= 0 \\ \frac{\partial \sigma'_z}{\partial z} + \frac{\partial \tau_{xz}}{\partial x} &= 0 \end{aligned}\right\} \quad \ldots\ldots \quad (3.1)$$

$$\left.\begin{aligned} \frac{\partial \sigma_y}{\partial y} + \frac{\partial \tau_{yz}}{\partial z} &= 0 \\ \frac{\partial \sigma_z}{\partial z} + \frac{\partial \tau_{yz}}{\partial y} &= 0 \end{aligned}\right\} \quad \ldots\ldots \quad (3.2)$$

Because of the symmetry of the system, the distributions of the direct stresses will be skew symmetrical about the centre-lines of each panel, whilst the shearing stresses will be symmetrical.

In order to model the anticipated distributions of stresses in the substitute system, as simply as possible, it is assumed that the shearing stresses may be expressed as parabolic distributions of the form,

$$\tau_{xz} = \frac{dr_o}{dz} + \left(\frac{x}{c}\right)^2 \frac{dr}{dz} \quad \ldots\ldots \quad (3.3)$$

$$\tau_{yz} = \frac{dr_1}{dz} + \left(\frac{y}{b}\right)^2 \frac{dr_2}{dz} \quad \ldots\ldots \quad (3.4)$$

where r_o, r, r_1 and r_2 are functions of the height coordinate z only.

Statically consistent distributions of the other stress components may then be obtained from the equilibrium conditions (3.1) and (3.2).

The total shear force S_1 at any level on face AB or DC is

$$S_1(z) = -t \int_{-c}^{c} \tau_{xz}\, dx \quad \ldots\ldots \quad (3.5)$$

where t is the thickness of equivalent uniform tube.

The total shear force S_2 on face AD or BC is, correspondingly,

$$S_2(z) = t \int_{-b}^{b} \tau_{yz}\, dy \qquad \ldots\ldots \quad (3.6)$$

The equation of torsional equilibrium at any level is,

$$2bS_1 + 2cS_2 = T(z) \qquad \ldots\ldots \quad (3.7)$$

where T(z) is the total applied twisting moment at that level.

Substituting equations (3.3), (3.4), (3.5) and (3.6) into equation (3.7) yields

$$-\frac{dr_o}{dz} - \tfrac{1}{3}\frac{dr}{dz} + \frac{dr_1}{dz} + \tfrac{1}{3}\frac{dr_2}{dz} = \frac{T}{4bct} \qquad \ldots\ldots \quad (3.8)$$

On substituting equations (3.3) and (3.4) into equations (3.1) and (3.2) and integrating, the vertical stresses σ_z' and σ_z are determined as,

$$\sigma_z' = -\frac{2x}{c^2} r \qquad \ldots\ldots \quad (3.9)$$

$$\sigma_z = -\frac{2y}{b^2} r_2 \qquad \ldots\ldots \quad (3.10)$$

For direct stresses the skew-symmetry of the stress-distribution was used to obtain the constants of integration involved.

The condition of vertical strain compatibility at the corners requires that,

$$\frac{1}{E}\,(\sigma'_z)_{x=c} = \frac{1}{E}\,(\sigma_z)_{y=b} = \frac{\sigma_c}{E} \qquad \ldots\ldots \quad (3.11)$$

in which σ_c is the axial stress in the corner column, given by,

$$\sigma_c = (\sigma'_z)_{x=c} = (\sigma_z)_{y=b} \qquad \ldots\ldots \quad (3.12)$$

Substituting equations (3.9) and (3.10) into equation (3.11) it is found that

$$r_2 = \frac{b}{c}\, r \qquad \ldots\ldots \quad (3.13)$$

The vertical stress σ_z, therefore, becomes

$$\sigma_z = -\frac{2y}{bc}\, r \qquad \ldots\ldots \quad (3.14)$$

The equation of equilibrium for the corner column may be shown to be (cf Fig. 3.3),

$$(\tau_{xz})_{x=c} + (\tau_{yz})_{y=b} = \frac{A_c}{t}\,\frac{\partial \sigma_c}{\partial z} \qquad \ldots\ldots \quad (3.15)$$

where A_c is the cross-sectional area of the corner column.

Substituting equations (3.3), (3.4), (3.9) and (3.12) into equation (3.14) gives

$$\frac{dr_o}{dz} + \frac{dr}{dz} + \frac{dr_1}{dz} + \frac{dr_2}{dz} = -\frac{2A_c}{ct}\,\frac{dr}{dz} \qquad \ldots\ldots \quad (3.16)$$

The functions r_o and r_1 are evaluated from equations (3.8), (3.13) and (3.16) in terms of the single function r as,

$$\frac{dr_o}{dz} = -\frac{T}{8bct} - \left(\tfrac{2}{3} + \tfrac{1}{3}\,\frac{b}{c} + \frac{A_c}{ct}\right)\frac{dr}{dz} \qquad \ldots\ldots \quad (3.17)$$

$$\frac{dr_1}{dz} = \frac{T}{8bct} - \left(\tfrac{1}{3} + \tfrac{2}{3}\,\frac{b}{c} + \frac{A_c}{ct}\right)\frac{dr}{dz} \qquad \ldots\ldots \quad (3.18)$$

The shear stresses τ_{xz} and τ_{yz} may, therefore, be expressed in terms of the single unknown function r(z) as,

$$\tau_{xz} = - \frac{T}{8bct} - \left[\tfrac{1}{3}(a + 3n + 2) - (\frac{x}{c})^2 \right] \frac{dr}{dz} \qquad (3.19)$$

$$\tau_{yz} = \frac{T}{8bct} - \left[\tfrac{1}{3}(2a + 3n + 1) - a(\frac{y}{b})^2 \right] \frac{dr}{dz} \qquad (3.20)$$

where $a = \frac{b}{c}$ and $n = \frac{A_c}{ct}$ ..... (3.21)

On substituting equations (3.19) and (3.20) into the equilibrium conditions (3.1) and (3.2) and integrating, the horizontal direct stress components are evaluated as

$$\sigma_x = c \left\{ \frac{1}{8bct} (\frac{x}{c}) \frac{dT}{dz} + \tfrac{1}{3} \left[(a + 3n + 2)(\frac{x}{c}) - (\frac{x}{c})^3 \right] \frac{d^2r}{dz^2} \right\}$$

..... (3.22)

$$\sigma_y = b \left\{ -\frac{1}{8bct} (\frac{y}{b}) \frac{dT}{dz} + \tfrac{1}{3} \left[(2a + 3n + 1)(\frac{y}{b}) - a(\frac{y}{b})^3 \right] \frac{d^2r}{dz^2} \right\}$$

..... (3.23)

The skew symmetry of the stress-distribution was again used to obtain the constants of integration.

The axial stress in the corner column becomes,

$$\sigma_c = (\sigma'_z)_{x=c} = - \frac{2}{c} r \qquad ..... \quad (3.24)$$

Because of the skew-symmetry of the rotational deformations, the axial stresses in the corner columns A and C will be opposite in sense from those in B and D.

The total strain energy, U, stored in the structure is

$$U = t \int_0^H \left\{ \int_{-c}^{c} \left[\frac{(\sigma'_z)^2}{E} + \frac{\tau_{xz}^2}{G} \right] dx + \right.$$

$$\int_{-b}^{b} \left[\frac{\sigma_z^2}{E} + \frac{\tau_{yz}^2}{G} \right] dy \Bigg\} \, dz + \frac{2A_c}{E} \int_0^H \sigma_c^2 \, dz \qquad (3.25)$$

It is assumed that, as a result of the high in-plane stiffness of the floor slabs, the horizontal strains are negligible, and the strain energy due to the horizontal direct stresses, σ_x and σ_y, may be ignored.

On substituting equations (3.9), (3.14), (3.19), (3.20) and (3.24) into equation (3.25) the total strain energy may be expressed as,

$$U = t \int_0^H \left[\frac{4}{Ec^4} \int_{-c}^{c} r^2 x^2 dx + \frac{1}{G} \int_{-c}^{c} \Bigg\{ \frac{T}{8bct} \right.$$

$$\left. + \left[\tfrac{1}{3}(a + 3n + 2) - \left(\frac{x}{c}\right)^2 \right] \frac{dr}{dz} \Bigg\}^2 dx \right.$$

$$+ \frac{4}{Eb^2c^2} \int_{-b}^{b} r^2 y^2 dy + \frac{1}{G} \int_{-b}^{b} \Bigg\{ \frac{T}{8bct} \right.$$

$$\left. - \left[\tfrac{1}{3}(2a + 3n + 1) - a\left(\frac{y}{b}\right)^2 \right] \frac{dr}{dz} \Bigg\}^2 dy \right.$$

$$\left. + \frac{8A_c}{Etc^2} r^2 \right] dz \qquad \ldots\ldots (3.26)$$

The strain energy integral must be a minimum, by virtue of the principle of least work. The condition for minimum U is that the variation of U, δU, must vanish, so that

$$\delta U = 2t \int_0^H \left[\frac{4}{Ec^4} \int_{-c}^{c} r \, \delta r \, x^2 \, dx + \frac{1}{G} \int_{-c}^{c} \Bigg\{ \frac{T}{8bct} + \right.$$

$$\left. \left[\tfrac{1}{3}(a + 3n + 2) - \left(\frac{x}{c}\right)^2 \right] \frac{dr}{dz} \Bigg\} \right.$$

$$\left\{ \tfrac{1}{3}\ (a + 3n + 2) - (\tfrac{x}{c})^2 \right\} \delta(\tfrac{dr}{dz})\, dx$$

$$+ \frac{4}{Eb^2c^2} \int_{-b}^{b} r\ \delta r\ y^2\, dy$$

$$+ \frac{1}{G} \int_{-b}^{b} \left\{ \frac{T}{8bct} - \left[\tfrac{1}{3}(2a + 3n + 1) - a(\tfrac{y}{b})^2 \right] \frac{dr}{dz} \right\} .$$

$$\left\{ - \left[\tfrac{1}{3}(2a + 3n + 1) - a(\tfrac{y}{b})^2 \right] \delta(\tfrac{dr}{dz}) \right\} dy$$

$$+ \frac{8A_c}{Etc^2} r\ \delta r \Bigg] dz = 0$$

Since $\delta(dr) = d(\delta r)$, there follows, by integration,

$$\int_0^H \Bigg[- \frac{1}{G}\frac{2c}{15}(a + 1)(3a^2 + 15n^2 + 10an + 2a + 10n + 3) \frac{d^2r}{dz^2}$$

$$+ \frac{1}{E}\frac{8}{3c}(a + 3n + 1)r + \frac{1}{G}\frac{1}{12bt}(a + 3n + 1)(a - 1)\frac{dT}{dz} \Bigg] dz\, \delta r$$

$$+ \Bigg[\frac{1}{G} \Bigg\{ \frac{2c}{15}(a + 1)(3a^2 + 15n^2 + 10an + 2a + 10n + 3) \frac{dr}{dz}$$

$$- \frac{1}{12bt}(a + 3n + 1)(a - 1)T \Bigg\} \delta r \Bigg]_0^H = 0 \qquad (3.27)$$

Since at the top σ_z' and $-\sigma_z$ are zero, it follows further that

$$\text{At } z = 0, \quad r = 0$$

$$\text{Hence at } z = 0, \quad \delta r = 0 \qquad \ldots\ldots \quad (3.28)$$

Also since $\delta r(z)$ is arbitrary, the integrands of the first term and the second term of equation (3.27) have to vanish separately, resulting in the following differential equation and the boundary condition for r(z):

$$\frac{d^2r}{dz^2} - 20\,\frac{G}{E}\left(\frac{H}{b}\right)^2 \frac{a^2(a + 3n + 1)}{(a + 1)(3a^2 + 15n^2 + 10an + 2a + 10n + 3)}\,\frac{r}{H^2}$$

$$= \frac{1}{8bct}\,\frac{5(a - 1)(a + 3n + 1)}{(a + 1)(3a^2 + 15n^2 + 10an + 2a + 10n + 3)}\,\frac{dT}{dz} \qquad \ldots\ldots \quad (3.29)$$

At $z = H$,

$$\frac{dr}{dz} - \frac{1}{8bct}\,\frac{5(a - 1)(a + 3n + 1)}{(a + 1)(3a^2 + 15n^2 + 10an + 2a + 10n + 3)}\,T = 0 \qquad \ldots\ldots \quad (3.30)$$

The differential equation (3.29) and the boundary condition (3.30) may be expressed as

$$\frac{d^2r}{dz^2} - \left(\frac{k}{H}\right)^2 r = \lambda^2 \frac{d\tau_s}{dz} \qquad \ldots\ldots \quad (3.31)$$

$$\text{At } z = H,\ \frac{dr}{dz} - \lambda^2 \tau_s = 0 \qquad \ldots\ldots \quad (3.32)$$

where the parameters k and λ may be defined as

$$k^2 = 20\,\frac{G}{E}\left(\frac{H}{b}\right)^2 \frac{a^2(a + 3n + 1)}{(a + 1)(3a^2 + 15n^2 + 10an + 2a + 10n + 3)}$$

$$\lambda^2 = \frac{5(a - 1)(a + 3n + 1)}{(a + 1)(3a^2 + 15n^2 + 10an + 2a + 10n + 3)} \qquad \ldots\ldots \quad (3.33)$$

For convenience, and to indicate the relationship between the perforated tube stresses and those derived from ordinary torsion theory of thin walled tubes, the right-hand side of equation (3.31) has been expressed in terms of τ_s, the St. Venant shear stress, given by,

$$\tau_s = \frac{T}{8bct} \qquad \ldots\ldots \quad (3.34)$$

The analogy between equations (3.31), (3.28) and (3.32) and the corresponding ones derived for the bending

of framed-tube structures in Chapter 2 (equations 2.45, 2.41 and 2.46) will be obvious.

In the particular case where the corner columns are of the same stiffness as the others, so that they can be included as a segment of the equivalent orthotropic plate, the concentrated corner area A_c is zero, and the parameters k^2 and λ^2 reduce to

$$k^2 = 20 \frac{G}{E} \left(\frac{H}{b}\right)^2 \frac{a^2}{3a^2 + 2a + 3} \quad \ldots\ldots (3.35)$$

$$\lambda^2 = \frac{5(a - 1)}{3a^2 + 2a + 3}$$

In equations (3.33) and (3.35), it is convenient to denote the greater side of the framed-tube by 2b, so that the aspect ratio a is always greater than or equal to unity. In that case, the parameters k^2 and λ^2 are always positive.

The homogeneous part of the solution of equation (3.31) may thus always be expressed in the form

$$r = K_1 \cosh \frac{k}{H} z + K_2 \sinh \frac{k}{H} z \quad \ldots\ldots (3.36)$$

in which K_1 and K_2 are integration constants to be determined from the boundary conditions.

The particular integral part of the solution will depend on the form of the applied torsional loading and the resultant St. Venant shear stress τ_s.

In the particular case of a square section, a = 1, and the parameter λ^2 becomes zero.

Solutions are derived for three standard load cases corresponding to those considered for bending actions

in Chapter 2.

Case 1 Concentrated torque T_o at the top

In this case, the St. Venant shear stress, τ_s, is constant and is given by

$$\tau_s = \frac{T_o}{8bct}$$

The particular integral is zero and the complete solution of equation (3.31), subject to the boundary conditions (3.28) and (3.32), becomes

$$r(\xi) = \frac{\lambda^2}{k} H \tau_s \frac{\sinh k\xi}{\cosh k} \quad \ldots\ldots \quad (3.37)$$

where ξ is the non-dimensional height coordinate given by

$$\xi = \frac{z}{H}$$

Case 2 Uniformly distributed twisting moment of intensity t_o per unit height

In this case, the total torque T at any level is given by

$$T = t_o z \quad \text{and} \quad \tau_s = \frac{t_o z}{8bct}$$

The particular integral is given by,

$$r = -\frac{\lambda^2}{k^2} \frac{t_o}{8bct} H^2$$

and the complete solution becomes,

$$r(\xi) = \frac{\lambda^2}{k^2} H \tau_s(H) \left[\frac{\cosh k(1-\xi) + k \sinh k\xi}{\cosh k} - 1 \right]$$

$\ldots\ldots$ (3.38)

where $\tau_s(H) = \frac{t_o H}{8bct}$

Case 3 Triangularly distributed torque

For a torque whose intensity varies linearly from zero at the base to a value of t_o per unit height at the top,

$$T = t_o(z - \frac{z^2}{2H}) \quad , \quad \tau_s = \frac{t_o}{8bct}\ (z - \frac{z^2}{2H})$$

The particular integral is given by,

$$r = - \frac{\lambda^2}{k^2}\ \frac{t_o H^2}{8bct}\ (1 - \frac{z}{H})$$

The complete solution becomes,

$$r(\xi) = \frac{2\lambda^2}{k^2}\ H\ \tau_s(H)\ .$$

$$\left[\frac{2k \cosh k(1 - \xi) + (k^2 - 2) \sinh k\xi}{2k \cosh k} - (1 - \xi) \right]$$

..... (3.39)

where $\tau_s(H) = \frac{t_o H}{16bct}$

3.3 DESIGN CURVES

The torsional loads will, in each of the three standard load cases, be given by a situation where the corresponding lateral load is offset from the central axis of the building.

In order to produce simple design curves, it is convenient to express the four important design stress components σ'_z, σ_z, τ_{xz} and τ_{yz} in the following forms,

$$\sigma'_z = - \frac{2x}{c^2}\ H\ \tau_s(H)\ R_1 R_2$$

$$\sigma_z = - \frac{2y}{bc}\ H\ \tau_s(H)\ R_1 R_2$$

$$\tau_{xz} = -\ \tau_s - \left[\tfrac{1}{3}(a + 3n + 2) - (\tfrac{x}{c})^2 \right]\ \tau_s(H)\ R_1 R_3$$

$$\tau_{yz} = \ \tau_s - \left[\tfrac{1}{3}(2a + 3n + 1) - a(\tfrac{y}{b})^2 \right]\ \tau_s(H)\ R_1 R_3$$

..... (3.40)

in which the parameters τ_s, $\tau_s(H)$, and the functions R_1, R_2 and R_3 are given in Table 3.1 for the three load cases. For convenience, the functions have been expressed in terms of the non-dimensional height coordinate ξ.

The terms τ_s and $\tau_s(H)$ are functions of load form only.

The function R_1, equal to λ^2, depends only on the cross-sectional shape (a) and the relative size of the corner columns (n). Fig. 3.4 shows the variation of the function R_1 with the two ratios a and n.

The functions R_2 and R_3 depend on the stiffness parameter k and the height ξ. The stiffness parameter k depends in turn on the ratios $\frac{G}{E}$, $\frac{H}{b}$, a and n. These functions are of the same form as the corresponding functions F_2 and F_3 derived for the bending of framed-tube structures (cf. Table 2.1 of Chapter 2). It is seen that in the case of a point torque at the top, the functions R_2 and R_3 are identical to the functions F_2 and F_3 for a point load at the top; in the case of a uniformly distributed torque, the value of functions R_2 and R_3 are half of the values of the functions F_2 and F_3 derived for a uniformly distributed lateral loading; and in the case of a triangularly distributed torque, the values of the functions R_2 and R_3 are $\frac{2}{3}$ of the values of

functions F_2 and F_3 derived for a triangularly distributed lateral loading.

The variations of the stress functions F_2 and F_3 with the parameters k and ξ were shown in Figs. 2.8 to 2.13 for the three corresponding lateral load cases in Chapter 2. Consequently the same curves may be used directly for the case of the corresponding torsional loadings if the functions R_2 and R_3 are derived by multiplying the corresponding values of F_2 and F_3 in Chapter 2 by the factor β (1, $\frac{1}{2}$, or $\frac{2}{3}$ as appropriate) as indicated in Table 3.1. It is thus unnecessary to reproduce the curves in this chapter.

In the case of a square tube, $\lambda^2 = 0$, and the values of the stresses reduce to

$$\sigma_z' = \sigma_z = 0$$

$$\sigma_x = x \frac{d\tau_s}{dz} \quad ; \quad \sigma_y = -y \frac{d\tau_s}{dz}$$

$$\tau_{xz} = -\tau_s \quad ; \quad \tau_{yz} = \tau_s$$

In this case, because of symmetry, the stress system degenerates to the case of a pure St. Venant torsional shear stress, and no warping occurs.

3.4 USE OF DESIGN CURVES

For a given structure, the values of the effective elastic and shear moduli, E and G, may be determined from the formulae given in Chapter 2 (Article 2.3). The values of a and n are obtained from equation (3.21) and the value of k from equation (3.33). The function R_1 (i.e., λ^2) may be interpolated from the curves of Fig.3.4

or evaluated directly from equation (3.33). For the standard load condition specified, the values of the functions R_2 and R_3 follow by factoring the values of F_2 and F_3 by β, F_2 and F_3 having been obtained at the level being investigated, from the appropriate curves in Chapter 2. For this purpose, the corresponding standard loadings are:

Concentrated torque T_o at top $\equiv$ Point load at top

Uniformly distributed torque $\equiv$ Uniformly distributed lateral load

Triangularly distributed torque $\equiv$ Triangularly distributed lateral load.

Knowing the values of τ_s and $\tau_s(H)$, the stress components at the level concerned are given by equations (3.40).

Design curves have not been given for the horizontal axial stresses σ_x and σ_y since they are generally small. However, if necessary, they may be determined from equations (3.22) and (3.23).

3.5 CALCULATION OF COLUMN AND BEAM FORCES

The results from the substitute continuous system must be transformed into the real discrete structure to give the shears, and hence moments, and axial forces in the beams and columns. These are obtained simply by integrating the stress distribution over the particular bay width or storey level as required.

The axial forces in the columns and the shearing forces in the columns and spandrel beams, for the two

mutually perpendicular panels are derived below. The axial force in the corner area A_c is also given.

PANELS AD & BC

(i) The axial force in column at position y_i is given by

$$N_i = t \int_{y_i - \frac{d}{2}}^{y_i + \frac{d}{2}} \sigma_z \, dy$$

On substituting the value of σ_z from the equation (3.14) and integrating, the axial force becomes,

$$N_i = - \frac{2td}{bc} y_i r \qquad \ldots\ldots (3.41)$$

(ii) The axial force in corner column is

$$N_1 = t \int_{b - \frac{d}{2}}^{b} \sigma_z \, dy$$

$$= - \frac{td}{bc} (b - \frac{d}{4}) r \qquad \ldots\ldots (3.42)$$

(iii) The shear force in column at position y_i is given by

$$S_{c_i} = t \int_{y_i - \frac{d}{2}}^{y_i + \frac{d}{2}} \tau_{yz} \, dy$$

$$= td \left[\tau_s - \frac{1}{3H} \left\{ (2a+3n+1) - \frac{a}{b^2}(3y_i^2 + \frac{d^2}{4}) \right\} \frac{dr}{d\xi} \right]$$

$\ldots\ldots$ (3.43)

(iv) The shear force in corner column becomes

$$S_{c_1} = t \int_{b-\frac{d}{2}}^{b} \tau_{yz} \, dy$$

$$= \frac{td}{2}\left[\tau_s - \frac{i}{3H}\left\{(2a+3n+1) - \frac{a}{b^2}(3b^2 - \frac{3}{2}bd + \frac{d^2}{4})\right\}\frac{dr}{d\xi}\right]$$

..... (3.44)

(v) The shear force in spandrel beam at position y_i and level z_j is given by

$$S_{b_i} = t \int_{z_j - \frac{h}{2}}^{z_j + \frac{h}{2}} \tau_{yz} \, dz$$

For a concentrated torque at the top or a uniformly distributed torque for the whole height, the shear force in the spandrel beam may be expressed as

$$S_{b_{ij}} = t\left[h\,\tau_s - \left\{\tfrac{1}{3}(2a+3n+1) - a(\frac{y_i}{b})^2\right\} \cdot \left\{r(z_j + \frac{h}{2}) - r(z_j - \frac{h}{2})\right\}\right] \quad (3.45)$$

In the case of triangularly distributed torque the shear force in the spandrel beam becomes

$$S_{b_{ij}} = t\left[2\,\frac{h}{H}\,\tau_s(H)\left\{z_j - \frac{1}{6H}(3z_j^2 + \frac{h^2}{4})\right\} - \left\{\tfrac{1}{3}(2a+3n+1) - a(\frac{y_i}{b})^2\right\}\left\{r(z_j + \frac{h}{2}) - r(z_j - \frac{h}{2})\right\}\right]$$

..... (3.46)

PANELS AB & DC

(i) The axial force in column at position x_i is

$$N_i = t \int_{x_i - \frac{d}{2}}^{x_i + \frac{d}{2}} \sigma_z' \, dx \qquad = -\frac{2td}{c^2}\, x_i\, r \qquad \ldots\ldots \quad (3.47)$$

(ii) The axial force in corner column is given by

$$N_1 = t \int_{c-\frac{d}{2}}^{c} \sigma'_z \, dx = -\frac{td}{c^2}\left(c - \frac{d}{4}\right)r \qquad \ldots\ldots (3.48)$$

(iii) The shear force in column at position x_i becomes

$$S_{c_i} = t \int_{x_i - \frac{d}{2}}^{x_i + \frac{d}{2}} \tau_{xz} \, dx$$

$$= -td\left[\tau_s + \frac{1}{3H}\left\{(a+3n+2) - \frac{1}{c^2}\left(3x_i^2 + \frac{d^2}{4}\right)\right\}\frac{dr}{d\xi}\right]$$

$\ldots\ldots$ (3.49)

(iv) The shear force in corner column is

$$S_{c_1} = t \int_{c-\frac{d}{2}}^{c} \tau_{xz} \, dx$$

$$= -\frac{td}{2}\left[\tau_s + \frac{1}{3H}\left\{(a+3n+2) - \frac{1}{c^2}\left(3c^2 - \frac{3}{2}cd + \frac{d^2}{4}\right)\right\}\frac{dr}{d\xi}\right]$$

$\ldots\ldots$ (3.50)

(v) The shear force in spandrel beam at position x_i and level z_j becomes

$$S_{b_{ij}} = t \int_{z_j - \frac{h}{2}}^{z_j + \frac{h}{2}} \tau_{xz} \, dz$$

In case of a concentrated torque at the top or uniformly distributed torque, the shear force in a spandrel beam becomes,

$$S_{b_{ij}} = -t\left[h\,\tau_s + \left\{\tfrac{1}{3}(a+3n+2) - \left(\frac{x_i}{c}\right)^2\right\}\left\{r\left(z_j + \frac{h}{2}\right) - r\left(z_j - \frac{h}{2}\right)\right\}\right]$$

$\ldots\ldots$ (3.51)

In case of a triangularly distributed torque the shear force in a spandrel beam is

$$S_{b_{ij}} = -t \left[2 \frac{h}{H} \tau_s(H) \left\{ z_j - \frac{1}{6H} (3z_j^2 + \frac{h^2}{4}) \right\} + \left\{ \frac{1}{3}(a+3n+2) - (\frac{x_i}{c})^2 \right\} \left\{ r(z_j + \frac{h}{2}) - r(z_j - \frac{h}{2}) \right\} \right] \quad \ldots\ldots (3.52)$$

CORNER AREA A_c

The axial force in the corner area A_c becomes

$$N_c = A_c \sigma_c$$

On substituting the value of σ_c from equation (3.24), N_c becomes

$$N_c = -2ntr \quad \ldots\ldots (3.53)$$

The total axial force in the corner column is the sum of the three values obtained by equations (3.42), (3.48) and (3.53).

3.6 ASSESSMENT OF ROTATION

The rotation at the top of the structure may again be evaluated by means of the principle of virtual work.

The stresses under a uniformly distributed torque t_o may be evaluated from equations (3.9), (3.14), (3.19), (3.20) and (3.24) and are expressed as

$$\sigma'_z = -\frac{\lambda^2}{k^2} \frac{t_o H^2}{4bc^3 t} x \left[\frac{\cosh k(1-\xi) + k \sinh k\xi}{\cosh k} - 1 \right]$$

$$\sigma_z = -\frac{\lambda^2}{k^2} \frac{t_o H^2}{4b^2 c^2 t} y \left[\frac{\cosh k(1-\xi) + k \sinh k\xi}{\cosh k} - 1 \right]$$

$$\sigma_c = -\frac{\lambda^2}{k^2}\frac{t_o H^2}{4bc^2 t}\left[\frac{\cosh k(1-\xi) + k \sinh k\xi}{\cosh k} - 1\right]$$

$$\tau_{xz} = -\frac{t_o H}{8bct}\left\{\xi + \frac{\lambda^2}{k}\left[\tfrac{1}{3}(a+3n+2) - (\tfrac{x}{c})^2\right] \cdot \left[\frac{k \cosh k\xi - \sinh k(1-\xi)}{\cosh k}\right]\right\}$$

$$\tau_{yz} = \frac{t_o H}{8bct}\left\{\xi - \frac{\lambda^2}{k}\left[\tfrac{1}{3}(2a+3n+1) - a(\tfrac{y}{b})^2\right] \cdot \left[\frac{k \cosh k\xi - \sinh k(1-\xi)}{\cosh k}\right]\right\} \quad (3.54)$$

From the stresses given in equation (3.54) the true strains can be evaluated by the stress-strain relationships

$$\epsilon = \frac{\sigma}{E} \quad ; \quad \gamma = \frac{\tau}{G}$$

A unit torque is applied at the top due to which the virtual stresses may be expressed as,

$$\sigma'_z = -\frac{\lambda^2}{k \cosh k}\frac{H}{4bc^3 t} \; x \sinh k\xi$$

$$\sigma_z = -\frac{\lambda^2}{k \cosh k}\frac{H}{4b^2c^2 t} \; y \sinh k\xi$$

$$\sigma_c = -\frac{\lambda^2}{k \cosh k}\frac{H}{4bc^2 t} \sinh k\xi \quad (3.55)$$

$$\tau_{xz} = -\frac{1}{8bct}\left\{1 + \frac{\lambda^2}{\cosh k}\left[\tfrac{1}{3}(a+3n+2) - (\tfrac{x}{c})^2\right] \cosh k\xi\right\}$$

$$\tau_{yz} = \frac{1}{8bct}\left\{1 - \frac{\lambda^2}{\cosh k}\left[\tfrac{1}{3}(2a+3n+1) - a(\tfrac{y}{b})^2\right] \cosh k\xi\right\}$$

The rotation θ at the top of the structure is

given by

$$\theta = 2\int_0^H \int_{-c}^{c} \sigma\epsilon\ t\ dx\ dz + 2\int_0^H \int_{-b}^{b} \sigma\epsilon\ t\ dy\ dz +$$

$$4\int_0^H (\sigma\epsilon)_c\ A_c\ dz \qquad \ldots\ldots (3.56)$$

On substituting the values of σ and ϵ in equation (3.56) and integrating with respect to x and y the rotation θ becomes

$$\theta = \frac{t_o H^4}{12b^2c^3t\ E}\ \frac{\lambda^4}{k^3\cosh k}\ (a + 3n + 1)\int_0^1 \sinh k\xi\ \cdot$$

$$\left[\frac{\cosh k(1-\xi) + k\sinh k\xi}{\cosh k} - 1\right] d\xi$$

$$+ \frac{t_o H^2}{16b^2ctG}\int_0^1 \left\{ (a+1)\xi - \frac{\lambda^2}{3\cosh k}(a-1)(a+3n+1)\cdot \right.$$

$$\xi\cosh k\xi - \frac{\lambda^2}{3k\cosh k}(a-1)(a+3n+1)\cdot$$

$$\left[k\cosh k\xi - \sinh k(1-\xi)\right]$$

$$+ \frac{\lambda^4}{15k\cosh^2 k}(a+1)(3a^2 + 15n^2 + 10an + 2a + 10n + 3)\cdot$$

$$\left. \cosh k\xi \left[k\cosh k\xi - \sinh k(1-\xi)\right]\right\} d\xi$$

Integrating with respect to ξ the rotation θ is found out as

$$\theta = \frac{t_o H^4}{24b^2c^3t\ E}(a+3n+1)\ \frac{\lambda^4}{k^4\cosh^2 k}\ (2\cosh k - 2\cosh^2 k$$

$$- k^2 + k\sinh k + k\sinh k\cosh k)$$

$$+ \frac{t_o H^2}{32b^2 ctG}(a+1)\left[1 - \frac{4(a-1)(a+3n+1)}{3(a+1)} \cdot \frac{\lambda^2}{k^2 \cosh k} \cdot (k \sinh k - \cosh k + 1)\right.$$

$$\left. + \frac{1}{15}(3a^2 + 15n^2 + 10an + 2a + 10n + 3) \cdot \frac{\lambda^4}{k \cosh^2 k} \cdot (k - \sinh k + \sinh k \cosh k)\right] \quad \ldots\ldots (3.57)$$

In the particular case of a square section ($\lambda^2 = 0$) of side 2b the rotation equation reduces to

$$\theta = \frac{t_o H^2}{16b^3 t G} \quad \ldots\ldots (3.58)$$

Similar expressions may be derived for the other standard load cases. In case of a concentrated torque T_o applied at the top, the rotation θ at the top may be expressed as,

$$\theta = \frac{T_o H^3}{24b^2 c^3 tE}(a+3n+1)\frac{\lambda^4}{k^2 \cosh^2 k}\left(\frac{\sinh 2k}{2k} - 1\right)$$

$$+ \frac{T_o H}{16b^2 ctG}(a+1)\left[1 - \frac{2(a-1)(a+3n+1)}{3(a+1)}\frac{\lambda^2}{k}\tanh k\right.$$

$$+ \frac{1}{30}(3a^2 + 15n^2 + 10an + 2a + 10n + 3)\frac{\lambda^4}{\cosh^2 k} \cdot \left.\left(\frac{\sinh 2k}{2k} + 1\right)\right] \quad \ldots\ldots (3.59)$$

3.7 ASSESSMENT OF WARPING

Due to the different senses of bending actions in the frame panels on opposite sides of the tube, warping

of the floor slabs will occur in rectangular tubes. The vertical strains which arise due to the direct stress σ'_z and σ_z may be summed up to give the total vertical movement at each corner at the top of the structure, in order to determine the maximum relative movement between the corners. This warping action may be of importance when considering the action of torsion on non-structural partitions as well as the floor system.

The total vertical movement, w, at the corner at the top of the structure is given by,

$$w = \int_0^H \frac{\sigma_c}{E} \, dz \qquad \ldots\ldots (3.60)$$

On substituting equation (3.24) into equation (3.60), the vertical movement w becomes

$$w = -\frac{2}{cE} \int_0^H r \, dz \qquad \ldots\ldots (3.61)$$

Solutions are derived for the three standard load cases mentioned earlier in Article 3.2.

Case 1 Concentrated torque T_o at the top

On substituting equation (3.37) into equation (3.61) and integrating, it is found that

$$w = -\frac{2}{cE} \frac{\lambda^2}{k^2} H^2 \tau_s \frac{\cosh k - 1}{\cosh k} \qquad \ldots\ldots (3.62)$$

where $\tau_s = \frac{T_o}{8bct}$

Case 2 Uniformly distributed twisting moment of intensity t_o per unit height

From equations (3.38) and (3.61) the vertical movement w is determined as

$$w = - \frac{2}{cE} \frac{\lambda^2}{k^2} H^2 \tau_s(H) \frac{\sinh k - k}{k \cosh k} \quad \ldots\ldots (3.63)$$

where $\tau_s(H) = \frac{t_o H}{8bct}$

Case 3 Triangularly distributed torque

For a torque whose intensity varies linearly from zero at the base to a value of t_o per unit height at the top, the stress function r was given earlier by equation (3.39). On substituting equation (3.39) into equation (3.61) and integrating, the vertical movement w becomes,

$$w = - \frac{2}{cE} \frac{\lambda^2}{k^2} H^2 \tau_s(H) \left[\frac{2 \sinh k + \frac{k^2 - 2}{k} (\cosh k - 1)}{k \cosh k} - 1 \right] \quad \ldots\ldots (3.64)$$

where $\tau_s(H) = \frac{t_o H}{16bct}$

3.8 NUMERICAL EXAMPLE

The high-rise building described in Article 2.9 is analysed here for the case where the lateral load of 1 kN/m height is offset from the central axis of the building by 0.1 times the total width of the building.

The thickness t of the equivalent orthotropic plate is given by

$$t = \frac{1.0 \times 0.3}{3.0} = 0.1 \text{ m}$$

$$H = 50 \times 3.6 = 180 \text{ m}$$

$$a = \frac{12}{6} = 2$$

$$A_c = 1.0 \times 0.3 = 0.3 \text{ m}^2$$

$$n = \frac{A_c}{ct} = \frac{0.3}{6 \times 0.1} = 0.5$$

The uniformly distributed twisting moment is given by

$$t_o = 1 \text{ kN/m} \times 2.4 \text{ m} = 2.4 \text{ kNm/m}$$

$$\tau_s(H) = \frac{t_o H}{8bct} = \frac{2.4 \times 180}{8 \times 12 \times 6 \times 0.1} = 7.5 \quad \text{kN/m}^2$$

$$I_h = \frac{0.3 \times 1.0^3}{12} = 0.025 \text{ m}^4$$

$$I_d = \frac{0.3 \times 0.6^3}{12} = 0.0054 \text{ m}^4$$

$$e = h - t_2 = 3.0 \text{ m}$$

$$l = d - t_1 = 2.0 \text{ m}$$

The value of $\frac{G}{E}$ is calculated from equation (2.20) and is given by

$$\frac{G}{E} = \frac{12 \times 0.025 \times 3.6}{1.0 \times 0.3 \times 27} \times \frac{1}{2.9753} = 0.044813$$

The values of k^2 and λ^2 are determined from equation (3.33) as

$$k^2 = 20 \times 0.044813 \times \left(\frac{180}{12}\right)^2 \frac{4 \times 4.5}{3 \times 37.75} = 32.0517$$

$$k = 5.6614$$

$$\lambda^2 = \frac{5 \times 1 \times 4.5}{3 \times 37.75} = 0.1987$$

$$\cosh k = 143.7772$$

$$\sinh k = 143.7737$$

The columns and beams are again numbered as shown in Fig. (2.14) of Chapter 2.

Axial forces in columns

The axial forces in the columns at the second floor level are evaluated as follows

$$\xi = \frac{z}{H} = 0.96$$

$$k\xi = 5.4349; \quad k(1-\xi) = 0.2265$$

$$\sinh k\xi = 114.6328$$

$$\cosh k(1-\xi) = 1.0258$$

The function $r(\xi)$ is calculated from equation (3.38) as

$$r = \frac{0.1987}{32.0517} \times 180 \times 3.5209 \quad \tau_s(II) = 3.9289\ \tau_s(II) \quad kN/m$$

The column axial forces in panels AD and BC (24 m sides) are found from equations (3.41) and (3.42) as

$$N_1 = -\frac{0.1 \times 3 \times 11.25}{12 \times 6} \times 3.9289 \times 7.5 = -1.3813\ kN$$

$$N_2 = -\frac{2 \times 0.1 \times 3}{12 \times 6} \times 9 \times 3.9289 \times 7.5 = -2.2100\ kN$$

$$N_3 = -\frac{2 \times 0.1 \times 3}{12 \times 6} \times 6 \times 3.9289 \times 7.5 = -1.4733\ kN$$

$$N_4 = -\frac{2 \times 0.1 \times 3}{12 \times 6} \times 3 \times 3.9289 \times 7.5 = -0.7367\ kN$$

$$N_5 = 0$$

Similarly the column axial forces in panels AB and DC (12 m sides) are determined from equations (3.47) and (3.48) as

$$N_1 = - \frac{0.1 \times 3}{36} \times 5.25 \times 3.9289 \times 7.5 = -1.2892 \text{ kN}$$

$$N_2 = - \frac{2 \times 0.1 \times 3}{36} \times 3 \times 3.9289 \times 7.5 = - 1.4733 \text{ kN}$$

$$N_3 = 0$$

The axial force in the corner area A_c is given by equation (3.53) as

$$N_c = - 2 \times 0.5 \times 0.1 \times 3.9289 \times 7.5 = - 2.9467 \text{ kN}$$

The total axial force in the corner column becomes

$$- 1.3813 - 1.2892 - 2.9467 = - 5.6172 \text{ kN}$$

The distribution of axial forces in columns are shown in Fig. 3.5.

Shear forces in columns

The shear forces in the columns at the middle of the third storey are determined as below.

$$\xi = 0.95$$

$$\tau_s = \xi \tau_s(H) = 0.95 \quad \tau_s(H)$$

$$k\xi = 5.3783 , \quad k(1 - \xi) = 0.2831$$

$$\cosh k\xi = 108.3291$$

$$\sinh k(1 - \xi) = 0.2869$$

$$\frac{dr}{d\xi} = \frac{\lambda^2}{k} H \tau_s(H) \left[\frac{k \cosh k\xi - \sinh k(1 - \xi)}{\cosh k} \right]$$

$$= \frac{0.1987}{5.6614} \times 180 \times 4.2636 \quad \tau_s(H)$$

$$= 26.9354 \ \tau_s(H) \quad \text{kN/m}$$

The shear forces in the columns in panels AD and BC are evaluated from equations (3.43) and (3.44) and

are given as

$$S_{c_1} = \frac{0.1 \times 3}{2} \times 7.5 \left\{ 0.95 - \frac{1}{540}(6.5 - 5.28125)26.9354 \right\}$$

$$= 1.0004 \text{ kN}$$

$$S_{c_2} = 0.1 \times 3 \times 7.5 \left\{ 0.95 - \frac{1}{540}(6.5 - 3.40625)26.9354 \right\}$$

$$= 1.7903 \text{ kN}$$

$$S_{c_3} = 0.1 \times 3 \times 7.5 \left\{ 0.95 - \frac{1}{540}(6.5 - 1.53125)26.9354 \right\}$$

$$= 1.5799 \text{ kN}$$

$$S_{c_4} = 0.1 \times 3 \times 7.5 \left\{ 0.95 - \frac{1}{540}(6.5 - 0.40625)26.9354 \right\}$$

$$= 1.4536 \text{ kN}$$

$$S_{c_5} = 0.1 \times 3 \times 7.5 \left\{ 0.95 - \frac{1}{540}(6.5 - 0.03125)26.9354 \right\}$$

$$= 1.4115 \text{ kN}.$$

From equations (3.49) and (3.50), the shear forces in columns in panels AB and DC become

$$S_{c_1} = - \frac{0.1 \times 3}{2} \times 7.5 \left\{ 0.95 + \frac{1}{540}(5.5-2.3125)26.9354 \right\}$$

$$= - 1.2476 \text{ kN}$$

$$S_{c_2} = - 0.1 \times 3 \times 7.5 \left\{ 0.95 + \frac{1}{540}(5.5-0.8125)26.9354 \right\}$$

$$= - 2.6636 \text{ kN}$$

$$S_{c_3} = - 0.1 \times 3 \times 7.5 \left\{ 0.95 + \frac{1}{540}(5.5 - 0.0625)26.9354 \right\}$$

$$= - 2.7478 \text{ kN}$$

The distribution of shear forces in columns are illustrated in Fig. 3.6.

<u>Shear forces in spandrel beams</u>

The shear forces in the spandrel beams at the second floor level are evaluated as follows.

$\xi = 0.96$

$z_j + \frac{h}{2} = 174.6$ m ; corresponding $\xi_1 = 0.97$

$z_j - \frac{h}{2} = 171.0$ m; corresponding $\xi_2 = 0.95$

$k\xi_1 = 5.4916$, $k(1-\xi_1) = 0.1698$

$\sinh k\xi_1 = 121.3205$

$\cosh k(1-\xi_1) = 1.0145$

$$r(z_j + \frac{h}{2}) = \frac{0.1987}{32.0517} \times 180 \times 3.7842 \ \tau_s(H) = 4.22273 \ \tau_s(H)$$

$k\xi_2 = 5.3783$, $k(1-\xi_2) = 0.2831$

$\sinh k\xi_2 = 108.3245$

$\cosh k(1-\xi_2) = 1.0403$

$$r(z_j - \frac{h}{2}) = \frac{0.1987}{32.0517} \times 180 \times 3.2726 \ \tau_s(H) = 3.65184 \ \tau_s(H)$$

$$\therefore r(z_j + \frac{h}{2}) - r(z_j - \frac{h}{2}) = 0.57089 \ \tau_s(H)$$

From equation (3.45) the shear forces in the spandrel beams for the panels AD and BC are

$$S_{b_1} = 0.1 \times 7.5 \left[3.6 \times 0.96 - \left\{ \frac{6.5}{3} - 2\left(\frac{10.5}{12}\right)^2 \right\} 0.57089 \right]$$

$$= 2.3199 \text{ kN}$$

$$S_{b_2} = 0.1 \times 7.5 \left[3.6 \times 0.96 - \left\{ \frac{6.5}{3} - 2\left(\frac{7.5}{12}\right)^2 \right\} 0.57089 \right]$$

$$= 1.9988 \text{ kN}$$

$$S_{b_3} = 0.1 \times 7.5 \left[3.6 \times 0.96 - \left\{ \frac{6.5}{3} - 2\left(\frac{4.5}{12}\right)^2 \right\} 0.57089 \right]$$

$$= 1.7847 \text{ kN}$$

$$S_{b_4} = 0.1 \times 7.5 \left[3.6 \times 0.96 - \left\{ \frac{6.5}{3} - 2\left(\frac{1.5}{12}\right)^2 \right\} 0.57089 \right]$$

$$= 1.6777 \text{ kN}$$

The shear forces in the spandrel beams for the panels AB and DC are evaluated from equation (3.51) as

$$S_{b_1} = - 0.1 \times 7.5 \left[3.6 \times 0.96 + \left\{ \frac{5.5}{3} - \left(\frac{4.5}{6}\right)^2 \right\} 0.57089 \right]$$

$$= - 3.1361 \text{ kN}$$

$$S_{b_2} = - 0.1 \times 7.5 \left[3.6 \times 0.96 + \left\{ \frac{5.5}{3} - \left(\frac{1.5}{6}\right)^2 \right\} 0.57089 \right]$$

$$= - 3.3502 \text{ kN}$$

The total rotation θ at the top of the building may be determined from equation (3.57) as

$$\theta = \frac{2.4 \times 180^4 \times 4.5}{24 \times 144 \times 216 \times 0.1 \times 22.24 \times 10^6} \times \frac{0.1987^2}{32.0517^2} \times 3.7130$$

$$+ \frac{2.4 \times 180^2 \times 3}{32 \times 144 \times 6 \times 0.1 \times 0.044813 \times 22.24 \times 10^6} (1 -$$

$$\frac{4 \times 4.5}{3 \times 3} \times \frac{0.1987}{32.0517} \times 4.6682 +$$

$$\frac{37.75}{15} \times \frac{0.1987^2}{5.6614} \times 0.9933)$$

$$= (0.9745 + 81.2352) \times 10^{-6}$$

$$= 82.2097 \times 10^{-6} \text{ radian}$$

	Torque T_o at top	Uniformly distributed torque t_o	Triangularly distributed torque $t_o(1 - \xi)$
τ_s	$\frac{T_o}{8bct}$	$\frac{t_o H \xi}{8bct}$	$\frac{t_o H}{8bct}\left(\xi - \frac{\xi^2}{2}\right)$
$\tau_{s(H)}$	$\frac{T_o}{8bct}$	$\frac{t_o H}{8bct}$	$\frac{t_o H}{16bct}$
R_1	λ^2	λ^2	λ^2
R_2	$\frac{\sinh k\xi}{k \cosh k}$	$\frac{1}{k^2}\left[\frac{\cosh k(1-\xi) + k \sinh k\xi}{\cosh k} - 1\right]$	$\frac{2}{k^2}\left[\frac{2k \cosh k(1-\xi) + (k^2-2)\sinh k\xi}{2 k \cosh k} - (1-\xi)\right]$
R_3	$\frac{\cosh k\xi}{\cosh k}$	$\frac{k \cosh k\xi - \sinh k(1-\xi)}{k \cosh k}$	$\frac{2}{k^2}\left[\frac{(k^2-2) \cosh k\xi - 2k \sinh k(1-\xi)}{2 \cosh k} + 1\right]$
$\beta\left(\frac{R_2}{F_2}; \frac{R_3}{F_3}\right)$	1	$\frac{1}{2}$	$\frac{2}{3}$

Table 3.1 Design Functions for Standard Load Cases

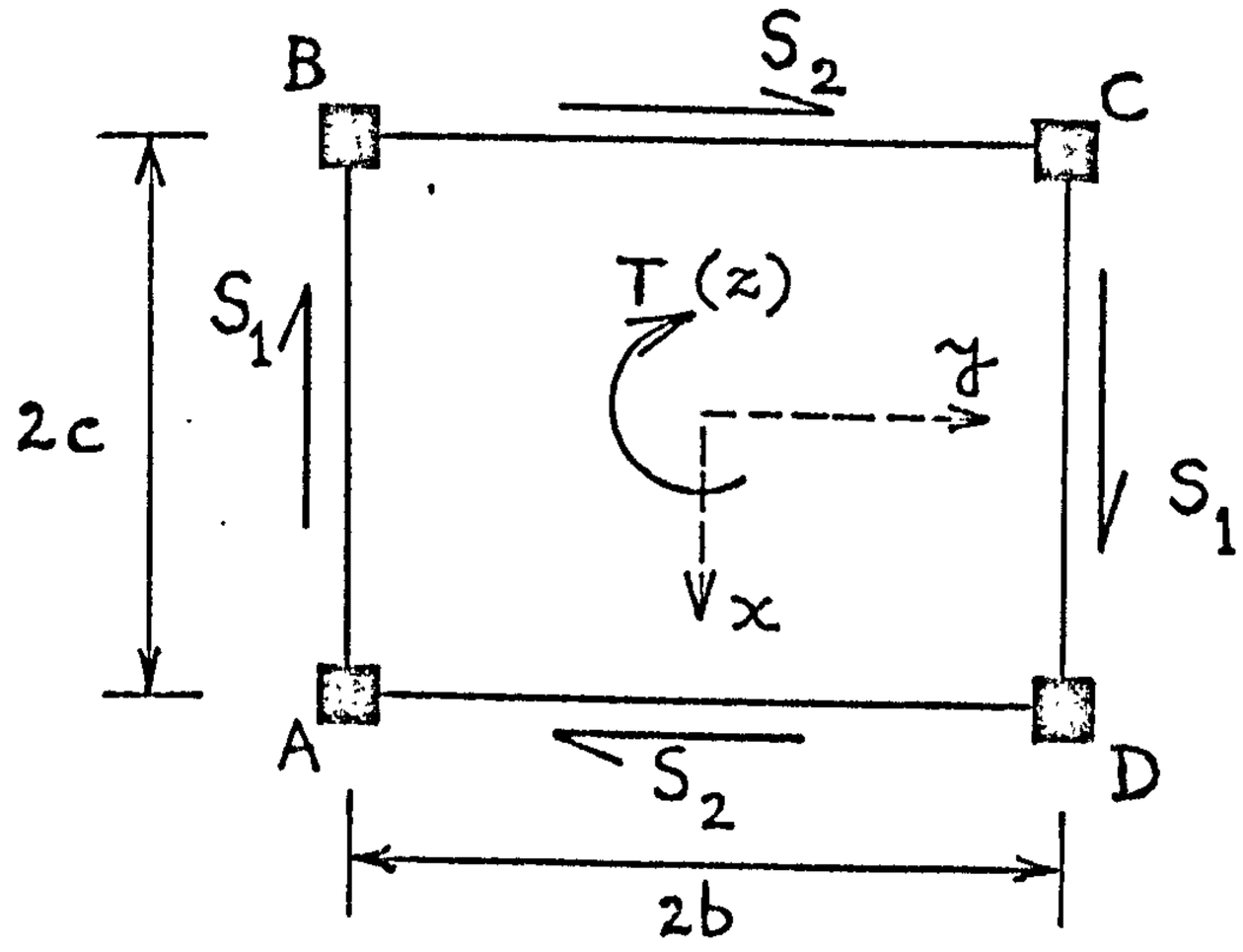

Fig. 3.1 Framed tube under torsion
(Plan view)

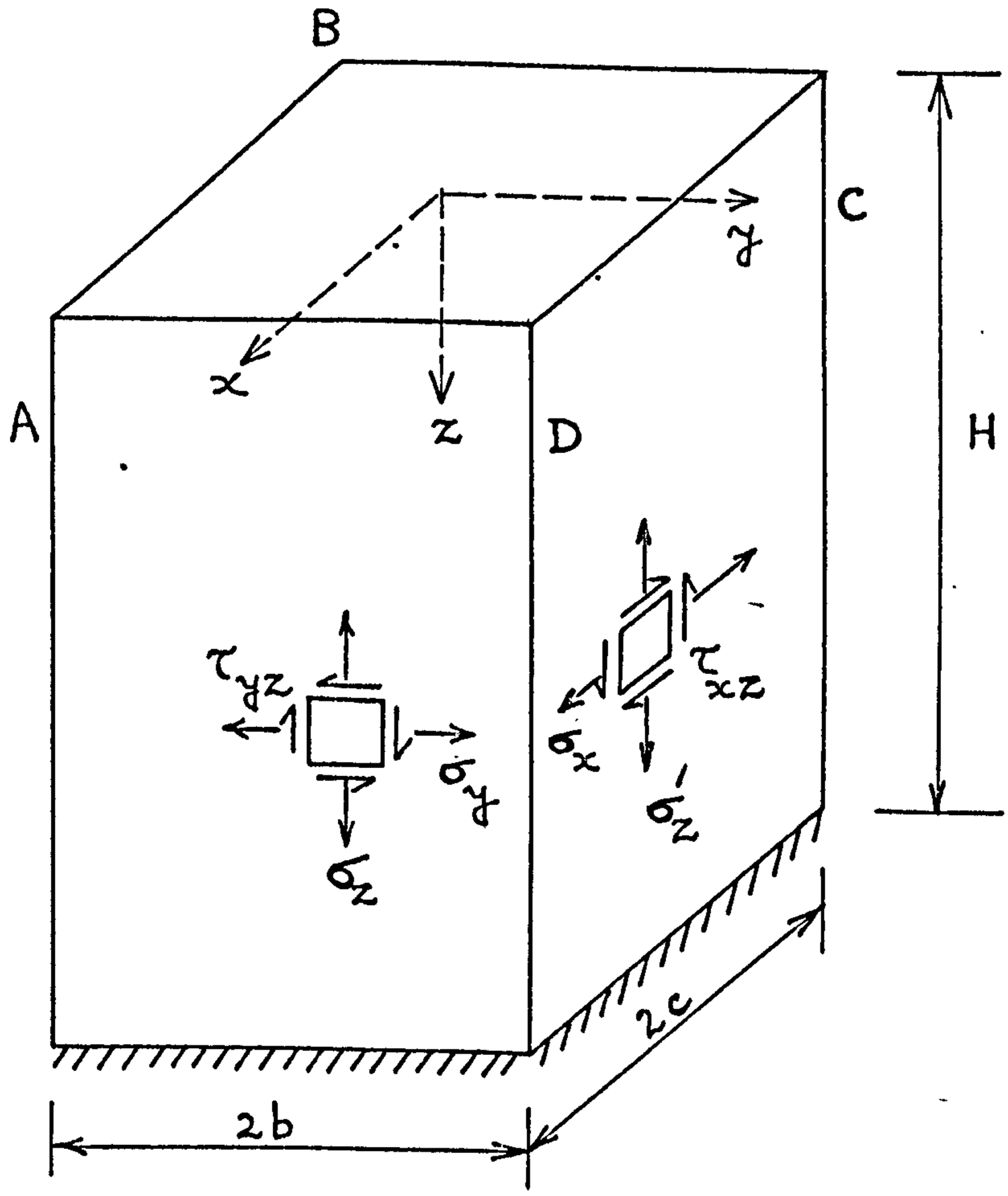

Fig. 3.2 Notation for stresses

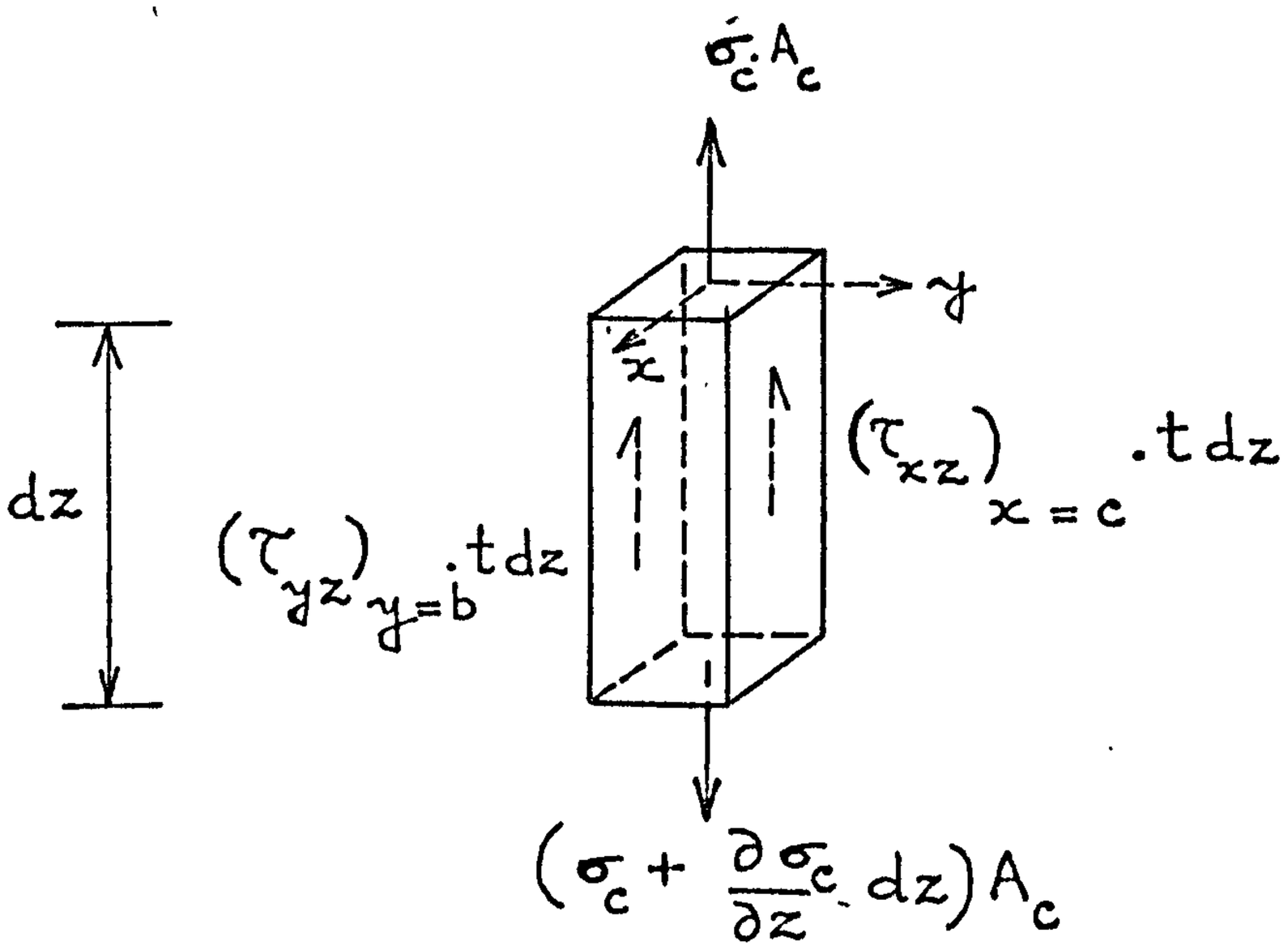

Fig. 3.3 Forces in Corner column

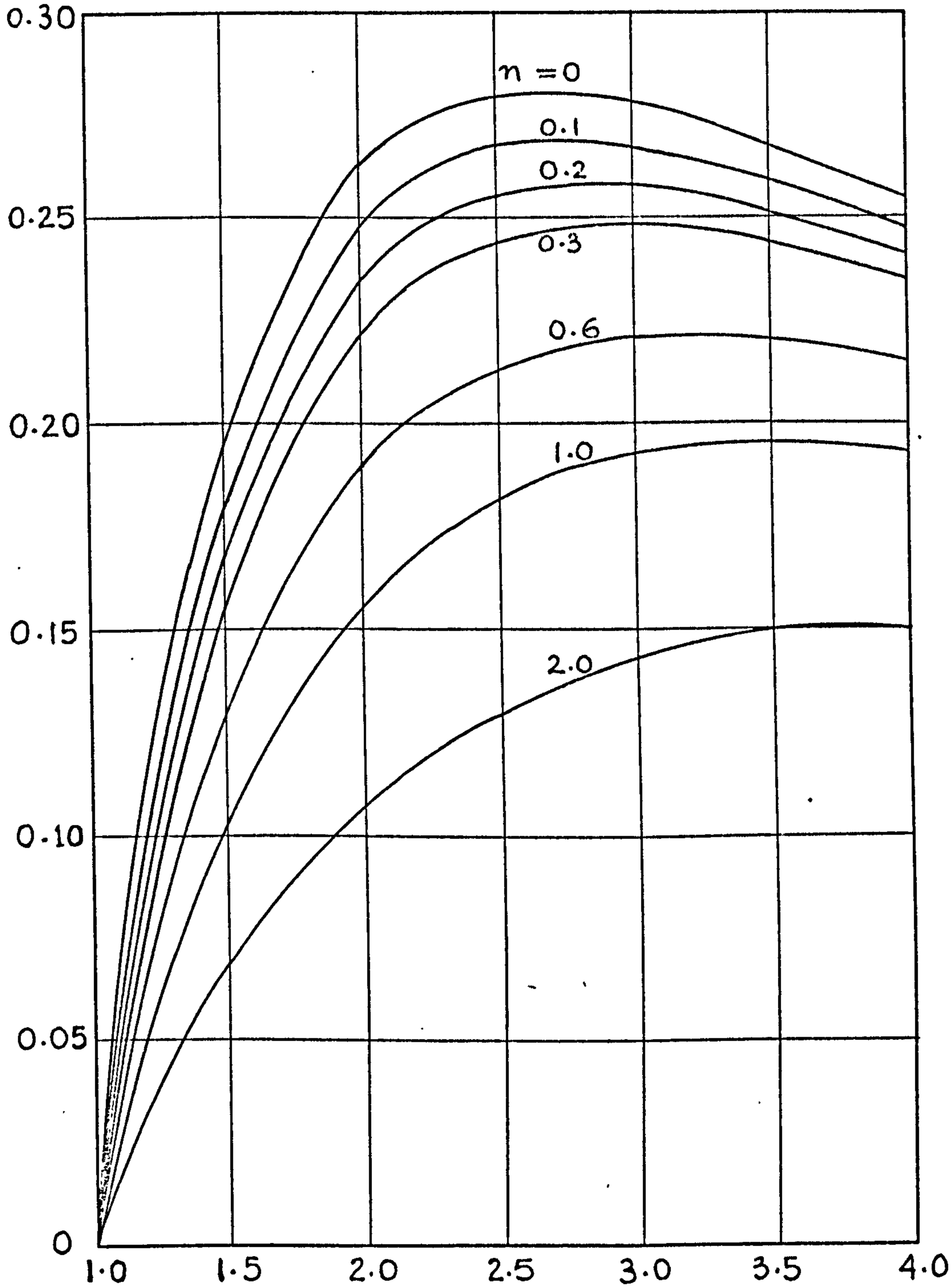

Fig. 3.4 Variation of Geometrical Function R_1 with Aspect ratio for various ratios of Corner column area

Fig. 3.5 AXIAL FORCES IN COLUMNS

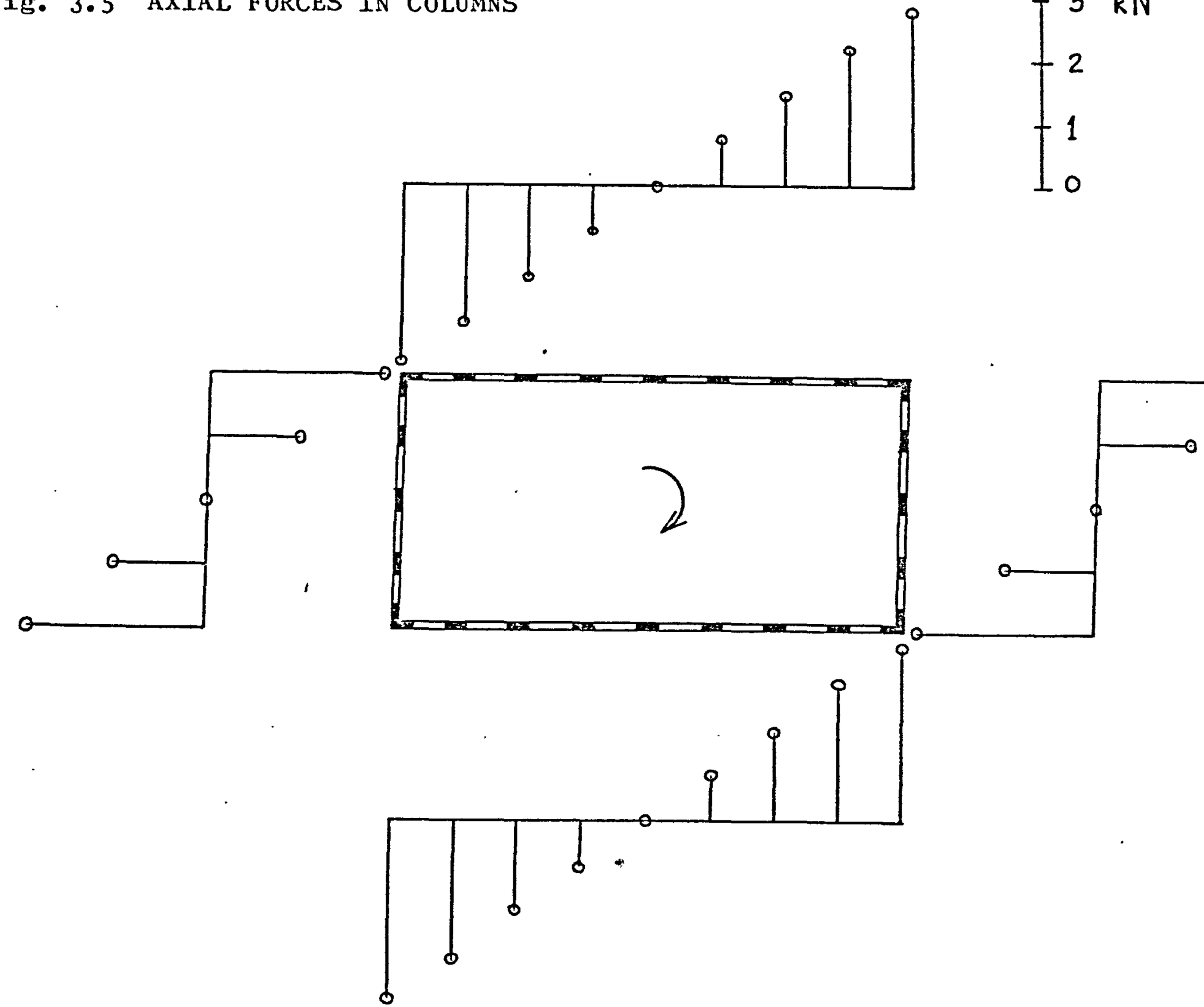

Fig. 3.6 SHEAR FORCES IN COLUMNS

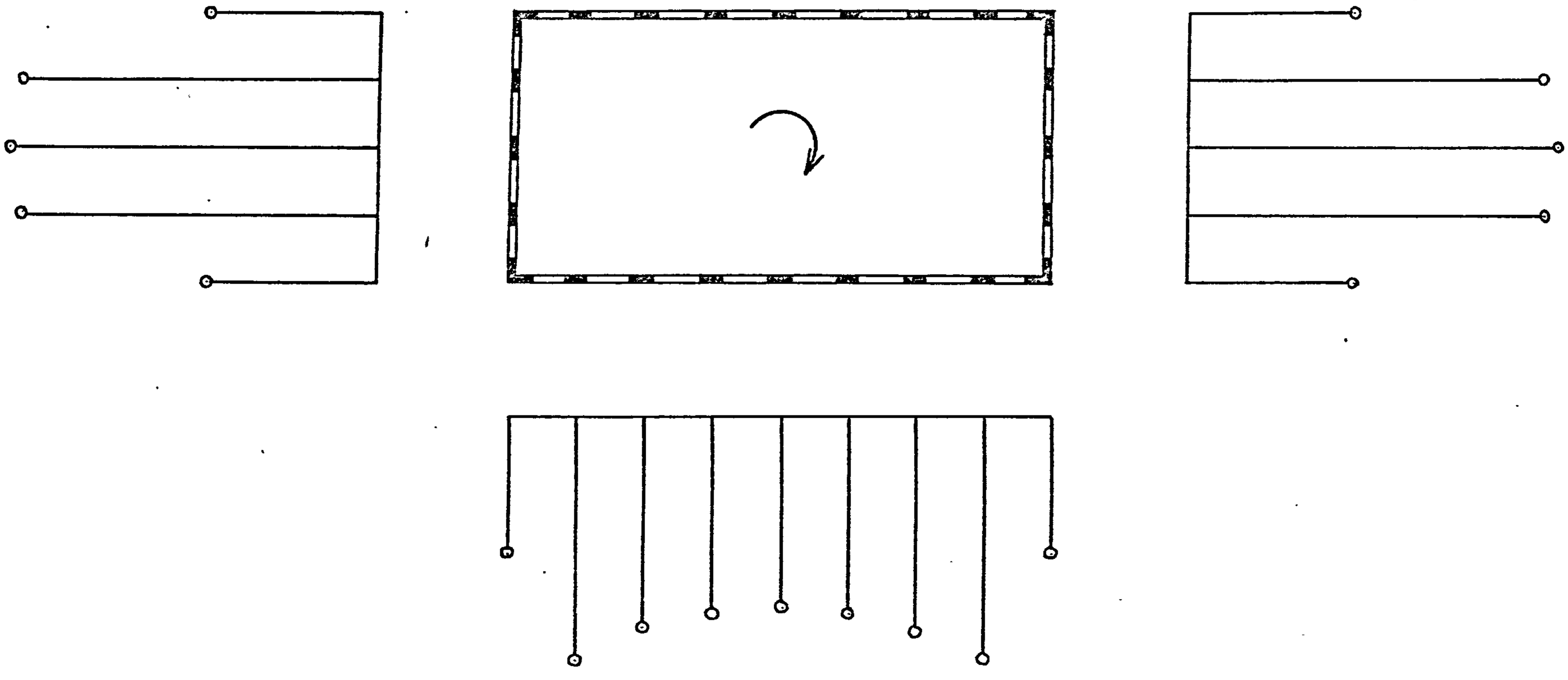

CHAPTER 4

FRAMED-TUBE STRUCTURE SUPPORTED ON ELASTIC BASE

NOTATION

The following symbols are used in this chapter:

A_c = area of corner column;

b = half breadth of framed tube;

c = half depth of framed tube;

E = equivalent elastic modulus;

G = equivalent shear modulus;

H = total height of building;

I = second moment of area of framed tube;

k = structural parameter;

k_o = modulus of supporting medium;

M = applied moment at any level;

m = geometrical ratio;

P = concentrated load at top;

p = intensity of lateral loading per unit height;

S = stress function;

t = thickness of equivalent orthotropic plate;

U = strain energy;

w = vertical displacement;

x, y = horizontal coordinates;

z, z' = vertical coordinates;

λ = geometrical ratio;

ξ = non-dimensional height coordinate $(\frac{z}{H})$;

σ = direct stress;

σ_b = direct stress according to engineer's beam theory.

4.1 INTRODUCTION

In the analysis of framed-tube structure presented in Chapters 2 and 3, it was assumed that the structure was supported on a rigid base. Closed form solutions were obtained for different loading conditions, which enabled design curves to be developed for the rapid approximate analyses of the structure under bending and torsional actions.

The assumption of rigid base is not strictly true and the structure may be founded on a number of piles or may be supported on transfer girders on a series of columns along the perimeter of the structure at first floor level. The discrete supporting elements may be replaced approximately by a continuous elastic medium, whose elastic stiffness properties are chosen to model the axial deformations of the supporting elements.

A similar simple analysis, based on the same basic assumptions regarding the structural behaviour, is presented in this chapter for the bending analysis of the framed-tube structure supported on an elastic base. The governing differential equation remains the same as that derived for the structure with rigid base, but the boundary condition at the base is modified to include the effect of deformation of the elastic base.

4.2 METHOD OF ANALYSIS

The wind forces acting on the structure will produce continuously distributed reaction forces in the supporting medium. It is assumed that the intensity of

the reaction forces at any point is proportional to the vertical displacement of the structure at that point. The reaction forces are assumed to be acting vertically and opposing the displacement of the structure. Hence where the displacement is directed downward there is compression in the supporting medium, but, on the other hand, where the displacement happens to be upward, tension is produced.

In addition to the vertical reactions there will be horizontal forces along the surfaces where the structure is in contact with the supporting medium. The influence of such horizontal forces on the total strain energy of the structure is neglected in the following analysis.

It is then assumed that each framework panel of columns and beams may be replaced by an equivalent uniform orthotropic plate, to form a substitute closed-tube structure. The derivation of the properties of the orthotropic plate to model the vertical, horizontal, and shearing stiffnesses of the frame panels was given in Article 2.3.

The direct and shear stresses in the normal and side panels are determined in terms of a single unknown function S(z) as in Article 2.4.

The stress-displacement relationship at the base of the structure for the normal panels may be expressed in the form

$$(\sigma_z)_{z=H} = k_o w \qquad \ldots\ldots \quad (4.1)$$

where w is the vertical displacement at the base, and k_o is defined as the modulus of the supporting medium.

If the structure is supported on relatively rigid girders founded on a number of columns, it is assumed that the girders are supported on a number of independent springs whose stiffnesses are chosen to model the axial deformations of the columns. The spring stiffnesses are then diffused to produce a continuous elastic base for which the value of k_o may be determined.

The energy stored in the supporting medium under the two normal panels is given by

$$U_{f_1} = t \int_{-b}^{b} (\sigma_z)_{z=H} \, w \, dy \qquad \ldots\ldots (4.2)$$

On substituting k_o from equation (4.1) U_{f_1} becomes

$$U_{f_1} = \frac{t}{k_o} \int_{-b}^{b} \left[\sigma_z^2 \, dy \right]_{z=H} \qquad \ldots\ldots (4.3)$$

The energy stored in the supporting medium under the side panels, and the concentrated corner elements are similarly determined. The total energy stored in the supporting medium, therefore, becomes

$$U_f = \left[\frac{t}{k_o} \int_{-b}^{b} \sigma_z^2 \, dy + \frac{t}{k_o} \int_{-c}^{c} (\sigma_z')^2 \, dx + \frac{2A_c}{k_o} \sigma_c^2 \right]_{z=H}$$

$\ldots\ldots$ (4.4)

On substituting equations (2.34), (2.35) and (2.36) into equation (4.4) it is found that

$$U_f = \left[\frac{t}{k_o} \int_{-b}^{b} \left\{ \frac{M}{I} c - \left[\tfrac{1}{3}m - \left(\frac{y}{b}\right)^2 \right] S \right\}^2 dy \right.$$

$$+ \frac{t}{k_o} \int_{-c}^{c} \left\{ \frac{M}{I} x + (1 - \tfrac{1}{3}m)\left(\frac{x}{c}\right)^3 S \right\}^2 dx$$

$$\left. + \frac{2A_c}{k_o} \left\{ \frac{M}{I} c + (1 - \tfrac{1}{3}m)S \right\}^2 \right]_{z=H} \qquad \ldots\ldots (4.5)$$

The energy stored in the framed-tube structure is given by equation (2.39). The total energy stored is, therefore, the sum of the two equations (2.39) and (4.5).

The variation of U_f, δU_f is given by

$$\delta U_f = \left[\frac{2t}{k_o} \int_{-b}^{b} \left\{ \frac{M}{I} c - \left[\tfrac{1}{3}m - \left(\frac{y}{b}\right)^2 \right] S \right\} \cdot \right.$$

$$\left\{ - \left[\tfrac{1}{3}m - \left(\frac{y}{b}\right)^2 \right] \right\} \cdot \delta S \, dy$$

$$+ \frac{2t}{k_o} \int_{-c}^{c} \left\{ \frac{M}{I} x + (1 - \tfrac{1}{3}m)\left(\frac{x}{c}\right)^3 S \right\} (1 - \tfrac{1}{3}m)\left(\frac{x}{c}\right)^3 \delta S \, dx$$

$$\left. + \frac{4A_c}{k_o} \left\{ \frac{M}{I} c + (1 - \tfrac{1}{3}m)S \right\} (1 - \tfrac{1}{3}m) \, \delta S \right]_{z=H}$$

$$\ldots\ldots (4.6)$$

On integration, δU_f becomes

$$\delta U_f = \frac{2t}{k_o} \left[\left\{ \frac{2b}{45}(5m^2 - 10m + 9) + \frac{2c}{7}(1 - \tfrac{1}{3}m)^2 \right.\right.$$

$$\left.\left. + \frac{2A_c}{t}(1 - \tfrac{1}{3}m)^2 \right\} \cdot S \, \delta S \right]_{z=H} \qquad \ldots\ldots (4.7)$$

The variation of the total strain energy is given by the sum of the equations (2.40) and (4.7). On

equating this variation to zero, the following governing differential equation is obtained.

$$\frac{d^2S}{dz^2} - \left(\frac{k}{H}\right)^2 S = \lambda^2 \frac{d^2\sigma_b}{dz^2} \qquad \ldots\ldots (4.8)$$

where the parameters k and λ are defined as

$$k^2 = 45 \frac{G}{E} \left(\frac{H}{b}\right)^2 \frac{7(5m^2-10m+9) + 5(3-m)^2 \frac{c}{b}(1 + 7 \frac{A_c}{ct})}{15(35m^2-42m+15) + 7\left(\frac{c}{b}\right)^3 (3-m)^2}$$

$$\lambda^2 = 45 \frac{7(5m - 3) - \left(\frac{c}{b}\right)^3 (3 - m)}{15(35m^2 - 42m + 15) + 7\left(\frac{c}{b}\right)^3 (3 - m)^2}$$

$\ldots\ldots$ (4.9)

The differential equation (4.8) and the parameters k and λ given by equation (4.9) are identical to the corresponding ones derived for the bending of framed-tube structures with a rigid base (equations 2.45 and 2.47).

The boundary conditions are

At $z = 0$, $\quad S = 0$ $\qquad \ldots\ldots (4.10)$

At $z = H$, $\frac{dS}{dz} + \frac{E}{k_o} \left(\frac{k}{H}\right)^2 S - \lambda^2 \frac{d\sigma_b}{dz} = 0$ $\qquad \ldots\ldots (4.11)$

On comparing the boundary condition (4.11) with (2.46) it is found that the equation (4.11) contains an extra term $\frac{E}{k_o}\left(\frac{k}{H}\right)^2 S$ on the left hand side of the equation. This term vanishes for a structure founded on a rigid base when $k_o = \infty$.

As before, the homogeneous part of the solution of equation (4.8) may be expressed in the form

$$S = A \cosh \frac{k}{H} z + B \sinh \frac{k}{H} z \qquad \ldots\ldots (4.12)$$

The particular integral parts of the solution are derived for the three standard load cases discussed earlier.

Case 1 Concentrated load P at the top

In this case, the applied moment M at any level z is given by

$$M = Pz$$

and the datum stress σ_b becomes

$$\sigma_b = \frac{Pc}{I} z$$

The equation (4.8) becomes homogeneous, so that the particular integral part of the solution vanishes.

The constants A and B in equation (4.12) are determined from the boundary conditions (4.10) and (4.11) as

$$A = 0$$

$$B = \frac{\lambda^2}{k} \sigma_b(H) \frac{1}{\cosh k + \frac{E}{k_o} \frac{k}{H} \sinh k}$$

The complete solution of equation (4.8) then becomes

$$S(\xi) = \frac{\lambda^2}{k} \sigma_b(H) \frac{\sinh k\xi}{\cosh k + \frac{E}{k_o} \frac{k}{H} \sinh k} \quad \ldots\ldots (4.13)$$

where $\sigma_b(H) = \frac{PcH}{I}$ and $\xi = \frac{z}{H}$.

When the base is rigid, $k_o = \infty$, and $S(\xi)$ reduces to that of equation (2.49) derived earlier.

Case 2 Uniformly distributed load p throughout the height

In this case,

$$M = \frac{pz^2}{2} \quad \text{and} \quad \sigma_b = \frac{pc}{2I} z^2$$

The particular integral part of the solution is

$$S = - \frac{\lambda^2}{k^2} \frac{pcH^2}{I}$$

The constants A and B are determined as

$$A = \frac{\lambda^2}{k^2} \frac{pcH^2}{I}$$

$$B = \frac{\lambda^2}{k^2} \frac{pcH^2}{I} \frac{k - \sinh k + \frac{E}{k_o} \frac{k}{H} (1 - \cosh k)}{\cosh k + \frac{E}{k_o} \frac{k}{H} \sinh k}$$

The complete solution becomes

$$S(\xi) = \frac{2\lambda^2}{k^2} \sigma_b(II) \left[\frac{1}{D} \left\{ \cosh k(1 - \xi) + k \sinh k\xi + \frac{E}{k_o} \frac{k}{H} \left[\sinh k (1 - \xi) + \sinh k\xi \right] \right\} - 1 \right] \quad \ldots\ldots (4.14)$$

where $D = \cosh k + \frac{E}{k_o} \frac{k}{H} \sinh k$ $\ldots\ldots$ (4.15)

For a rigid base the equation (4.14) reduces to that of equation (2.50) determined earlier.

Case 3 Triangularly distributed load

For a load intensity which varies linearly from 0 at $z = H$ to p at $z = 0$,

$$M = \frac{p}{2}(z^2 - \frac{z^3}{3H})$$

and $$\sigma_b = \frac{pc}{2I}(z^2 - \frac{z^3}{3H})$$

The particular integral part of the solution is given by

$$S = - \frac{\lambda^2}{k^2} \frac{pcH^2}{I} \left(1 - \frac{z}{H}\right)$$

The constants A and B are found out as

$$A = \frac{\lambda^2}{k^2} \frac{pcH^2}{I}$$

$$B = \frac{\lambda^2}{k^2} \frac{pcH^2}{2I} \frac{k - \frac{2}{k} - 2 \sinh k - 2 \frac{E}{k_o} \frac{k}{H} \cosh k}{\cosh k + \frac{E}{k_o} \frac{k}{H} \sinh k}$$

The complete solution of equation (4.8) then becomes

$$S(\xi) = \frac{3\lambda^2}{k^2} \sigma_b(H) \left[\frac{1}{2D} \left\{ 2 \cosh k (1-\xi) + (k - \frac{2}{k}) \sinh k\xi + 2 \frac{E}{k_o} \frac{k}{H} \sinh k(1-\xi) \right\} - (1-\xi) \right]$$

..... (4.16)

where D was given by equation (4.15).

For a structure supported on rigid base the equation (4.16) reduces to equation (2.51) derived earlier.

CHAPTER 5

FRAMED-TUBE STRUCTURE WITH DIFFERENT STIFFNESS REGIONS

NOTATION

The following symbols are used in this chapter:

A_{c_1}, A_{c_2}	areas of corner columns;
b	half breadth of framed tube;
c	half depth of framed tube;
E_1, E_2	elastic moduli of equivalent tubes;
G_1, G_2	shear moduli of equivalent tubes;
H	total height of building;
H_1	level of building where the lower region begins;
I_1, I_2	second moments of area of framed tube;
k_1, k_2	structural parameters;
M	applied moment at any level;
m	geometrical ratio;
p	intensity of lateral loading per unit height;
S_1, S_1', S_1'', S_2	stress functions;
t_1, t_2	thicknesses of equivalent tubes;
U	total strain energy;
x, y	horizontal coordinates;
z, z'	vertical coordinates;
σ	direct stress;
σ_b	direct stress according to engineer's beam theory;
τ	shear stress.

5.1 INTRODUCTION

In the analysis of framed tube structures described in the earlier chapters, the spacings of beams and columns were assumed uniform throughout the height, as is usually the case in practice. In addition, in order to simplify the analysis, it was assumed that both the beams and columns were of uniform section throughout the height. This latter assumption is not strictly necessary and in practice the structure may include a number of regions in which the beams and columns have constant stiffnesses.

A simple method of analysis, similar to the one described in Chapter 2, is presented here for structures with variable beam and column stiffnesses in different regions. The spacings of beams and columns need not necessarily be the same throughout the height but in a particular region the spacings must be uniform.

In many cases, the four corner columns are considerably stiffer than the other columns, and provision is again made in the analysis to include stiffer corner elements.

5.2 METHOD OF ANALYSIS

The framed tube structure, shown in Fig. 5.1, includes two regions in each of which the beams and columns have constant stiffnesses and uniform spacings. The framework panel in each region, consisting of columns and spandrel beams is replaced by an equivalent uniform orthotropic plate, to form a substitute closed-tube structure. The properties of the orthotropic plate must

be so chosen that, under the action of identical axial or shear forces, the axial and shear deformations of both framework and equivalent orthotropic plate will be equal (Chapter 2).

The equations of equilibrium for the normal and side panels of the substitute tube may be expressed as,

$$\left.\begin{aligned} \frac{\partial \sigma_y}{\partial y} + \frac{\partial \tau_{yz}}{\partial z} &= 0 \\ \frac{\partial \sigma_z}{\partial z} + \frac{\partial \tau_{yz}}{\partial y} &= 0 \end{aligned}\right\} \quad \ldots\ldots (5.1)$$

$$\left.\begin{aligned} \frac{\partial \sigma_x}{\partial x} + \frac{\partial \tau_{xz}}{\partial z} &= 0 \\ \frac{\partial \sigma'_z}{\partial z} + \frac{\partial \tau_{xz}}{\partial x} &= 0 \end{aligned}\right\} \quad \ldots\ldots (5.2)$$

The vertical stress distributions σ_z and σ'_z in the normal and side panels of the upper region ($0 \leqslant z \leqslant H_1$) may be expressed in the form, (cf. Fig. 5.2),

$$\sigma_z = \frac{M}{I_1} c + S'_1 + \left(\frac{y}{b}\right)^2 S_1 \quad \ldots\ldots (5.3)$$

$$\sigma'_z = \frac{M}{I_1} x + \left(\frac{x}{c}\right)^3 S''_1 \quad \ldots\ldots (5.4)$$

In equations (5.3) and (5.4) I_1 is the second moment of area of the substitute tube cross-section in the upper region, given by

$$I_1 = \frac{4}{3} t_1 c^2 (3b + c) + 4A_{c_1} \cdot c^2$$

where 2b and 2c are the lengths of normal and side panels, t_1 is the effective thickness of the orthotropic tube, and

A_{c_1} is the area of the corner element.

The condition of vertical strain compatibility at the corner requires that

$$\frac{\sigma_z}{E_1}(\pm b, z) = \frac{\sigma'_z}{E_1}(c, z) = \frac{\sigma_c}{E_1} \qquad \ldots\ldots (5.5)$$

where E_1 is the elastic modulus of the upper region, and σ_c is the axial stress in the corner column given by, on using equation (5.3),

$$\sigma_c = (\sigma_z)_{y=b} = \frac{M}{I_1} c + S'_1 + S_1 \qquad \ldots\ldots (5.6)$$

Substitution of equations (5.3) and (5.4) into equation (5.5) yields,

$$S''_1 = S'_1 + S_1 \qquad \ldots\ldots (5.7)$$

The condition of overall moment equilibrium at any height is,

$$2\int_{-b}^{b} \sigma_z t_1 c \, dy + 2\int_{-c}^{c} \sigma'_z t_1 x \, dx + 4A_{c_1} c \sigma_c = M(z) \qquad \ldots\ldots (5.8)$$

where M(z) is the total bending moment at any level.

On substituting equations (5.3), (5.4), (5.6) and (5.7) into equation (5.8), it is found that,

$$S'_1 = -\tfrac{1}{3} m S_1$$

$$\text{where} \quad m = \frac{5b + 3c + 15\frac{A_{c_1}}{t_1}}{5b + c + 5\frac{A_{c_1}}{t_1}}$$

The stresses σ_z and σ'_z may, therefore, be expressed in terms of the single unknown function $S_1(z)$ as,

$$\sigma_z = \frac{M}{I_1} c - \left[\frac{1}{3} m - \left(\frac{y}{b}\right)^2 \right] S_1 \qquad \ldots\ldots (5.9)$$

$$\sigma'_z = \frac{M}{I_1} x + \left(1 - \frac{1}{3}m\right)\left(\frac{x}{c}\right)^3 S_1 \qquad \ldots\ldots (5.10)$$

The stress σ_c in the corner column becomes,

$$\sigma_c = \frac{M}{I_1} c + \left(1 - \frac{1}{3}m\right) S_1 \qquad \ldots\ldots (5.11)$$

On substituting equations (5.9) and (5.10) into the equilibrium conditions (5.1) and (5.2), and integrating, the shear stress components τ_{yz} and τ_{xz} become

$$\tau_{yz} = - y \left\{ \frac{c}{I_1} \frac{dM}{dz} - \frac{1}{3} \left[m - \left(\frac{y}{b}\right)^2 \right] \frac{dS_1}{dz} \right\} \qquad \ldots\ldots (5.12)$$

$$\tau_{xz} = \frac{c^2}{2I_1} \left[1 + 2\frac{b}{c} + \frac{2A_{c_1}}{ct_1} - \left(\frac{x}{c}\right)^2 \right] \frac{dM}{dz} +$$

$$\left(1 - \frac{1}{3}m\right) \frac{c}{4} \left[\frac{1}{5} - \left(\frac{x}{c}\right)^4 \right] \frac{dS_1}{dz} \qquad \ldots\ldots (5.13)$$

The boundary conditions for evaluating the integration constants are similar to those described in Chapter 2.

Similarly the various stress components in the lower region ($H_1 \leqslant z \leqslant H$) can be found as,

$$\sigma_z = \frac{M}{I_2} c - \left[\frac{1}{3} m - \left(\frac{y}{b}\right)^2 \right] S_2$$

$$\sigma'_z = \frac{M}{I_2} x + \left(1 - \frac{1}{3}m\right)\left(\frac{x}{c}\right)^3 S_2$$

$$\sigma_c = \frac{M}{I_2} c + \left(1 - \frac{1}{3}m\right) S_2$$

$$\tau_{yz} = - y \left\{ \frac{c}{I_2} \frac{dM}{dz} - \frac{1}{3} \left[m - \left(\frac{y}{b}\right)^2 \right] \frac{dS_2}{dz} \right\}$$

$$\tau_{xz} = \frac{c^2}{2I_2}\left[1 + 2\,\frac{b}{c} + \frac{2A_{c_2}}{ct_2} - \left(\frac{x}{c}\right)^2\right]\frac{dM}{dz} +$$

$$(1 - \tfrac{1}{3}m)\,\frac{c}{4}\left[\frac{1}{5} - \left(\frac{x}{c}\right)^4\right]\frac{dS_2}{dz} \qquad \ldots\ldots (5.14)$$

where S_2 is a function of height coordinate z only.

In equation (5.14) I_2 is the second moment of area of the equivalent tube for the lower region of the structure, given by,

$$I_2 = \frac{4}{3}\,t_2\,c^2\,(3b + c) + 4\,A_{c_2}.c^2$$

where t_2 is the thickness of the substitute tube and A_{c_2} is the area of concentrated corner element.

In deriving equation (5.14) it has been assumed that,

$$\frac{A_{c_1}}{t_1} = \frac{A_{c_2}}{t_2} \qquad \ldots\ldots (5.15)$$

Equation (5.15) follows from the assumption that the corner columns in the two regions are proportional to the interior columns, with the result that the geometrical ratio m remains the same throughout the height of the building. This is not strictly necessary and different values of m may be used for the two regions if required.

The total strain energy U stored in the structure is given by,

$$U = t_1\int_0^{H_1}\left[\frac{1}{E_1}\int_{-b}^{b}\left\{\frac{M}{I_1}\,c - \left[\tfrac{1}{3}m - \left(\frac{y}{b}\right)^2\right]S_1\right\}^2 dy\right.$$

$$\left. + \frac{1}{G_1}\int_{-b}^{b} y^2\left\{\frac{c}{I_1}\frac{dM}{dz} - \tfrac{1}{3}\left[m - \left(\frac{y}{b}\right)^2\right]\frac{dS_1}{dz}\right\} dy\right.$$

$$+ \frac{1}{E_1} \int_{-c}^{c} \left\{ \frac{M}{I_1} x + (1 - \tfrac{1}{3}m)\left(\frac{x}{c}\right)^3 S_1 \right\}^2 dx$$

$$+ \frac{1}{G_1} \int_{-c}^{c} \left\{ \frac{c^2}{2I_1} \cdot \left[1 + 2\,\frac{b}{c} + \frac{2A_{c_1}}{ct_1} - \left(\frac{x}{c}\right)^2 \right] \frac{dM}{dz} + \right.$$

$$\left. (1 - \tfrac{1}{3}m)\,\frac{c}{4} \left[\frac{1}{5} - \left(\frac{x}{c}\right)^4 \right] \frac{dS_1}{dz} \right\}^2 dx$$

$$+ \frac{2A_{c_1}}{t_1 E_1} \left\{ \frac{M}{I_1}\, c + (1 - \tfrac{1}{3}m)\, S_1 \right\}^2 \Bigg] dz$$

$$+ t_2 \int_{H_1}^{H} \left[\frac{1}{E_2} \int_{-b}^{b} \left\{ \frac{M}{I_2}\, c - \left[\tfrac{1}{3}m - \left(\frac{y}{b}\right)^2 \right] S_2 \right\}^2 dy \right.$$

$$+ \frac{1}{G_2} \int_{-b}^{b} y^2 \left\{ \frac{c}{I_2}\, \frac{dM}{dz} - \tfrac{1}{3} \left[m - \left(\frac{y}{b}\right)^2 \right] \frac{dS_2}{dz} \right\}^2 dy$$

$$+ \frac{1}{E_2} \int_{-c}^{c} \left\{ \frac{M}{I_2} x + (1 - \tfrac{1}{3}m)\left(\frac{x}{c}\right)^3 S_2 \right\}^2 dx$$

$$+ \frac{1}{G_2} \int_{-c}^{c} \left\{ \frac{c^2}{2I_2} \left[1 + 2\,\frac{b}{c} + \frac{2A_{c_2}}{ct_2} - \left(\frac{x}{c}\right)^2 \right] \frac{dM}{dz} + \right.$$

$$\left. (1 - \tfrac{1}{3}m)\,\frac{c}{4} \left[\frac{1}{5} - \left(\frac{x}{c}\right)^4 \right] \frac{dS_2}{dz} \right\}^2 dx$$

$$+ \frac{2A_{c_2}}{t_2 E_2} \left\{ \frac{M}{I_2}\, c + (1 - \tfrac{1}{3}m) S_2 \right\}^2 \Bigg] dz \qquad \ldots\ldots \quad (5.16)$$

The condition for a minimum of U is that the variation of U vanishes. This gives

$$t_1 \int_{0}^{H_1} \left\{ - \frac{1}{G_1} \frac{2b^3}{14175} \left[15(35m^2 - 42m + 15) + 7\left(\frac{c}{b}\right)^3 (3-m)^2 \right] \right. \frac{d^2 S_1}{dz^2}$$

$$+ \frac{1}{E_1} \frac{2b}{315} \left[7(5m^2-10m+9)+5\left(\frac{c}{b}\right)(3-m)^2 + 35 \frac{A_{c_1}}{bt_1}(3-m)^2 \right] S_1$$

$$+ \frac{1}{G_1} \frac{2b^3c}{315I_1} \left[7(5m-3) - \left(\frac{c}{b}\right)^3(3-m) \right] \frac{d^2M}{dz^2} \Bigg\} dz\, \delta S_1(z)$$

$$+ \frac{t_1}{G_1} \Bigg[\Bigg\{ \frac{2b^3}{14175} \left[15(35m^2-42m+15) + 7\left(\frac{c}{b}\right)^3(3-m)^2 \right] \frac{dS_1}{dz}$$

$$- \frac{2b^3c}{315I_1} \left[7(5m-3) - \left(\frac{c}{b}\right)^3(3-m) \right] \frac{dM}{dz} \Bigg\} \delta S_1(z) \Bigg]_0^{H_1}$$

$$+ t_2 \int_{H_1}^{H} \Bigg\{ - \frac{1}{G_2} \frac{2b^3}{14175} \left[15(35m^2-42m+15)+7\left(\frac{c}{b}\right)^3(3-m)^2 \right] \frac{d^2S_2}{dz^2}$$

$$+ \frac{1}{E_2} \frac{2b}{315} \left[7(5m^2-10m+9) + 5\left(\frac{c}{b}\right)(3-m)^2 + 35 \frac{A_{c_2}}{bt_2}(3-m)^2 \right] S_2$$

$$+ \frac{1}{G_2} \frac{2b^3c}{315I_2} \left[7(5m-3)-\left(\frac{c}{b}\right)^3(3-m) \right] \frac{d^2M}{dz^2} \Bigg\} dz \;\; \delta S_2(z)$$

$$+ \frac{t_2}{G_2} \Bigg[\Bigg\{ \frac{2b^3}{14175} \left[15(35m^2-42m+15)+ 7\left(\frac{c}{b}\right)^3(3-m)^2 \right] \frac{dS_2}{dz}$$

$$- \frac{2b^3c}{315I_2} \left[7(5m-3)-\left(\frac{c}{b}\right)^3(3-m) \right] \frac{dM}{dz} \Bigg\} \delta S_2(z) \Bigg]_{H_1}^{H} = 0$$

..... (5.17)

The stresses σ_z and σ'_z are zero at the top, so that

at $z = 0$, $S_1 = 0$ ..... (5.18)

Hence at $z = 0$, $\delta S_1 = 0$

At $z = H_1$, because of vertical equilibrium, the stresses in the two regions are inversely proportional to

the thicknesses of the orthotropic plates. This gives

$$\text{at } z = H_1$$

$$\frac{S_1}{S_2} = \frac{t_2}{t_1} = \frac{I_2}{I_1} \qquad \ldots\ldots \quad (5.19)$$

Hence at $z = H_1$

$$\delta S_2 = \frac{I_1}{I_2}\, \delta S_1$$

On substituting equations (5.18) and (5.19) into equation (5.17) it is found that

$$t_1 \int_0^{H_1} \Bigg\{ -\frac{1}{G_1}\frac{2b^3}{14175}\left[15(35m^2-42m+15)+7\left(\frac{c}{b}\right)^3(3-m)^2\right]\frac{d^2S_1}{dz^2}$$

$$+\frac{1}{E_1}\frac{2b}{315}\left[7(5m^2-10m+9)+5\left(\frac{c}{b}\right)(3-m)^2+35\frac{A_{c_1}}{bt_1}(3-m)^2\right]S_1$$

$$+\frac{1}{G_1}\frac{2b^3c}{315I_1}\left[7(5m-3)-\left(\frac{c}{b}\right)^3(3-m)\right]\frac{d^2M}{dz^2}\Bigg\}\, dz\ \delta S_1(z)$$

$$+ t_2 \int_{H_1}^{H} \Bigg\{ -\frac{1}{G_2}\frac{2b^3}{14175}\left[15(35m^2-42m+15)+7\left(\frac{c}{b}\right)^3(3-m)^2\right]\frac{d^2S_2}{dz^2}$$

$$+\frac{1}{E_2}\frac{2b}{315}\left[7(5m^2-10m+9)+5\left(\frac{c}{b}\right)(3-m)^2+35\frac{A_{c_2}}{bt_2}(3-m)^2\right]S_2$$

$$+\frac{1}{G_2}\frac{2b^3c}{315I_2}\left[7(5m-3)-\left(\frac{c}{b}\right)^3(3-m)\right]\frac{d^2M}{dz^2}\Bigg\}\, dz\ \delta S_2(z)$$

$$+\Bigg\{\frac{2b^3}{14175}\left[15(35m^2-42m+15)+7\left(\frac{c}{b}\right)^3(3-m)^2\right]\cdot$$

$$\left(\frac{t_1}{G_1}\frac{dS_1}{dz}-\frac{t_2}{G_2}\frac{I_1}{I_2}\frac{dS_2}{dz}\right)$$

$$- \frac{2b^3c}{315I_1}\left[7(5m-3) - \left(\frac{c}{b}\right)^3(3-m)\right]\left(\frac{t_1}{G_1} - \frac{t_2}{G_2}\frac{I_1^2}{I_2^2}\right)\frac{dM}{dz}\Bigg\}^{H_1}\delta S_1(H_1)$$

$$+\frac{t_2}{G_2}\Bigg\{\frac{2b^3}{14175}\left[15(35m^2-42m+15) + 7\left(\frac{c}{b}\right)^3(3-m)^2\right]\frac{dS_2}{dz}$$

$$- \frac{2b^3c}{315I_2}\left[7(5m-3)-\left(\frac{c}{b}\right)^3(3-m)\right]\frac{dM}{dz}\Bigg\}^{H}\delta S_2(H) = 0$$

..... (5.20)

The variations $\delta S_1(z)$ and $\delta S_2(z)$ are arbitrary values. Therefore, the integrand of the first and second term in equation (5.20) will each be equal to zero. Also the third and fourth term will each be equal to zero. This results in the following differential equations and boundary conditions for S_1 and S_2:

$$\frac{d^2S_1}{dz^2} - 45\frac{G_1}{E_1}\left(\frac{H}{b}\right)^2\frac{7(5m^2-10m+9) + 5(3-m)^2\frac{c}{b}\left(1+7\frac{A_{c_1}}{ct_1}\right)}{15(35m^2-42m+15) + 7\left(\frac{c}{b}\right)^3(3-m)^2}\frac{S_1}{H^2}$$

$$= 45\frac{7(5m-3) - \left(\frac{c}{b}\right)^3(3-m)}{15(35m^2-42m+15)+ 7\left(\frac{c}{b}\right)^3(3-m)^2}\frac{d^2\sigma_{b_1}}{dz^2} \quad (5.21)$$

$$\frac{d^2S_2}{dz^2} - 45\frac{G_2}{E_2}\left(\frac{H}{b}\right)^2\frac{7(5m^2-10m+9) + 5(3-m)^2\frac{c}{b}\left(1+7\frac{A_{c_2}}{ct_2}\right)}{15(35m^2-42m+15)+ 7\left(\frac{c}{b}\right)^3(3-m)^2}\frac{S_2}{H^2}$$

$$= 45\frac{7(5m-3) - \left(\frac{c}{b}\right)^3(3-m)}{15(35m^2-42m+15) + 7\left(\frac{c}{b}\right)^3(3-m)^2}\frac{d^2\sigma_{b_2}}{dz^2}$$

..... (5.22)

At $z = H_1$

$$\frac{dS_1}{dz} = \frac{G_1}{G_2}\frac{dS_2}{dz} - \left(1 - \frac{G_1}{G_2}\frac{I_1}{I_2}\right).$$

$$45\,\frac{7(5m-3)-(\frac{c}{b})^3(3-m)}{15(35m^2-42m+15)+7(\frac{c}{b})^3(3-m)^2}\,\frac{d\sigma_{b_1}}{dz}=0 \qquad \ldots\ldots (5.23)$$

At $z = H$

$$\frac{dS_2}{dz}-45\,\frac{7(5m-3)-(\frac{c}{b})^3(3-m)}{15(35m^2-42m+15)+7(\frac{c}{b})^3(3-m)^2}\,\frac{d\sigma_{b_2}}{dz}=0 \qquad \ldots\ldots (5.24)$$

The stresses σ_{b_1} and σ_{b_2} are given by

$$\sigma_{b_1}=\frac{M}{I_1}c\ ,\qquad \sigma_{b_2}=\frac{M}{I_2}c \qquad \ldots\ldots (5.25)$$

The equations (5.21) and (5.22) and the boundary conditions (5.23) and (5.24) may be expressed in the form

$$\frac{d^2S_1}{dz^2}-(\frac{k_1}{H})^2 S_1=\lambda^2\,\frac{d^2\sigma_{b_1}}{dz^2} \qquad \ldots\ldots (5.26)$$

$$\frac{d^2S_2}{dz^2}-(\frac{k_2}{H})^2 S_2=\lambda^2\,\frac{d^2\sigma_{b_2}}{dz^2} \qquad \ldots\ldots (5.27)$$

At $z = H_1$

$$\frac{dS_1}{dz}-\frac{G_1}{G_2}\,\frac{dS_2}{dz}-(1-\frac{G_1}{G_2}\cdot\frac{I_1}{I_2})\,\lambda^2\,\frac{d\sigma_{b_1}}{dz}=0 \qquad \ldots (5.28)$$

At $z = H$, $\frac{dS_2}{dz}-\lambda^2\,\frac{d\sigma_{b_2}}{dz}=0$ $\qquad \ldots\ldots (5.29)$

where $k_1^2=45\,\frac{G_1}{E_1}(\frac{H}{b})^2\,\frac{7(5m^2-10m+9)+5(3-m)^2\,\frac{c}{b}(1+7\,\frac{A_{c_1}}{ct_1})}{15(35m^2-42m+15)+7(\frac{c}{b})^3(3-m)^2}$

$$k_2^2=45\,\frac{G_2}{E_2}(\frac{H}{b})^2\,\frac{7(5m^2-10m+9)+5(3-m)^2\,\frac{c}{b}(1+7\,\frac{A_{c_2}}{ct_2})}{15(35m^2-42m+15)+7(\frac{c}{b})^3(3-m)^2}$$

$$\lambda^2 = 45 \frac{7(5m - 3) - \left(\frac{c}{b}\right)^3 (3 - m)}{15(35m^2 - 42m + 15) + 7\left(\frac{c}{b}\right)^3 (3 - m)^2}$$

Comparing k_1^2 and k_2^2 it is found that,

$$\frac{k_1^2}{k_2^2} = \frac{G_1}{G_2} \frac{E_2}{E_1}$$

For practical structures, the values of k_1^2 and k_2^2 are positive for all values of $\frac{b}{c}$ and $\frac{A_{c_1}}{ct_1}$.

Consequently, the homogeneous part of the solution of equation (5.26) may be expressed as,

$$S_1 = A_1 \cosh \frac{k_1}{H} z + B_1 \sinh \frac{k_1}{H} z \qquad \ldots\ldots (5.30)$$

The homogeneous part of the solution of equation (5.27) becomes,

$$S_2 = A_2 \cosh \frac{k_2}{H} z + B_2 \sinh \frac{k_2}{H} z \qquad \ldots\ldots (5.31)$$

In the case of uniformly distributed load p throughout the height,

$$M = \frac{pz^2}{2}$$

$$\sigma_{b_1} = \frac{pc}{2I_1} z^2 \; ; \qquad \sigma_{b_2} = \frac{pc}{2I_2} z^2$$

The particular integrals for the equations (5.26) and (5.27) are

$$S_1 = - \frac{\lambda^2}{k_1^2} \frac{pcH^2}{I_1}$$

$$S_2 = - \frac{\lambda^2}{k_2^2} \frac{pcH^2}{I_2}$$

The constants of integration A_1, B_1, A_2 and B_2 are evaluated from the boundary conditions (5.18), (5.19), (5.28) and (5.29) and may be expressed in the form,

$$A_1 = \frac{\lambda^2}{k_1^2} \quad \frac{pcH^2}{I_1}$$

$$A_2 = \frac{\lambda^2}{k_2^2} \quad \frac{pcH^2}{I_2} \frac{1}{D} \left\{ \frac{k_2}{k_1} \cosh k_2 \left[1 - (1 - \frac{k_1^2}{k_2^2}) \cosh \frac{k_1 H_1}{H} \right.\right.$$

$$\left. + (1 - \frac{G_1}{G_2} \cdot \frac{I_1}{I_2}) \frac{k_1 H_1}{H} \cdot \sinh \frac{k_1 H_1}{H} \right]$$

$$-k_2 \left[\frac{k_1}{k_2} \cosh \frac{k_1 H_1}{H} \sinh \frac{k_2 H_1}{H} - \frac{G_1}{G_2} \frac{I_1}{I_2} \sinh \frac{k_1 H_1}{H} \cosh \frac{k_2 H_1}{H} \right] \Bigg\}$$

$$B_1 = \frac{\lambda^2}{k_1^2} \quad \frac{pcH^2}{I_1} \quad \frac{1}{D} \left\{ \frac{k_1}{k_2} \cosh k_2 (1 - \frac{H_1}{H}) \left[(1 - \frac{G_1}{G_2} \frac{I_1}{I_2}) \frac{k_1 H_1}{H} \right.\right.$$

$$\left. - \sinh \frac{k_1 H_1}{H} \right] + \frac{G_1}{G_2} \cdot \frac{I_1}{I_2} \cdot$$

$$\left. \left[(1 - \frac{k_1^2}{k_2^2} - \cosh \frac{k_1 H_1}{H}) \sinh k_2 (1 - \frac{H_1}{H}) + \frac{k_1^2}{k_2} \right] \right\}$$

$$B_2 = - \frac{\lambda^2}{k_2^2} \quad \frac{pcH^2}{I_2} \frac{1}{D} \left\{ \frac{k_2}{k_1} \sinh k_2 \left[1 - (1 - \frac{k_1^2}{k_2^2}) \cosh \frac{k_1 H_1}{H} \right.\right.$$

$$\left. + (1 - \frac{G_1}{G_2} \frac{I_1}{I_2}) \cdot \frac{k_1 H_1}{H} \sinh \frac{k_1 H_1}{H} \right]$$

$$- k_2 \left[\frac{k_1}{k_2} \cosh \frac{k_1 H_1}{H} \cosh \frac{k_2 H_1}{H} - \right.$$

$$\left. \left. \frac{G_1}{G_2} \frac{I_1}{I_2} \sinh \frac{k_1 H_1}{H} \sinh \frac{k_2 H_1}{H} \right] \right\}$$

where

$$D = \frac{k_1}{k_2} \cosh \frac{k_1 H_1}{H} \cosh k_2\left(1 - \frac{H_1}{H}\right) + \frac{G_1}{G_2} \frac{I_1}{I_2} \sinh \frac{k_1 H_1}{H} \cdot \sinh k_2\left(1 - \frac{H_1}{H}\right)$$

Substituting the values of the integration constants the stress functions S_1 and S_2 become

$$S_1 = \frac{\lambda^2}{k_1^2} \frac{pcH^2}{I_1} \left[\frac{1}{D} \left\{ \frac{k_1}{k_2} \cosh k_2\left(1 - \frac{H_1}{H}\right) \left[\cosh \frac{k_1 H_1}{H}\left(1 - \frac{z}{H_1}\right) + \left(1 - \frac{G_1}{G_2} \frac{I_1}{I_2}\right) \frac{k_1 H_1}{H} \cdot \sinh \frac{k_1 z}{H} \right] + \frac{G_1}{G_2} \frac{I_1}{I_2} \cdot \left[\sinh k_2\left(1 - \frac{H_1}{H}\right) \sinh \frac{k_1 H_1}{H} \left(1 - \frac{z}{H_1}\right) + \left\{ \left(1 - \frac{k_1^2}{k_2^2}\right) \sinh k_2\left(1 - \frac{H_1}{H}\right) + \frac{k_1^2}{k_2} \right\} \cdot \sinh \frac{k_1 z}{H} \right] \right\} - 1 \right] \quad \ldots\ldots \quad (5.32)$$

$$S_2 = \frac{\lambda^2}{k_2^2} \frac{pcH^2}{I_2} \left[\frac{1}{D} \left\{ \frac{k_2}{k_1} \left[1 - \left(1 - \frac{k_1^2}{k_2^2}\right) \cosh \frac{k_1 H_1}{H} + \left(1 - \frac{G_1}{G_2} \frac{I_1}{I_2}\right) \frac{k_1 H_1}{H} \sinh \frac{k_1 H_1}{H} \right] \cdot \cosh k_2\left(1 - \frac{z}{H}\right) + k_2 \frac{G_1}{G_2} \frac{I_1}{I_2} \sinh \frac{k_1 H_1}{H} \cosh \frac{k_2 H_1}{H}\left(\frac{z}{H_1} - 1\right) + k_1 \cosh \frac{k_1 H_1}{H} \sinh \frac{k_2 H_1}{H} \left(\frac{z}{H_1} - 1\right) \right\} - 1 \right] \quad \ldots\ldots \quad (5.33)$$

In the case of uniform column and beam stiffnesses throughout the height the equations (5.32) and (5.33) reduce to

$$S_1 = S_2 = \frac{\lambda^2}{k^2} \frac{pcH^2}{I} \left[\frac{\cosh k(1 - \frac{z}{H}) + k \sinh \frac{kz}{H}}{\cosh k} - 1 \right]$$

where k_1 amd k_2 are equal and denoted by k and I_1 and I_2 are equal and denoted by I.

Other standard load cases may be considered and the equations (5.26) and (5.27) solved subject to the boundary conditions (5.18), (5.19), (5.28) and (5.29).

In the case where the structure includes more than two regions, with different beam and column stiffnesses, the nature of the governing differential equations for stress functions will be similar to equations (5.26) and (5.27). For every additional region there will be two more boundary conditions similar to the boundary conditions (5.19) and (5.28). Once the differential equations for the stress functions and boundary conditions are known, it is a simple but tedious matter to solve the equations to determine the stress function at any level of the structure for any type of load conditions.

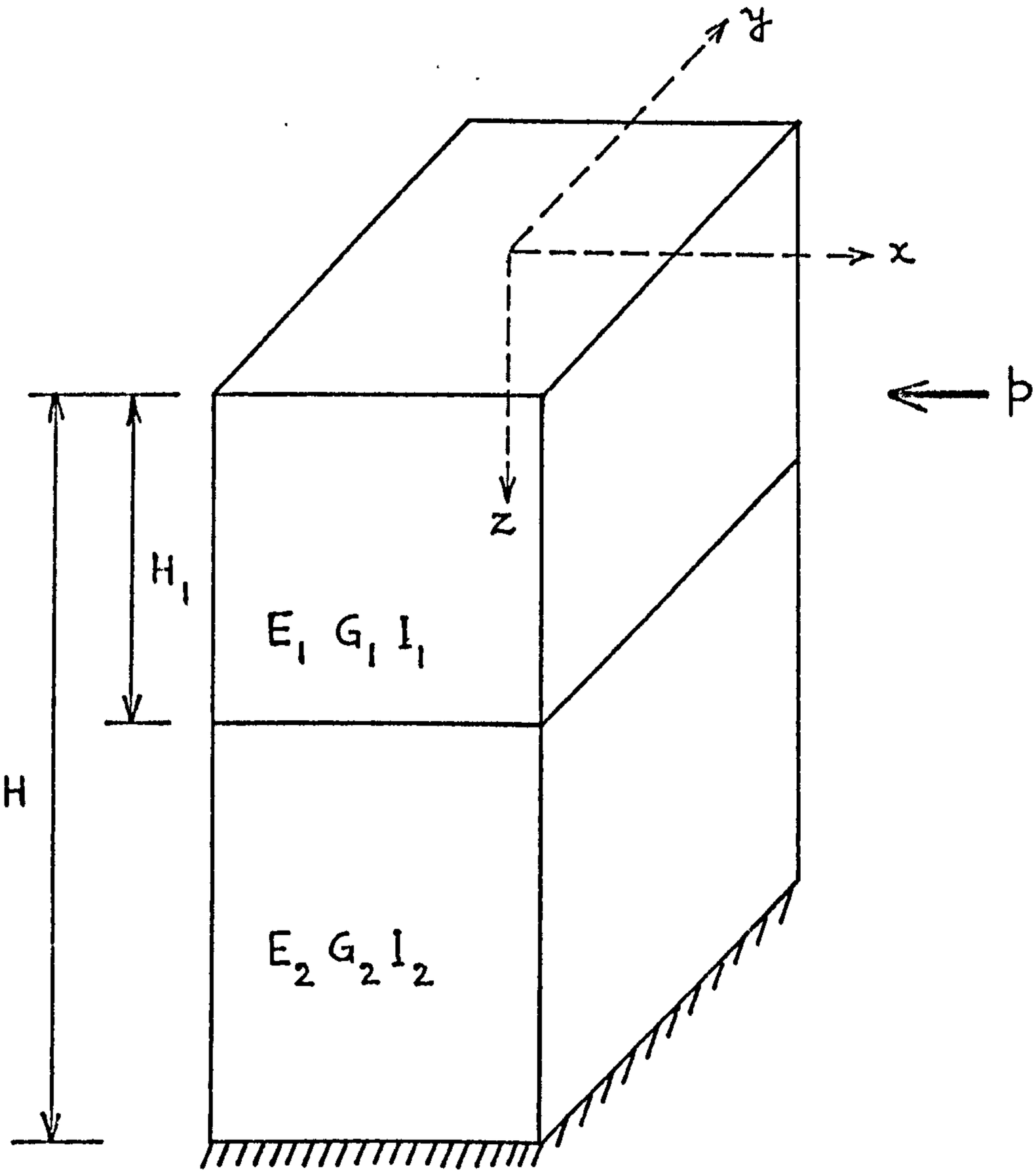

Fig. 5.1 Substitute Tube Structure

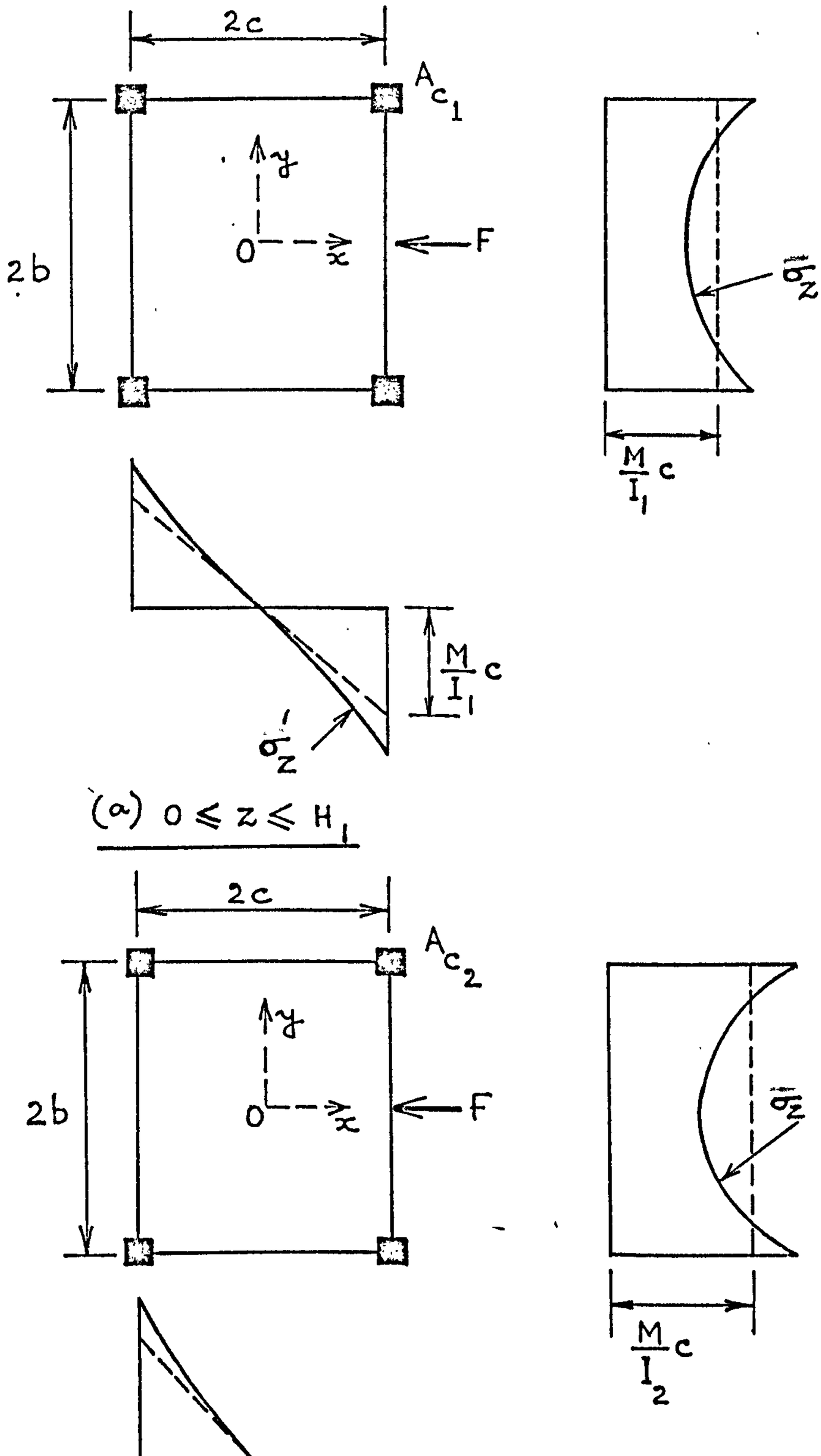

Fig. 5.2 Shear lag in tube

CHAPTER 6

ANALYSIS OF BUNDLED TUBE STRUCTURE

NOTATION

The following symbols are used in this chapter:

A_1, A_2 = areas of columns at the intersections of flange and web panels;

a = aspect ratio $(\frac{b}{c})$;

b = half breadth of bundled tube;

c = half depth of bundled tube;

d = bay width;

E = elastic modulus;

F = applied shear force at any level;

f_1, f_2, f_3, f_4 = stress functions;

G = equivalent shear modulus;

H = total height of building;

I = second moment of area of bundled tube;

k, k_1, k_2 = structural parameters;

M = applied moment at any level;

n_1 = $\frac{A_1}{ct}$;

n_2 = $\frac{A_2}{ct}$;

S, S_o, S_1 = stress functions;

t = thickness of equivalent orthotropic plate;

U = strain energy ;

x, y = horizontal coordinates;

z, z' = vertical coordinates;

α_1, α_2 = geometrical ratios;

β_1, β_2 = structural parameters;

λ, λ_1, λ_2 = geometrical ratios;

ξ = non-dimensional height coordinate $(\frac{z}{H})$;

σ = direct stress;

σ_b = direct stress according to engineer's beam theory;

τ = shear stress.

6.1 INTRODUCTION

Conventional square or rectangular framed tubes, relying on facade frames, exhibit a large amount of shear lag with consequent loss of cantilever efficiency. The Bundled Tube or Modular Tube system, which basically consists of a bundling of smaller size tubes, was evolved to reduce the shear lag effect, thereby inducing more effective participation of the core columns or interior columns in resisting lateral loads. In this system additional frames are provided in each direction which are engaged to perimeter frames with the result that the axial load distribution line exhibits peak points at each intersection of the web frame and the flange frame. This improved behaviour can be seen in Fig. 6.1 where the shear lag is confined to only the width of a modular tube. The structural premium for height (extra structural weight per square metre in tall buildings to provide wind resistance) is reduced considerably due to improved tubular behaviour.

Apart from its improved structural efficiency, the Bundled Tube system is particularly suitable to satisfy the

modularisation of space. This consists of "step back" in which the floor areas are systematically reduced at various heights. The modular step back is accomplished by termination of columns pertaining to the particular tube while other columns continue. It is claimed that such modulation of rental space maximises rental revenue.

6.2 ANALYSIS OF STRUCTURE WITH TWO TUBES

In the simplest form of bundled tube structure shown in Fig. 6.2, one additional web frame is added to the usual perimeter frames of the framed tube structure. The perforated walls of each tube consist of closely spaced columns and deep spandrel beams at each floor level. The two adjacent framed tubes share one set of columns and beams. The basic character of the frame is maintained throughout the height of the building.

As already discussed in Chapter 2, each framework panel of columns and spandrel beams is replaced by an equivalent uniform orthotropic plate, to form a substitute structure with two adjacent closed tubes. The substitute structure is shown in Fig. 6.3, in which the stress systems on small elements on the normal and side panels are given.

The equations of equilibrium for the normal and side panels are

$$\frac{\partial \sigma_y}{\partial y} + \frac{\partial \tau_{yz}}{\partial z} = 0$$

$$\frac{\partial \sigma_z}{\partial z} + \frac{\partial \tau_{yz}}{\partial y} = 0 \qquad \ldots\ldots (6.1)$$

$$\frac{\partial \sigma_x}{\partial x} + \frac{\partial \tau_{xz}}{\partial z} = 0$$

$$\frac{\partial \sigma'_z}{\partial z} + \frac{\partial \tau_{xz}}{\partial x} = 0 \qquad \ldots\ldots (6.2)$$

It is assumed that the structure possesses two horizontal axes of symmetry, passing through the vertical central axis, so that the stress systems in the side perimeter panels 1 and 2 (Fig. 6.4) are identical and those in the normal panels are equal and opposite. Since the additional web panel 3 and the side perimeter panels are identical and their deflection profiles are also the same, it is assumed that the vertical stress distributions in the three web panels are identical. It is further assumed that the axial load distribution curve in the normal panel of each tube is symmetrical about the vertical centre line of the panel, so that the peak stresses at the intersections of web and flange panels are all equal in magnitude (Fig. 6.4). These assumptions are necessary to reduce the number of unknown functions and produce a simple solution to the problem of shear lag in bundled-tube structure.

The simplest approximation which may be made for the vertical stress distribution σ_z in the normal panel, modified by the shear lag effect, is a parabolic distribution. The stress distribution σ_z in panel 4 (Fig. 6.4) may thus be expressed in the form,

$$\sigma_z = \frac{M}{I} c + S_o + 4\left(\frac{y}{b} - \tfrac{1}{2}\right)^2 S \qquad \ldots\ldots (6.3)$$

where S_o and S are functions of the height coordinate z only.

In equation (6.3) I is the second moment of area of the equivalent tube cross-section, given by

$$I = 2tc^2(2b + c) + 4A_1c^2 + 2A_2c^2$$

where 2b and 2c are the overall cross-sectional dimensions of the bundled tube, normal and parallel to the wind directions respectively, and A_1 and A_2 are the cross-sectional areas of the stiffer columns at the intersections of the flange and web panels.

The distribution of vertical stresses σ_z' in the web panels may be expressed as,

$$\sigma_z' = \frac{M}{I} x + \left(\frac{x}{c}\right)^3 S_1 \qquad \ldots\ldots (6.4)$$

where S_1 is a function of the height coordinate z only.

Because of the skew-symmetry of the stress distribution only odd powers of the polynomial have been used in equation (6.4) for the web panels.

The condition of vertical strain compatibility at the intersections of flange and web panels requires that

$$\left(\frac{\sigma_z}{E}\right)_{y=0 \text{ or } b} = \left(\frac{\sigma_z'}{E}\right)_{x=c} = \frac{\sigma_c}{E} \qquad \ldots\ldots (6.5)$$

where σ_c is the axial stress in the column at the intersection of normal and side panels given by, on using equation (6.3),

$$\sigma_c = (\sigma_z)_{y=0 \text{ or } b} = \frac{M}{I} c + S_o + S \qquad \ldots\ldots (6.6)$$

On substituting equations (6.3) and (6.4) into

equation (6.5) it is found that

$$S_1 = S_o + S \qquad \ldots\ldots\ldots (6.7)$$

The condition of overall moment equilibrium at any height may be expressed in the form,

$$4\int_0^b \sigma_z \, tcdy + 3\int_{-c}^{c} \sigma'_z \, txdx + (4A_1 + 2A_2)c\,\sigma_c = M(z) \qquad \ldots\ldots\ldots (6.8)$$

where M(z) is the total bending moment at that level caused by the applied lateral loading.

On substituting equations (6.3), (6.4), (6.6) and (6.7) into the equilibrium condition (6.8) and integrating, it is found that

$$S_o = -\tfrac{1}{3}\, m\, S \qquad \ldots\ldots\ldots (6.9)$$

where $$m = \frac{10b + 9c + 30\,\frac{A_1}{t} + 15\,\frac{A_2}{t}}{10b + 3c + 10\,\frac{A_1}{t} + 5\,\frac{A_2}{t}}$$

which is always greater than unity.

The vertical stresses σ_z and σ'_z may, therefore, be expressed in terms of the single unknown function S as,

$$\sigma_z = \frac{M}{I}\, c + \left[(1 - \tfrac{1}{3}m) - 4\left(\frac{y}{b}\right) + 4\left(\frac{y}{b}\right)^2 \right] S \qquad \ldots\ldots (6.10)$$

$$\sigma'_z = \frac{M}{I}\, x + (1 - \tfrac{1}{3}m)\left(\frac{x}{c}\right)^3 S \qquad \ldots\ldots\ldots (6.11)$$

The stress σ_c then becomes

$$\sigma_c = (\sigma_z)_{y=0 \text{ or } b} = \frac{M}{I}\, c + (1 - \tfrac{1}{3}m)S \qquad \ldots\ldots\ldots (6.12)$$

On substituting equation (6.10) into equation (6.1) and integrating, the shear stress τ_{yz} is given by

$$\tau_{yz} = -y \left[\frac{c}{I} \frac{dM}{dz} + \left\{ (1 - \tfrac{1}{3}m) - 2\left(\frac{y}{b}\right) + \frac{4}{3}\left(\frac{y}{b}\right)^2 \right\} \frac{dS}{dz} \right] + C_1$$

..... (6.13)

where C_1 is the constant of integration; that is, constant with respect to y.

At y = 0, $\tau_{yz} = C_1$ ..... (6.14)

At y = b, $\tau_{yz} = -\frac{bc}{I}\frac{dM}{dz} + \frac{b}{3}(m - 1)\frac{dS}{dz} + C_1$

..... (6.15)

Similarly on substituting equation (6.11) into the equilibrium equation (6.2) and integrating, the shear stress τ_{xz} is found out as

$$\tau_{xz} = -\frac{x^2}{2I}\frac{dM}{dz} - \tfrac{1}{4}(1 - \tfrac{1}{3}m)\frac{x^4}{c^3}\frac{dS}{dz} + C_2 \quad \text{..... (6.16)}$$

At x = c,

$$\tau_{xz} = -\frac{c^2}{2I}\frac{dM}{dz} - \frac{c}{4}(1 - \tfrac{1}{3}m)\frac{dS}{dz} + C_2 \quad \text{..... (6.17)}$$

The constants of integration are evaluated from the equilibrium equations for the columns at the intersections of flange and web panels.

The equation of equilibrium for the column at the intersection of panels 1 and 4 is given by

$$(\tau_{xz})_{x=c} + (\tau_{yz})_{y=b} = \frac{A_1}{t}\frac{\partial \sigma_c}{\partial z} \quad \text{..... (6.18)}$$

For the column at the intersection of panels 3 and 4 the equilibrium equation becomes

$$(\tau_{xz})_{x=c} - 2(\tau_{yz})_{y=0} = \frac{A_2}{t}\frac{\partial \sigma_c}{\partial z} \quad \text{..... (6.19)}$$

On substituting equations (6.14), (6.15) and (6.17) into the equilibrium equations (6.18) and (6.19), the constants of integration C_1 and C_2 are determined as

$$C_1 = \frac{c^2}{3I}\left(\frac{b}{c} + \frac{A_1}{ct} - \frac{A_2}{ct}\right)\frac{dM}{dz} - \frac{c}{3}\left[\frac{1}{3}(m-1)\frac{b}{c} - (1-\tfrac{1}{3}m)\left(\frac{A_1}{ct} - \frac{A_2}{ct}\right)\right]\frac{dS}{dz} \quad \ldots\ldots (6.20)$$

$$C_2 = \frac{c^2}{6I}\left(\frac{9}{5} + \frac{8}{3-m}\frac{b}{c}\right)\frac{dM}{dz} + \frac{c}{20}(1-\tfrac{1}{3}m)\frac{dS}{dz} \quad \ldots\ldots (6.21)$$

The shear stresses τ_{yz} and τ_{xz} may, therefore, be expressed in the form

$$\tau_{yz} = \frac{bc}{3I}\left[1 + \frac{c}{b}\left(\frac{A_1}{ct} - \frac{A_2}{ct}\right) - 3\left(\frac{y}{b}\right)\right]\frac{dM}{dz}$$

$$- b\left[\frac{1}{9}(m-1) - \tfrac{1}{3}(1-\tfrac{1}{3}m)\frac{c}{b}\left(\frac{A_1}{ct} - \frac{A_2}{ct}\right)\right.$$

$$\left. + (1-\tfrac{1}{3}m)\left(\frac{y}{b}\right) - 2\left(\frac{y}{b}\right)^2 + \frac{4}{3}\left(\frac{y}{b}\right)^3\right]\frac{dS}{dz} \quad \ldots\ldots (6.22)$$

$$\tau_{xz} = \frac{c^2}{6I}\left[\frac{9}{5} + \frac{8}{3-m}\frac{b}{c} - 3\left(\frac{x}{c}\right)^2\right]\frac{dM}{dz}$$

$$+ (1-\tfrac{1}{3}m)\frac{c}{4}\left[\frac{1}{5} - \left(\frac{x}{c}\right)^4\right]\frac{dS}{dz} \quad \ldots\ldots (6.23)$$

The horizontal direct stresses σ_x and σ_y are small compared to the vertical stresses σ_z and σ'_z and are not evaluated.

The total strain energy stored in the structure is given by,

$$U = t\int_0^H \left\{2\int_0^b \left[\frac{\sigma_z^2}{E} + \frac{\tau_{yz}^2}{G}\right]dy + \right.$$

$$\frac{3}{2}\int_{-c}^{c}\left[\frac{(\sigma_z')^2}{E}+\frac{\tau_{xz}^2}{G}\right]dx\Bigg\}\,dz+\frac{2A_1+A_2}{E}\int_0^H\sigma_c^2\,dz \qquad \ldots\ldots (6.24)$$

On substituting equations (6.10), (6.11), (6.12), (6.22) and (6.23) into equation (6.24), U becomes

$$\begin{aligned}U = t\int_0^H\Bigg[\frac{2}{E}\int_0^b\Bigg\{&\frac{M}{I}c+\left[(1-\tfrac{1}{3}m)-4(\tfrac{y}{b})+4(\tfrac{y}{b})^2\right]S\Bigg\}^2dy\\
&+\frac{2}{G}\int_0^b\Bigg\{\frac{bc}{3I}\left[1+\frac{c}{b}(\frac{A_1}{ct}-\frac{A_2}{ct})-3(\tfrac{y}{b})\right]\frac{dM}{dz}\\
&-b\left[\tfrac{1}{9}(m-1)-\tfrac{1}{3}(1-\tfrac{1}{3}m)\frac{c}{b}(\frac{A_1}{ct}-\frac{A_2}{ct})\right.\\
&\left.+(1-\tfrac{1}{3}m)(\tfrac{y}{b})-2(\tfrac{y}{b})^2+\tfrac{4}{3}(\tfrac{y}{b})^3\right]\frac{dS}{dz}\Bigg\}^2dy\\
&+\frac{3}{2E}\int_{-c}^{c}\Bigg\{\frac{M}{I}x+(1-\tfrac{1}{3}m)(\tfrac{x}{c})^3S\Bigg\}^2dx\\
&+\frac{3}{2G}\int_{-c}^{c}\Bigg\{\frac{c^2}{6I}\left[\frac{9}{5}+\frac{8}{3-m}\frac{b}{c}-3(\tfrac{x}{c})^2\right]\frac{dM}{dz}\\
&+(1-\tfrac{1}{3}m)\frac{c}{4}\left[\frac{1}{5}-(\tfrac{x}{c})^4\right]\frac{dS}{dz}\Bigg\}^2dx\\
&+\frac{2A_1+A_2}{tE}\left\{\frac{M}{I}c+(1-\tfrac{1}{3}m)S\right\}^2\Bigg]dz \qquad \ldots\ldots (6.25)\end{aligned}$$

The variation of U, δU, may be expressed as,

$$\begin{aligned}\delta U = 2t\int_0^H\Bigg[\frac{2}{E}\int_0^b\Bigg\{&\frac{M}{I}c+\left[(1-\tfrac{1}{3}m)-4(\tfrac{y}{b})+4(\tfrac{y}{b})^2\right]S\Bigg\}\\
&\left[(1-\tfrac{1}{3}m)-4(\tfrac{y}{b})+4(\tfrac{y}{b})^2\right]\delta S\,dy\end{aligned}$$

$$+ \frac{2}{G} \int_0^b \left\{ \frac{bc}{3I} \left[1 + \frac{c}{b} \left(\frac{A_1}{ct} - \frac{A_2}{ct} \right) - 3\left(\frac{y}{b}\right) \right] \frac{dM}{dz} \right.$$

$$- b \left[\frac{1}{9}(m - 1) - \tfrac{1}{3}(1 - \tfrac{1}{3}m) \frac{c}{b}\left(\frac{A_1}{ct} - \frac{A_2}{ct} \right) \right.$$

$$\left. \left. + (1 - \tfrac{1}{3}m)\left(\frac{y}{b}\right) - 2\left(\frac{y}{b}\right)^2 + \frac{4}{3}\left(\frac{y}{b}\right)^3 \right] \frac{dS}{dz} \right\} .$$

$$\left\{ - b \left[\frac{1}{9}(m - 1) - \tfrac{1}{3}(1 - \tfrac{1}{3}m) \frac{c}{b}\left(\frac{A_1}{ct} - \frac{A_2}{ct} \right) \right. \right.$$

$$\left. \left. + (1 - \tfrac{1}{3}m)\left(\frac{y}{b}\right) - 2\left(\frac{y}{b}\right)^2 + \frac{4}{3}\left(\frac{y}{b}\right)^3 \right] \frac{d(\delta S)}{dz} \right\} dy$$

$$+ \frac{3}{2E} \int_{-c}^{c} \left\{ \frac{M}{I} x + (1 - \tfrac{1}{3}m)\left(\frac{x}{c}\right)^3 S \right\} (1 - \tfrac{1}{3}m)\left(\frac{x}{c}\right)^3 \delta S \, dx$$

$$+ \frac{3}{2G} \int_{-c}^{c} \left\{ \frac{c^2}{6I} \left[\frac{9}{5} + \frac{8}{3 - m} \frac{b}{c} - 3\left(\frac{x}{c}\right)^2 \right] \frac{dM}{dz} \right.$$

$$\left. + (1 - \tfrac{1}{3}m) \frac{c}{4} \left[\frac{1}{5} - \left(\frac{x}{c}\right)^4 \right] \frac{dS}{dz} \right\} .$$

$$(1 - \tfrac{1}{3}m) \frac{c}{4} \left[\frac{1}{5} - \left(\frac{x}{c}\right)^4 \right] \frac{d(\delta S)}{dz} dx$$

$$+ \frac{2A_1 + A_2}{t E} \left\{ \frac{M}{I} c + (1 - \tfrac{1}{3}m) S \right\} .(1 - \tfrac{1}{3}m) \delta S \Big] dz$$

..... (6.26)

To obtain the minimum value of strain energy U, the variation δU must vanish. On integrating equation (6.26) and equating to zero, the following equation is obtained.

$$\int_0^H \left\{ - \frac{1}{G} \left[\frac{2b^3}{2835} (35m^2 - 49m + 20) + \frac{2b^2 c}{27}(m-1)(1-\tfrac{1}{3}m)\left(\frac{A_1}{ct} - \frac{A_2}{ct} \right) \right. \right.$$

$$+ \frac{2}{9}\, bc^2(1 - \tfrac{1}{3}m)^2 \left(\frac{A_1}{ct} - \frac{A_2}{ct}\right)^2 + \frac{c^3}{75}(1 - \tfrac{1}{3}m)^2 \Bigg] \frac{d^2S}{dz^2}$$

$$+ \frac{1}{E}\left[\frac{2b}{45}(5m^2 - 10m + 9) + \frac{3c}{7}(1 - \tfrac{1}{3}m)^2 + \frac{2A_1 + A_2}{t}(1 - \tfrac{1}{3}m)^2\right] S$$

$$+ \frac{1}{G}\left[\frac{b^3c}{135I}(10m - 7) + \frac{2b^2c^2}{27I}(2 - m)\left(\frac{A_1}{ct} - \frac{A_2}{ct}\right)\right.$$

$$\left. - \frac{2bc^3}{9I}(1 - \tfrac{1}{3}m)\left(\frac{A_1}{ct} - \frac{A_2}{ct}\right)^2 - \frac{c^4}{35I}(1 - \tfrac{1}{3}m)\right] \frac{d^2M}{dz^2}\Bigg\}\, dz\, \delta S$$

$$+ \frac{1}{G}\left[\left\{\left[\frac{2b^3}{2835}(35m^2 - 49m + 20) + \frac{2b^2c}{27}(m-1)(1 - \tfrac{1}{3}m)\left(\frac{A_1}{ct} - \frac{A_2}{ct}\right)\right.\right.\right.$$

$$\left.\left.\left. + \frac{2}{9}\, bc^2(1 - \tfrac{1}{3}m)^2\left(\frac{A_1}{ct} - \frac{A_2}{ct}\right)^2 + \frac{c^3}{75}(1 - \tfrac{1}{3}m)^2\right] \frac{dS}{dz}\right.\right.$$

$$\left.\left. - \left[\frac{b^3c}{135I}(10m - 7) + \frac{2b^2c^2}{27I}(2 - m)\left(\frac{A_1}{ct} - \frac{A_2}{ct}\right)\right.\right.\right.$$

$$\left.\left.\left. - \frac{2bc^3}{9I}(1 - \tfrac{1}{3}m)\left(\frac{A_1}{ct} - \frac{A_2}{ct}\right)^2 - \frac{c^4}{35I}(1 - \tfrac{1}{3}m)\right] \frac{dM}{dz}\right\} \delta S\right]_0^H$$

$$= 0 \qquad \ldots\ldots (6.27)$$

The governing differential equation may, therefore, be expressed in the form

$$\frac{d^2S}{dz^2} - \left(\frac{k}{H}\right)^2 S = \lambda^2 \frac{d^2\sigma_b}{dz^2} \qquad \ldots\ldots (6.28)$$

where

$$k^2 = 45\, \frac{G}{E} \left(\frac{H}{b}\right)^2 \frac{1}{D_1}\left[14(5m^2 - 10m + 9) + 5(3 - m)^2 \cdot \left(\frac{c}{b}\right) \cdot \left(3 + 7\, \frac{2A_1 + A_2}{ct}\right)\right]$$

$$\lambda^2 = 15 \times \frac{1}{D_1}\left[7(10m - 7) + 70(2 - m)\left(\frac{c}{b}\right)\left(\frac{A_1}{ct} - \frac{A_2}{ct}\right)\right.$$

$$- 70(3 - m)\left(\frac{c}{b}\right)^2\left(\frac{A_1}{ct} - \frac{A_2}{ct}\right)^2 - 9(3 - m)\left(\frac{c}{b}\right)^3 \Bigg]$$

where $D_1 = 10(35m^2 - 49m + 20) + 7(3 - m)\left(\frac{c}{b}\right)$.

$$\Bigg[50(m-1)\left(\frac{A_1}{ct} - \frac{A_2}{ct}\right) + 50(3-m)\left(\frac{c}{b}\right)\left(\frac{A_1}{ct} - \frac{A_2}{ct}\right)^2$$

$$+ 3(3 - m)\left(\frac{c}{b}\right)^2 \Bigg]$$

For the case of a structure rigidly fixed at the base and free at the top, the boundary conditions are

$$\text{At } z = 0, \quad S = 0 \qquad \ldots\ldots (6.29)$$

$$\text{At } z = H, \quad \frac{dS}{dz} - \lambda^2 \frac{d\sigma_b}{dz} = 0 \qquad \ldots\ldots (6.30)$$

It is found that the governing differential equation (6.28) and the boundary conditions (6.29) and (6.30) derived for a bundled tube structure are identical to the governing differential equation (2.45) and boundary conditions (2.41) and (2.46) respectively suitable for a framed-tube structure. The solution of the equation for different lateral loading conditions will, therefore, be identical. The same design curves Figs.2.8 to 2.13 may be used to evaluate the direct and shear stresses. The function F_1, equal to λ^2, may be calculated directly from equation (6.28).

In the particular case where the columns at the intersections of the flange and web frames have suitable stiffnesses (the same as other columns at the intersection of panels 1 and 4, and $\frac{3}{2}$ times the other columns at the intersection of panels 3 and 4), so that they can be included as a segment of the equivalent orthotropic plates,

the concentrated areas A_1 and A_2 are zero, and the parameters k^2 and λ^2 reduce to,

$$k^2 = 162 \frac{G}{E} \left(\frac{H}{b}\right)^2 \frac{(3 - m)(5m^2 + 15m - 6)}{385m^3 - 714m^2 + 597m - 160}$$

$$\lambda^2 = -\frac{9}{2} \frac{790m^3 - 1593m^2 + 228m + 323}{(3 - m)(385m^3 - 714m^2 + 597m - 160)}$$

where the geometrical ratio m is given by

$$m = \frac{10b + 9c}{10b + 3c} .$$

6.3 NUMERICAL EXAMPLE

In the bundled tube structure shown in Fig. 6.5, one additional web frame has been added to the perimeter frames of the framed-tube structure analysed in Article 2.9. The building has the same dimensions and is subjected to a uniform lateral load of 1 kN/m height.

With the given data it is found that

$t = 0.1$ m

$A_1 = 0.3$ m^2

$A_2 = 0.105$ m^2

$I = 266.76$ m^4

$m = 1.6147$

$\sigma_{b(H)} = 364.37$ kN/m^2

$\lambda^2 = 2.4568$

$\frac{G}{E} = 0.044813$

$k^2 = 157.55$

$k = 12.5519$

The function S at the second floor level ($\xi = 0.96$), given by equation (2.50), becomes

$$S = 0.2057 \quad \sigma_b(H)$$

The axial force in column 1 of flange panel is given by (Fig. 6.5)

$$N_1 = t \int_{b-\frac{d}{2}}^{b} \sigma_z \, dy$$

On substituting σ_z from equation (6.10) and integrating N_1 becomes

$$N_1 = \frac{td}{2} \left\{ \sigma_b + \left[(1 - \tfrac{1}{3}m) - \frac{d}{b^2} (b - \frac{d}{3}) \right] S \right\}$$

The axial force in column in the flange panel at position y_i may be expressed as

$$N_i = t \int_{y_i - \frac{d}{2}}^{y_i + \frac{d}{2}} \sigma_z \, dy$$

which on the substitution of the value of σ_z becomes,

$$N_i = td \left\{ \sigma_b + \left[(1 - \tfrac{1}{3}m) - \frac{4}{b} y_i + \frac{4}{3b^2}(3y_i^2 + \frac{d^2}{4}) \right] S \right\}$$

The axial force in column 5 of the flange panel is double the axial force in column 1.

The axial forces N_1 in column 1 and N_i in column at position x_i in the web panel may be expressed as

$$N_1 = \frac{td}{2c}(c - \frac{d}{4}) \left\{ \sigma_b + (1 - \tfrac{1}{3}m) \frac{1}{c^2}(c^2 - \frac{cd}{2} + \frac{d^2}{8})S \right\}$$

and

$$N_i = \frac{tdx_i}{c} \left\{ \sigma_b + (1 - \tfrac{1}{3}m) \frac{1}{c^2} (x_i^2 + \frac{d^2}{4})S \right\}$$

In the concentrated areas A_1 and A_2, the axial

forces N_{c_1} and N_{c_2} respectively are given by

$$N_{c_1} = A_1 \left\{ \sigma_b + (1 - \tfrac{1}{3}m)S \right\}$$

and $$N_{c_2} = A_2 \left\{ \sigma_b + (1 - \tfrac{1}{3}m)S \right\}$$

From the above equations the axial forces in the columns of the flange panel may be evaluated as

$N_2 = 94.7285$ kN

$N_3 = 89.1071$ kN

$N_4 = 94.7285$ kN

The axial forces in the columns of the web panel are

$N_2 = 51.9930$ kN

$N_3 = 0$

The total axial forces N_1 and N_5 in the columns at the intersections of the flange and web panels are determined as

$N_1 = 211.7335$ kN

$N_5 = 192.4880$ kN

Comparing the results of the present analysis with the analysis of Article 2.9 it is found that while the second moment of area of the section of the bundled-tube structure has increased by 8.97 per cent over that of the framed-tube structure, the ratio of minimum to maximum stress in the columns of the flange panel has also increased from 0.6256 in the case of framed-tube structure to 0.8417 in the case of bundled tube structure. Thus the shear lag effect is considerably reduced by the addition of an extra web frame.

6.4 MORE GENERAL ANALYSIS OF STRUCTURE WITH TWO TUBES

The vertical stress σ_z' in the web panel, given by equation (6.11), had for its first term the basic beam theory stress, and the perturbation consisted of a cubic term in the coordinate x. It seems more appropriate to include linear and cubic terms in addition to the linear basic beam theory stress term. In order to achieve this the vertical stresses σ_z and σ_z' in the flange and web panels are expressed in more general terms as (Fig. 6.6),

$$\sigma_z = f_1 + 4\left(\frac{y}{b} - \frac{1}{2}\right)^2 f_2 \qquad \ldots\ldots (6.31)$$

$$\sigma_z' = \left(\frac{x}{c}\right) f_3 + \left(\frac{x}{c}\right)^3 f_4 \qquad \ldots\ldots (6.32)$$

where f_1, f_2, f_3 and f_4 are functions of coordinate z only.

The condition of vertical strain compatibility at the intersections of the flange and web panels requires that,

$$\frac{1}{E}(f_1 + f_2) = \frac{1}{E}(f_3 + f_4) = \frac{\sigma_c}{E} \qquad \ldots\ldots (6.33)$$

The condition of moment equilibrium at any height is given by equation (6.8). On substituting equations (6.31), (6.32) and (6.33) into the equilibrium condition (6.8) it is found that

$$f_1 = \frac{M}{I} c - \frac{2a + 6n_1 + 3n_2 + 3}{3(2a + 2n_1 + n_2 + 1)} f_2 + \frac{2}{5(2a + 2n_1 + n_2 + 1)} f_4$$

$\ldots\ldots$ (6.34)

where $a = \frac{b}{c}$

$$n_1 = \frac{A_1}{ct} \quad , \quad n_2 = \frac{A_2}{ct}$$

On substituting equation (6.34) into equation (6.33) the function f_3 may be expressed as,

$$f_3 = \frac{M}{I} c + \frac{4a}{3(2a+2n_1+n_2+1)} f_2 - \frac{10a + 10n_1 + 5n_2 + 3}{5(2a + 2n_1 + n_2 + 1)} f_4$$

..... (6.35)

The vertical stresses σ_z and σ'_z may, therefore, be expressed in terms of only two unknown functions f_2 and f_4 as,

$$\sigma_z = \frac{M}{I} c + 4\left[\frac{a}{3(2a + 2n_1 + n_2 + 1)} - \left(\frac{y}{b}\right) + \left(\frac{y}{b}\right)^2\right] f_2$$

$$+ \frac{2}{5(2a + 2n_1 + n_2 + 1)} f_4 \quad ..... (6.36)$$

$$\sigma'_z = \frac{M}{I} x + \frac{4a}{3(2a + 2n_1 + n_2 + 1)} \left(\frac{x}{c}\right) f_2$$

$$- \left[\frac{10a + 10n_1 + 5n_2 + 3}{5(2a + 2n_1 + n_2 + 1)} \left(\frac{x}{c}\right) - \left(\frac{x}{c}\right)^3\right] f_4$$

..... (6.37)

The stress in the corner column then becomes,

$$\sigma_c = \frac{M}{I} c + \frac{4a}{3(2a + 2n_1 + n_2 + 1)} f_2 + \frac{2}{5(2a + 2n_1 + n_2 + 1)} f_4$$

..... (6.38)

The equations of equilibrium for the flange and web panels are given by equations (6.1) and (6.2). On substituting equation (6.36) into the equation of equilibrium (6.1) and integrating, the shear stress τ_{yz} is given by

$$\tau_{yz} = - y\left\{ \frac{c}{I}\frac{dM}{dz} + 4\left[\frac{a}{3(2a+2n_1+n_2+1)} - \frac{y}{2b} + \frac{y^2}{3b^2}\right]\frac{df_2}{dz}\right.$$

$$\left. + \frac{2}{5(2a+2n_1+n_2+1)}\ \frac{df_4}{dz}\ \right\} + C_3 \qquad \ldots\ldots (6.39)$$

where C_3 represents the constant of integration.

At $y = 0$, $\quad \tau_{yz} = C_3$ $\qquad \ldots\ldots (6.40)$

$$\text{At } y = b,\ \tau_{yz} = -b\left\{ \frac{c}{I}\frac{dM}{dz} - \frac{2(2n_1 + n_2 + 1)}{3(2a+2n_1+n_2+1)}\ \frac{df_2}{dz}\right.$$

$$\left. + \frac{2}{5(2a+2n_1+n_2+1)}\ \frac{df_4}{dz}\ \right\} + C_3 \qquad (6.41)$$

The shear stress τ_{xz} may also be determined on substituting equation (6.37) into the equilibrium equation (6.2), and is given by

$$\tau_{xz} = - \frac{x^2}{2I}\ \frac{dM}{dz} - \frac{2a}{3(2a+2n_1+n_2+1)}\ \frac{x^2}{c}\ \frac{df_2}{dz}$$

$$+ \tfrac{1}{2}\left[\frac{10a + 10n_1 + 5n_2 + 3}{5(2a + 2n_1 + n_2 + 1)}\ \frac{x^2}{c} - \frac{x^4}{2c^3}\right]\frac{df_4}{dz} + C_4$$

$\ldots\ldots (6.42)$

where C_4 is another constant of integration.

$$\text{At } x = c,\ \tau_{xz} = - \frac{c^2}{2I}\frac{dM}{dz} - \frac{2a}{3(2a + 2n_1 + n_2 + 1)}c\ \frac{df_2}{dz}$$

$$+ \frac{10a + 10n_1 + 5n_2 + 1}{20(2a + 2n_1 + n_2 + 1)}\ c\ \frac{df_4}{dz} + C_4 \qquad (6.43)$$

The equations of equilibrium for the columns at the intersections of flange and web panels are given by equations (6.18) and (6.19). On substituting equations (6.40), (6.41) and (6.43) into the equilibrium equations

(6.18) and (6.19), the constants C_3 and C_4 are evaluated as

$$C_3 = (a + n_1 - n_2)\frac{c^2}{3I}\frac{dM}{dz} - \frac{2a(3n_2+1)}{9(2a+2n_1+n_2+1)}c\frac{df_2}{dz}$$

$$+ \frac{2}{15}\frac{a + n_1 - n_2}{2a + 2n_1 + n_2 + 1}c\frac{df_4}{dz} \qquad \ldots\ldots (6.44)$$

$$C_4 = (4a + 4n_1 + 2n_2 + 3)\frac{c^2}{6I}\frac{dM}{dz} + \frac{2a}{9(2a+2n_1+n_2+1)}c\frac{df_2}{dz}$$

$$- \frac{14a + 14n_1 + 7n_2 + 3}{60(2a + 2n_1 + n_2 + 1)}c\frac{df_4}{dz} \qquad \ldots\ldots (6.45)$$

The shear stresses τ_{yz} and τ_{xz} may, therefore, be expressed in terms of two variables f_2 and f_4 as,

$$\tau_{yz} = \frac{c^2}{3I}\left[(a + n_1 - n_2) - 3a\left(\frac{y}{b}\right)\right]\frac{dM}{dz} - 2b\left[\frac{3n_2 + 1}{9(2a+2n_1+n_2+1)}\right.$$

$$\left. + \frac{2a}{3(2a + 2n_1 + n_2 + 1)}\left(\frac{y}{b}\right) - \left(\frac{y}{b}\right)^2 + \frac{2}{3}\left(\frac{y}{b}\right)^3\right]\frac{df_2}{dz}$$

$$+ \frac{2b}{15a(2a+2n_1+n_2+1)}\left[(a + n_1 - n_2) - 3a\left(\frac{y}{b}\right)\right]\frac{df_4}{dz}$$

$\ldots\ldots$ (6.46)

$$\tau_{xz} = \frac{c^2}{6I}\left[(4a + 4n_1 + 2n_2 + 3) - 3\left(\frac{x}{c}\right)^2\right]\frac{dM}{dz}$$

$$+ \frac{2a}{9(2a + 2n_1 + n_2 + 1)}c\left[1 - 3\left(\frac{x}{c}\right)^2\right]\frac{df_2}{dz}$$

$$- \frac{c}{2}\left[\frac{14a+14n_1+7n_2+3}{30(2a+2n_1+n_2+1)} - \frac{10a+10n_1+5n_2+3}{5(2a+2n_1+n_2+1)}\left(\frac{x}{c}\right)^2\right.$$

$$\left. + \frac{1}{2}\left(\frac{x}{c}\right)^4\right]\frac{df_4}{dz} \qquad \ldots\ldots (6.47)$$

It is found that each web frame carries one third of the total shear force caused due to the lateral load, so that

$$t \int_{-c}^{c} \tau_{xz} \, dx = \frac{1}{3} \frac{dM}{dz} = \frac{F}{3}$$

The total strain energy stored in the structure is expressed by equation (6.24). On substituting equations (6.36), (6.37), (6.38), (6.46) and (6.47) into the equation (6.24), the total strain energy U may be expressed as,

$$U = t \int_0^H \left[\frac{2}{E} \int_0^b \left\{ \frac{M}{I} c + 4 \left[\frac{a}{3(2a+2n_1+n_2+1)} - \left(\frac{y}{b}\right)+\left(\frac{y}{b}\right)^2 \right] f_2 \right.\right.$$

$$\left.\left. + \frac{2}{5(2a + 2n_1 + n_2 + 1)} f_4 \right\}^2 dy \right.$$

$$+ \frac{2}{G} \int_0^b \left\{ \frac{c^2}{3I} \left[(a+n_1-n_2) - 3a\left(\frac{y}{b}\right) \right] \frac{dM}{dz} - 2b \left[\frac{3n_2 + 1}{9(2a+2n_1+n_2+1)} \right.\right.$$

$$\left. + \frac{2a}{3(2a+2n_1+n_2+1)} \left(\frac{y}{b}\right) - \left(\frac{y}{b}\right)^2 + \frac{2}{3}\left(\frac{y}{b}\right)^3 \right] \frac{df_2}{dz}$$

$$\left. + \frac{2b}{15a(2a+2n_1+n_2+1)} \left[(a+n_1-n_2) - 3a\left(\frac{y}{b}\right) \right] \frac{df_4}{dz} \right\}^2 dy$$

$$+ \frac{3}{2E} \int_{-c}^{c} \left\{ \frac{M}{I} x + \frac{4a}{3(2a + 2n_1 + n_2 + 1)} \left(\frac{x}{c}\right) f_2 \right.$$

$$\left. - \left[\frac{10a + 10n_1 + 5n_2 + 3}{5(2a + 2n_1 + n_2 + 1)} \left(\frac{x}{c}\right) - \left(\frac{x}{c}\right)^3 \right] f_4 \right\}^2 dx$$

$$+ \frac{3}{2G} \int_{-c}^{c} \left\{ \frac{c^2}{6I} \left[(4a + 4n_1 + 2n_2 + 3) - 3\left(\frac{x}{c}\right)^2 \right] \frac{dM}{dz} \right.$$

$$+ \frac{2a}{9(2a+2n_1+n_2+1)}\, c \left[1 - 3\left(\frac{x}{c}\right)^2\right] \frac{df_2}{dz}$$

$$- \frac{c}{2}\left[\frac{14a+14n_1+7n_2+3}{30(2a+2n_1+n_2+1)} - \frac{10a+10n_1+5n_2+3}{5(2a+2n_1+n_2+1)} \left(\frac{x}{c}\right)^2 \right.$$

$$\left. + \tfrac{1}{2}\left(\frac{x}{c}\right)^4\right] \frac{df_4}{dz} \Bigg\}^2 dx$$

$$+ \frac{2A_1 + A_2}{t\,E}\left\{\frac{M}{I}\, c + \frac{4a}{3(2a+2n_1+n_2+1)}\, f_2 \right.$$

$$\left. + \frac{2}{5(2a+2n_1+n_2+1)}\, f_4\right\}^2 \Bigg] dz$$

..... (6.48)

For minimum U, the variation δU must vanish. On minimising U, the following equation is obtained.

$$\int_0^{II} \Big\{ - \frac{1}{G}\,\frac{4c^3a^2}{63}\,(6a^3 + 468an_1^2 + 117an_2^2 + 54a^2n_1 + 27a^2n_2$$

$$- 162an_1n_2 + 27a^2 + 258an_1 + 24an_2 + 47a + 42)\,\frac{d^2f_2}{dz^2}$$

$$+ \frac{1}{E}\, 8ca(2a^2 + 12n_1^2 + 3n_2^2 + 14an_1 + 7an_2 + 12n_1n_2$$

$$+ 7a + 12n_1 + 6n_2 + 3)\, f_2$$

$$+ \frac{1}{G}\,\frac{c^3a}{105}\,(42a^3 - 420an_1^2 - 210an_2^2 + 462a^2n_1 + 21a^2n_2$$

$$+ 630an_1n_2 + 161a^2 - 70an_1 + 70an_2 + 240a + 240n_1$$

$$+ 120n_2 + 36)\frac{d^2f_4}{dz^2} - \frac{1}{E}\, 12ca(2a + 2n_1 + n_2 + 1)\, f_4$$

$$+ \frac{1}{G}\,\frac{c^4a}{6I}\,(2a + 2n_1 + n_2 + 1)(6a^3 - 60an_1^2 - 30an_2^2 + 66a^2n_1$$

$$+ 3a^2n_2 + 90an_1n_2 + 23a^2 - 10an_1 + 10an_2 - 12)\frac{d^2M}{dz^2}\Big\}dz\,\delta f_2$$

$$+\int_0^H\Big\{\frac{1}{G}\,\frac{c^3a}{105}\,(42a^3 + 420an_1^2 - 210an_2^2 + 462a^2n_1 + 21a^2n_2$$

$$+ 630an_1n_2 + 161a^2 - 70an_1 + 70an_2 + 240a + 240n_1$$

$$+ 120n_2 + 36)\frac{d^2f_2}{dz^2} - \frac{1}{E}\,12ca(2a + 2n_1 + n_2 + 1)\,f_2$$

$$- \frac{1}{G}\,\frac{2c^3}{175}\,(70a^3 + 70an_1^2 + 70an_2^2 - 70a^2n_1 + 70a^2n_2$$

$$- 140an_1n_2 + 180a^2 + 180n_1^2 + 45n_2^2 + 360an_1 + 180an_2$$

$$+ 180n_1n_2 + 60a + 60n_1 + 30n_2 + 6)\,\frac{d^2f_4}{dz^2}$$

$$+ \frac{1}{E}\,\frac{18c}{35}(40a^2 + 40n_1^2 + 10n_2^2 + 80an_1 + 40an_2 + 40n_1n_2$$

$$+ 26a + 26n_1 + 13n_2 + 3)\,f_4$$

$$- \frac{1}{G}\,\frac{c^4}{35I}\,(2a + 2n_1 + n_2 + 1)(70a^3 + 70an_1^2 + 70an_2^2 - 70a^2n_1$$

$$+ 70a^2n_2 - 140an_1n_2 - 60a - 60n_1 - 30n_2 - 9)\,\frac{d^2M}{dz^2}\Big\}dz\,\delta f_4$$

$$+ \frac{1}{G}\Big[\Big\{\frac{4c^3a^2}{63}(6a^3 + 468an_1^2 + 117an_2^2 + 54a^2n_1 + 27a^2n_2$$

$$- 162an_1n_2 + 27a^2 + 258an_1 + 24an_2 + 47a + 42)\,\frac{df_2}{dz}$$

$$- \frac{c^3a}{105}\,(42a^3 - 420an_1^2 - 210an_2^2 + 462a^2n_1 + 21a^2n_2$$

$$+ 630an_1n_2 + 161a^2 - 70an_1 + 70an_2 + 240a + 240n_1$$

$$+ 120n_2 + 36)\frac{df_4}{dz} - \frac{c^4a}{6I}(2a + 2n_1 + n_2 + 1)(6a^3$$

$$- 60an_1^2 - 30an_2^2 + 66a^2n_1 + 3a^2n_2 + 90an_1n_2$$

$$+ 23a^2 - 10an_1 + 10an_2 - 12)\frac{dM}{dz}\Big\}\,\delta f_2\Big]_0^H$$

$$+ \frac{1}{G}\Big[\Big\{-\frac{c^3a}{105}(42a^3 - 420an_1^2 - 210an_2^2 + 462a^2n_1 + 21a^2n_2$$

$$+ 630an_1n_2 + 161a^2 - 70an_1 + 70an_2 + 240a$$

$$+ 240n_1 + 120n_2 + 36)\frac{df_2}{dz} + \frac{2c^3}{175}(70a^3 + 70an_1^2$$

$$+ 70an_2^2 - 70a^2n_1 + 70a^2n_2 - 140an_1n_2 + 180a^2$$

$$+ 180n_1^2 + 45n_2^2 + 360an_1 + 180an_2 + 180n_1n_2$$

$$+ 60a + 60n_1 + 30n_2 + 6)\frac{df_4}{dz}$$

$$+ \frac{c^4}{35I}(2a + 2n_1 + n_2 + 1)(70a^3 + 70an_1^2 + 70an_2^2 - 70a^2n_1$$

$$+ 70a^2n_2 - 140an_1n_2 - 60a - 60n_1 - 30n_2 - 9)\frac{dM}{dz}\Big\}\,\delta f_4\Big]_0^H$$

$$= 0 \qquad \ldots\ldots (6.49)$$

The governing differential equations for the functions f_2 and f_4 may, therefore, be expressed as

$$\frac{d^2f_2}{dz^2} - \left(\frac{k_1}{H}\right)^2 f_2 - \alpha_1^2\frac{d^2f_4}{dz^2} + \left(\frac{\beta_1}{H}\right)^2 f_4 = \lambda_1^2\frac{d^2\sigma_b}{dz^2}$$

$$\ldots\ldots (6.50)$$

$$\frac{d^2f_2}{dz^2} - \left(\frac{k_2}{H}\right)^2 f_2 - \alpha_2^2\frac{d^2f_4}{dz^2} + \left(\frac{\beta_2}{H}\right)^2 f_4 = \lambda_2^2\frac{d^2\sigma_b}{dz^2}$$

$$\ldots\ldots (6.51)$$

where

$$k_1^2 = 126\ \frac{G}{E}\ \left(\frac{H}{b}\right)^2\ \frac{1}{D_2}\ a(2a + 2n_1 + n_2 + 1)(a + 6n_1 + 3n_2 + 3)$$

$$\alpha_1^2 = \frac{3}{20}\ \frac{1}{aD_2}\ (42a^3 - 420an_1^2 - 210\ an_2^2 + 462a^2n_1 + 21a^2n_2$$

$$+ 630an_1n_2 + 161a^2 - 70an_1 + 70an_2$$

$$+ 240a + 240n_1 + 120n_2 + 36)$$

$$\beta_1^2 = 189\ \frac{G}{E}\ \left(\frac{H}{b}\right)^2\ \frac{1}{D_2}\ a(2a + 2n_1 + n_2 + 1)$$

$$\lambda_1^2 = \frac{21}{8}\ \frac{1}{aD_2}\ (2a + 2n_1 + n_2 + 1)(6a^3 - 60an_1^2 - 30an_2^2$$

$$+ 66a^2n_1 + 3a^2n_2 + 90an_1n_2 + 23a^2$$

$$- 10an_1 + 10an_2 - 12) \qquad (6.52)$$

$$k_2^2 = 1260\ \frac{G}{E}\ \left(\frac{H}{b}\right)^2\ \frac{1}{D_3}\ a^2(2a + 2n_1 + n_2 + 1)$$

$$\alpha_2^2 = \frac{6}{5}\ \frac{1}{aD_3}\ (70a^3 + 70an_1^2 + 70an_2^2 - 70a^2n_1 + 70a^2n_2$$

$$- 140an_1n_2 + 180a^2 + 180n_1^2 + 45n_2^2 + 360an_1$$

$$+ 180an_2 + 180n_1n_2 + 60a + 60n_1 + 30n_2 + 6)$$

$$\beta_2^2 = 54\ \frac{G}{E}\ \left(\frac{H}{b}\right)^2\ \frac{1}{D_3}\ a(2a + 2n_1 + n_2 + 1)(20a + 20n_1 + 10n_2 + 3)$$

$$\lambda_2^2 = 3\ \frac{1}{aD_3}\ (2a + 2n_1 + n_2 + 1)(70a^3 + 70an_1^2 + 70an_2^2$$

$$- 70a^2n_1 + 70a^2n_2 - 140an_1n_2 - 60a - 60n_1$$

$$- 30n_2 - 9)$$

In equation (6.52) D_2 and D_3 are constants, given by

$$D_2 = 6a^3 + 468an_1^2 + 117an_2^2 + 54a^2n_1 + 27a^2n_2$$

$$- 162an_1n_2 + 27a^2 + 258an_1 + 24an_2 + 47a + 42$$

$$D_3 = 42a^3 - 420an_1^2 - 210an_2^2 + 462a^2n_1 + 21a^2n_2 + 630an_1n_2$$

$$+ 161a^2 - 70an_1 + 70an_2 + 240a + 240n_1 + 120n_2 + 36 \qquad (6.53)$$

The boundary conditions become

$$\text{At } z = 0, \quad f_2 = 0 \qquad (6.54)$$

$$\text{At } z = 0, \quad f_4 = 0 \qquad (6.55)$$

$$\text{At } z = H, \quad \frac{df_2}{dz} - \alpha_1^2 \frac{df_4}{dz} - \lambda_1^2 \frac{d\sigma_b}{dz} = 0 \qquad (6.56)$$

$$\text{At } z = H, \quad \frac{df_2}{dz} - \alpha_2^2 \frac{df_4}{dz} - \lambda_2^2 \frac{d\sigma_b}{dz} = 0 \qquad (6.57)$$

It may be noted that the differential equations (6.50) and (6.51) and the boundary conditions (6.54) to (6.57) are again identical to the differential equations (2.88) and (2.89) and the boundary conditions (2.86), (2.87), (2.90) and (2.91) derived in Chapter 2 for a framed tube structure. Hence the solutions of the equations will also be identical. For different loading conditions f_2 and f_4 were derived in Chapter 2.

In the particular case where there are no stiffer columns at junctions of web and flange panels, so that n_1 and n_2 are each equal to zero, the parameters k_1, α_1, β_1, λ_1, k_2, α_2, β_2 and λ_2 reduce to

$$k_1^2 = 126 \frac{G}{E} \left(\frac{H}{b}\right)^2 \frac{a(2a + 1)(a + 3)}{6a^3 + 27a^2 + 47a + 42}$$

$$\alpha_1^2 = \frac{3}{20} \frac{42a^3 + 161a^2 + 240a + 36}{a(6a^3 + 27a^2 + 47a + 42)}$$

$$\beta_1^2 = 189 \frac{G}{E} \left(\frac{H}{b}\right)^2 \frac{a(2a + 1)}{6a^3 + 27a^2 + 47a + 42}$$

$$\lambda_1^2 = \frac{21}{8} \frac{(2a + 1)(6a^3 + 23a^2 - 12)}{a(6a^3 + 27a^2 + 47a + 42)}$$

$$k_2^2 = 1260 \frac{G}{E} \left(\frac{H}{b}\right)^2 \frac{a^2(2a + 1)}{42a^3 + 161a^2 + 240a + 36}$$

$$\alpha_2^2 = \frac{12}{5} \frac{35a^3 + 90a^2 + 30a + 3}{a(42a^3 + 161a^2 + 240a + 36)}$$

$$\beta_2^2 = 54 \frac{G}{E} \left(\frac{H}{b}\right)^2 \frac{a(2a + 1)(20a + 3)}{42a^3 + 161a^2 + 240a + 36}$$

$$\lambda_2^2 = 3 \frac{(2a + 1)(70a^3 - 60a - 9)}{a(42a^3 + 161a^2 + 240a + 36)}$$

6.5 BUNDLED-TUBE STRUCTURE WITH NINE TUBES

6.5.1 INTRODUCTION

For a high-rise building with a large plan area bundling of a relatively large number of tubes may be required to develop high cantilever efficiency. In the bundled tube system of the Sears Tower, Chicago two additional web frames in each direction are engaged to perimeter frames. In other words, nine small tubes are bundled together to create the large overall tube. The improved behaviour of the tube due to the large reduction of shear lag effect can be seen in Fig. 6.7.

The analysis of such a structure without the aid of a computer presents some difficulty. The rigidly

jointed frame panels may be replaced by equivalent orthotropic plates as shown in Chapter 2. The plan of the structure is symmetrical about the horizontal coordinates and only one quarter of the structure need be considered for the analysis. The vertical stress distribution in the different panels due to lateral load may be expressed most simply in the form (Fig. 6.8)

$$\text{for panel 1, } \sigma_z = a_1 + b_1 y^2$$

$$\text{for panel 2, } \sigma_z = a_2 + b_2 y + c_2 y^2$$

$$\text{for panel 3, } \sigma_z = a_3 + b_3 y^2$$

$$\text{for panel 4, } \sigma_z = a_4 + b_4 y + c_4 y^2$$

$$\text{for panel 5, } \sigma'_z = a_5 x + b_5 x^3 \qquad (6.58)$$

$$\text{for panel 6, } \sigma'_z = a_6 + b_6 x + c_6 x^3$$

$$\text{for panel 7, } \sigma'_z = a_7 x + b_7 x^3$$

$$\text{and for panel 8, } \sigma'_z = a_8 + b_8 x + c_8 x^3$$

where a_1, b_1, a_2, b_2, c_2, a_3, b_3, a_4, b_4, c_4, a_5, b_5, a_6, b_6, c_6, a_7, b_7, a_8, b_8 and c_8 are functions of the height coordinate z only.

The condition of vertical strain compatibility at the junctions of the different panels will yield 8 equations and the condition of overall moment equilibrium at any level will give one more equation. This will leave 11 unknown functions to be dealt with.

Some additional simplifying assumptions must

therefore be made to reduce the number of functions to a manageable limit. The simple approximate analyses of bundled tube structure are discussed in Articles 6.5.2 and 6.5.3.

6.5.2 SIMPLIFIED ANALYSIS

The vertical stresses in the interior panels 3 and 4 are small (nearly a third of the maximum vertical stress in the flange panels 1 and 2) and the moments resisted by them are still smaller (nearly a ninth of the moment resisted by panels 1 and 2). The effect of panels 3 and 4 in resisting lateral load is, therefore, neglected in the first instance (Fig. 6.9).

It is then assumed that the vertical bending stress distribution curves in the normal panels 1 and 2 are symmetrical about the vertical central axes of the two panels, so that the peak stresses in the panels are all equal in magnitude.

It is further assumed that the stress distribution in the panels 5 and 6 is expressed by a continuous curve and that the stress distribution in the panels 7 and 8 is identical to the one for panels 5 and 6.

Using equation (6.58) the following 16 relations between the 20 unknown functions are obtained.

$$a_2 = a_1 + \frac{4b^2}{9} b_1$$

$$b_2 = - \frac{4b}{3} b_1$$

$$c_2 = b_1$$

$$a_3 = b_3 = a_4 = b_4 = c_4 = 0$$

$$a_5 = b_6 = a_7 = b_8$$

$$b_5 = c_6 = b_7 = c_8 \cdot$$

$$a_6 = a_8 = 0$$

The vertical stress distributions in the different panels reduce to

for panel 1, $\sigma_z = a_1 + b_1 y^2$

for panel 2, $\sigma_z = a_1 + b_1 (y - \frac{2b}{3})^2$ (6.59)

for panels 5-6 and 7-8

$$\sigma_z' = a_5 x + b_5 x^3$$

The condition of vertical strain compatibility at the junctions of flange and web panels and the condition of overall moment equilibrium at any level will give two additional equations, still leaving two unknown functions.

In order to further simplify the analysis the distribution of vertical stresses σ_z in the normal panel 1 may be expressed in the form (cf Fig. 6.9)

$$\sigma_z = \frac{M}{I} c + S_o + 9(\frac{y}{b})^2 S \quad - \quad \ldots\ldots \quad (6.60)$$

where S_o and S are functions of height coordinate z only.

The second moment of area I of equivalent tube cross-section in equation (6.60) is given by

$$I = 4c^2 t \ (b + \tfrac{2}{3}c)$$

where 2b and 2c are the overall cross-sectional dimensions of the bundled tube, normal and parallel to the wind directions respectively, and t is the thickness of the

equivalent uniform orthotropic plate.

The stiffnesses of the columns at the intersections of web and flange panels are assumed to be just adequate to form a segment of the equivalent orthotropic plates. If, however, they are stiffer the effect may be included in the analysis.

Similarly the distribution of vertical stresses in normal panel 2 may be expressed as

$$\sigma_z = \frac{M}{I} c + S_o + 9\left(\frac{y}{b} - \frac{2}{3}\right)^2 S \qquad \ldots\ldots \quad (6.61)$$

The distribution of vertical stresses σ_z' in the web panels 5-6 and 7-8 may be expressed in the form

$$\sigma_z' = \frac{M}{I} x + \left(\frac{x}{c}\right)^3 S_1 \qquad \ldots\ldots \quad (6.62)$$

where S_1 is a function of height coordinate z.

The condition of vertical strain compatibility at the intersections of flange and web panels requires that

$$\left(\frac{\sigma_z}{E}\right)_{y=\frac{b}{3} \text{ or } b} = \left(\frac{\sigma_z'}{E}\right)_{x = c} \qquad \ldots\ldots \quad (6.63)$$

On substituting equations (6.60) to (6.62) into equation (6.63) it is found that

$$S_o + S = S_1 \qquad \ldots\ldots \quad (6.64)$$

The condition of overall moment equilibrium at any level z may be expressed in the form

$$2\int_{-\frac{b}{3}}^{\frac{b}{3}} \sigma_z \, t \, c \, dy + 4\int_{\frac{b}{3}}^{b} \sigma_z \, t \, c \, dy + 4\int_{-c}^{c} \sigma_z' \, tx \, dx = M(z) \qquad \ldots\ldots \quad (6.65)$$

where M(z) is the total bending moment at that level

caused by the applied lateral loading.

On substituting equations (6.60), (6.61), (6.62) and (6.64) into the equilibrium condition (6.65) and integrating, it is found that

$$S_o = -\frac{1}{3} mS \qquad \ldots\ldots (6.66)$$

where the geometrical ratio m is given by

$$m = \frac{5b + 6c}{5b + 2c}$$

which is always greater than 1.

The vertical stresses σ_z and σ_z' in the flange and web panels may, therefore, be expressed in terms of the single unknown function S as,

for panel 1,

$$\sigma_z = \frac{M}{I} c - \left[\frac{1}{3}m - 9\left(\frac{Y}{b}\right)^2 \right] S \qquad \ldots\ldots (6.67)$$

for panel 2,

$$\sigma_z = \frac{M}{I} c - \left[\frac{1}{3}m - 4 + 12\left(\frac{Y}{b}\right) - 9\left(\frac{Y}{b}\right)^2 \right] S \qquad \ldots\ldots (6.68)$$

for web panels,

$$\sigma_z' = \frac{M}{I} x + \left(1 - \frac{1}{3}m\right)\left(\frac{x}{c}\right)^3 S \qquad \ldots\ldots (6.69)$$

The equations of equilibrium for a small element in the flange and web panels are given by equations (6.1) and (6.2).

On substituting equation (6.67) into the equilibrium condition (6.1) and integrating, the shear stress component τ_{yz} in panel 1 may be expressed as

$$\tau_{yz} = -y\left\{ \frac{c}{I}\frac{dM}{dz} - \left[\frac{1}{3}m - 3\left(\frac{y}{b}\right)^2 \right] \frac{dS}{dz} \right\} \qquad \ldots\ldots (6.70)$$

The constant of integration is zero as τ_{yz} is skew-symmetric with respect to the axis y = 0.

At $y = \frac{b}{3}$ the shear stress $(\tau_{yz})_1$ is found to be

$$(\tau_{yz})_1 = -\frac{b}{3}\left\{\frac{c}{I}\frac{dM}{dz} - \tfrac{1}{3}(m-1)\frac{dS}{dz}\right\} \quad \ldots\ldots (6.71)$$

On substituting equation (6.68) into equation (6.1) and integrating, the shear stress τ_{yz} in panel 2 may be expressed in the form

$$\tau_{yz} = -y\left\{\frac{c}{I}\frac{dM}{dz} - \left[\tfrac{1}{3}m - 4 + 6\left(\frac{y}{b}\right) - 3\left(\frac{y}{b}\right)^2\right]\frac{dS}{dz}\right\} + C_5 \quad \ldots\ldots (6.72)$$

where C_5 is the constant of integration.

The shear stresses $(\tau_{yz})_2$ and $(\tau_{yz})_3$ at $y = \frac{b}{3}$ and y = b respectively are

$$(\tau_{yz})_2 = -\frac{b}{3}\left\{\frac{c}{I}\frac{dM}{dz} + \tfrac{1}{3}(7-m)\frac{dS}{dz}\right\} + C_5 \quad \ldots\ldots (6.73)$$

$$(\tau_{yz})_3 = -b\left\{\frac{c}{I}\frac{dM}{dz} + (1 - \tfrac{1}{3}m)\frac{dS}{dz}\right\} + C_5 \quad \ldots\ldots (6.74)$$

On substituting equation (6.69) into the equilibrium condition (6.2) and integrating, the shear stress component τ_{xz} in the web panels may be found to be

$$\tau_{xz} = -\frac{x^2}{2I}\frac{dM}{dz} - \tfrac{1}{4}(1 - \tfrac{1}{3}m)\frac{x^4}{c^3}\frac{dS}{dz} + C_6 \quad \ldots\ldots (6.75)$$

where C_6 is another constant of integration.

The shear stress $(\tau_{xz})_1$ in the web panel at x = c is evaluated as

$$(\tau_{xz})_1 = -\frac{c^2}{2I}\frac{dM}{dz} - (1 - \tfrac{1}{3}m)\frac{c}{4}\frac{dS}{dz} + C_6 \quad \ldots\ldots (6.76)$$

Considering the equilibrium of shear forces at the

intersections of the flange and web panels it may be seen that

$$(\tau_{yz})_1 - (\tau_{yz})_2 = -(\tau_{xz})_1 \qquad \ldots\ldots (6.77)$$

and

$$(\tau_{yz})_3 = -(\tau_{xz})_1 \qquad \ldots\ldots (6.78)$$

On substituting equations (6.71), (6.73), (6.74) and (6.76) into the equations (6.77) and (6.78), the constants C_5 and C_6 are determined as

$$C_5 = \frac{bc}{2I}\frac{dM}{dz} + \frac{b}{6}(5 - m)\frac{dS}{dz} \qquad \ldots\ldots (6.79)$$

$$C_6 = \frac{c^2}{2I}(1 + \frac{b}{c})\frac{dM}{dz} + \frac{c}{4}\left[(1 - \tfrac{1}{3}m) - \tfrac{2}{3}(m - 1)\frac{b}{c}\right]\frac{dS}{dz} \qquad \ldots\ldots (6.80)$$

The shear stresses τ_{yz} in the normal panel 2 and τ_{xz} in the web panels may, therefore be expressed as,

for panel 2

$$\tau_{yz} = \frac{bc}{2I}\left[1 - 2(\frac{y}{b})\right]\frac{dM}{dz} + b\left[\frac{1}{6}(5 - m) + (\tfrac{1}{3}m - 4)(\frac{y}{b}) + 6(\frac{y}{b})^2 - 3(\frac{y}{b})^3\right]\frac{dS}{dz} \qquad \ldots\ldots (6.81)$$

$$\tau_{xz} = \frac{c^2}{2I}\left[1 + \frac{b}{c} - (\frac{x}{c})^2\right]\frac{dM}{dz} + (1 - \tfrac{1}{3}m)\frac{c}{4}\left[\frac{1}{5} - (\frac{x}{c})^4\right]\frac{dS}{dz} \qquad \ldots\ldots (6.82)$$

On calculating $(\tau_{yz})_1$, $(\tau_{yz})_2$, $(\tau_{yz})_3$ and $(\tau_{xz})_1$ it is found that

$$\tfrac{1}{2}(\tau_{yz})_1 = -(\tau_{yz})_2 = \tfrac{1}{3}(\tau_{yz})_3 = -\tfrac{1}{3}(\tau_{xz})_1 \qquad \ldots\ldots (6.83)$$

It is also found that each web panel carries one quarter of the total applied shear, so that

$$t\int_{-c}^{c} \tau_{xz}\, dx = \tfrac{1}{4}\frac{dM}{dz} = \frac{F}{4} \qquad \ldots\ldots (6.84)$$

The total strain energy U, stored in the structure is then given by

$$U = t\int_0^H \left[\frac{1}{E}\int_{\frac{-b}{3}}^{\frac{b}{3}} \left\{ \frac{M}{I}\, c - \left[\tfrac{1}{3}m - 9\left(\frac{y}{b}\right)^2 \right] S \right\}^2 dy \right.$$

$$+ \frac{1}{G}\int_{\frac{-b}{3}}^{b/3} y^2 \left\{ \frac{c}{I}\frac{dM}{dz} - \left[\tfrac{1}{3}m - 3\left(\frac{y}{b}\right)^2 \right] \frac{dS}{dz} \right\}^2 dy$$

$$+ \frac{2}{E}\int_{\frac{b}{3}}^{b} \left\{ \frac{M}{I}\, c - \left[\tfrac{1}{3}m - 4 + 12\left(\frac{y}{b}\right) - 9\left(\frac{y}{b}\right)^2 \right] S \right\}^2 dy$$

$$+ \frac{2}{G}\int_{\frac{b}{3}}^{b} \left\{ \frac{bc}{2I}\left[1 - 2\left(\frac{y}{b}\right) \right] \frac{dM}{dz} + b\left[\frac{1}{6}(5-m) + \left(\tfrac{1}{3}m - 4\right)\left(\frac{y}{b}\right) \right.\right.$$

$$\left.\left. + 6\left(\frac{y}{b}\right)^2 - 3\left(\frac{y}{b}\right)^3 \right] \frac{dS}{dz} \right\}^2 dy$$

$$+ \frac{2}{E}\int_{-c}^{c} \left\{ \frac{M}{I}\, x + \left(1 - \tfrac{1}{3}m\right)\left(\frac{x}{c}\right)^3 S \right\}^2 dx$$

$$+ \frac{2}{G}\int_{-c}^{c} \left\{ \frac{c^2}{2I}\left[1 + \frac{b}{c} - \left(\frac{x}{c}\right)^2 \right] \frac{dM}{dz} + \right.$$

$$\left. \left(1 - \tfrac{1}{3}m\right)\frac{c}{4}\left[\frac{1}{5} - \left(\frac{x}{c}\right)^4 \right] \frac{dS}{dz} \right\}^2 dx \Bigg] dz \quad \ldots\ldots\ (6.85)$$

The variation of U, δU may be expressed as

$$\delta U = 2t\int_0^H \left[\frac{1}{E}\int_{-b/3}^{b/3} \left\{ \frac{M}{I}\, c - \left[\tfrac{1}{3}m - 9\left(\frac{y}{b}\right)^2 \right] S \right\} \cdot \right.$$

$$\left. \left\{ - \left[\tfrac{1}{3}m - 9\left(\frac{y}{b}\right)^2 \right] \delta S \right\} dy \right.$$

$$+ \frac{1}{G}\int_{-b/3}^{b/3} y^2\left\{\frac{c}{I}\frac{dM}{dz} - \left[\tfrac{1}{3}m - 3\left(\frac{y}{b}\right)^2\right]\frac{dS}{dz}\right\}$$

$$\left\{-\left[\tfrac{1}{3}m - 3\left(\frac{y}{b}\right)^2\right]\frac{d(\delta S)}{dz}\right\} dy$$

$$+ \frac{2}{E}\int_{b/3}^{b}\left\{\frac{M}{I}c - \left[\tfrac{1}{3}m - 4 + 12\left(\frac{y}{b}\right) - 9\left(\frac{y}{b}\right)^2\right] S\right\}$$

$$\left\{-\left[\tfrac{1}{3}m - 4 + 12\left(\frac{y}{b}\right) - 9\left(\frac{y}{b}\right)^2\right]\delta S\right\} dy$$

$$+ \frac{2}{G}\int_{b/3}^{b}\left\{\frac{bc}{2I}\left[1 - 2\left(\frac{y}{b}\right)\right]\frac{dM}{dz} + b\left[\frac{1}{6}(5 - m)\right.\right.$$

$$\left.\left. + \left(\tfrac{1}{3}m-4\right)\left(\frac{y}{b}\right) + 6\left(\frac{y}{b}\right)^2 - 3\left(\frac{y}{b}\right)^3\right]\frac{dS}{dz}\right\}.$$

$$\left\{b\left[\frac{1}{6}(5-m) + \left(\tfrac{1}{3}m-4\right)\left(\frac{y}{b}\right) + 6\left(\frac{y}{b}\right)^2 - 3\left(\frac{y}{b}\right)^3\right]\frac{d(\delta S)}{dz}\right\} dy$$

$$+ \frac{2}{E}\int_{-c}^{c}\left\{\frac{M}{I}x + \left(1-\tfrac{1}{3}m\right)\left(\frac{x}{c}\right)^3 S\right\}\cdot\left(1-\tfrac{1}{3}m\right)\left(\frac{x}{c}\right)^3 \delta S\, dx$$

$$+ \frac{2}{G}\int_{-c}^{c}\left\{\frac{c^2}{2I}\left[1 + \frac{b}{c} - \left(\frac{x}{c}\right)^2\right]\frac{dM}{dz} + \left(1-\tfrac{1}{3}m\right)\frac{c}{4}\left[\frac{1}{5} - \left(\frac{x}{c}\right)^4\right]\frac{dS}{dz}\right\}.$$

$$\left\{\left(1-\tfrac{1}{3}m\right)\frac{c}{4}\left[\frac{1}{5} - \left(\frac{x}{c}\right)^4\right]\frac{d(\delta S)}{dz}\right\} dx\ \Bigg] dz \qquad \ldots\ (6.86)$$

On integration δU may be expressed in the form

$$\delta U = 2t\int_0^H\left\{-\frac{1}{G}\frac{b^3}{17010}\,\frac{315m^3 - 637m^2 + 521m - 135}{3 - m}\,\frac{d^2S}{dz^2}\right.$$

$$+ \frac{1}{E}\frac{4b}{315}\left(5m^2 + 15m - 6\right) S$$

$$\left. - \frac{1}{G}\frac{b^3c}{5670I}\,\frac{915m^3 - 1961m^2 + 561m + 261}{(3 - m)^2}\,\frac{d^2M}{dz^2}\right\} dz\, \delta S(z)$$

$$+ \frac{2t}{G}\left[\left\{\frac{b^3}{17010}\ \frac{315m^3 - 637m^2 + 521m - 135}{3 - m}\ \frac{dS}{dz}\right.\right.$$

$$\left.\left. + \frac{b^3 c}{5670I}\ \frac{915m^3 - 1961m^2 + 561m + 261}{(3 - m)^2}\ \frac{dM}{dz}\right\} \delta S\right]_0^H$$

..... (6.87)

For minimum U, the variation δU must vanish. On equating δU to zero, the following governing differential equation is obtained.

$$\frac{d^2S}{dz^2} - \left(\frac{k}{H}\right)^2 S = \lambda^2\ \frac{d^2\sigma_b}{dz^2} \qquad \text{..... (6.88)}$$

where

$$k^2 = 216\ \frac{G}{E}\left(\frac{H}{b}\right)^2\ \frac{(3 - m)(5m^2 + 15m - 6)}{315m^3 - 637m^2 + 521m - 135}$$

$$\lambda^2 = -\ 3\ \frac{915m^3 - 1961m^2 + 561m + 261}{(3-m)(315m^3 - 637m^2 + 521m - 135)}$$

For the case of a structure built in at the base and free at the top, the boundary conditions become

At $z = 0$, $S = 0$ ..... (6.89)

At $z = H$, $\frac{dS}{dz} - \lambda^2 \frac{d\sigma_b}{dz} = 0$ ..... (6.90)

It may be noted that the governing differential equation (6.88) and the boundary conditions (6.89) and (6.90) are identical to the governing differential equation (2.45) and the boundary conditions (2.41) and (2.46) respectively. Hence the same design curves Fig. 2.8 to 2.13 may be used to evaluate the direct and shear stresses in the structure. The function F_1, equal to λ^2, may be evaluated directly from equation (6.88).

In the above analysis the effects of panels 3 and 4 in resisting the lateral load were not considered. Once the structure has been analysed and the stresses determined, the uniform vertical stresses acting in panels 3 and 4 may be evaluated from the strains at the junction 456 or 3478 (Fig. 6.9). The resultant moment, ΔM_1, resisted by these panels may, then, be determined. The main structure (with the panels 3 and 4 omitted) is now considered with the applied moment $M - \Delta M_1$. Due to the reduced moment all stresses are also reduced proportionately. The new stresses in the panels 3 and 4 and the resultant moment, ΔM_2 ($\Delta M_2 < \Delta M_1$) resisted by them are calculated. The structure is then analysed for the moment $M - \Delta M_2$. The process may be repeated until the difference in results between two consecutive steps is within tolerable limits.

6.5.3 MORE GENERAL ANALYSIS

In order to analyse a bundled tube structure with nine tubes subjected to lateral load, certain simplifying assumptions regarding the stress distributions in the various panels of the structure were made in Article 6.5.2. The panels 3, 4 in Fig. 6.10 were omitted in the first iteration and a simple closed solution was obtained. By a process of iteration the stresses in the different panels were subsequently determined.

In the following more general analysis the same simplifying assumptions regarding the distribution of stresses are made. The effect of panels 3 and 4 in

resisting lateral load is neglected in the first instance.

The distribution of vertical stresses σ_z in the flange panel 1 may be expressed in the form

$$\sigma_z = f_1 + 9\left(\frac{y}{b}\right)^2 f_2 \qquad \ldots\ldots \quad (6.91)$$

where f_1 and f_2 are functions of the height coordinate z only.

For the flange panel 2, the distribution of vertical stresses σ_z may be expressed as

$$\sigma_z = f_1 + 9\left(\frac{y}{b} - \frac{2}{3}\right)^2 f_2 \qquad \ldots\ldots \quad (6.92)$$

The distribution of stresses σ'_z in the web panels 5-6 and 7-8 may be expressed in the form

$$\sigma'_z = \left(\frac{x}{c}\right) f_3 + \left(\frac{x}{c}\right)^3 f_4 \qquad \ldots\ldots \quad (6.93)$$

where f_3 and f_4 are also functions of coordinate z.

Comparing the equations (6.91) to (6.93) with the equation (6.59) it is found that

$$f_1 = a_1$$

$$\frac{9}{b^2} f_2 = b_1$$

$$\frac{f_3}{c} = a_5$$

and $$\frac{f_4}{c^3} = b_5$$

The condition of vertical strain compatibility at the intersections of flange and web panels yields

$$f_1 + f_2 = f_3 + f_4 \qquad \ldots\ldots \quad (6.94)$$

The condition of overall moment equilibrium at any level was given in Article 6.5.2 (equation 6.65). On substituting equations (6.91) to (6.94) into the equilibrium condition and integrating, it is found that,

$$f_1 = \frac{M}{I} c - \frac{a + 2}{3a + 2} f_2 + \frac{4}{5(3a + 2)} f_4 \qquad \ldots\ldots (6.95)$$

where $a = \frac{b}{c}$.

On substituting equation (6.95) into equation (6.94), the function f_3 is found to be

$$f_3 = \frac{M}{I} c + \frac{2a}{3a + 2} f_2 - \frac{3(5a + 2)}{5(3a + 2)} f_4 \qquad \ldots\ldots (6.96)$$

The distribution of vertical stresses σ_z and σ_z' in the flange and web panels may be expressed in terms of two unknown functions f_2 and f_4 as,

for flange panel 1,

$$\sigma_z = \frac{M}{I} c - \left[\frac{a + 2}{3a + 2} - 9\left(\frac{y}{b}\right)^2\right] f_2 + \frac{4}{5(3a + 2)} f_4 \qquad (6.97)$$

for flange panel 2,

$$\sigma_z = \frac{M}{I} c + \left[\frac{11a + 6}{3a + 2} - 12\left(\frac{y}{b}\right) + 9\left(\frac{y}{b}\right)^2\right] f_2 + \frac{4}{5(3a + 2)} f_4$$

$\ldots\ldots (6.98)$

for web panels,

$$\sigma_z' = \frac{M}{I} x + \frac{2a}{3a + 2} \left(\frac{x}{c}\right) f_2 - \left[\frac{3(5a + 2)}{5(3a + 2)} \left(\frac{x}{c}\right) - \left(\frac{x}{c}\right)^3\right] f_4$$

$\ldots\ldots (6.99)$

The equations of equilibrium for small elements in the flange and web panels are given by equations (6.1) and (6.2) respectively.

On substituting equation (6.97) into the equilibrium equation (6.1) and integrating, the shear stress τ_{yz} in panel 1 is found to be,

$$\tau_{yz} = -y\left\{\frac{c}{I}\frac{dM}{dz} - \left[\frac{a+2}{3a+2} - 3\left(\frac{y}{b}\right)^2\right]\frac{df_2}{dz} + \frac{4}{5(3a+2)}\frac{df_4}{dz}\right\} \quad \ldots\ldots (6.100)$$

The constant of integration is zero as τ_{yz} is skew-symmetric with respect to the axis y = 0.

At $y = \frac{b}{3}$, the shear stress $(\tau_{yz})_1$ becomes

$$(\tau_{yz})_1 = -\frac{b}{3}\left[\frac{c}{I}\frac{dM}{dz} - \frac{4}{3(3a+2)}\frac{df_2}{dz} + \frac{4}{5(3a+2)}\frac{df_4}{dz}\right] \quad \ldots\ldots (6.101)$$

The shear stress in panel 2 is similarly determined as

$$\tau_{yz} = -y\left\{\frac{c}{I}\frac{dM}{dz} + \left[\frac{11a+6}{3a+2} - 6\left(\frac{y}{b}\right) + 3\left(\frac{y}{b}\right)^2\right]\frac{df_2}{dz} + \frac{4}{5(3a+2)}\frac{df_4}{dz}\right\} + C_7 \quad \ldots\ldots (6.102)$$

where C_7 is the constant of integration.

The shear stresses $(\tau_{yz})_2$ and $(\tau_{yz})_3$ at $y = \frac{b}{3}$ and y = b respectively become

$$(\tau_{yz})_2 = -\frac{b}{3}\left\{\frac{c}{I}\frac{dM}{dz} + \frac{2(9a+4)}{3(3a+2)}\frac{df_2}{dz} + \frac{4}{5(3a+2)}\frac{df_4}{dz}\right\} + C_7 \quad \ldots\ldots (6.103)$$

$$(\tau_{yz})_3 = -b\left\{\frac{c}{I}\frac{dM}{dz} + \frac{2a}{3a+2}\frac{df_2}{dz} + \frac{4}{5(3a+2)}\frac{df_4}{dz}\right\} + C_7 \quad \ldots\ldots (6.104)$$

On substituting equation (6.99) into the equilibrium equation (6.2) and integrating, the shear stress τ_{xz} for the web panels may be expressed as

$$\tau_{xz} = -\frac{x^2}{2I}\frac{dM}{dz} - \frac{a}{3a+2}\frac{x^2}{c}\frac{df_2}{dz} + \left[\frac{3(5a+2)}{10(3a+2)}\frac{x^2}{c} - \frac{x^4}{4c^3}\right]\frac{df_4}{dz} + C_8 \qquad (6.105)$$

where C_8 is a constant of integration.

The shear stress $(\tau_{xz})_1$ at x = c is found to be

$$(\tau_{xz})_1 = -\frac{c^2}{2I}\frac{dM}{dz} - \frac{a}{3a+2}c\frac{df_2}{dz} + \frac{15a+2}{20(3a+2)}c\frac{df_4}{dz} + C_8$$

..... (6.106)

Considering the equilibrium of shear forces at the intersections of the flange and web panels it is found that

$$(\tau_{yz})_1 - (\tau_{yz})_2 = -(\tau_{xz})_1 \qquad ..... \qquad (6.107)$$

and $$(\tau_{yz})_3 = -(\tau_{xz})_1 \qquad ..... \qquad (6.108)$$

On substituting equations (6.101), (6.103), (6.104) and (6.106) into equations(6.107) and (6.108), the constants C_7 and C_8 become

$$C_7 = \frac{c^2}{2I}\, a\frac{dM}{dz} + \frac{2(3a+1)}{3(3a+2)}\, b\frac{df_2}{dz} + \frac{2a}{5(3a+2)}\, c\frac{df_4}{dz}$$

..... (6.109)

$$C_8 = \frac{c^2}{2I}(a+1)\frac{dM}{dz} + \frac{1}{3(3a+2)}\, b\frac{df_2}{dz} - \frac{7a+2}{20(3a+2)}\, c\frac{df_4}{dz}$$

..... (6.110)

The distribution of shear stresses τ_{yz} in panel 2 and τ_{xz} in web panels are given by,

for panel 2,

$$\tau_{yz} = \frac{bc}{2I}\left[1 - 2\left(\frac{y}{b}\right)\right]\frac{dM}{dz} + b\left[\frac{2(3a+1)}{3(3a+2)} - \frac{11a+6}{3a+2}\left(\frac{y}{b}\right)\right.$$

$$+ 6\left(\frac{y}{b}\right)^2 - 3\left(\frac{y}{b}\right)^3 \Bigg] \frac{df_2}{dz} + \frac{2b}{5(3a+2)} \left[1 - 2\left(\frac{y}{b}\right)\right] \frac{df_4}{dz}$$

..... (6.111)

for side panels,

$$\tau_{xz} = \frac{c^2}{2I}\left[(a+1) - \left(\frac{x}{c}\right)^2\right]\frac{dM}{dz} + \frac{ca}{3(3a+2)}\left[1 - 3\left(\frac{x}{c}\right)^2\right]\frac{df_2}{dz}$$

$$- \frac{c}{20}\left[\frac{7a+2}{3a+2} - \frac{6(5a+2)}{3a+2}\left(\frac{x}{c}\right)^2 + 5\left(\frac{x}{c}\right)^4\right]\frac{df_4}{dz}$$

..... (6.112)

The total strain energy U, stored in the structure becomes,

$$U = t\int_0^H \Bigg[\frac{1}{E}\int_{-b/3}^{b/3}\left\{\frac{M}{I}c - \left[\frac{a+2}{3a+2} - 9\left(\frac{y}{b}\right)^2\right]f_2 + \frac{4}{5(3a+2)}f_4\right\}^2 dy$$

$$+ \frac{1}{G}\int_{-b/3}^{b/3} y^2\left\{\frac{c}{I}\frac{dM}{dz} - \left[\frac{a+2}{3a+2} - 3\left(\frac{y}{b}\right)^2\right]\frac{df_2}{dz} + \frac{4}{5(3a+2)}\frac{df_4}{dz}\right\}^2 dy$$

$$+ \frac{2}{E}\int_{b/3}^{b}\left\{\frac{M}{I}c + \left[\frac{11a+6}{3a+2} - 12\left(\frac{y}{b}\right) + 9\left(\frac{y}{b}\right)^2\right]f_2 + \frac{4}{5(3a+2)}f_4\right\}^2 dy$$

$$+ \frac{2}{G}\int_{b/3}^{b}\left\{\frac{bc}{2I}\left[1 - 2\left(\frac{y}{b}\right)\right]\frac{dM}{dz} + b\left[\frac{2(3a+1)}{3(3a+2)} - \frac{11a+6}{3a+2}\left(\frac{y}{b}\right)\right.\right.$$

$$\left.\left. + 6\left(\frac{y}{b}\right)^2 - 3\left(\frac{y}{b}\right)^3\right]\frac{df_2}{dz} + \frac{2b}{5(3a+2)}\left[1 - 2\left(\frac{y}{b}\right)\right]\frac{df_4}{dz}\right\}^2 dy$$

$$+ \frac{2}{E}\int_{-c}^{c}\left\{\frac{M}{I}x + \frac{2a}{3a+2}\left(\frac{x}{c}\right)f_2 - \left[\frac{3(5a+2)}{5(3a+2)}\left(\frac{x}{c}\right) - \left(\frac{x}{c}\right)^3\right]f_4\right\}^2 dx$$

$$+ \frac{2}{G}\int_{-c}^{c}\left\{\frac{c^2}{2I}\left[(a+1) - \left(\frac{x}{c}\right)^2\right]\frac{dM}{dz} + \frac{ca}{3(3a+2)}\left[1 - 3\left(\frac{x}{c}\right)^2\right]\frac{df_2}{dz}\right.$$

$$- \frac{c}{20}\left[\frac{7a+2}{3a+2} - \frac{6(5a+2)}{3a+2}\left(\frac{x}{c}\right)^2 + 5\left(\frac{x}{c}\right)^4\right]\frac{df_4}{dz}\Bigg\}^2 dx\Bigg] dz \quad \ldots\ldots (6.113)$$

On minimising the integral by the calculus of variations, the following equation is obtained.

$$\int_0^H \Bigg\{ - \frac{1}{G}\frac{20c^3a^2}{567}(9a^3 + 54a^2 + 137a + 189)\frac{d^2f_2}{dz^2}$$

$$+ \frac{1}{E} 10ca(3a + 2)(a + 4)f_2$$

$$+ \frac{1}{G}\frac{4c^3a}{189}(21a^3 + 119a^2 + 270a + 54)\frac{d^2f_4}{dz^2}$$

$$- \frac{1}{E} 20ca(3a + 2) f_4$$

$$+ \frac{1}{G}\frac{5c^4a}{27I}(3a + 2)(3a^3 + 17a^2 - 18)\frac{d^2M}{dz^2}\Bigg\} dz\ \delta f_2$$

$$+ \int_0^H \Bigg\{ \frac{1}{G}\frac{4c^3a}{189}(21a^3 + 119a^2 + 270a + 54)\frac{d^2f_2}{dz^2}$$

$$- \frac{1}{E} 20ca(3a + 2) f_2$$

$$- \frac{1}{G}\frac{4c^3}{105}(35a^3 + 135a^2 + 60a + 8)\frac{d^2f_4}{dz^2}$$

$$+ \frac{1}{E}\frac{24c}{7}(5a + 1)(3a + 2) f_4$$

$$- \frac{1}{G}\frac{c^4}{21I}(3a + 2)(35a^3 - 60a - 12)\frac{d^2M}{dz^2}\Bigg\} dz\ \delta f_4$$

$$+ \frac{1}{G}\Bigg[\Bigg\{\frac{20c^3a^2}{567}(9a^3 + 54a^2 + 137a + 189)\frac{df_2}{dz}$$

$$- \frac{4c^3a}{189}(21a^3 + 119a^2 + 270a + 54)\frac{df_4}{dz}$$

$$- \frac{5c^4a}{27I} (3a + 2)(3a^3 + 17a^2 - 18) \frac{dM}{dz} \Big\} \delta f_2 \Big]_0^H$$

$$+ \frac{1}{G} \Big[\Big\{ - \frac{4c^3a}{189} (21a^3 + 119a^2 + 270a + 54) \frac{df_2}{dz}$$

$$+ \frac{4c^3}{105} (35a^3 + 135a^2 + 60a + 8) \frac{df_4}{dz}$$

$$+ \frac{c^4}{21I} (3a + 2)(35a^3 - 60a - 12) \frac{dM}{dz} \Big\} \delta f_4 \Big]_0^H$$

$$= 0 \qquad \ldots\ldots (6.114)$$

The governing differential equations may, therefore, be expressed as

$$\frac{d^2f_2}{dz^2} - \left(\frac{k_1}{H}\right)^2 f_2 - \alpha_1^2 \frac{d^2f_4}{dz^2} + \left(\frac{\beta_1}{H}\right)^2 f_4 = \lambda_1^2 \frac{d^2\sigma_b}{dz^2} \qquad (6.115)$$

and

$$\frac{d^2f_2}{dz^2} - \left(\frac{k_2}{H}\right)^2 f_2 - \alpha_2^2 \frac{d^2f_4}{dz^2} + \left(\frac{\beta_2}{H}\right)^2 f_4 = \lambda_2^2 \frac{d^2\sigma_b}{dz^2} \qquad (6.116)$$

in which

$$k_1^2 = \frac{567}{2} \frac{G}{E} \left(\frac{H}{b}\right)^2 \frac{a(3a + 2)(a + 4)}{9a^3 + 54a^2 + 137a + 189}$$

$$\alpha_1^2 = \frac{3}{5} \frac{21a^3 + 119a^2 + 270a + 54}{a(9a^3 + 54a^2 + 137a + 189)}$$

$$\beta_1^2 = 567 \frac{G}{E} \left(\frac{H}{b}\right)^2 \frac{a(3a + 2)}{9a^3 + 54a^2 + 137a + 189}$$

$$\lambda_1^2 = \frac{21}{4} \frac{(3a + 2)(3a^3 + 17a^2 - 18)}{a(9a^3 + 54a^2 + 137a + 189)}$$

$$k_2^2 = 945 \frac{G}{E} \left(\frac{H}{b}\right)^2 \frac{a^2(3a + 2)}{21a^3 + 119a^2 + 270a + 54}$$

$$\alpha_2^2 = \frac{9}{5} \frac{35a^3 + 135a^2 + 60a + 8}{a(21a^3 + 119a^2 + 270a + 54)}$$

$$\beta_2^2 = 162 \frac{G}{E} \left(\frac{H}{b}\right)^2 \frac{a(5a + 1)(3a + 2)}{21a^3 + 119a^2 + 270a + 54}$$

and

$$\lambda_2^2 = \frac{9}{4} \frac{(3a + 2)(35a^3 - 60a - 12)}{a(21a^3 + 119a^2 + 270a + 54)}$$

For the case of a structure rigidly built-in at the base and free at the top, the appropriate boundary conditions are

$$\text{at } z = 0, \quad f_2 = 0 \qquad \ldots\ldots (6.117)$$

$$\text{at } z = 0, \quad f_4 = 0 \qquad \ldots\ldots (6.118)$$

$$\text{at } z = H, \quad \frac{df_2}{dz} - \alpha_1^2 \frac{df_4}{dz} - \lambda_1^2 \frac{d\sigma_b}{dz} = 0 \qquad (6.119)$$

and

$$\text{at } z = H, \quad \frac{df_2}{dz} - \alpha_2^2 \frac{df_4}{dz} - \lambda_2^2 \frac{d\sigma_b}{dz} = 0 \qquad (6.120)$$

The equations (6.115) to (6.120) are identical to the corresponding equations for the bending of framed-tube structures in Chapter 2 (equations 2.88, 2.89, 2.86, 2.87, 2.90 and 2.91). Hence the solutions of the equations for different loading cases will be the same.

In the particular case of a bundled tube structure with a square cross-section of sides 2b, the aspect ratio a becomes 1, and the parameters are reduced to

$$k_1^2 = 18.2198 \frac{G}{E} \left(\frac{H}{b}\right)^2$$

$$\alpha_1^2 = 0.7157$$

$$\beta_1^2 = 7.2879 \frac{G}{E} \left(\frac{H}{b}\right)^2$$

$$\lambda_1^2 = 0.1350$$

$$k_2^2 = 10.1832 \frac{G}{E} \left(\frac{H}{b}\right)^2$$

$$\alpha_2^2 = 0.9233$$

$$\beta_2^2 = 10.4741 \frac{G}{E} \left(\frac{H}{b}\right)^2$$

$$\lambda_2^2 = - 0.8971$$

The process of iteration, described in Article 6.5.2 is also carried out in the present analysis and the stresses in the various panels of the structure determined.

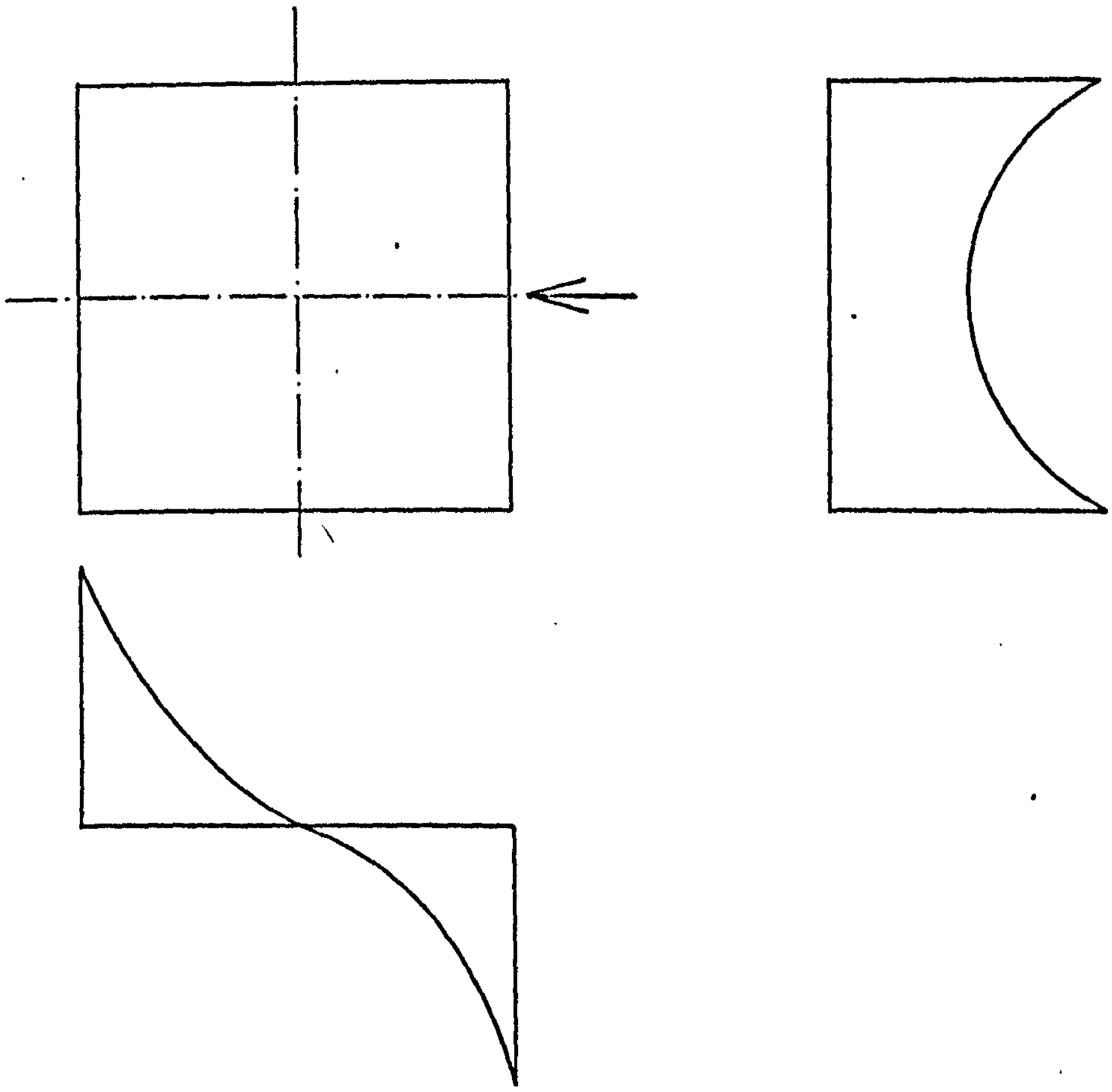

Fig. 6.1 Shear lag in Framed Tube and Bundled Tube Structures

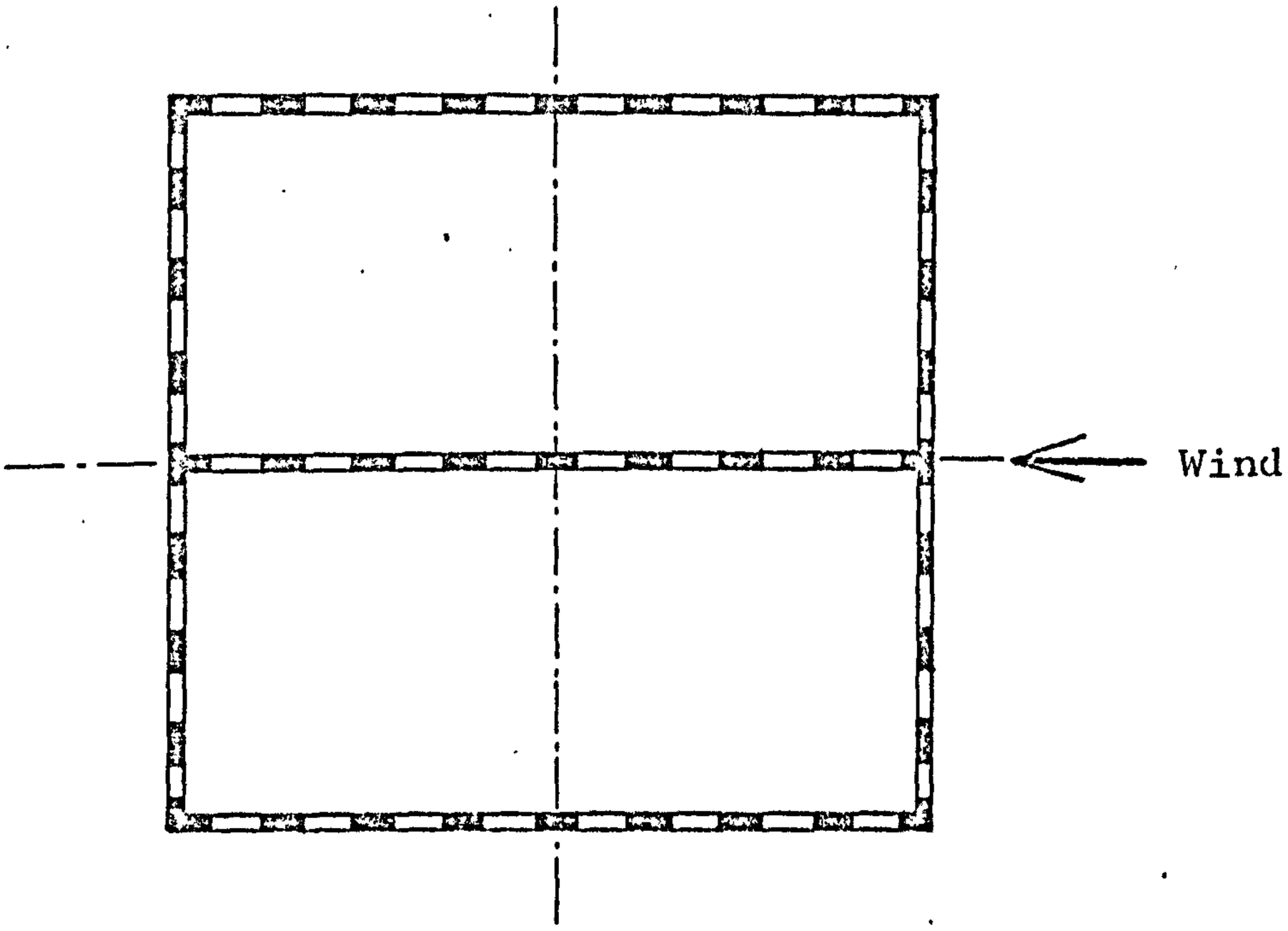

Fig. 6.2 Plan of Bundled-Tube Structure

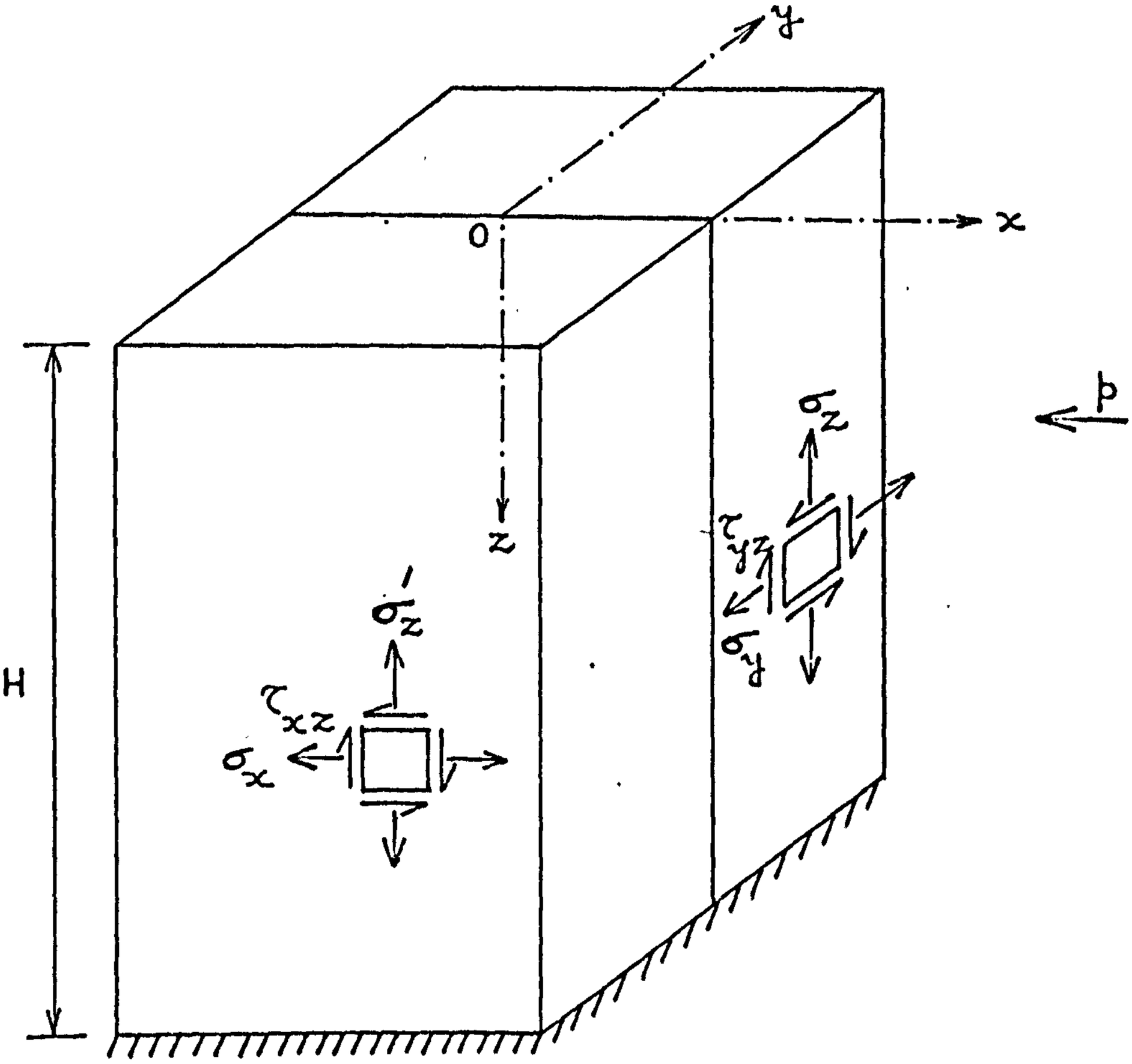

Fig. 6.3 Notation for stresses

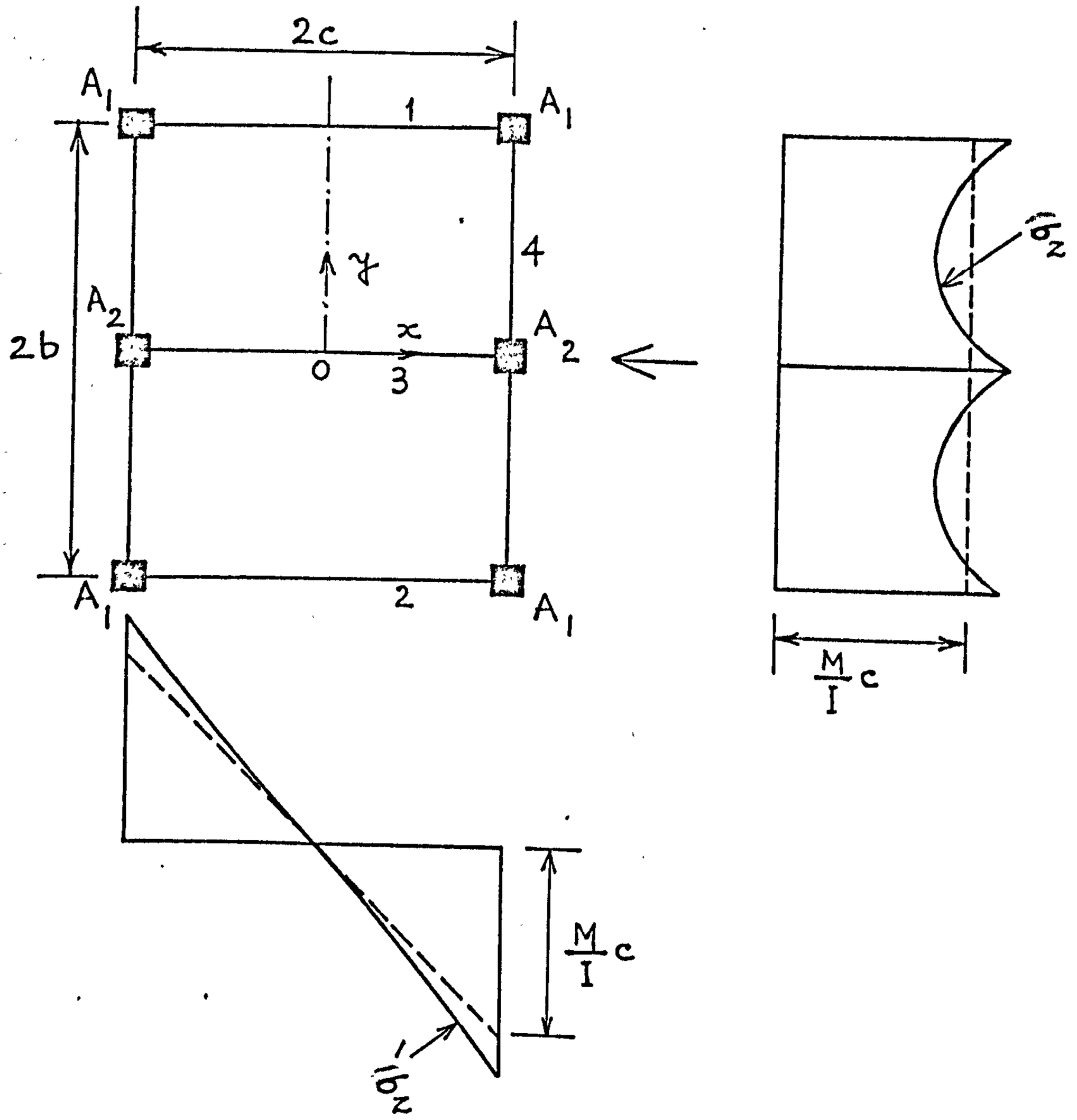

Fig. 6.4 Vertical stresses in Substitute Structure

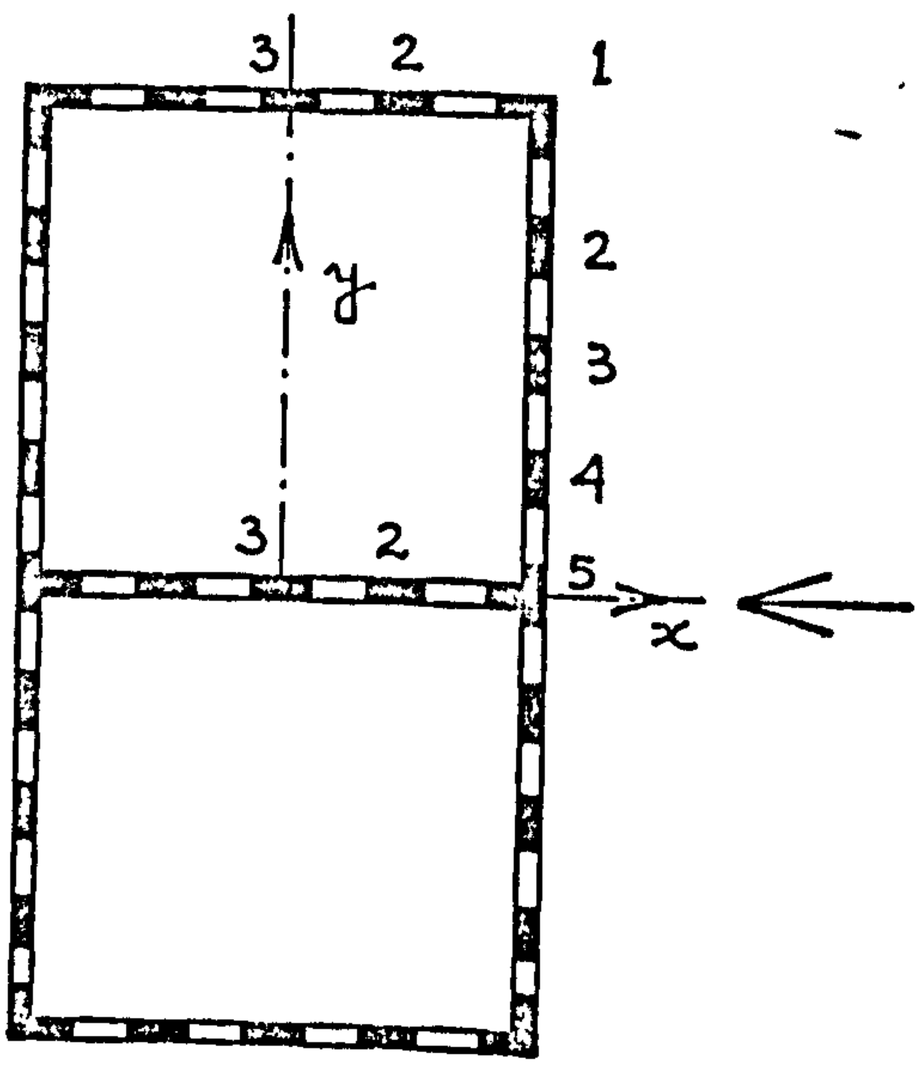

Fig. 6.5 Typical plan of a building

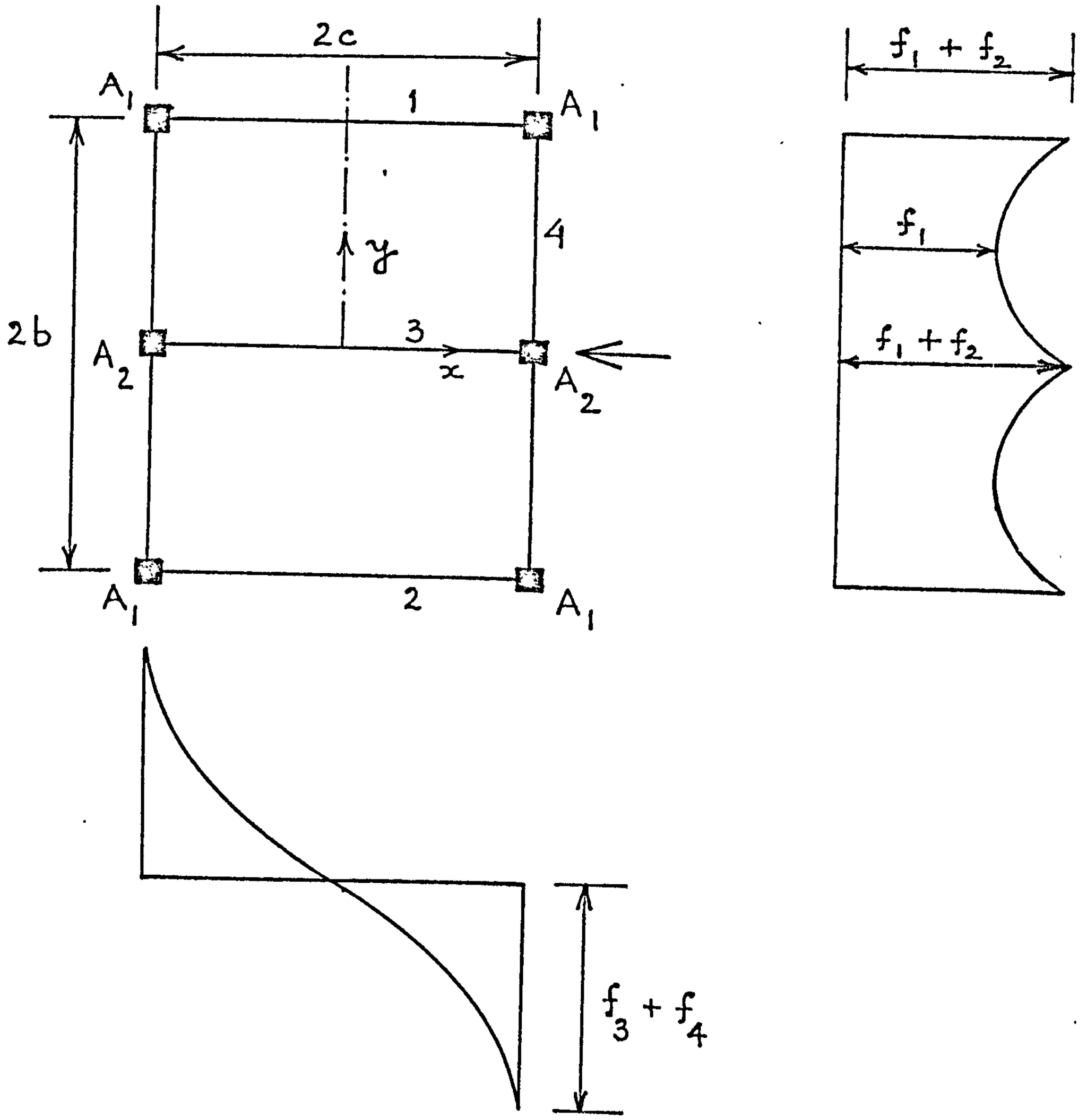

Fig. 6.6 Vertical Stresses in Structure

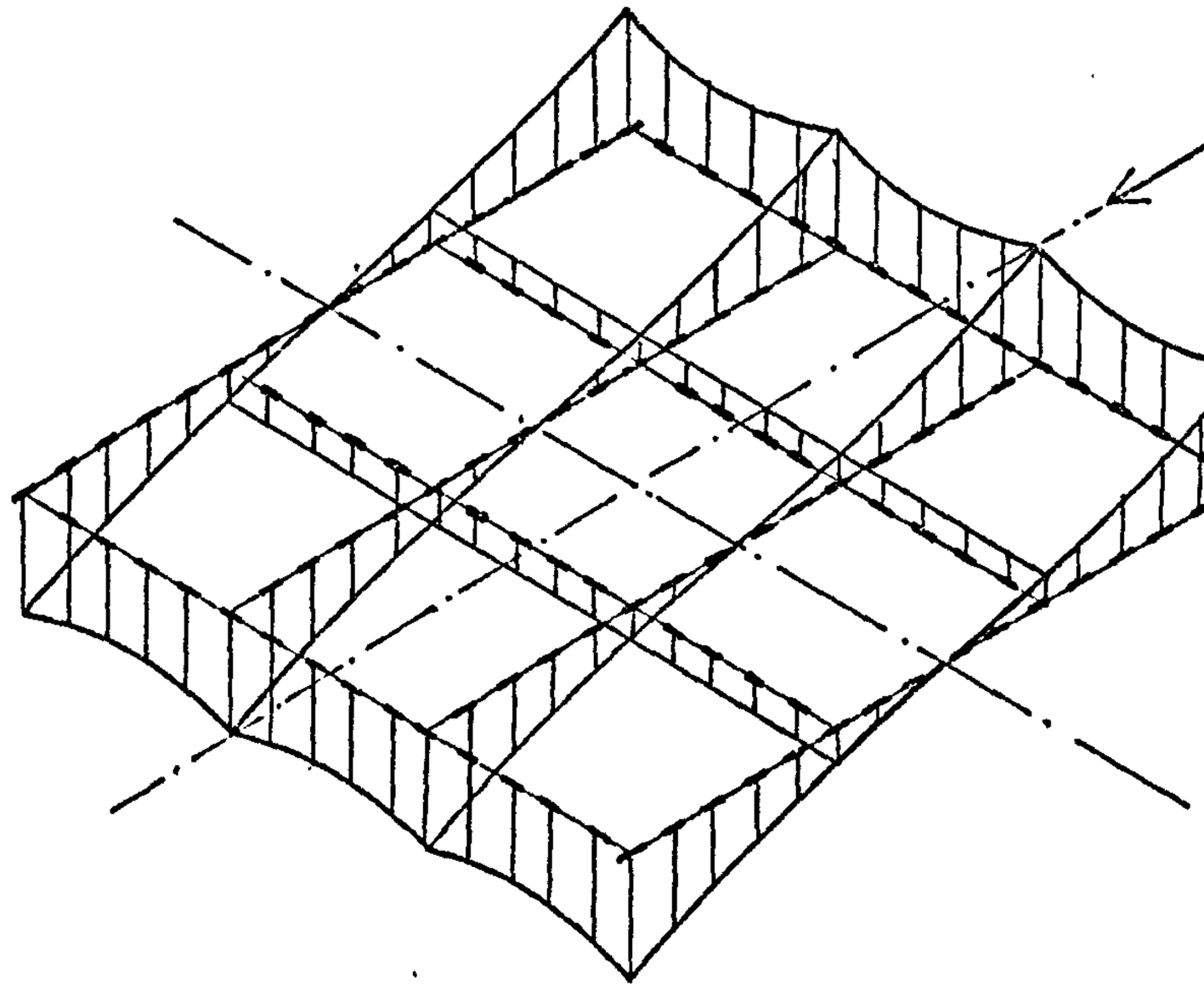

Fig. 6.7 Column axial load distribution showing shear lag effects

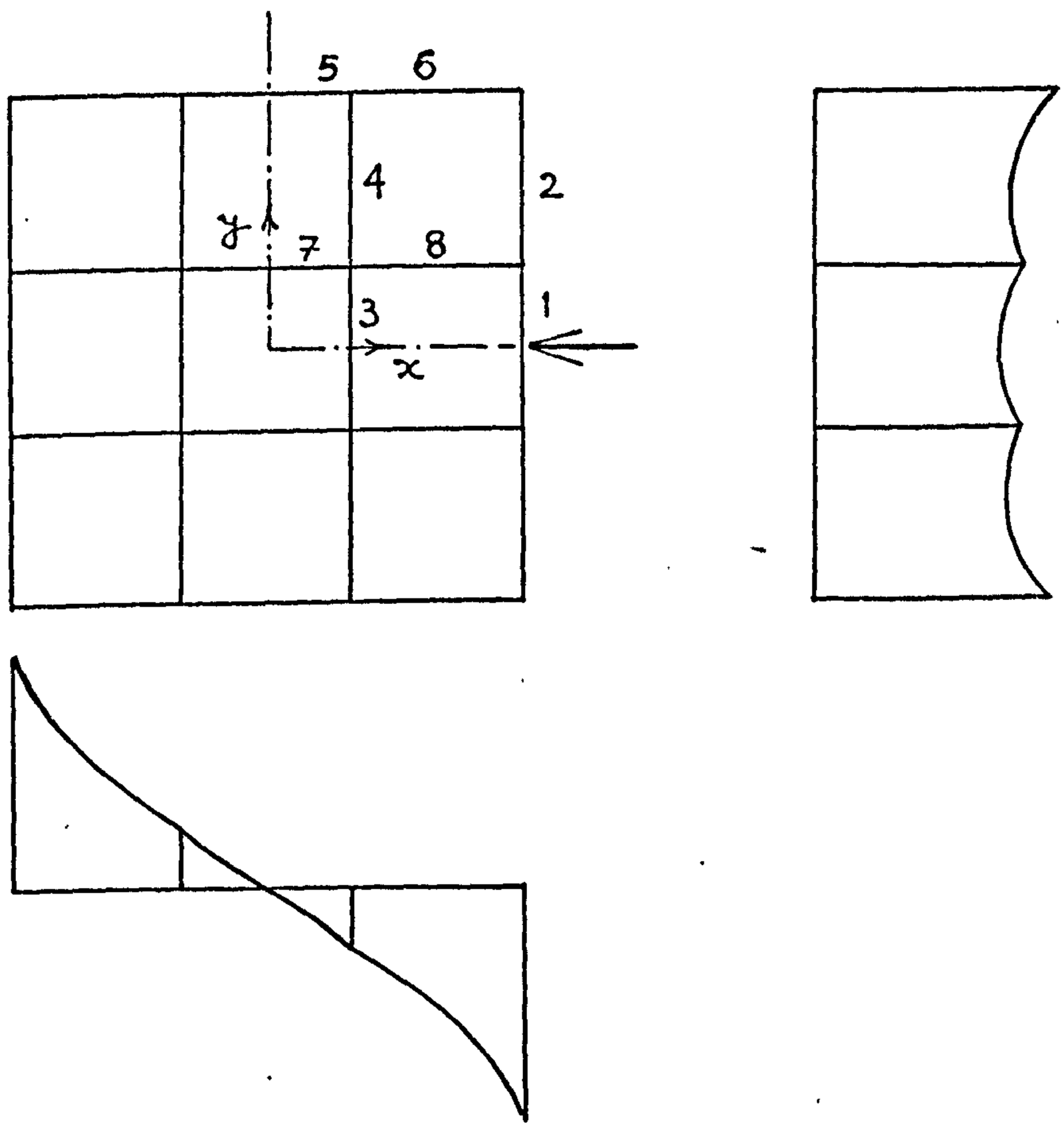

Fig. 6.8 Stress distribution in Substitute Structure

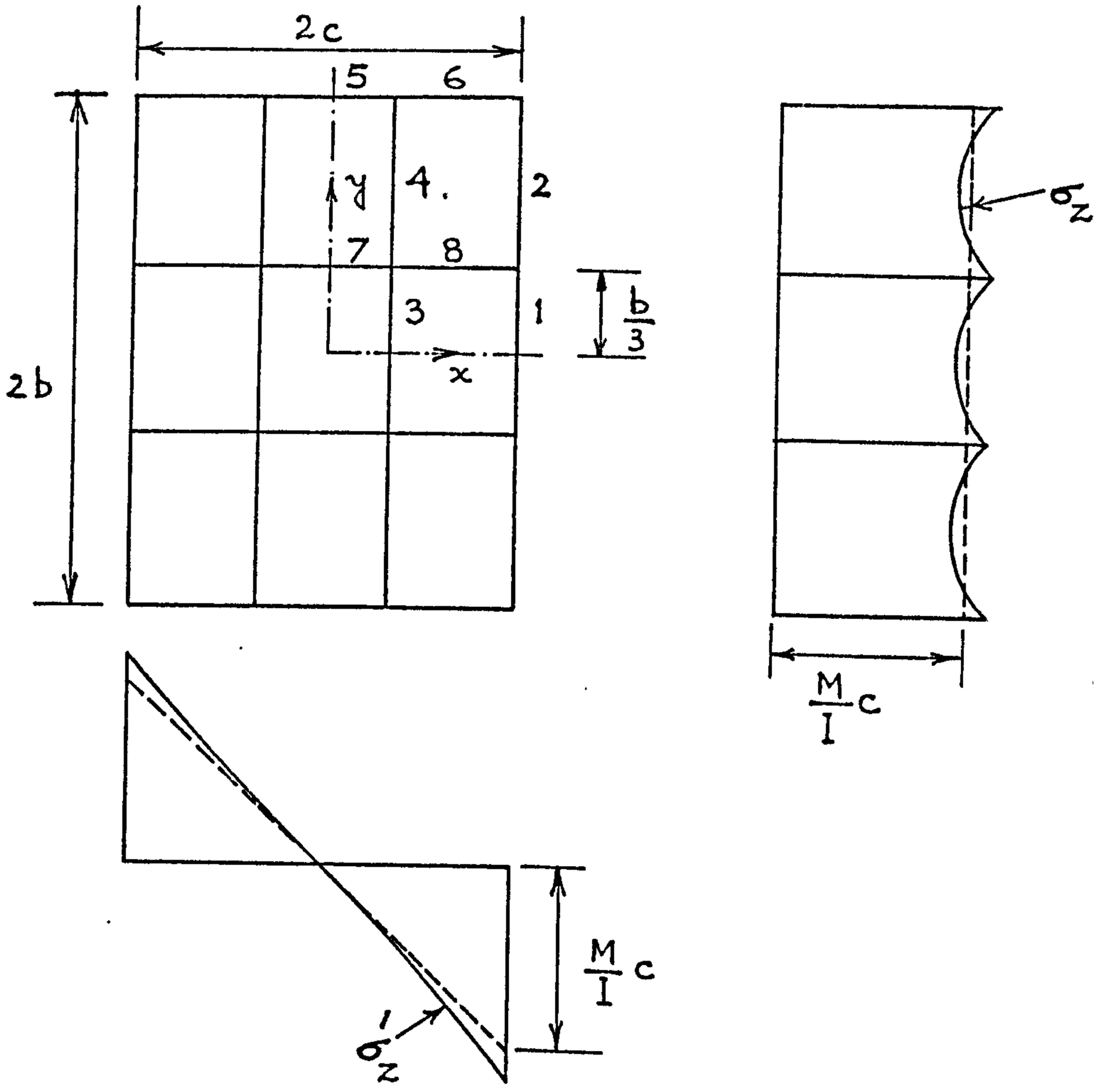

Fig. 6.9 Vertical stress distribution in flange and web panels

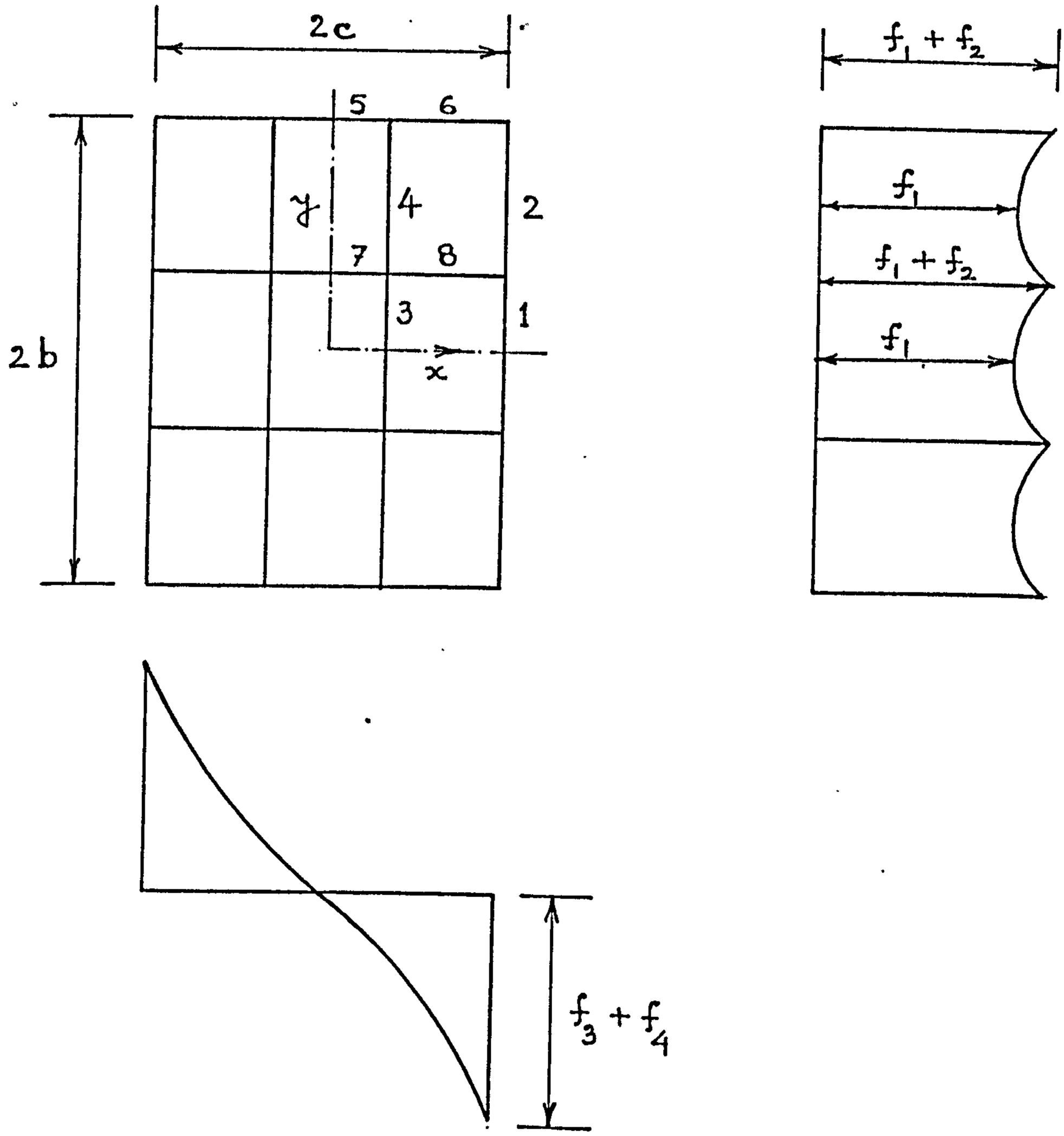

Fig. 6.10 Vertical stress distribution showing shear lag effect

CHAPTER 7

FRAMED-TUBE STRUCTURE UNDER VERTICAL FORCES

NOTATION

The following symbols are used in this chapter:

A = area of cross-section of framed-tube;

A_c = area of corner column;

a = aspect ratio;

b = half breadth of framed-tube;

c = half depth of framed-tube;

E = elastic modulus;

f_1, f_2, f_3, f_4 = stress functions;

G = equivalent shear modulus;

H = total height of building;

k_1, k_2 = structural parameters;

n = $\frac{A_c}{ct}$;

t = thickness of equivalent orthotropic plate;

U = strain energy;

W = applied force at any level;

x, y = horizontal coordinates;

z, z' = vertical coordinates;

α_1, α_2 = geometrical ratios;

β_1, β_2 = structural parameters;

ξ = non-dimensional height coordinate $(\frac{z}{H})$;

ρ_s = force per unit volume due to self weight;

ρ_{f_1}, ρ_{f_2} = maximum vertical forces in the panels induced due to the loads on the floor areas;

σ = direct stress;

τ = shear stress.

7.1 INTRODUCTION

The analysis of framed-tube structures subjected to lateral wind load was considered in Chapter 2. By replacing the discrete structure by an equivalent orthotropic tube, and making simplifying assumptions regarding the stress distribution in the structure a simple closed solution was obtained.

In addition to the lateral load the structure is subjected to vertical forces due to the dead load of the structure and the live load acting on the floor areas. The dead load includes the weight of (a) the exterior structural wall consisting of columns and spandrel beams, (b) the floor system of deep girders or trusses, the metal deck and the concrete slab, and (c) the light weight elements and glass for interior partitions and exterior cladding.

The magnitude of the live load depends on the purpose for which the floor areas are used and are different for office areas, mechanical rooms, public spaces and plaza areas.

The vertical force acting on the panels is not uniform and a redistribution of vertical stresses in the panels may take place due to the flexibility of the spandrel beams. A simple procedure is described in this chapter to examine any redistribution which may take place.

In many practical structures, the four corner columns are considerably stiffer than the other columns, and provision is again made in the analysis to include

stiffer individual corner elements.

7.2 METHOD OF ANALYSIS

In the framed-tube structure with stiffer corner columns shown in plan is Fig. 7.1, the vertical load is resisted primarily by the axial deformations of the four frame panels. The interactions between the orthogonal panels consist mainly of vertical interactive forces along the corners A, B, C and D.

The spacings of the beams and columns are assumed uniform throughout the height, as is usually the case in practice. In addition, in order to simplify the analysis, it is assumed that both beams and columns are of uniform section throughout the height. This is not strictly necessary, and it is straightforward to extend the analysis to include a number of regions in which the beams and columns have constant stiffnesses. The analysis of framed-tube structureswith different stiffness regions was discussed in Chapter 5 for bending action and a similar procedure may be followed for vertical forces.

It is then assumed that each framework panel of columns and spandrel beams may be replaced by an equivalent uniform orthotropic plate, to form a substitute closed-tube structure. The substitute tube is assumed to have a uniform equivalent thickness t, with vertical elastic modulus E and shear modulus G. The derivation of the properties of the orthotropic plate to model the vertical, horizontal, and shearing stiffnesses of the frame panels was given in Chapter 2.

The vertical force caused due to the weight of the structure itself consisting of closely spaced columns and deep spandrel beams, and exterior cladding may be considered as a uniform force ρ_s per unit volume of the equivalent tube structure.

The weight of the floor system and the interior partitions, and the live load acting on the floor areas are transferred to the four panels of the equivalent tube at every floor level. It is assumed that the vertical forces along the frame panels at every floor level may be expressed as parabolic distributions.(21) On dividing the force per unit width by the thickness t of the equivalent tube and the storey height h, the vertical forces in the panels AD and DC may be expressed as a continuous force per unit volume for the whole height of the building of the form,

$$\rho = \rho_{f_1} \left[1 - \left(\frac{y}{b}\right)^2 \right] \qquad \ldots\ldots (7.1)$$

$$\rho' = \rho_{f_2} \left[1 - \left(\frac{x}{c}\right)^2 \right] \qquad \ldots\ldots (7.2)$$

where ρ_{f_1} and ρ_{f_2} are constant terms independent of the height coordinate z.

These parabolic distributions of vertical forces will modify the distributions of vertical stresses in the panels, expressed ordinarily by the average stress $\frac{W}{A}$, and induce horizontal direct stresses and shear stresses.

The assumption is now made that the stresses may be expressed with sufficient accuracy as a power series in the horizontal coordinate, x or y, the coefficients of the

series being arbitrary functions of the height coordinate z. The simplest approximation which may be made for the symmetrical distributions of vertical stresses σ_z and σ'_z in the panels AD and DC respectively are parabolic distributions. The stress distribution, σ_z, for panel AD may thus be expressed as,

$$\sigma_z = f_1 + \left(\frac{y}{b}\right)^2 f_2 \qquad \ldots\ldots (7.3)$$

in which f_1 and f_2 are functions of the height coordinate z only.

In the same way, the distribution of vertical stresses, σ'_z, in the panel DC may be expressed in the form,

$$\sigma'_z = f_3 + \left(\frac{x}{c}\right)^2 f_4 \qquad \ldots\ldots (7.4)$$

in which f_3 and f_4 are also functions of the coordinate z.

The condition of vertical strain compatibility at the corner requires,

$$\frac{\sigma_z}{E}(\pm b, z) = \frac{\sigma'_z}{E}(\pm c, z) = \frac{\sigma_c}{E} \qquad \ldots\ldots (7.5)$$

in which σ_c is the axial stress in the corner column of area A_c, given by, on using equation (7.3),

$$\sigma_c = (\sigma_z)_{y=b} = f_1 + f_2 \qquad \ldots\ldots (7.6)$$

On substituting equations (7.3) and (7.4) into equation (7.5), it is found that

$$f_1 + f_2 = f_3 + f_4 \qquad \ldots\ldots (7.7)$$

The condition of vertical force equilibrium at any level is

$$2\int_{-b}^{b} \sigma_z\, t\, dy + 2\int_{-c}^{c} \sigma'_z\, t\, dx + 4A_c\, \sigma_c = -W(z) \qquad (7.8)$$

in which W(z) is the total vertical force at that level, given by

$$W = 2\int_{-b}^{b} \rho\, t\, dy\, z + 2\int_{-c}^{c} \rho'\, t\, dx\, z + \left[4(b+c)t + 4A_c\right].$$

$$\rho_s.\ z \qquad \ldots\ldots \qquad (7.9)$$

On substituting equations (7.1) and (7.2) into equation (7.9), the total vertical force W becomes,

$$W = 4tz\left[\tfrac{2}{3}b\,\rho_{f_1} + \tfrac{2}{3}c\,\rho_{f_2} + \left(b + c + \frac{A_c}{t}\right)\rho_s\right] \ldots\ldots\ldots (7.10)$$

On substituting equations (7.3) and (7.4) into equation (7.8) and integrating, it is found that,

$$4t\left[b\left(f_1 + \tfrac{1}{3}f_2\right) + c\left(f_3 + \tfrac{1}{3}f_4\right) + \frac{A_c}{t}\left(f_1 + f_2\right)\right] = -W$$

$$\ldots\ldots \qquad (7.11)$$

The functions f_1 and f_3 may, therefore, be determined from equations (7.7) and (7.11) as,

$$f_1 = -\frac{W}{A} - \frac{a + 3n + 3}{3(a + n + 1)}\, f_2 + \frac{2}{3(a + n + 1)} f_4 \qquad (7.12)$$

$$f_3 = -\frac{W}{A} + \frac{2a}{3(a + n + 1)}\, f_2 - \frac{3a + 3n + 1}{3(a + n + 1)}\, f_4 \qquad (7.13)$$

in which $a = \dfrac{b}{c}$

and $n = \dfrac{A_c}{ct}$

In equations (7.12) and (7.13), A is the area of the equivalent tube cross-section, given by

$$A = 4(b + c)t + 4A_c \qquad \ldots\ldots \qquad (7.14)$$

The vertical stresses, σ_z and σ'_z, may thus be expressed in terms of the two unknown functions $f_2(z)$ and $f_4(z)$ as,

$$\sigma_z = -\frac{W}{A} - \left[\frac{a + 3n + 3}{3(a + n + 1)} - \left(\frac{y}{b}\right)^2\right] f_2 + \frac{2}{3(a + n + 1)} f_4 \quad \ldots\ldots \quad (7.15)$$

$$\sigma'_z = -\frac{W}{A} + \frac{2a}{3(a + n + 1)} f_2 - \left[\frac{3a + 3n + 1}{3(a + n + 1)} - \left(\frac{x}{c}\right)^2\right] f_4 \quad \ldots\ldots \quad (7.16)$$

The stress in the corner element then becomes

$$\sigma_c = -\frac{W}{A} + \frac{2a}{3(a + n + 1)} f_2 + \frac{2}{3(a + n + 1)} f_4 \quad (7.17)$$

The equations of equilibrium for the panel AD are

$$\frac{\partial \sigma_y}{\partial y} + \frac{\partial \tau_{yz}}{\partial z} = 0$$

$$\frac{\partial \sigma_z}{\partial z} + \frac{\partial \tau_{yz}}{\partial y} + \rho_s + \rho_{f_1}\left[1 - \left(\frac{y}{b}\right)^2\right] = 0 \quad (7.18)$$

The equilibrium conditions for the panel DC are

$$\frac{\partial \sigma_x}{\partial x} + \frac{\partial \tau_{xz}}{\partial z} = 0$$

$$\frac{\partial \sigma'_z}{\partial z} + \frac{\partial \tau_{xz}}{\partial x} + \rho_s + \rho_{f_2}\left[1 - \left(\frac{x}{c}\right)^2\right] = 0 \quad (7.19)$$

On substituting equations (7.15) and (7.16) into the equilibrium conditions (7.18) and (7.19), and integrating, the remaining stress components become

$$\sigma_y = \frac{b^2}{6}\left[\frac{a+5n+5}{2(a+n+1)} - \frac{a+3n+3}{a+n+1}\left(\frac{y}{b}\right)^2 + \frac{1}{2}\left(\frac{y}{b}\right)^4\right] \frac{d^2 f_2}{dz^2}$$

$$- \frac{b^2}{3(a + n + 1)}\left[1 - \left(\frac{y}{b}\right)^2\right] \frac{d^2 f_4}{dz^2}$$

$$\tau_{yz} = \frac{y}{3}\left\{\left[\frac{a + 3n + 3}{a + n + 1} - \left(\frac{y}{b}\right)^2\right]\left(\frac{df_2}{dz} - \rho_{f_1}\right)\right.$$

$$\left. - \frac{2}{a + n + 1}\left(\frac{df_4}{dz} - \rho_{f_2}\right)\right\}$$

$$\sigma_x = - \frac{ac^2}{3(a + n + 1)}\left[1 - \left(\frac{x}{c}\right)^2\right]\frac{d^2f_2}{dz^2}$$

$$+ \frac{c^2}{6}\left[\frac{5a + 5n + 1}{2(a + n + 1)} - \frac{3a + 3n + 1}{a + n + 1}\left(\frac{x}{c}\right)^2 + \tfrac{1}{2}\left(\frac{x}{c}\right)^4\right]\frac{d^2f_4}{dz^2}$$

$$\tau_{xz} = \frac{x}{3}\left\{- \frac{2a}{a + n + 1}\left(\frac{df_2}{dz} - \rho_{f_1}\right)\right.$$

$$\left. + \left[\frac{3a + 3n + 1}{a + n + 1} - \left(\frac{x}{c}\right)^2\right]\left(\frac{df_4}{dz} - \rho_{f_2}\right)\right\} \quad \ldots\ldots (7.20)$$

The integration constants were evaluated from the following boundary conditions:

At $y = \pm b$, $\quad \sigma_y = 0$

At $x = \pm c$, $\quad \sigma_x = 0$

In addition τ_{yz} and τ_{xz} are skew symmetric with respect to the axes $y = 0$ and $x = 0$ respectively.

It is seen that the following equation of equilibrium at the corner column is automatically satisfied.

$$(\tau_{xz})_{x=c} + (\tau_{yz})_{y=b} = \frac{A_c}{t}\left(\frac{d\sigma_c}{dz} + \rho_s\right)$$

The total strain energy, U, stored in the structure is

$$U = t\int_0^H \left\{\int_{-b}^{b}\left[\frac{\sigma_z^2}{E} + \frac{\tau_{yz}^2}{G}\right]dy + \int_{-c}^{c}\left[\frac{(\sigma'_z)^2}{E} + \frac{\tau_{xz}^2}{G}\right]dx\right\}dz$$

$$+ \frac{2A_c}{E} \int_0^H \sigma_c^2 \, dz \qquad \ldots\ldots \qquad (7.21)$$

The strain energy due to the horizontal direct stresses, σ_x and σ_y, is small and may be neglected.

On substituting equations (7.15), (7.16), (7.17) and (7.20) into equation (7.21), the strain energy U may be expressed as,

$$U = t \int_0^H \left[\frac{1}{E} \int_{-b}^{b} \left\{ - \frac{W}{A} - \left[\frac{a+3n+3}{3(a+n+1)} - \left(\frac{y}{b}\right)^2 \right] f_2 + \frac{2}{3(a+n+1)} f_4 \right\}^2 dy \right.$$

$$+ \frac{1}{G} \int_{-b}^{b} \frac{y^2}{9} \left\{ \left[\frac{a + 3n + 3}{a + n + 1} - \left(\frac{y}{b}\right)^2 \right] \left(\frac{df_2}{dz} - \rho_{f_1} \right) \right.$$

$$\left. - \frac{2}{a + n + 1} \left(\frac{df_4}{dz} - \rho_{f_2} \right) \right\}^2 dy$$

$$+ \frac{1}{E} \int_{-c}^{c} \left\{ - \frac{W}{A} + \frac{2a}{3(a+n+1)} f_2 - \left[\frac{3a+3n+1}{3(a+n+1)} - \left(\frac{x}{c}\right)^2 \right] f_4 \right\}^2 dx$$

$$+ \frac{1}{G} \int_{-c}^{c} \frac{x^2}{9} \left\{ - \frac{2a}{a + n + 1} \left(\frac{df_2}{dz} - \rho_{f_1} \right) \right.$$

$$\left. + \left[\frac{3a + 3n + 1}{a + n + 1} - \left(\frac{x}{c}\right)^2 \right] \left(\frac{df_4}{dz} - \rho_{f_2} \right) \right\}^2 dx$$

$$\left. + \frac{2A_c}{tE} \left\{ - \frac{W}{A} + \frac{2a}{3(a + n + 1)} f_2 + \frac{2}{3(a + n + 1)} f_4 \right\}^2 \right] dz$$

$\ldots\ldots$ (7.22)

The variation, δU, of the strain energy may be determined by the calculus of variations and is given by,

$$\delta U = 2t \int_0^H \left[\frac{1}{E} \int_{-b}^{b} \left\{ - \frac{W}{A} - \left[\frac{a+3n+3}{3(a+n+1)} - \left(\frac{y}{b}\right)^2 \right] f_2 + \frac{2}{3(a+n+1)} f_4 \right\} \right.$$

$$\left\{ - \left[\frac{a + 3n + 3}{3(a+n+1)} - \left(\frac{y}{b}\right)^2 \right] \delta f_2 + \frac{2}{3(a+n+1)} \delta f_4 \right\} dy$$

$$+ \frac{1}{G} \int_{-b}^{b} \frac{y^2}{9} \left\{ \left[\frac{a + 3n + 3}{a + n + 1} - \left(\frac{y}{b}\right)^2 \right] \left(\frac{df_2}{dz} - \rho_{f_1} \right) \right.$$

$$\left. - \frac{2}{a + n + 1} \left(\frac{df_4}{dz} - \rho_{f_2} \right) \right\} \cdot$$

$$\left\{ \left[\frac{a+3n+3}{a+n+1} - \left(\frac{y}{b}\right)^2 \right] \frac{d(\delta f_2)}{dz} - \frac{2}{a+n+1} \frac{d(\delta f_4)}{dz} \right\} dy$$

$$+ \frac{1}{E} \int_{-c}^{c} \left\{ - \frac{W}{A} + \frac{2a}{3(a+n+1)} f_2 - \left[\frac{3a+3n+1}{3(a+n+1)} - \left(\frac{x}{c}\right)^2 \right] f_4 \right\} \cdot$$

$$\left\{ \frac{2a}{3(a+n+1)} \delta f_2 - \left[\frac{3a + 3n + 1}{3(a + n + 1)} - \left(\frac{x}{c}\right)^2 \right] \delta f_4 \right\} dx$$

$$+ \frac{1}{G} \int_{-c}^{c} \frac{x^2}{9} \left\{ - \frac{2a}{a + n + 1} \left(\frac{df_2}{dz} - \rho_{f_1} \right) \right.$$

$$\left. + \left[\frac{3a + 3n + 1}{a + n + 1} - \left(\frac{x}{c}\right)^2 \right] \left(\frac{df_4}{dz} - \rho_{f_2} \right) \right\} \cdot$$

$$\left\{ - \frac{2a}{a+n+1} \frac{d(\delta f_2)}{dz} + \left[\frac{3a+3n+1}{a+n+1} - \left(\frac{x}{c}\right)^2 \right] \frac{d(\delta f_4)}{dz} \right\} dx$$

$$+ \frac{2A_c}{tE} \left\{ - \frac{W}{A} + \frac{2a}{3(a+n+1)} f_2 + \frac{2}{3(a + n + 1)} f_4 \right\} \cdot$$

$$\left. \left\{ \frac{2a}{3(a + n + 1)} \delta f_2 + \frac{2}{3(a + n + 1)} \delta f_4 \right\} \right] dz$$

..... (7.23)

In order to minimise the strain energy the variation δU must be equal to zero, which gives

$$\int_0^H \Bigg[-\frac{2a^2c^3}{G}\left(2a^3+18a^2n+18a^2+51an^2+102an+51a+35\right)\frac{d^2f_2}{dz^2}$$

$$+\frac{42ac}{E}\left(a^2+7an+7a+6n^2+12n+6\right)f_2$$

$$+\frac{14ac^3}{G}\left(a^3+6a^2n+6a^2+6a+6n+1\right)\frac{d^2f_4}{dz^2}$$

$$-\frac{210\ ac}{E}\left(a+n+1\right)f_4\Bigg]\,dz\ \delta f_2$$

$$+\int_0^H \Bigg[\frac{14ac^3}{G}\left(a^3+6a^2n+6a^2+6a+6n+1\right)\frac{d^2f_2}{dz^2}$$

$$-\frac{210\ ac}{E}\left(a+n+1\right)f_2$$

$$-\frac{2c^3}{G}\left(35a^3+51a^2+102an+18a+51n^2+18n+2\right)\frac{d^2f_4}{dz^2}$$

$$+\frac{42c}{E}\left(6a^2+12an+7a+6n^2+7n+1\right)f_4\Bigg]\,dz\ \delta f_4$$

$$+\Bigg[\frac{1}{G}\Bigg\{2a^2c^3(2a^3+18a^2n+18a^2+51an^2+102an+51a+35)\left(\frac{df_2}{dz}-\rho_{f_1}\right)$$

$$-14ac^3(a^3+6a^2n+6a^2+6a+6n+1)\left(\frac{df_4}{dz}-\rho_{f_2}\right)\Bigg\}\delta f_2\Bigg]_0^H$$

$$+\Bigg[\frac{1}{G}\Bigg\{-14ac^3(a^3+6a^2n+6a^2+6a+6n+1)\left(\frac{df_2}{dz}-\rho_{f_1}\right)$$

$$+2c^3(35a^3+51a^2+102an+18a+51n^2+18n+2)\left(\frac{df_4}{dz}-\rho_{f_2}\right)\Bigg\}\ \delta f_4\Bigg]_0^H$$

$$=0 \qquad \ldots\ldots \quad (7.24)$$

The governing differential equations may, therefore, be expressed as

$$\frac{d^2f_2}{dz^2} - \left(\frac{k_1}{H}\right)^2 f_2 - \alpha_1^2 \frac{d^2f_4}{dz^2} + \left(\frac{\beta_1}{H}\right)^2 f_4 = 0 \qquad (7.25)$$

and

$$\frac{d^2f_2}{dz^2} - \left(\frac{k_2}{H}\right)^2 f_2 - \alpha_2^2 \frac{d^2f_4}{dz^2} + \left(\frac{\beta_2}{H}\right)^2 f_4 = 0 \qquad (7.26)$$

in which

$$k_1^2 = 21 \frac{G}{E} \left(\frac{H}{b}\right)^2 \frac{a(a + 6n + 6)(a + n + 1)}{2a^3 + 18a^2n + 18a^2 + 51an^2 + 102an + 51a + 35}$$

$$\alpha_1^2 = 7 \frac{a^3 + 6a^2n + 6a^2 + 6a + 6n + 1}{a(2a^3 + 18a^2n + 18a^2 + 51an^2 + 102an + 51a + 35)}$$

$$\beta_1^2 = 105 \frac{G}{E}\left(\frac{H}{b}\right)^2 \frac{a(a + n + 1)}{2a^3 + 18a^2n + 18a^2 + 51an^2 + 102an + 51a + 35}$$

$$k_2^2 = 15 \frac{G}{E} \left(\frac{H}{b}\right)^2 \frac{a^2(a + n + 1)}{a^3 + 6a^2n + 6a^2 + 6a + 6n + 1}$$

$$\alpha_2^2 = \frac{1}{7} \frac{35a^3 + 51a^2 + 102an + 18a + 51n^2 + 18n + 2}{a(a^3 + 6a^2n + 6a^2 + 6a + 6n + 1)}$$

and

$$\beta_2^2 = 3 \frac{G}{E} \left(\frac{H}{b}\right)^2 \frac{a(a + n + 1)(6a + 6n + 1)}{a^3 + 6a^2n + 6a^2 + 6a + 6n + 1}$$

For the case of a framed-tube rigidly built-in at the base and free at the top, the boundary conditions are

At $z = 0$, $f_2 = 0$ ..... (7.27)

At $z = 0$, $f_4 = 0$ ..... (7.28)

$$\text{At } z = H, \quad \frac{df_2}{dz} - \rho_{f_1} - \alpha_1^2 \left(\frac{df_4}{dz} - \rho_{f_2}\right) = 0 \qquad (7.29)$$

$$\text{At } z = H, \quad \frac{df_2}{dz} - \rho_{f_1} - \alpha_2^2 \left(\frac{df_4}{dz} - \rho_{f_2}\right) = 0 \qquad (7.30)$$

If it is assumed that the structure is supported on an elastic base, the boundary conditions (7.29) and (7.30) will be modified to include the effects of the elasticity of the base. A procedure similar to the one described in Chapter 4 may be followed to determine this modification and hence the effect of elastic base on the redistribution of vertical forces in the panels.

The equations (7.25) and (7.26) are identical to the homogeneous parts corresponding to the equations (2.88) and (2.89), derived for the bending of framed-tube structures. The solutions of the equations were given in Chapter 2 as,

$$f_2 = (\alpha_1^2 m_1^2 - \frac{\beta_1^2}{H^2})(A_1 \cosh m_1 z + A_2 \sinh m_1 z)$$

$$+ (\alpha_1^2 m_2^2 - \frac{\beta_1^2}{H^2})(A_3 \cosh m_2 z + A_4 \sinh m_2 z) \qquad (7.31)$$

$$f_4 = (m_1^2 - \frac{k_1^2}{H^2})(A_1 \cosh m_1 z + A_2 \sinh m_1 z)$$

$$+ (m_2^2 - \frac{k_1^2}{H^2})(A_3 \cosh m_2 z + A_4 \sinh m_2 z) \qquad (7.32)$$

where m_1 and m_2 are given by

$$m^2 = \frac{1}{2H^2(\alpha_1^2 - \alpha_2^2)} \left[(\alpha_1^2 k_2^2 - \alpha_2^2 k_1^2 + \beta_1^2 - \beta_2^2) \pm \right.$$

$$\left. \sqrt{(\alpha_1^2 k_2^2 - \alpha_2^2 k_1^2 + \beta_1^2 - \beta_2^2)^2 - 4(\alpha_1^2 - \alpha_2^2)(\beta_1^2 k_2^2 - \beta_2^2 k_1^2)} \right]$$

..... (7.33)

The constants A_1, A_2, A_3 and A_4 are determined with

the help of the four boundary conditions. They are

$$A_1 = 0$$

$$A_2 = - \frac{(m_2^2H^2 - k_1^2)\, \rho_{f_1} - (\alpha_1^2 m_2^2 H^2 - \beta_1^2)\, \rho_{f_2}}{(\alpha_1^2 k_1^2 - \beta_1^2)(m_1^2 - m_2^2) m_1 \cosh m_1 H}$$

$$A_3 = 0$$

$$A_4 = \frac{(m_1^2H^2 - k_1^2)\, \rho_{f_1} - (\alpha_1^2 m_1^2 H^2 - \beta_1^2)\, \rho_{f_2}}{(\alpha_1^2 k_1^2 - \beta_1^2)(m_1^2 - m_2^2)\, m_2 \cosh m_2 H} \qquad (7.34)$$

The complete solutions become

$$f_2 = (\alpha_1^2 m_1^2 - \frac{\beta_1^2}{H^2})\, A_2 \sinh m_1 H\xi + (\alpha_1^2 m_2^2 - \frac{\beta_1^2}{H^2}) \cdot A_4 \sinh m_2 H \xi \qquad (7.35)$$

$$f_4 = (m_1^2 - \frac{k_1^2}{H^2})\, A_2 \sinh m_1 H \xi + (m_2^2 - \frac{k_1^2}{H^2}) A_4 \sinh m_2 H \xi \qquad (7.36)$$

Considering equations (7.34) to (7.36) it may be seen that the uniform force ρ_s has no effect on the functions f_2 and f_4.

In the particular case where the cross-section of the framed tube is square, of side 2b, the aspect ratio a becomes equal to unity. The constants ρ_{f_1} and ρ_{f_2} are equal and may be denoted by ρ_f. The parameters k_1^2, α_1^2, β_1^2, k_2^2, α_2^2 and β_2^2 reduce to

$$k_1^2 = 21 \frac{G}{E} (\frac{H}{b})^2 \frac{(6n + 7)(n + 2)}{51n^2 + 120n + 106}$$

$$\alpha_1^2 = \frac{14(6n + 7)}{51n^2 + 120n + 106}$$

$$\beta_1^2 = 105 \frac{G}{E} \left(\frac{H}{b}\right)^2 \frac{n + 2}{51n^2 + 120n + 106}$$

$$k_2^2 = \frac{15}{2} \frac{G}{E} \left(\frac{H}{b}\right)^2 \frac{n + 2}{6n + 7}$$

$$\alpha_2^2 = \frac{51n^2 + 120n + 106}{14(6n + 7)}$$

and $$\beta_2^2 = \frac{3}{2} \frac{G}{E} \left(\frac{H}{b}\right)^2 (n + 2)$$

The following relations between the parameters may be noted.

$$\alpha_1^2 \alpha_2^2 = 1$$

$$\alpha_1^2 k_2^2 = \beta_1^2$$

and $$\alpha_1^2 \beta_2^2 = k_1^2$$

The constants m_1 and m_2 reduce to

$$m_1^2 = \frac{1}{H^2} \frac{\beta_1^2 + k_1^2}{\alpha_1^2 + 1}$$

and

$$m_2^2 = \frac{1}{H^2} \frac{\beta_1^2 - k_1^2}{\alpha_1^2 - 1}$$

The constant A_2 reduces to zero and A_4 becomes

$$A_4 = - \frac{(\alpha_1^2 - 1) H^2 \rho_f}{(\alpha_1^2 k_1^2 - \beta_1^2) m_2 \cosh m_2 H}$$

The functions f_2 and f_4 become equal and may be denoted by f. It is found that

$$f = \frac{\rho_f \sinh m_2 H \xi}{m_2 \cosh m_2 H} \qquad \ldots\ldots \quad (7.37)$$

The distributions of stresses in all the four panels are identical. For the face AD, they may be expressed as,

$$\sigma_z = -\frac{W}{A} - \left[\frac{3n + 2}{3(n + 2)} - \left(\frac{y}{b}\right)^2 \right] f \qquad \ldots\ldots\ldots \quad (7.38)$$

$$\tau_{yz} = \frac{y}{3} \left[\frac{3n + 2}{n + 2} - \left(\frac{y}{b}\right)^2 \right] \left(\frac{df}{dz} - \rho_f\right) \qquad \ldots\ldots\ldots \quad (7.39)$$

$$\sigma_y = \frac{b^2}{6} \left[\frac{5n + 2}{2(n + 2)} - \frac{3n + 2}{n + 2} \left(\frac{y}{b}\right)^2 + \tfrac{1}{2}\left(\frac{y}{b}\right)^4 \right] \frac{d^2 f}{dz^2}$$

$$\ldots\ldots\ldots \quad (7.40)$$

The framed-tube structure with variable ρ_s and ρ_f in different regions may be analysed by a procedure similar to the one described in Chapter 5.

7.3 NUMERICAL EXAMPLE

A 50-storey concrete high-rise building of square cross-section, shown in plan in Fig. 7.2, is considered with the following dimensions:

h = storey height = 3.6 m

d = bay width = 3.0 m

2b = side of the cross-section = 24.0 m

t_1 = width of the column = 1 m

t_2 = depth of the spandrel beam = 0.6 m

t_w = thicknesses of column and beam = 0.3 m

The corner column is twice the area of other columns.

The building is subjected to vertical forces defined by,

$$\rho_s = 1 \text{ kN/m}^3$$
$$\rho_f = 3.5 \text{ kN/m}^3 .$$

With the given data it is found that,

$t = 0.1$ m

$n = 0.25$

$A = 10.8 \text{ m}^2$

$$k_1^2 = 2.8855 \frac{G}{E} \left(\frac{H}{b}\right)^2$$

$$\alpha_1^2 = 0.8550$$

$$\beta_1^2 = 1.6974 \frac{G}{E} \left(\frac{H}{b}\right)^2$$

$$\frac{G}{E} = 0.044813$$

$m_2 = 0.050497 \text{ m}^{-1}$

At the second floor level ($\xi = 0.96$) it is found that,

$W = 5736.96$ kN

$f = 48.18$ kN/m^2

The axial force in column 1 is given by (Fig. 7.2),

$$N_1 = t \int_{b - \frac{d}{2}}^{b} \sigma_z \, dy$$

On substituting equation (7.38) into the above equation and integrating, it is found that

$$N_1 = - \frac{td}{2} \left\{ \frac{W}{A} + \frac{1}{3} \left[\frac{3n + 2}{n + 2} - \frac{1}{b^2} \left(3b^2 - \frac{3}{2} b.d + \frac{d^2}{4} \right) \right] f \right\}$$

The axial force in column at position y_i may be expressed as

$$N_i = t \int_{y_i - \frac{d}{2}}^{y_i + \frac{d}{2}} \sigma_z \, dy$$

On substituting equation (7.38) again into the above equation and integrating, N_i becomes,

$$N_i = -td \left\{ \frac{W}{A} + \frac{1}{3} \left[\frac{3n + 2}{n + 2} - \frac{1}{b^2} (3y_i^2 + \frac{d^2}{4}) \right] f \right\}$$

The axial force in the corner element A_c is given by

$$N_c = A_c \left[- \frac{W}{A} + \frac{4}{3(n + 2)} f \right]$$

From the equations given above the axial forces in the columns are found to be,

$N_1 = - 303.3209$ kN

$N_2 = - 157.0431$ kN

$N_3 = - 161.5600$ kN

$N_4 = - 164.2700$ kN

$N_5 = - 165.1734$ kN

If stiffer spandrel beams of depth 1.5 m are used it is found that

$\frac{G}{E} = 0.28404$

$m_2 = 0.127131 \quad m^{-1}$

$f = 11.0221 \quad kN/m^2$

The axial forces in columns become

$N_1 = -315.1971 \quad kN$

$N_2 = -158.8300 \quad kN$

$N_3 = -159.8633 \quad kN$

$N_4 = -160.4833 \quad kN$

$N_5 = -160.6899 \quad kN$

Comparing the results of the two cases, it appears that the flexibility of spandrel beams has small effect on the distribution of vertical stresses in the panels.

The shear forces in columns and beams are very small and are not evaluated here.

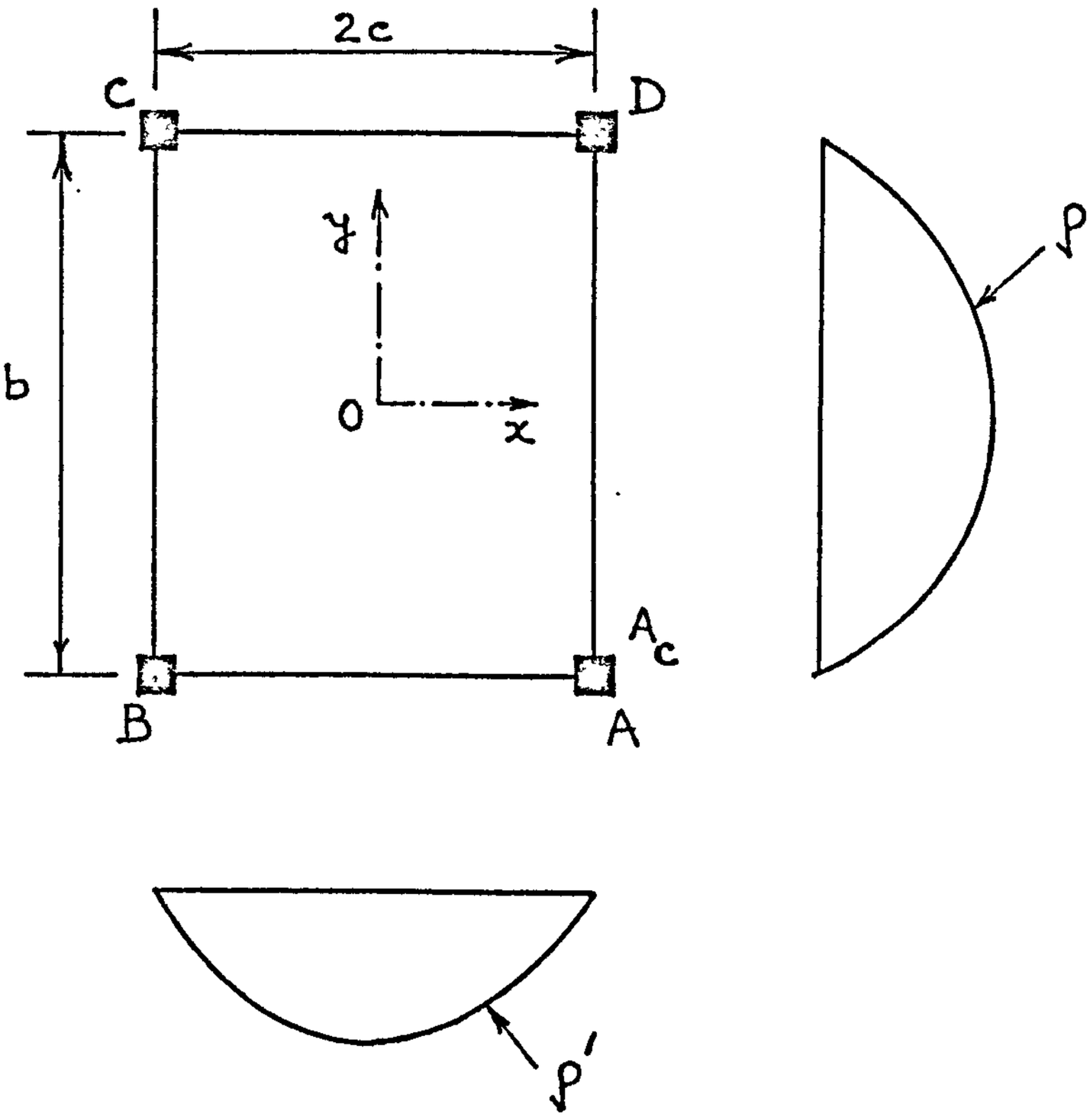

Fig. 7.1 Vertical forces due to floor load

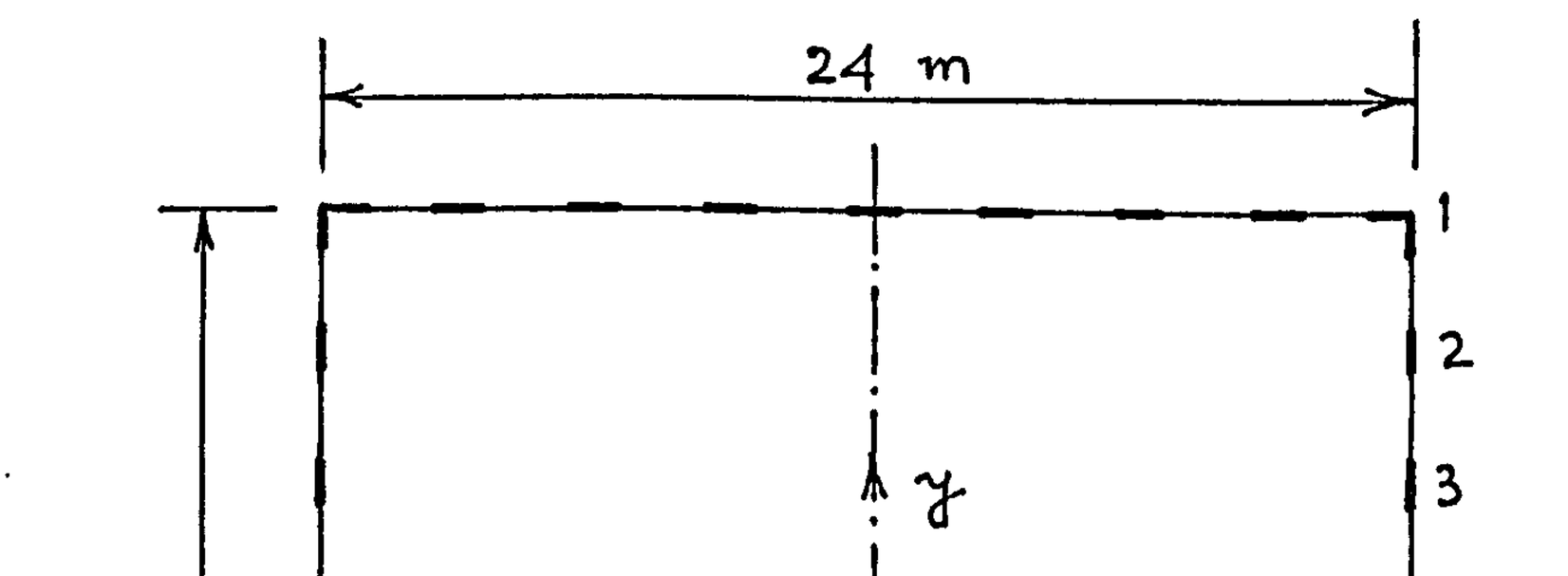

Fig. 7.2 Typical plan of a building

CHAPTER 8

EXPERIMENTAL INVESTIGATION

8.1 INTRODUCTION

In view of the limited number of published works regarding the structural behaviour of the framed-tube and bundled-tube type of structures, it was considered imperative to carry out experimental investigations in order to provide an understanding of their behaviour under lateral loads and torsional moments. The results of the various tests on the structural models were compared with the corresponding analytical solutions in order to assess the validity of the assumptions which were made in the derivation of the simple approximate methods of analysis.

In the earlier analyses of Chapter 6 it was found that the bundling of tubes improves the cantilever effectiveness of the structure by reducing the shear lag effects. It was decided to verify this improved behaviour of the bundled-tube structure over the framed-tube structure by suitable model tests.

A list of models tested is given below.

Model 1 : 15-storey, 28-column framed-tube structure of square cross-section.

Model 2 : Model 1 with strips glued to the corner columns.

Model 3 : 15-storey, 24-column framed-tube structure of rectangular cross-section.

Model 4 : Model 3 with an additional web frame glued to

form a bundled-tube structure with two modular tubes.

8.2 CHOICE OF MATERIAL

The selection of a suitable material for a structural model depends upon several requirements. The material must be such that the laws of similitude are satisfied and certain practical needs are met. The material must be easily available in a wide range of sizes, easily fabricated, easily cast into shape and relatively cheap and it must have reproducible mechanical properties and geometric stability. The most commonly used materials for constructing models are plastics, cementitious materials (plain and reinforced) and metals. Specific materials in each of these categories, and their properties, advantages and limitations were discussed by Roll[23] and Breen.[24]

For models designed to simulate the elastic response of the prototype, various plastics have proved to be extremely effective as model materials. Comprehensive studies of plastics suitable for models were made by Fialho.[25]

In addition to being easily available and relatively inexpensive, plastics possess various properties which make them suitable for model materials. They generally exhibit linear stress-strain relationship in the usual range of strains used in models, and the elastic moduli are low so that measurable strains and deflections are obtained without requiring large loads. Most plastics

can be considered to be isotropic and homogeneous. One important advantage of plastics is the ease with which models made from them can be fabricated and machined.

Some characteristics of plastics are disadvantageous and introduce some difficulties in interpretation of test results. For example, the mechanical properties of plastics may be affected by temperature, humidity, strain rate and duration of load. It is, therefore, essential that the testing of plastic models is conducted under controlled environmental conditions. A serious disadvantage of plastics is their low thermal conductivity. One method of handling this problem, when using electrical resistance strain gauges, is to simultaneously switch into the measuring circuit an active (measuring) gauge and a dummy (compensating) gauge. Another property that can lead to errors is the time-dependent strain, known as creep. It is common practice to allow a sufficiently long time to elapse between application of load and reading of gauges so that creep is essentially terminated and to use an asymptotic value of modulus of elasticity E for all gauges.

Of the available plastic materials Araldite and Perspex are the most widely used for shear wall and framed-tube models. Araldite is the more suitable of the two as it can be readily machined and exhibits negligible creep under low loads. It is, however, expensive and for complex models, where a large quantity of material is needed, the cost would be rather high. It was, therefore, decided to construct the models using the less expensive alternative, Perspex acrylic sheets. The properties of

Perspex are affected by changes of temperature and humidity, it creeps under load and is comparatively difficult to machine. Detailed properties of Perspex and the various cementing techniques have been given in I.C.I. Publications.[26,27] If experiments are carried out under controlled environmental conditions and necessary precautions are taken during testing, results of reasonable accuracy may be obtained from models using Perspex sheets.

8.3 MODEL CONSTRUCTION

The various panels of each model were cut by band saw to their approximate size from Perspex sheets of 5 mm thickness. The panels were then milled to their correct profile.

Openings in the panels were made by 4 mm diameter slot drill leaving the columns and beams of the required dimensions with 2 mm radius fillets at all intersections of columns and beams. The fillets help to avoid stress concentrations and the resultant cracks developing at beam-column connections. All the panels were cut with an extra length of material at the base for fixing to the base plate.

I.C.I. Tensol cement No. 7, which has properties similar to those of Perspex when cured, was used throughout the assembly of the models.

The rigid foundation required for each model was provided by cementing the extra length of each framed panel into slots cut in a 25 mm thick Perspex base plate. The

panels were held perpendicular to the base plate and at the correct level while the slots were completely filled with cement and until the cement had hardened sufficiently.

The models were numbered in the order in which they were tested and their dimensions are given in Figs. 8.1 to 8.4. Models under test are illustrated in Figs. 8.5 to 8.8.

For models 1 and 2, 3 mm thick diaphragms with a number of holes were glued at the free end and also at the eighth floor level. 3 mm thick rectangular pieces with central openings to fit the model were used in models 3 and 4. These diaphragms were used to maintain the shape of the models. The holes in the diaphragm prevent any coupling action between the columns except through the spandrel beams.

To minimise the cost of the experimental work, the models were constructed in stages, each completed stage tested fully before the addition of some component part required for the next model. Thus model 2 was built by cementing additional strips to the corner columns of model 1. Model 3 was built with a slot all through the central column of each of the flange panels to accommodate an additional web panel to form model 4.

The cementing of the various components of the model was done in stages so that the strains induced by shrinkage of the cement after setting would remain as low as possible. At least a week after the final construction of the model, the experimental investigation was started.

8.4 TEST FRAME

The test frame consisted of a pair of vertical mounting units set up parallel to each other at some distance apart and interconnected by horizontal and inclined bracings to form a stiff self supporting box frame. Since the model was set up inside the box, it was protected from accidental damage and disturbance (Figs. 8.5 to 8.8).

Each mounting unit consisted of two $\frac{1}{2}$" (12.7 mm) thick by 6" (152.4 mm) wide steel plates, provided with a regular array of holes for use in fixing the models to the test frame. The ends of each plate were welded to the vertical legs which consisted of 3" x $1\frac{1}{2}$" (76.2 mm x 38.1mm) steel channels welded to 6" x 5" (152.4 mm x 127.0) rectangular base plates. The bracings consisted of 2" x 1" (50.8 mm x 25.4 mm) rectangular hollow sections with welded end plates which were bolted to the vertical legs. There was a third unit similar to the two mounting units and placed one metre distant from the nearer mounting unit to form the complete box and give the test frame its stability.

The base plate of the model was positioned on the mounting unit and fixed by four $\frac{3}{4}$" (19.05 mm) diameter bolts through the base plate. Extra $\frac{1}{2}$" (12.7 mm) thick plates and 2" x 1" (50.8 mm and 25.4 mm) hollow tube lengths were used to clamp the base and minimise the rotation of the base. The correct positioning of the model was carried out by means of a spirit level and plumb line before the start of the test.

8.5 MEASURING DEVICES

8.5.1 DEFLECTION MEASUREMENT

The deflections were measured by "John Bull" dial gauges, manufactured by British Indicators Limited. To measure the deflections of the model under test the gauges were supported on a framework bolted to the test frame. The gauges were positioned directly above the two side frames of the model at every third floor level. At the second floor level additional gauges were positioned. The gauges used were generally type 2U which were very sensitive and could read 0.002 mm per division of the dial with a maximum travel of 12 mm. Near the free end of the model, where the deflection is large, gauges of type 2S with a sensitivity of 0.01 mm per division and a travel of 25 mm were used. Gauges of type 2U, supported by magnetic stands, were used to detect any deformation of the Perspex base plate.

8.5.2 STRAIN MEASUREMENT

The strains induced in the model due to the applied loads were measured by electrical resistance strain gauges. The gauges were glued to the columns at positions midway between the second and the third floors. The position of the gauges was selected close to the base to give measurable strains but not too close to be affected by any local effects caused by the base to frame connection. The location of the gauges also helped to avoid any local effect caused by beam-column interaction.

The strain gauges, Japanese type PL-10, and the terminal strips for the wire leads were glued to the Perspex model by M Bond 200 adhesive. All strain gauges were insulated against small changes in temperature and humidity by a coat of M-coat A. The resistance of each gauge was checked by the Solartron 4440 Digital Multimeter for any fault in the gauge or the connection.

The strain gauges were wired to Baldwin-Lima-Hamilton BLH Model 220 Switching units which in turn were connected to Baldwin-Lima-Hamilton BLH Type 20 Strain indicator. The dummy gauges were provided by a Perspex model not under test which had the same thickness and was fitted with identical strain gauges to the model under test.

The model 220 Switching unit provides a means of monitoring 10 strain gauge outputs in succession on one strain indicator. When monitoring of more than 10 strain gauge outputs is necessary, two or more switching units can be stacked and their output terminals connected in parallel to the indicating instrument. Each gauge and its compensator were wired to one channel of the 10-channel Switching unit.

The BLH Portable type 20 Strain indicator was used with a self contained battery power pack for measuring strains. It used a manually operated null-balance system with digital readout for fast accurate reading. The indicator had a total range of 0 to $\pm$ 30,000 microinches per inch and could read strains as low as 5 microinches per inch.

8.6 TEST PROCEDURE

The model was bolted to the test frame and the correct positioning of the model was checked by means of a spirit level and plumb line. Uniform lateral load was simulated by applying point loads at each of the two side frames at every alternate floor level. For combined bending and torsion the loads were applied at one of the side frames at every alternate floor level. The loads were placed on light hangers which were suspended by terylene threads. The load applied at the free end of the model was half the loads at other points.

With no weights on the hangers the readings for each strain gauge and dial gauge were recorded. The load was applied at every alternate floor level in increments of 4 kgf for model 1 and 2, 1 kgf for model 3 and 1.6 kgf for model 4. The loads were placed on the hangers with the utmost care to avoid any impact effect. A time interval of 10 minutes was allowed after the addition of each load increment before the readings were taken to permit the gauges to settle to reasonably stable values. Deflections and strain readings were recorded for four increments.

After the application of the maximum load the model was unloaded by equal decrements and a separate set of readings were recorded. The mean of the results obtained from loading and unloading was used.

After the model was completely unloaded at least an interval of 24 hours was allowed before starting new

experiments with the same model.

Model no. 1 was tested in one position, then rotated through 180^{o} and was retested.

Each test was carried out at least three times and the best of the results was used.

8.7 DETERMINATION OF MODULUS OF ELASTICITY

In order to evaluate the stresses induced in the models from the strain gauge readings and to determine the deflection using the theoretical analysis the modulus of elasticity of Perspex was evaluated.

The specimens for the test, 5 mm x 50 mm x 300 mm, were cut from the same sheets of Perspex as were used to make the models. An electrical resistance strain gauge, as used in the models, was fixed longitudinally on one face near the mid point of each of the specimens. The exact width and thickness of the specimen in the region near the gauge were measured by means of a vernier and a micrometer respectively.

The specimen was tested in bending, between level supports, 240 mm apart with equal loads at the third points of the span to induce constant bending and no shear in the region of the strain gauge. During a test on one specimen the strain gauge of the other specimen of the same thickness was used as a dummy gauge. A dial gauge was used to measure the deflection of the specimen at the centre of the span.

The specimen was loaded gradually by small increments of 200 gf and the readings of dial gauge and

strain gauge were recorded. After four increments the specimen was gradually unloaded. The specimen was tested twice, once with the strain gauge on the upper face and then with the strain gauge on the lower face.

From the results of the test the load-deflection and load-strain graphs were plotted. The best straight line in each case was drawn by eye and the value of the modulus of elasticity was evaluated.

The average values of Young's modulus for the specimens, based on deflection and strain results, are given in Table 8.1.

8.8 EVALUATION OF STRAINS AND DEFLECTIONS

From the test results the readings recorded from any gauge were plotted to scale against the load increments and the best straight line through the points was drawn. The slope of the line was determined in each set of readings to obtain the strain or deflection per unit load (N/mm) for that gauge.

The stress distribution in columns at the middle of the third storey, and the deflections at different storey levels for the four models were plotted as shown in Figs. 8.9 to 8.24.

Specimen	E in N/mm^2 based on deflection results	E in N/mm^2 based on strain results
1	2857.3	3138.1
2	2857.3	3074.2

Table 8.1 Young's modulus of Perspex used for models

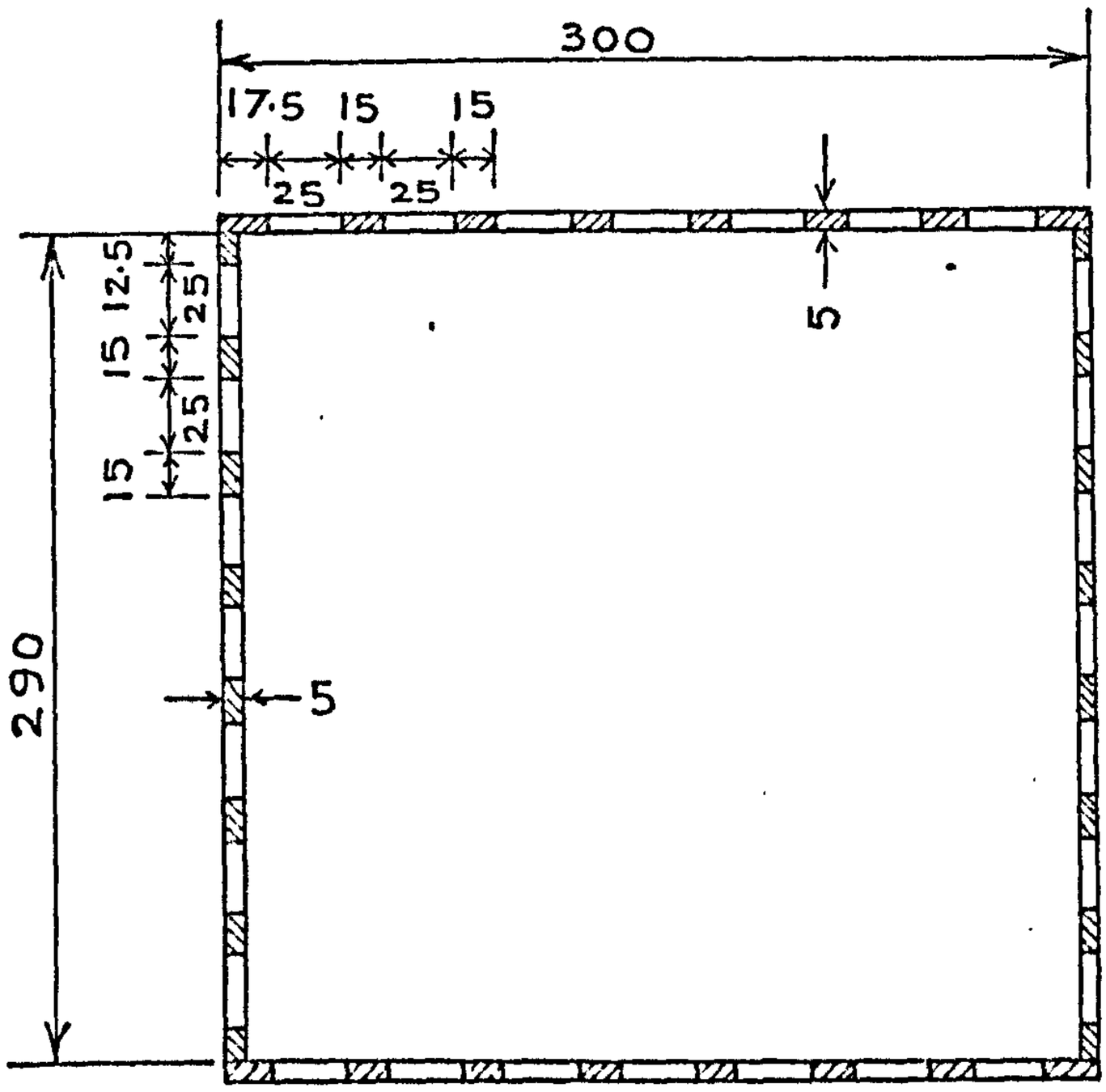

(a) Plan of Framed-Tube structure

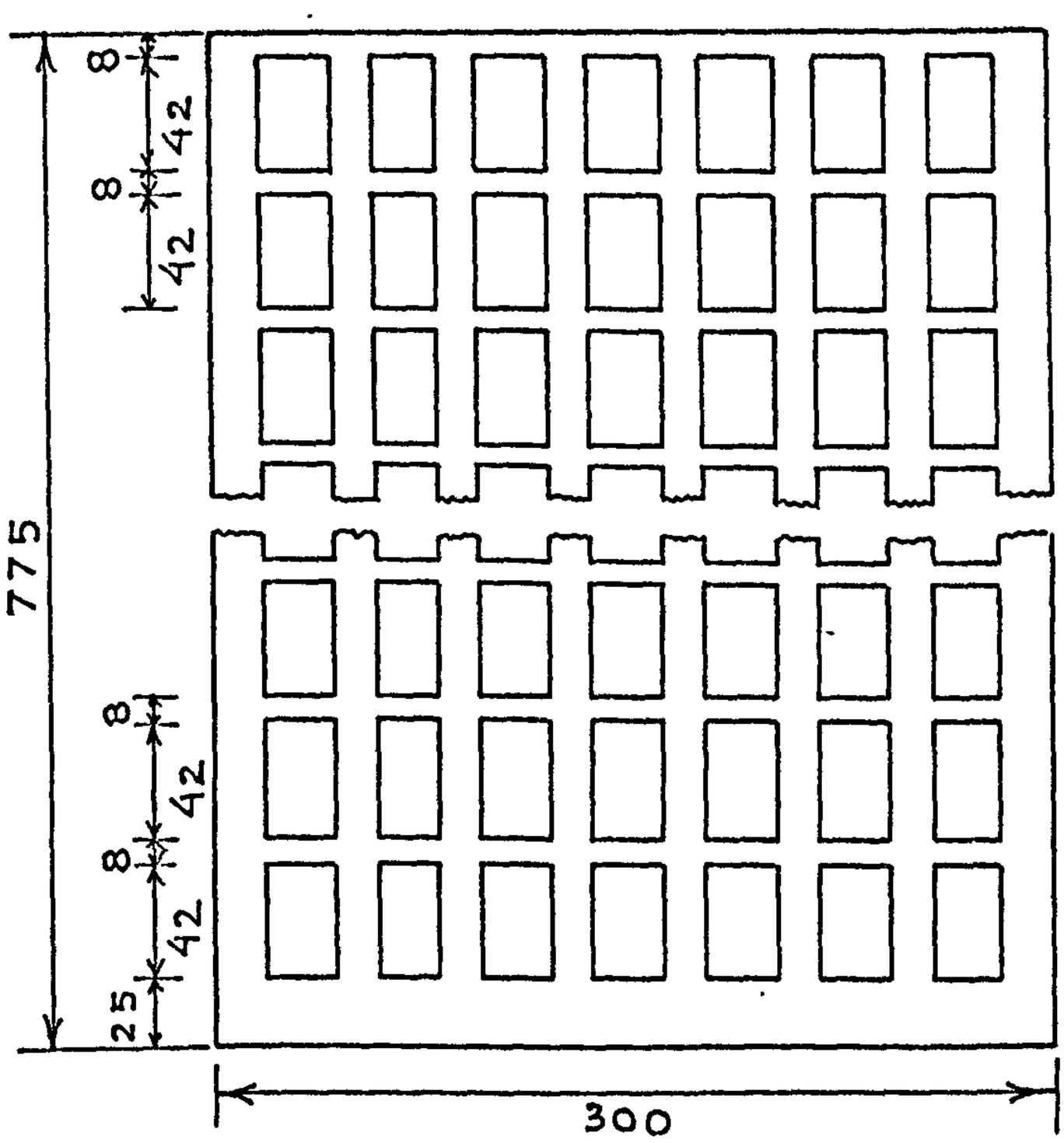

(b) Elevation of Framed-Tube Structure

(All dimensions in mm)

Fig. 8.1 Model 1

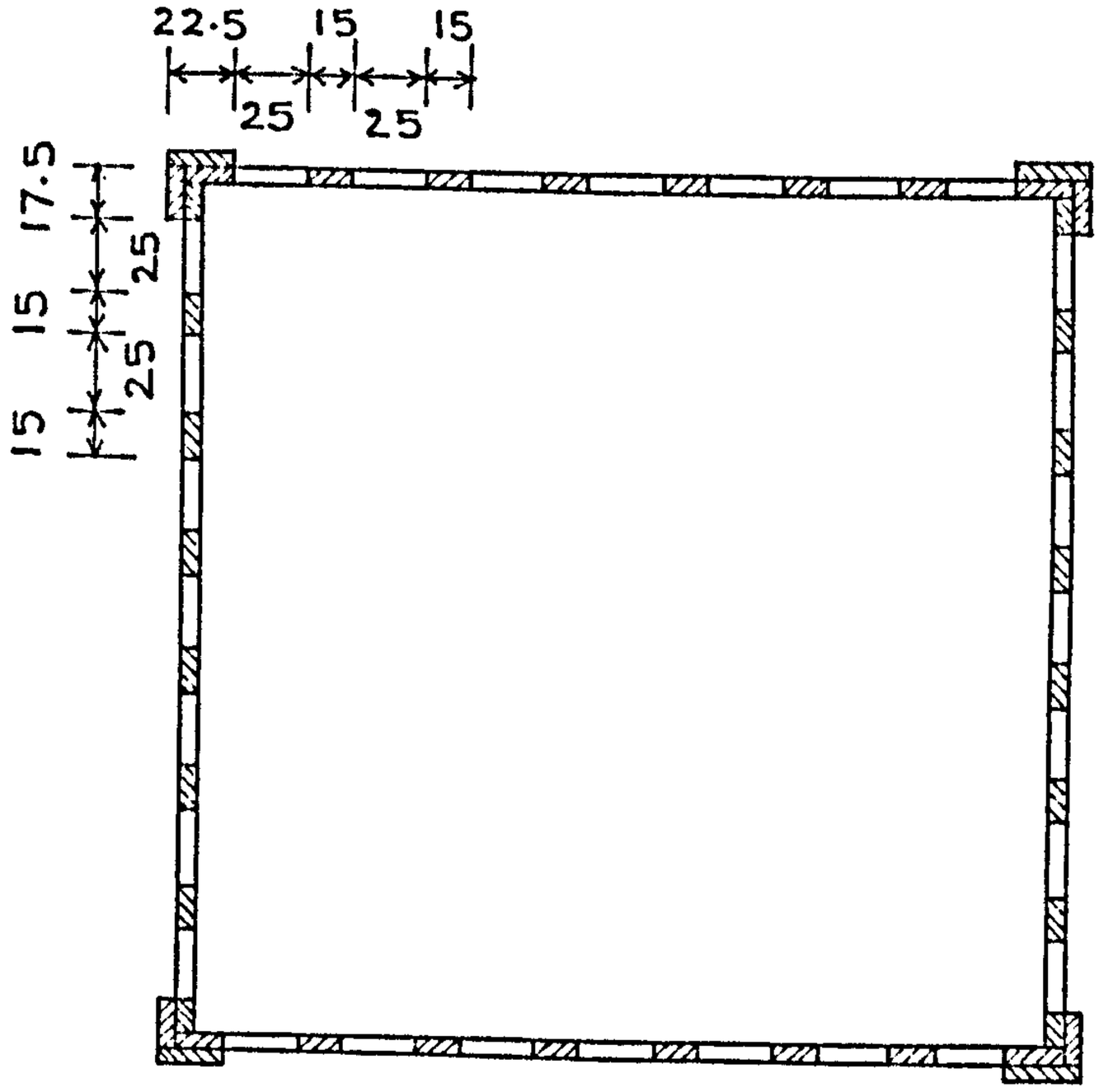

(All dimensions in mm)

Fig. 8.2 Plan of Model-2

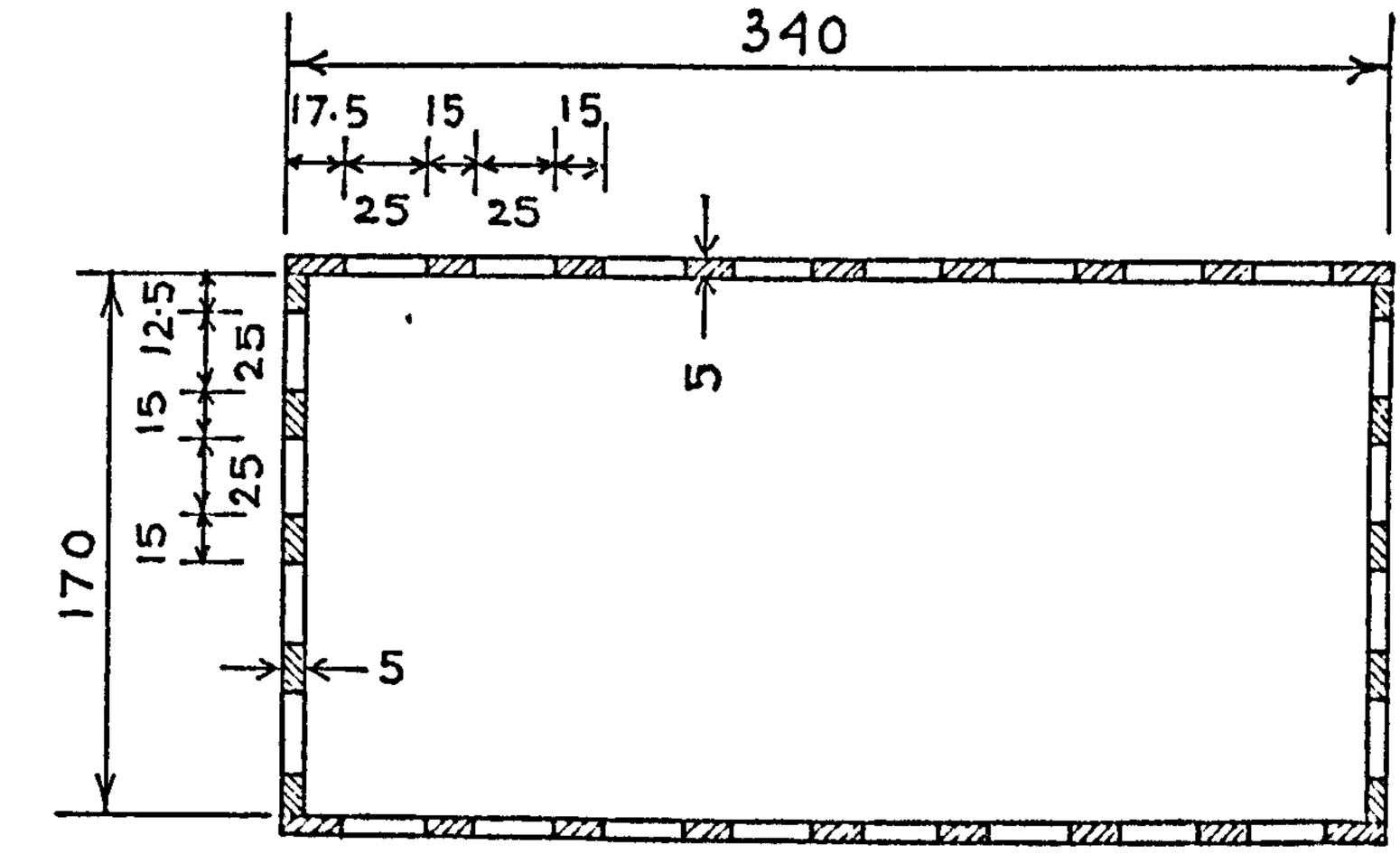

(a) Plan of Framed-Tube Structure

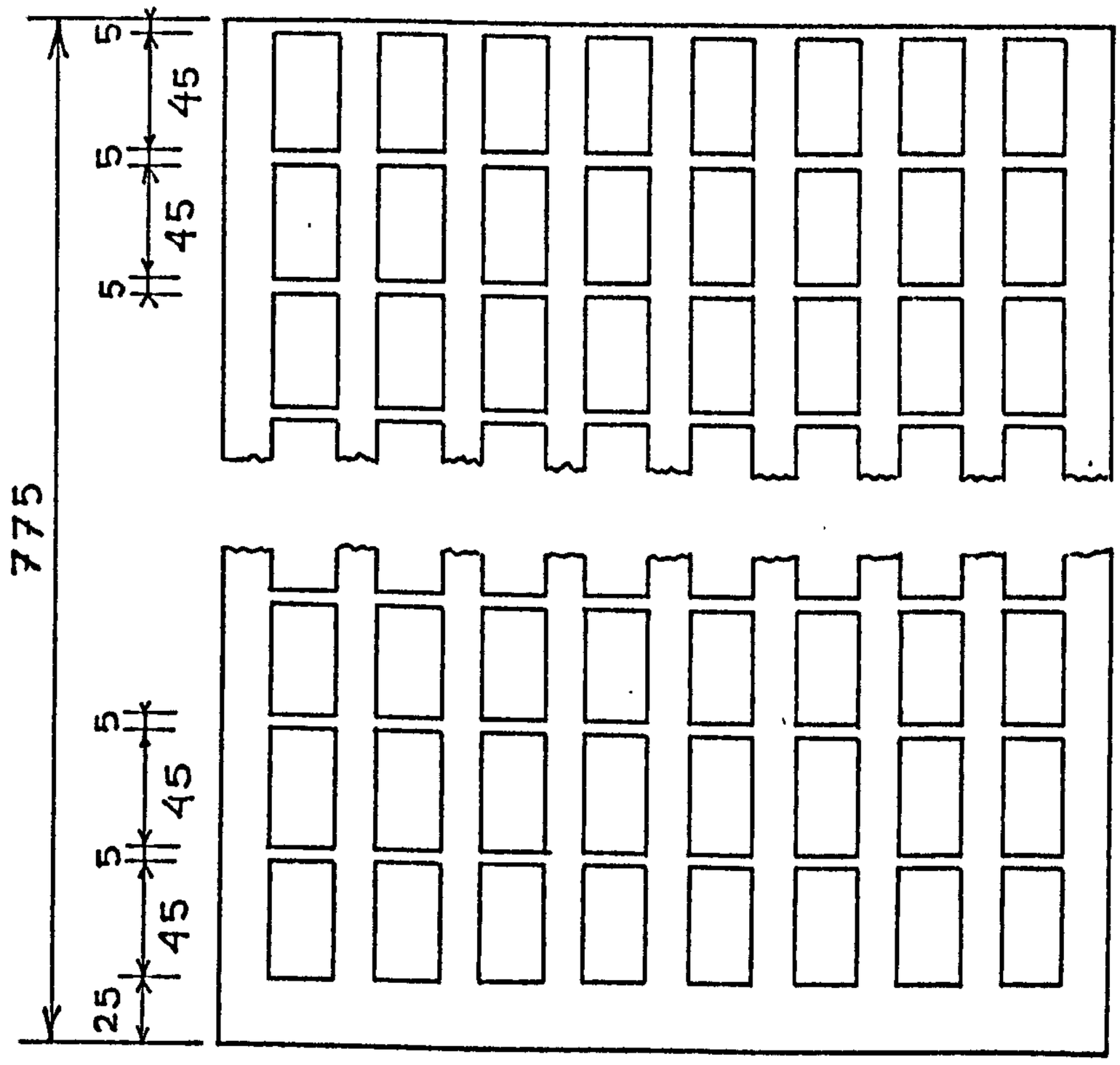

(b) Elevation of Framed-Tube Structure
(All dimensions in mm)

Fig. 8.3 Model 3

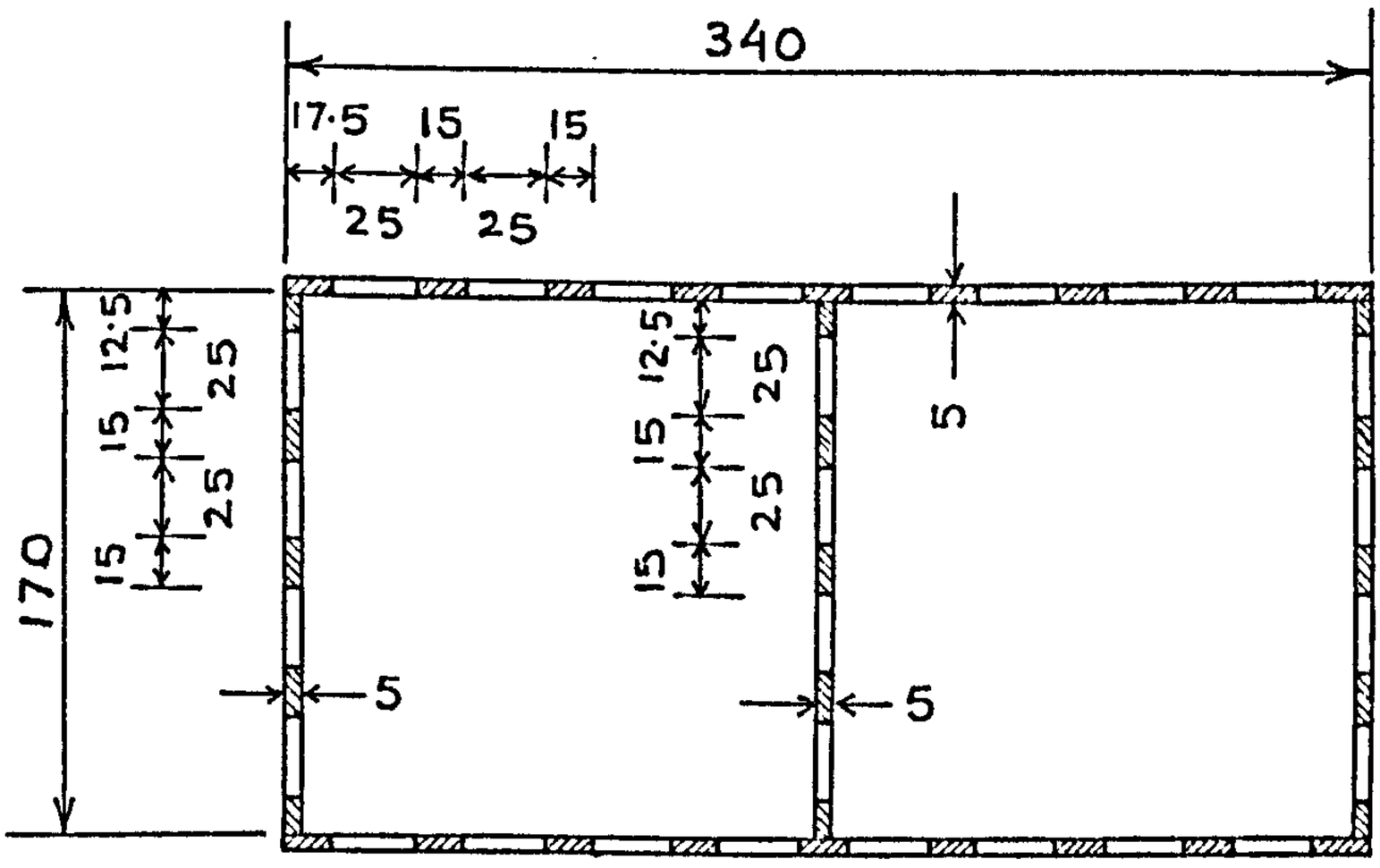

(All dimensions in mm)

Fig. 8.4 Plan of Model 4

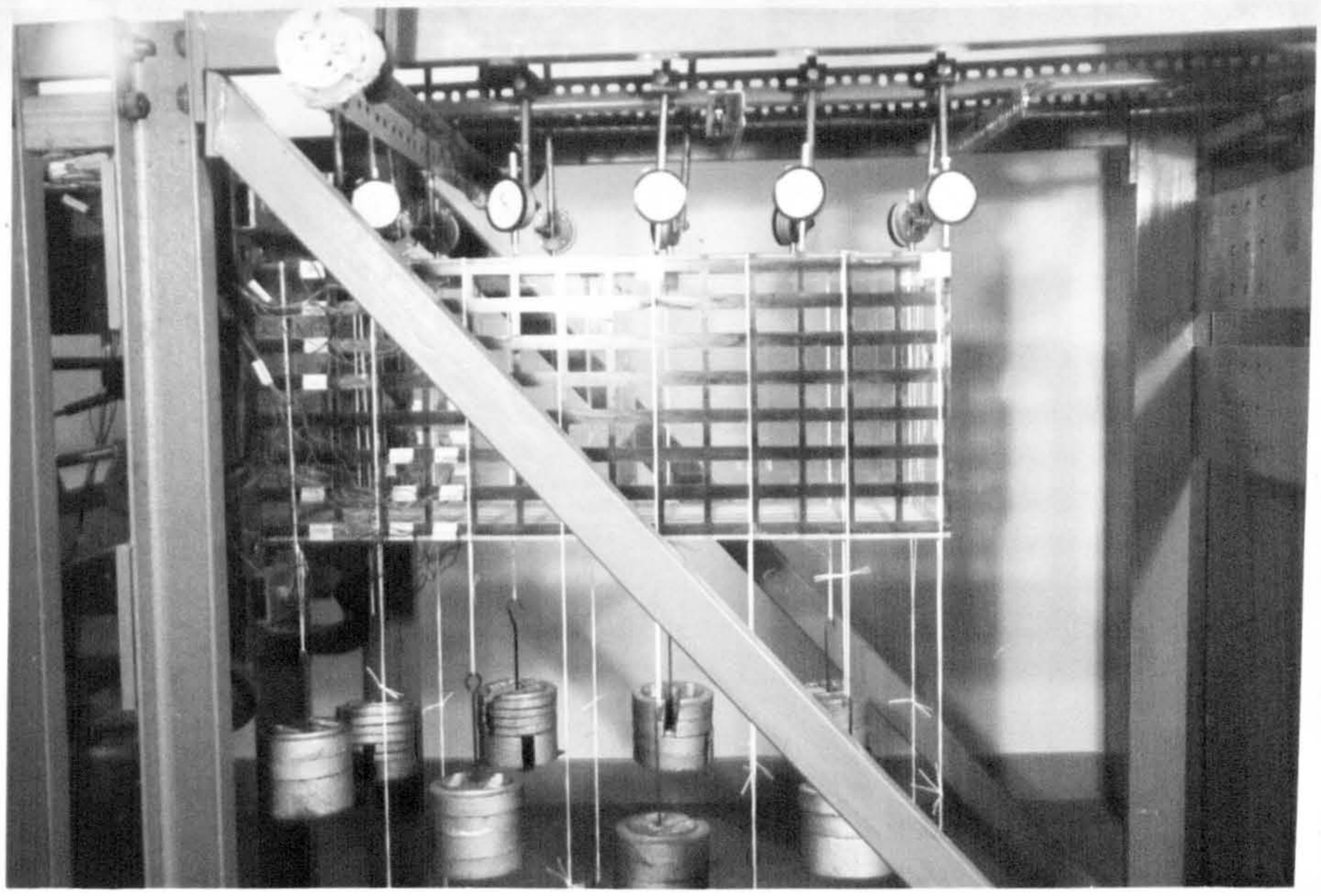

Fig. 8.5 Framed-tube model showing fixing arrangement at the base

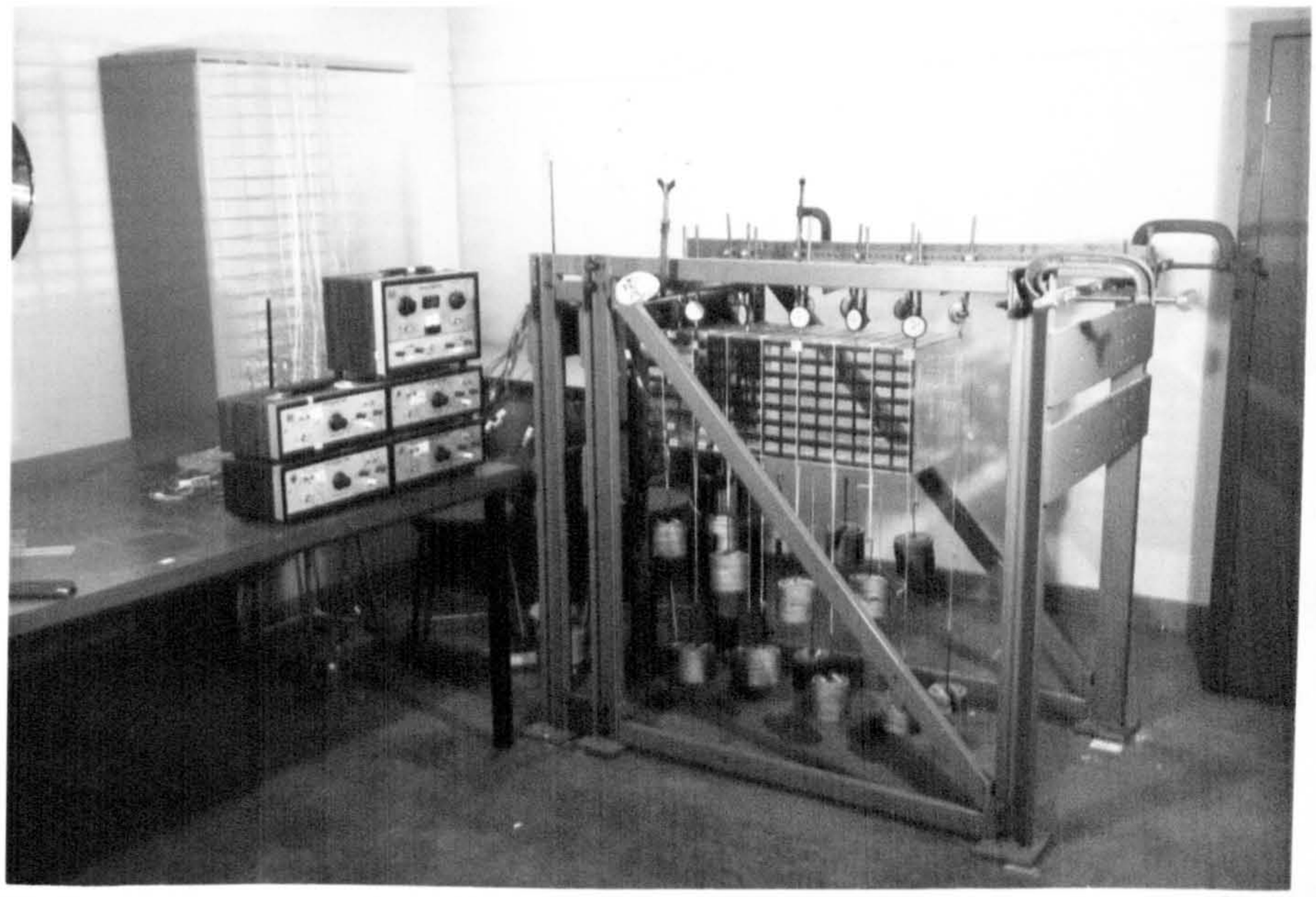

Fig. 8.6 Framed-tube model showing measuring devices and compensating gauges

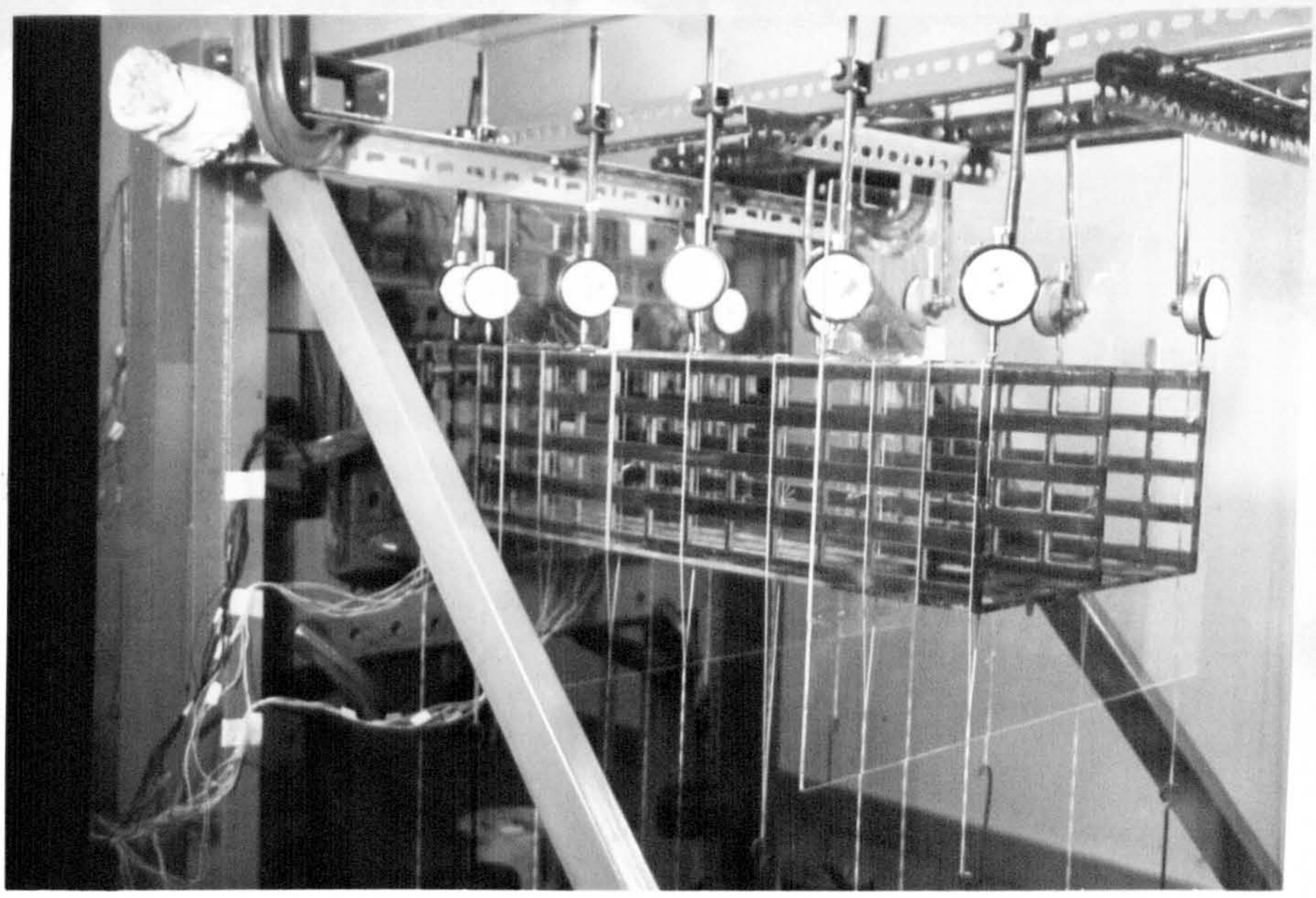

Fig. 8.7 Bundled-tube model showing fixing arrangement at the base

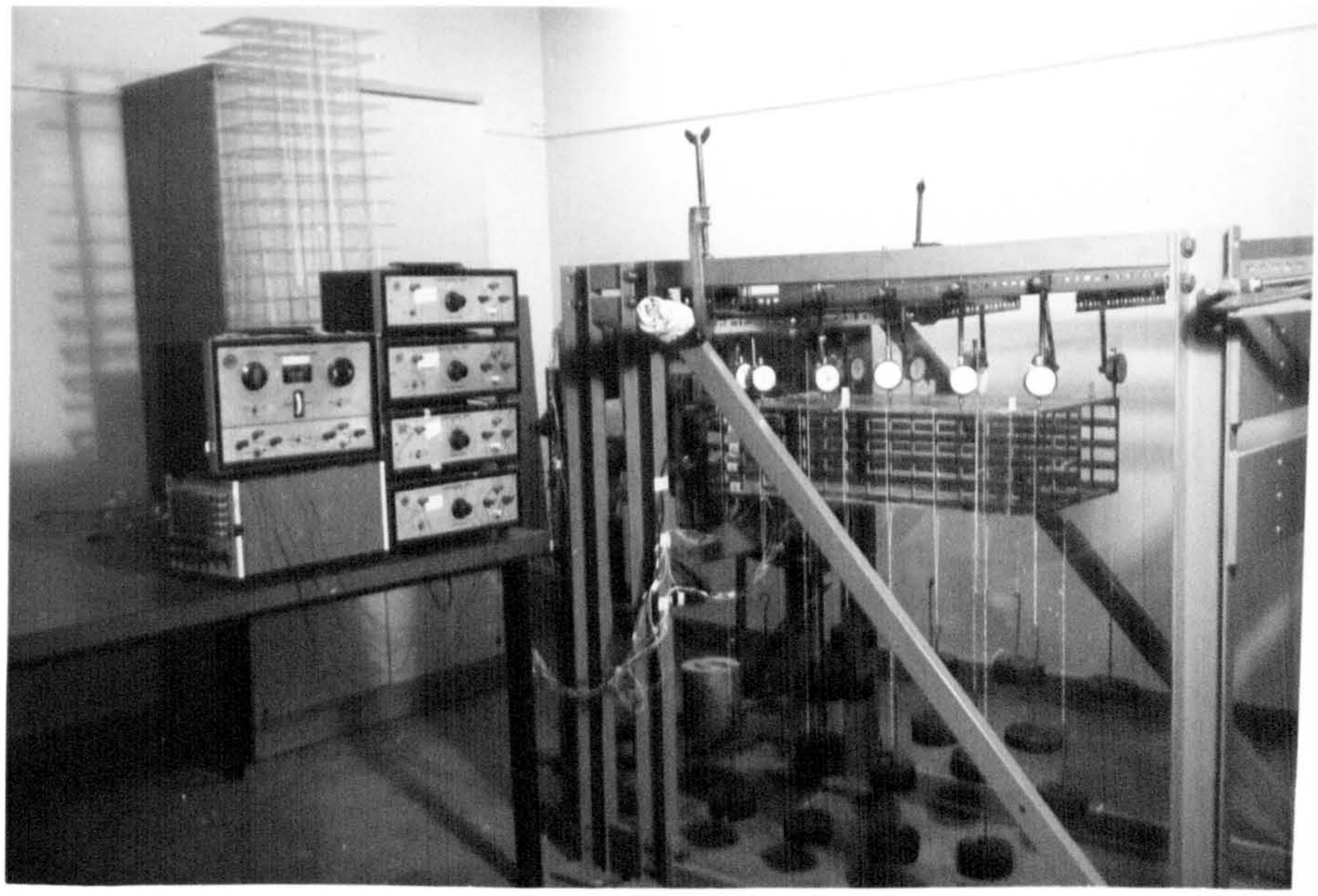

Fig. 8.8 Bundled-tube model showing measuring devices and compensating gauges

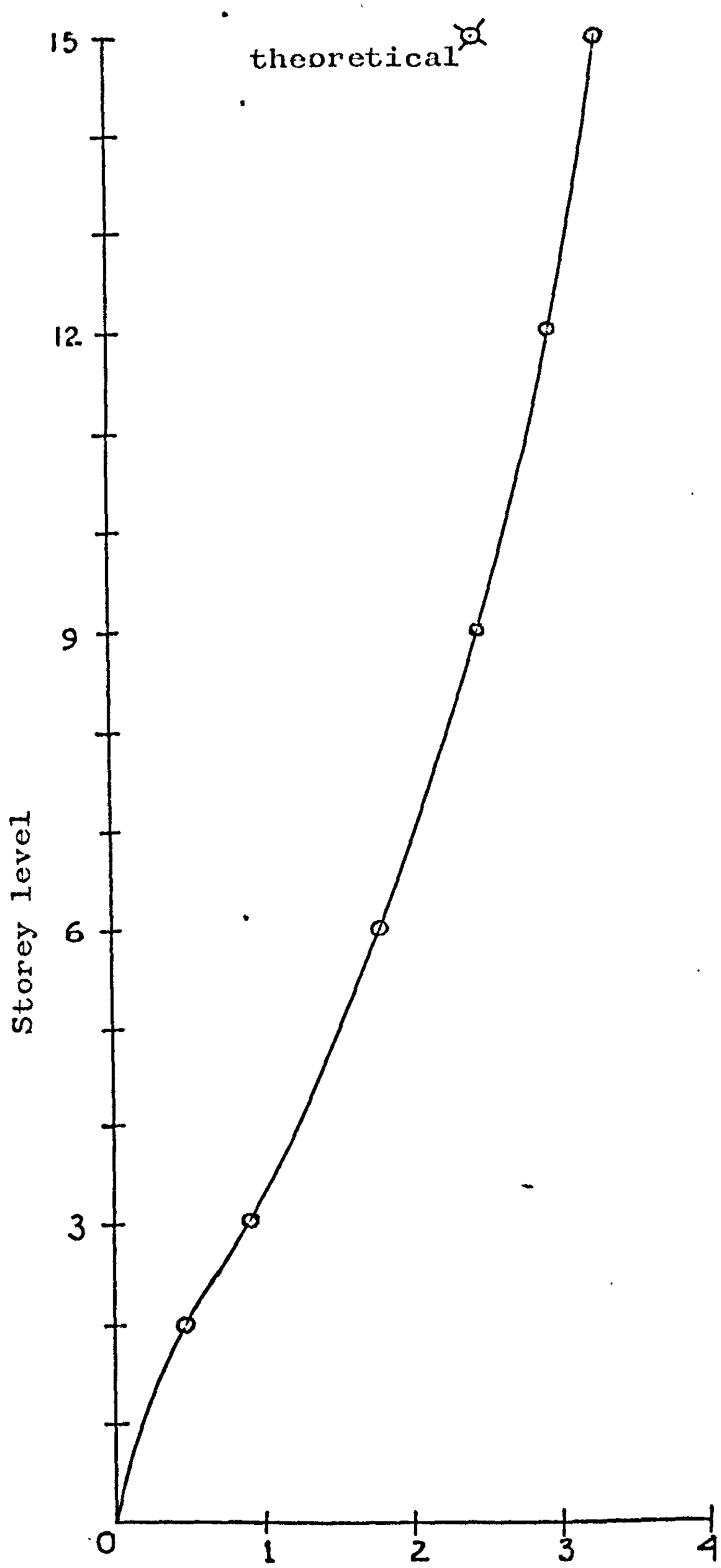

Fig. 8.9 Deflection profile
Model 1, Bending Test

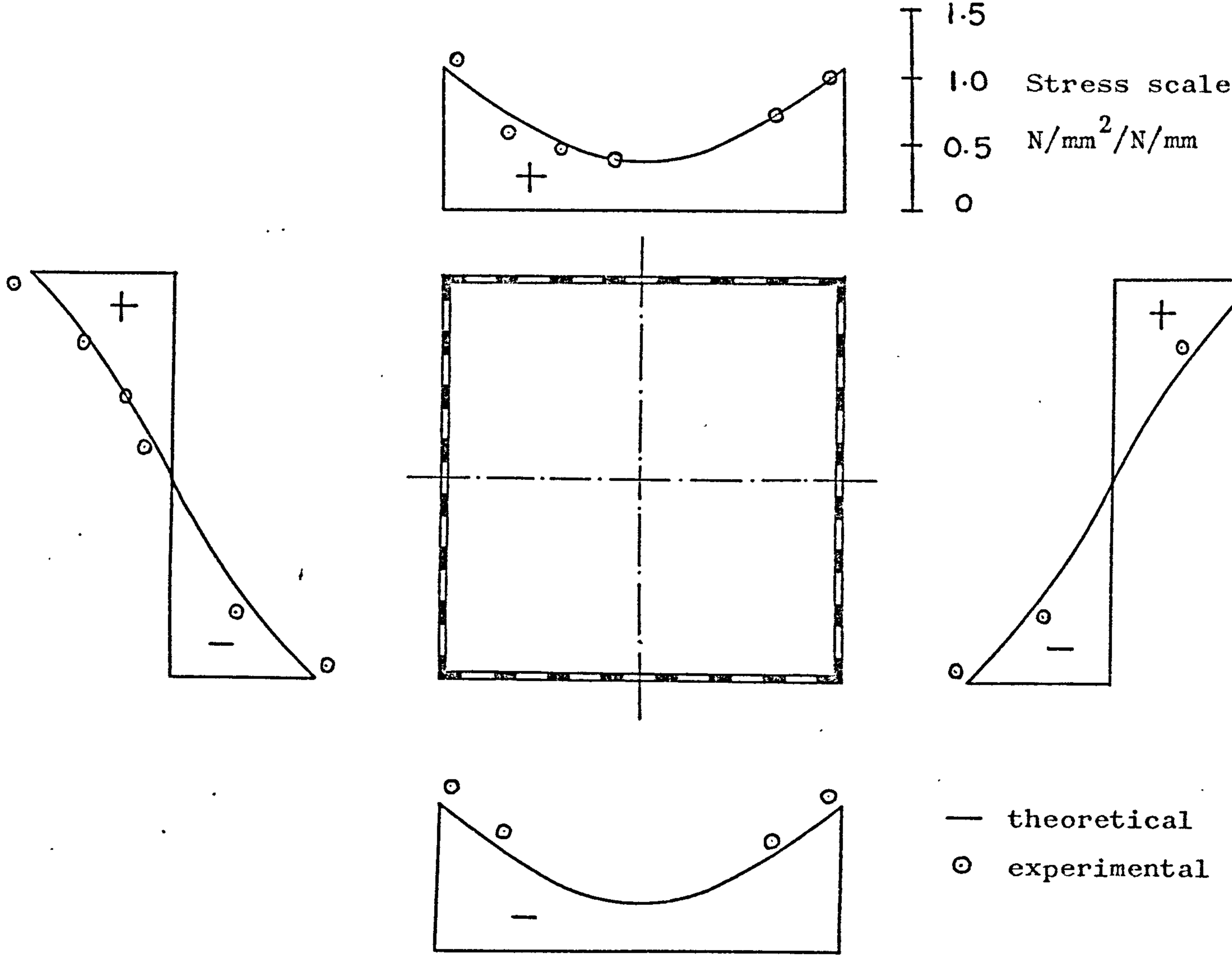

Fig. 8.10 Stress distribution, Model 1, Bending test

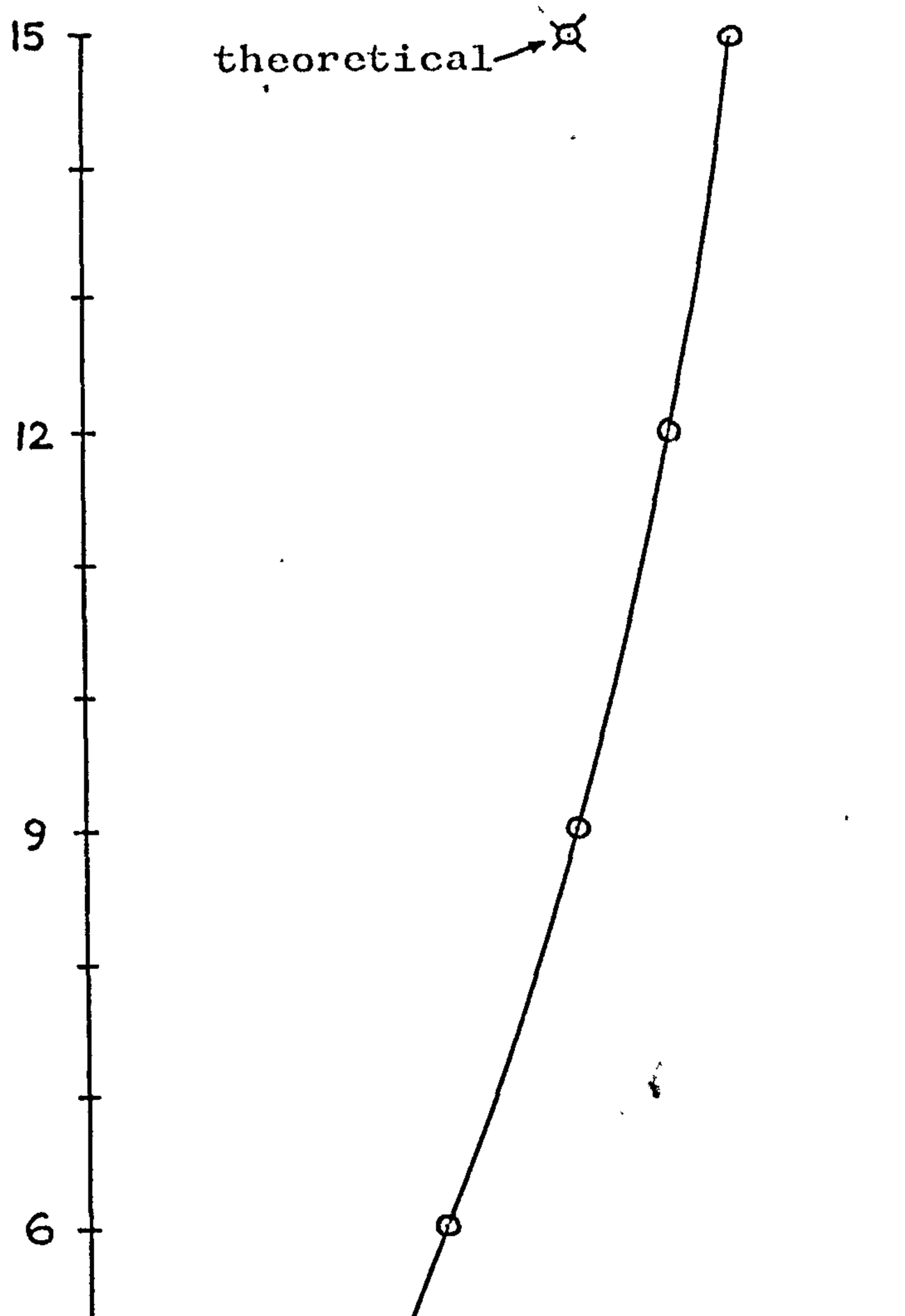

Fig. 8.11 Deflection profile
Model 1, Bending test
(model turned 180°)

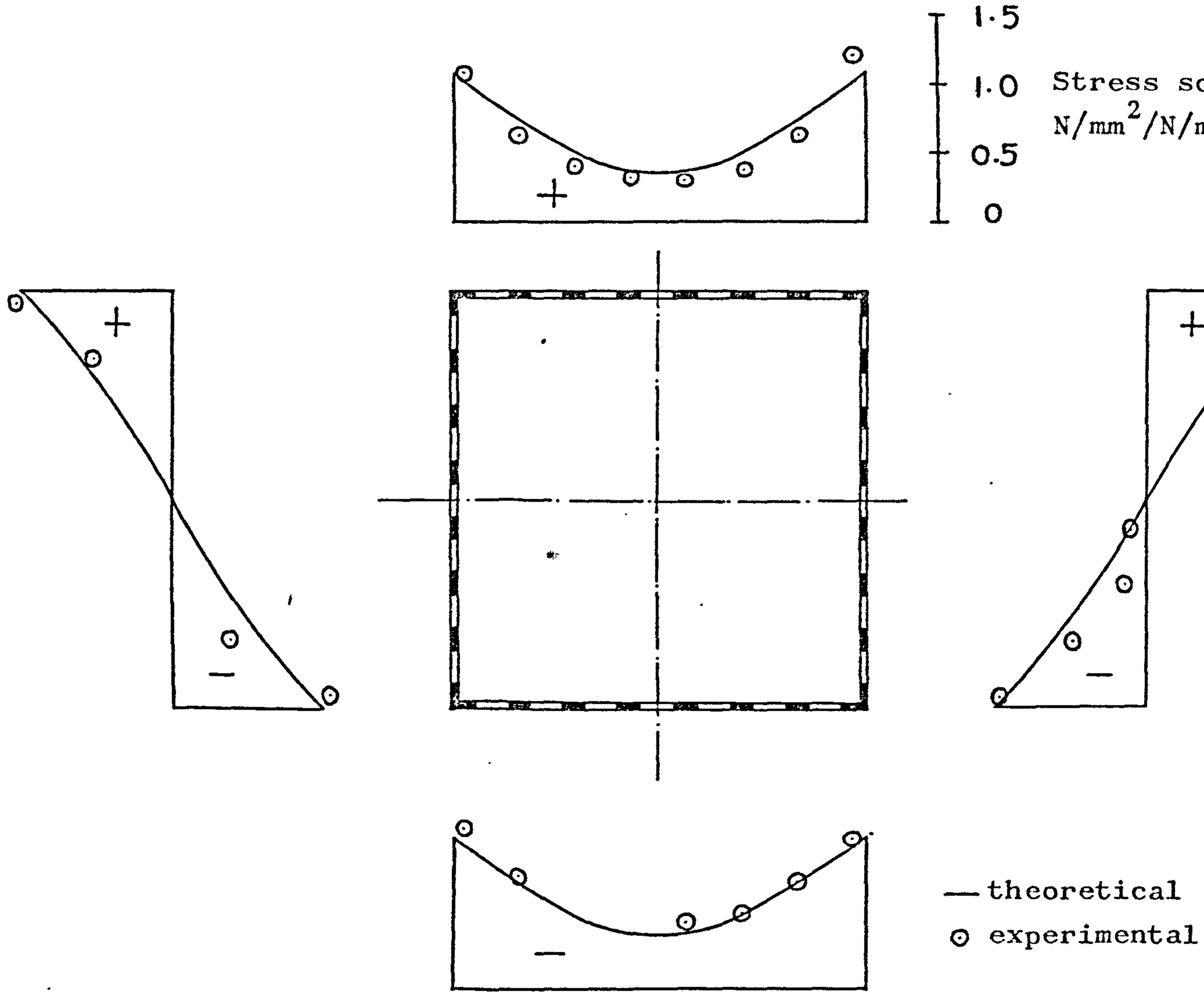

Fig. 8.12 Stress distribution, Model 1, Bending test (model turned 180°)

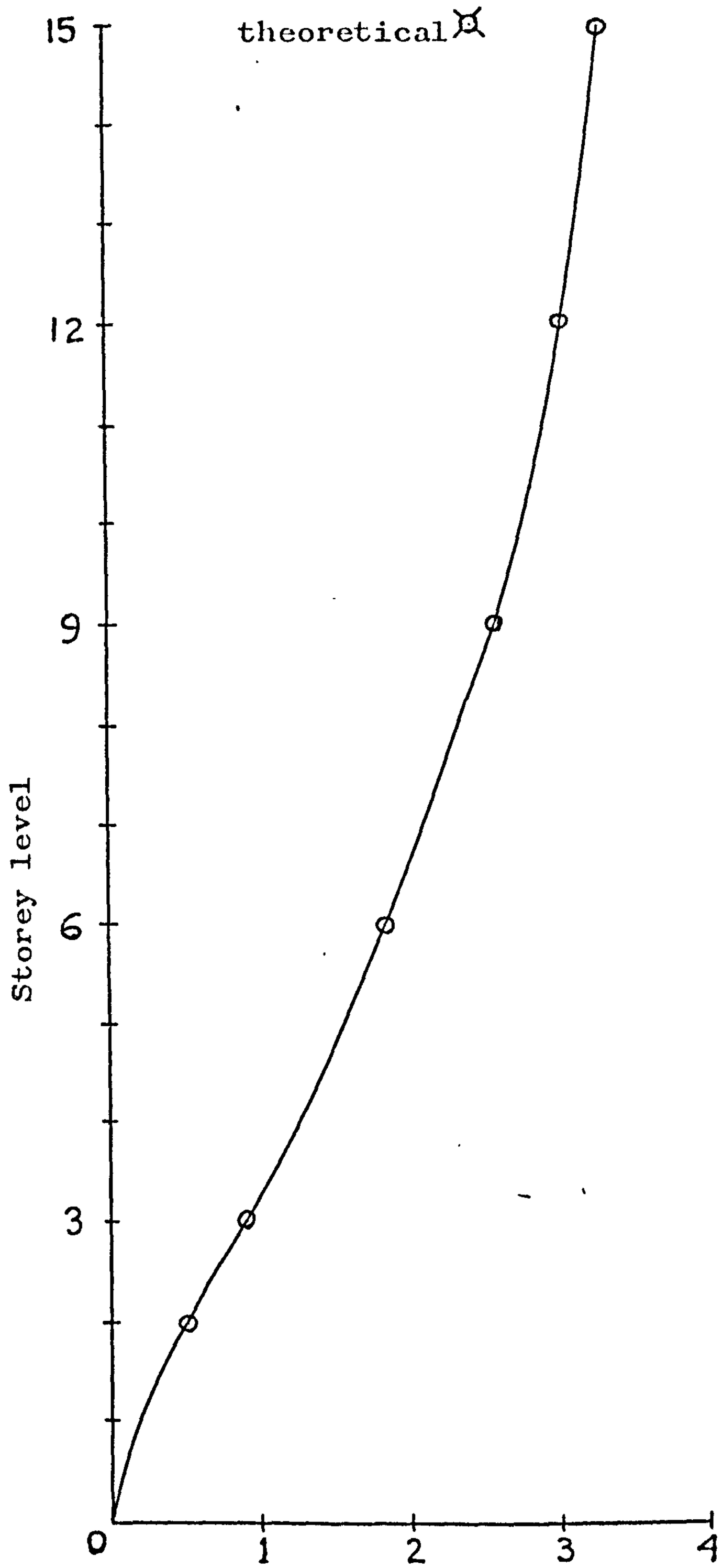

Fig. 8.13 Deflection profile
Model 1, Combined bending & torsion

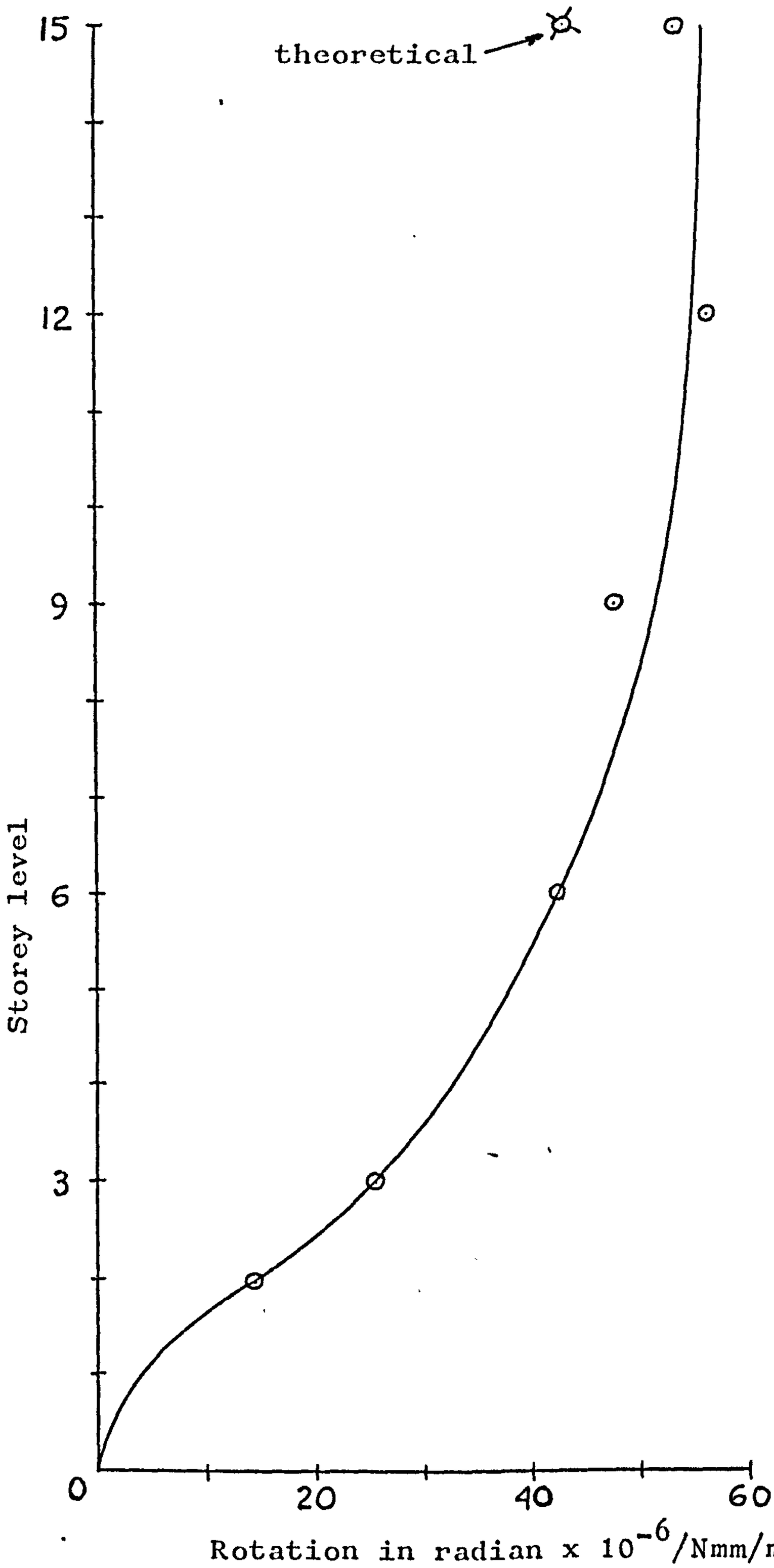

Fig. 8.14 Rotation profile
Model 1, Combined bending & torsion

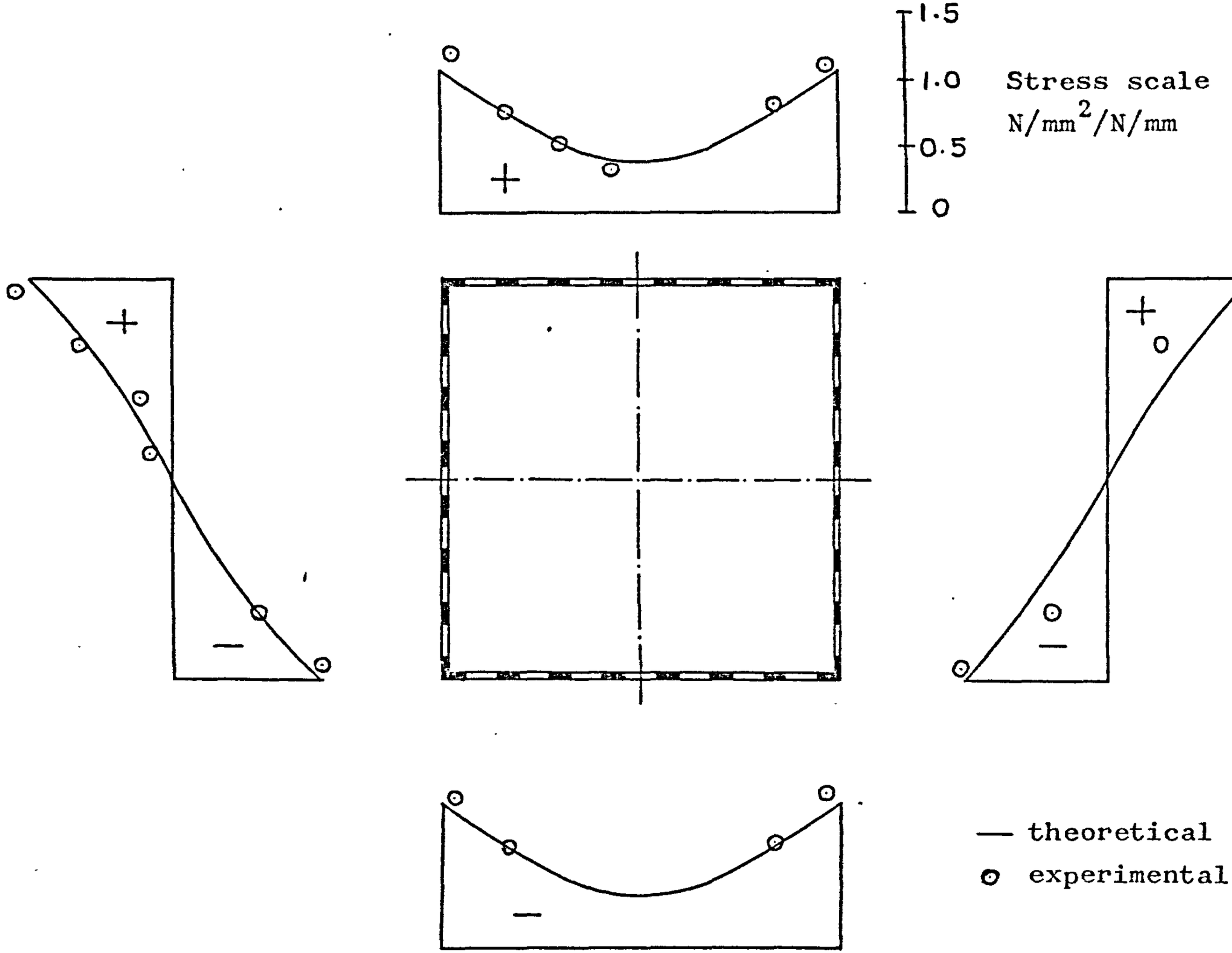

Fig. 8.15 Stress distribution, Model 1, Combined bending & torsion

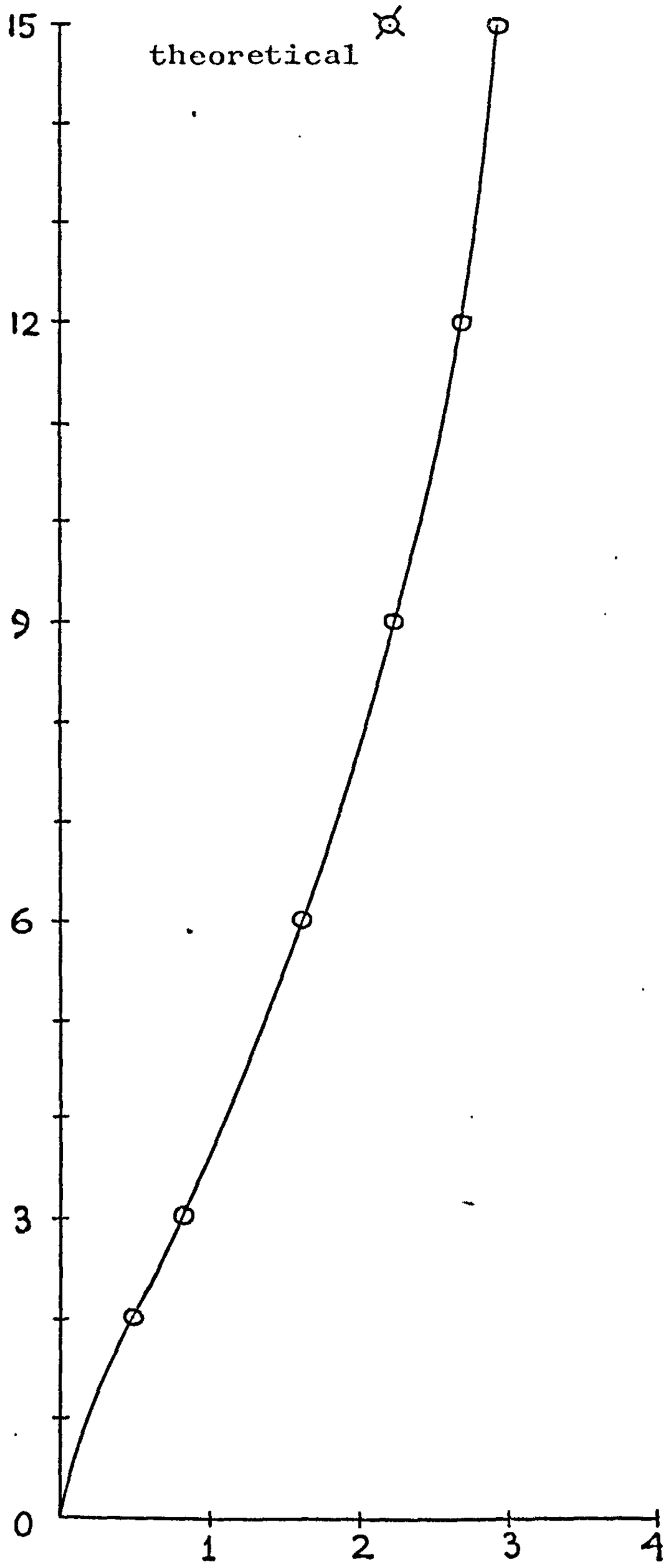

Fig. 8.16 Deflection profile
Model 2, Bending test

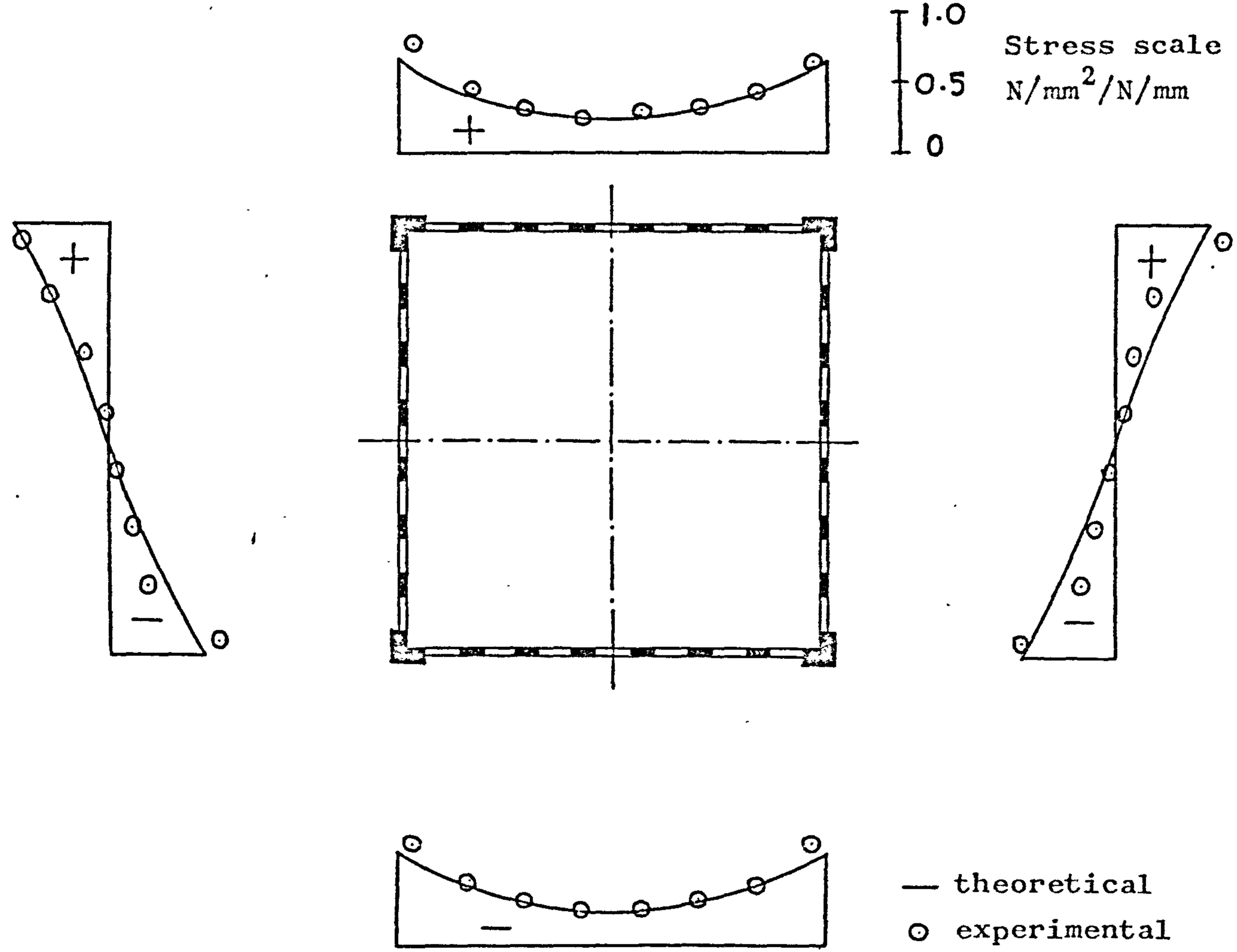

Fig. 8.17 Stress distribution, Model 2, Bending test

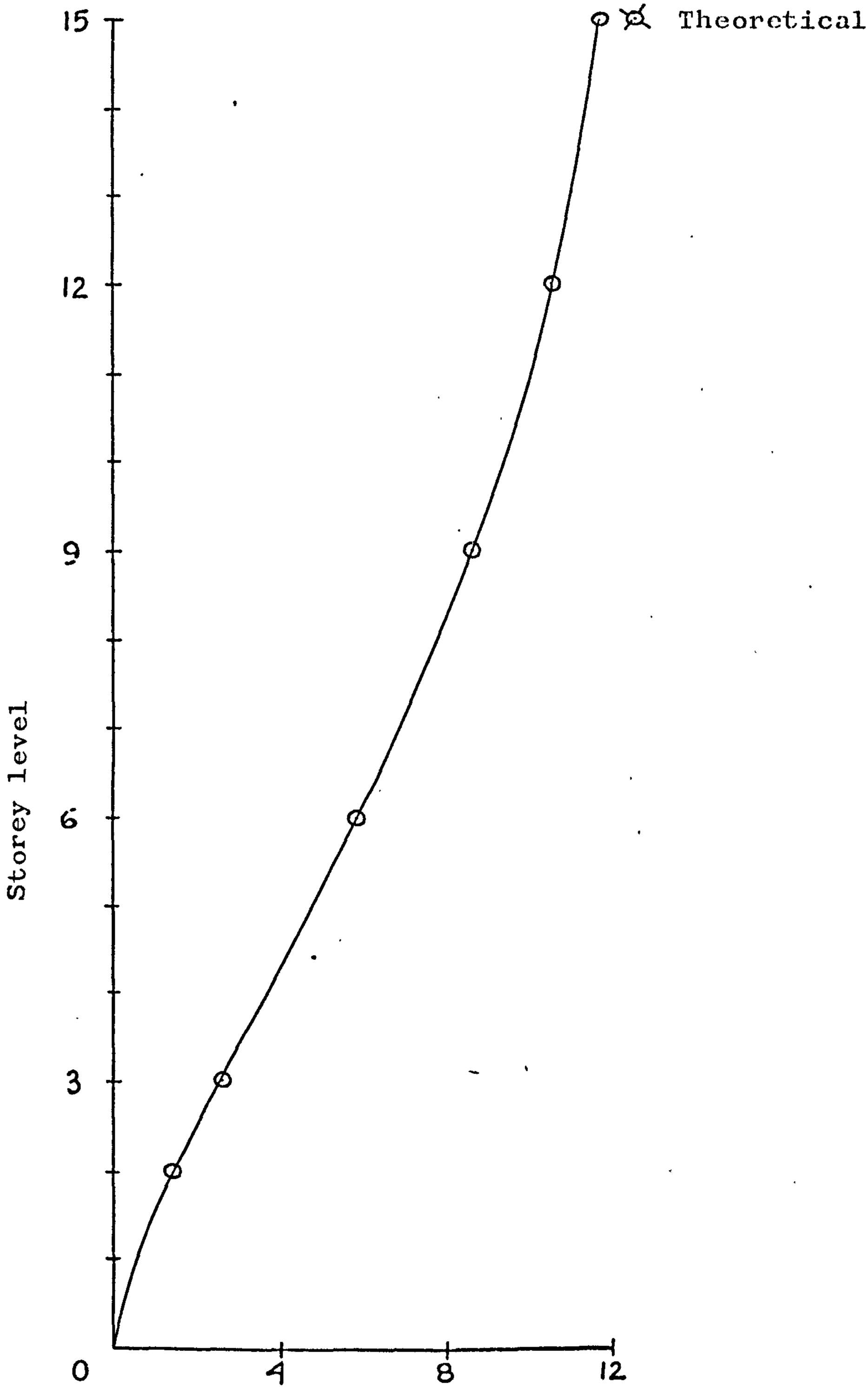

Fig. 8.18 Deflection profile
Model 3, Bending test

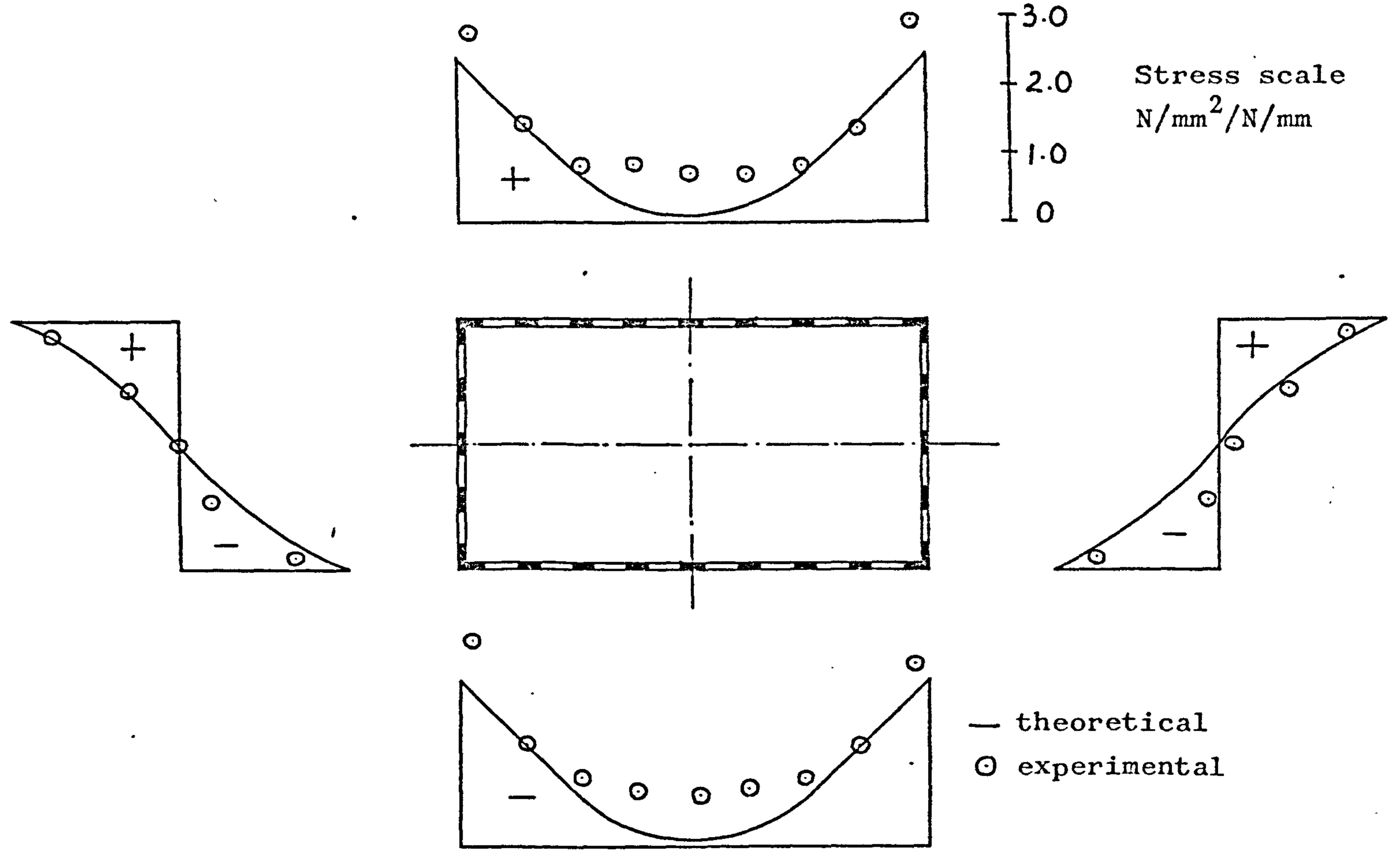

Fig. 8.19 Stress distribution, Model 3, Bending test

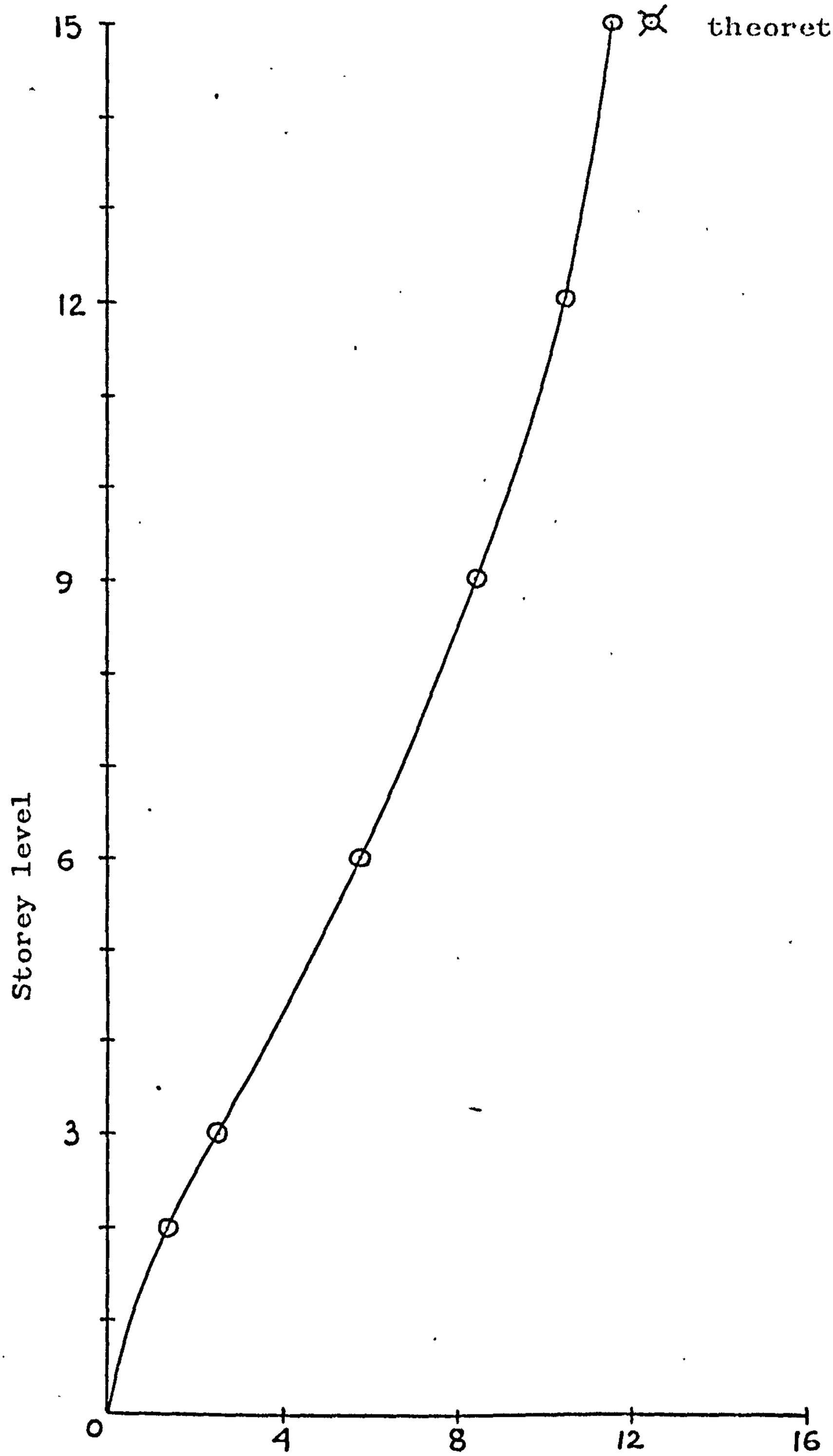

Fig. 8.20 Deflection profile
Model 3, Combined bending & torsion

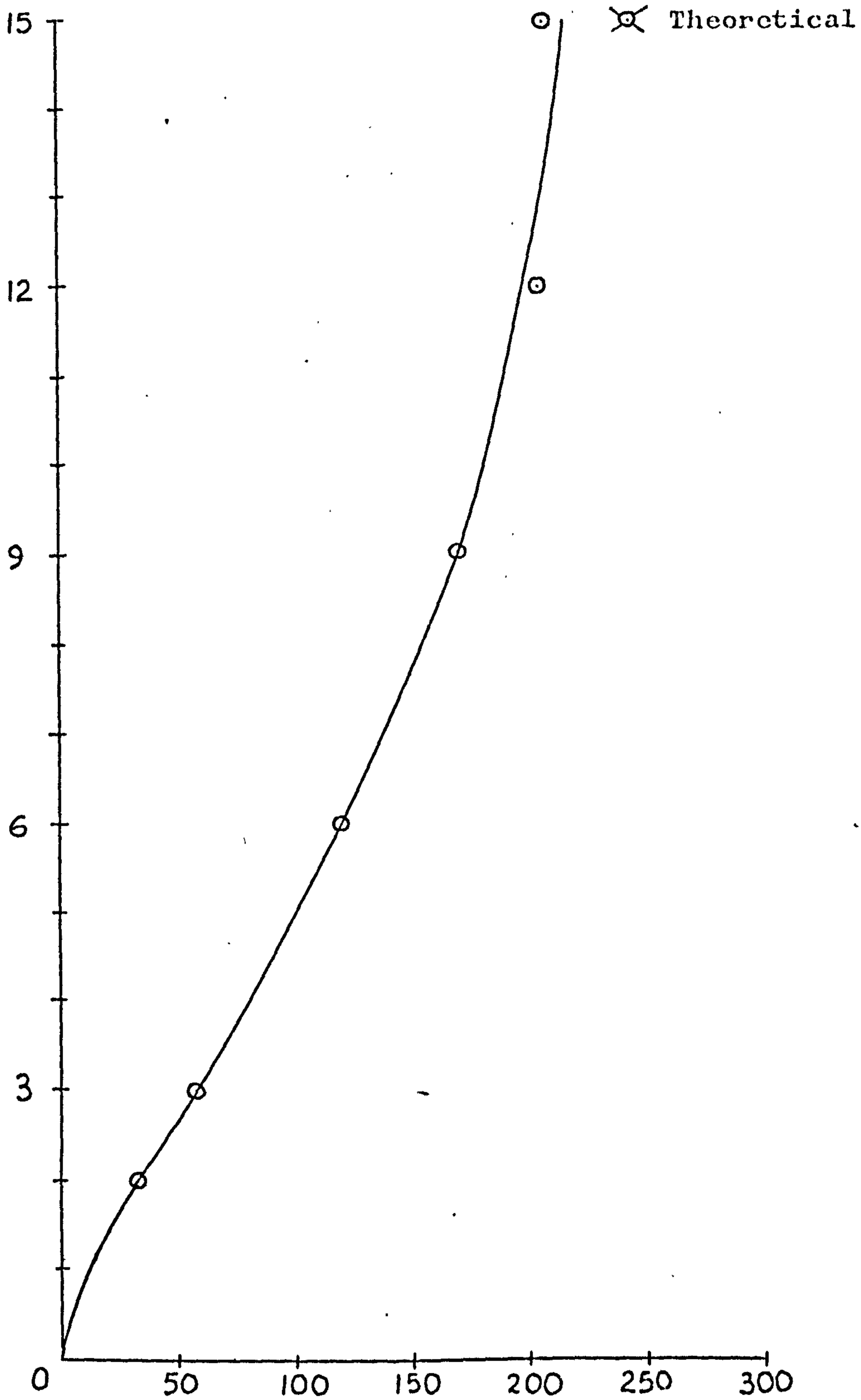

Fig. 8.21 Rotation profile,
Model 3, Combined bending & torsion

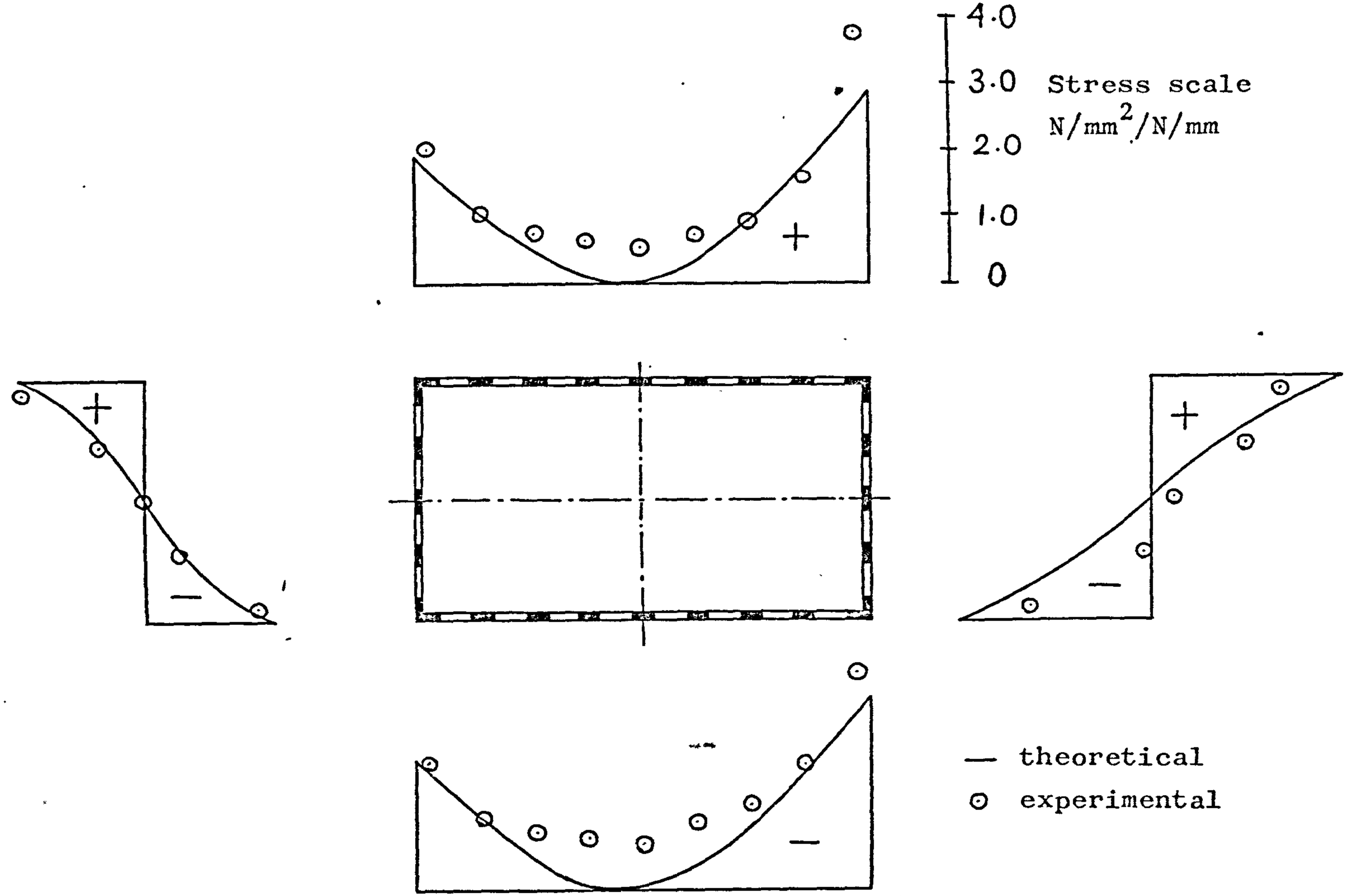

Fig. 8.22 Stress distribution, Model 3, Combined bending & torsion

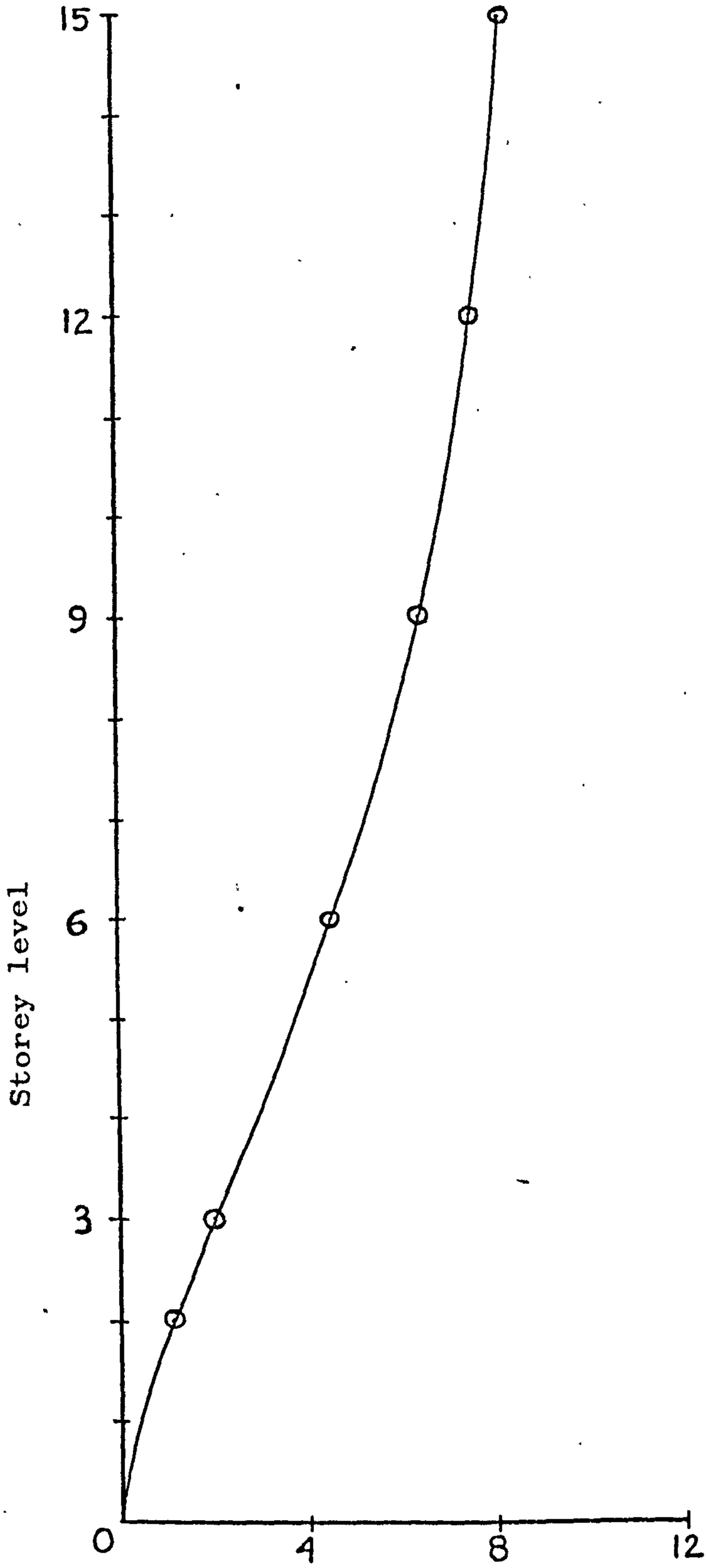

Fig. 8.23 Deflection profile
Model 4, Bending test

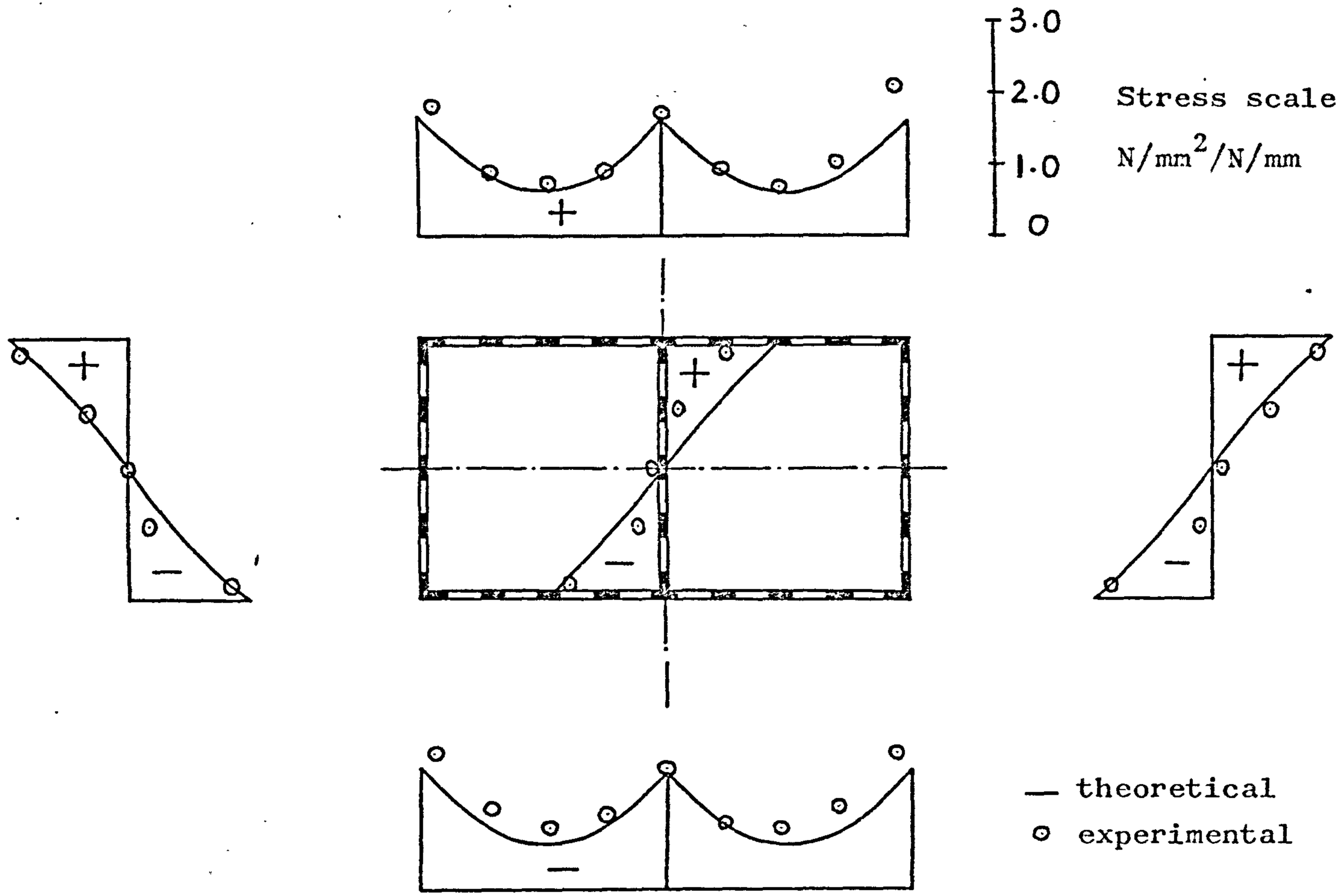

Fig. 8.24 Stress distribution, Model 4, Bending test

CHAPTER 9

DISCUSSION AND CONCLUSIONS

9.1 DISCUSSION OF RESULTS

9.1.1 EXPERIMENTAL RESULTS

The rigorous test procedure outlined in Chapter 8 was meant to eliminate or reduce as far as possible as many of the sources of error which occur as a result of the inherent deficiencies in the model material and the testing equipment used. However, a number of sources of error still continued to exist. Some of the possible sources of error encountered in the course of the experimental work and their likely effects on the test results are discussed below.

The conditions at the bases of the models which were required to be rigid could introduce some error in the measured displacements. Two dial gauges were positioned on the base plate, one near the top flange and another near the bottom flange, to measure the movement of the base plate. It was found that the deflection at the free end of the model caused by the rigid body movement at the base was less than 1 per cent of the deflection due to the applied loads. Deformations must also have occurred within the depth of the Perspex base plate due to its own elasticity, but it was not practical to measure these deformations by positioning gauges on the other side of the base plate as well; although presumably the deformations would have been too small to be measured by

such devices. These deformations could affect the accuracy of the test results by tending to give results for deflection of the model in excess of the results if the base was truly rigid.

Simulation of a uniformly distributed load was carried out by applying dead weights on hangers suspended from the two perimeter web frames at every alternate floor level. A combination of a uniformly distributed load and a torsional moment was simulated by hanging weights from one of the perimeter web frames at alternate floor levels. When the individual weights were applied on or removed from the hangers the model underwent rapid changes of deflection. Great care was taken to ensure that the increments and decrements were carried out smoothly in order to minimise the effect of impact on the model. The effect of impact will be of no significance if the material of the model is perfectly elastic and the yield stress is nowhere exceeded. However Perspex is not perfectly elastic, and some error could be introduced from this source.

As noted in section 8.2, Perspex undergoes considerable creep under sustained loading conditions which can lead to serious errors if not accounted for. It was found that the gauge readings became reasonably constant 10 minutes after the application of the loads, suggesting that the creep had essentially terminated. It was, therefore, decided to allow a waiting time of 10 minutes to eliminate to a considerable extent the errors caused due to creep in Perspex. The modulus of elasticity E of

Perspex was also determined from the deflection and strain readings allowing the same waiting time of 10 minutes.

One possible source of error encountered in using Perspex as model material is the low thermal conductivity of Perspex. Because of the low conductivity, heating of the strain gauges and the material under the gauge occurs when the measuring current is passed through it. This local heating may affect the mechanical properties of Perspex. The heating of the gauge causes a drift in the measuring circuit so that the output changes with time. Furthermore, it is not possible to separate the portion of the output due to structural response and that due to drifting caused by the heating of the gauge. The compensating dummy gauges together with a low-voltage strain indicator were used to minimise the effects of gauge heating.

The fabrication of the components and the assembling of each model to the correct dimensions were of utmost importance. The model required a number of panels each with a large number of openings which were made by slot drill of 4 mm diameter. As the depth of the spandrel beams was small, any small discrepancy could have serious effects on the experimental results and great care was taken while cutting these openings. The presence of fillets at all the intersections could also affect the accuracy of the result.

The measuring devices used were precision instruments and only negligible error could be introduced by them. Small errors may be introduced by the dial gauges if the

ball of the dial gauge bears on an uneven surface. The chances of this type of error were remote as the dial gauges were everywhere bearing on smooth surfaces of the Perspex model. The dial gauges were supported by a framework made from Dexion angles which was securely bolted to the test frame. The Dexion is comparatively flexible and might introduce some error were it to be disturbed during the test.

The adhesive with which the strain gauges were glued might stiffen the Perspex locally which could affect the test results to some extent.

The value of modulus of elasticity, as used to evaluate the stresses in the model from the results of the strain gauge readings was assumed to be constant in both tension and compression throughout the sheet. This could also introduce errors in the results since the elastic properties of Perspex are known to differ in tension and compression and also to vary within the single sheet.

The only means available to assess the accuracy of the strain readings was to check the statics of the structure by comparing the magnitude of the moment obtained from the experimental values of the strain in all the columns with the moment induced due to the applied loads, and also by comparing the total tensile force with the total compressive force at the section.

9.1.2 THEORETICAL RESULTS

The analyses of models 1, 2 and 3 (Framed-tubes) subjected to bending were carried out by the simplified

analysis discussed in section 2.4. For torsion the analysis of section 3.2 was used. Model 4 (Bundled-tube) was analysed for bending using the simplified analysis suggested in section 6.2. The theoretical results presented in graphical form at the end of chapter 8 were evaluated using the physical dimensions and structural conditions which most accurately represented the models under test.

For the analyses of the models the beams and columns were assumed to be uniform, the storey height and the bay width were taken to be constant throughout the height of the models. In order to represent the model as accurately as possible each of the dimensions used in the analyses was measured at a number of places and the mean value was used. The base of the model was assumed to be rigid. The elastic properties of the model material were assumed to be constant throughout the model. The variations in any of these properties could not be accommodated in the analyses.

The modulus of elasticity of Perspex was determined on the basis of the deflection and the strain results of the test specimens. They were found to differ by nearly 10 per cent which might be attributed to the local stiffening of Perspex due to the adhesive used for the purpose of gluing the strain gauges to the model. The value of the modulus of elasticity evaluated on the basis of deflection results was used in the analysis to determine the maximum deflection at the free end of the model.

Since the columns were closely spaced and the spandrel beams relatively deep, the finite size of the joint relative to the free column height and beam span was taken into consideration in the analysis. A simple method to consider this was suggested in section 2.3.

9.1.3 COMPARISON BETWEEN EXPERIMENTAL AND THEORETICAL RESULTS

The theoretical and experimental results for models 1 to 4 are illustrated in Figs. 8.9 to 8.24. The graphs are largely self explanatory and hence only general features are discussed below.

The deflection profiles are double-curvature curves, thus indicating the frame-tube interaction present in the structure. The experimental values of the maximum deflection at the free end of models 1 and 2 exceed the theoretical values by as much as 35 per cent. The large discrepancy cannot be attributed to any deficiency in the theory developed for evaluating the deflection, since the same theory gives the value of maximum deflection for model 3 which is in excess of the experimental value by nearly 5 per cent. The deflection profile of model 1 indicates no marked change when it is rotated through 180 degrees. Models 1 and 3 were tested in combined bending and torsion. Deflection profiles in this case agree closely with the respective profiles for simple bending.

The rotation of the model at any level was determined from the readings of the two dial gauges

positioned over the two web frames at that level. The difference of the two readings was divided by the width of the flange frame to give the rotation in radians. The rotation profiles also exhibit double curvature. The percentage agreement between the experimental results and the analytical solutions is again markedly poor, the experimental result being 20 per cent greater than the analytical solution for model 1 and 15 per cent less for model 3.

The stresses in the columns of the models, as derived from the strain gauge readings taken during the tests, yield a general form of stress distribution which bears a very consistent relationship to the stress distributions predicted by the analytical solutions. The non-uniform nature of the stress distribution in the flange panels is due to shear lag effects. In framed-tube models 1, 2 and 3 the flexibility of the spandrel beams produces a large deviation from the ordinary beam theory stress, increasing the axial stress in the corner columns and reducing them in the inner columns of the flange panels. This deviation is considerably reduced in the bundled-tube model 4, which is fabricated by incorporating an extra web frame in the framed-tube model 3. In the web panels, the stress distribution is non-linear.

Inspection of some of the graphs (8.19 and 8.22) would indicate that the effect of shear lag in the flange panels has been overestimated and the stresses in the centre columns are much higher than the analytical solution would suggest. This may be due to experimental errors or

due to the inadequacy of the proposed simplified analysis which assumes a simple parabolic stress distribution in the flange panel.

The stresses indicated by the strain gauges attached to the corner columns of flange frames and web frames generally agree, thus indicating efficient corner joints.

A statical check for the applied and internal moments and for the tensile and compressive forces in the cross-section was carried out. The results of the check for models 2 to 4 are given in the table 9.1.

The difference between the internal moment and the applied moment never exceeds 11 per cent which compares favourably with the earlier experiments on simpler plane models.

9.2 SUGGESTIONS FOR FUTURE RESEARCH

In this thesis an attempt has been made to produce a simplified analyses of framed-tube and bundled-tube structures which can be carried out without the aid of a computer. There still remain many related problems which need to be investigated. Some of these are summarised below.

1. In the analyses suggested for framed-tube and bundled-tube structures the distributions of vertical stresses in the flange and web panels were assumed. The elementary beam theory stress distributions were modified to include the effects of shear lag caused by the flexibility of the spandrel beams. It would be desirable to find a solution to the problem by assuming the vertical displacements in the flange and web panels. The principle of minimum potential energy may be applied to obtain the solution.

Model No.	Applied moment (N mm)	Internal moment (N mm)	Difference (% of applied moment)	Axial* forces (N)
2 (Framed-tube of square section; bending test	76982.20	78280.88	+ 1.69	+ 288.00 - 277.64
3 (Framed-tube of rectangular section; bending test)	19245.55	21326.69	+10.81	+ 132.57 - 126.81
3 (Framed-tube of rectangular section; combined bending and torsion test)	"	21052.31	+ 9.39	+ 134.65 - 123.81
4 (Bundled-tube; bending test)	30792.88	31422.78	+ 2.05	+ 191.37 - 192.75

* Plus sign indicates tension and minus sign indicates compression.

Table 9.1 Statical check of Structural Models.

2. The effectiveness of a framed-tube structure is increased by incorporating a central core which is connected to the outer frames by the floor slabs. The interaction between the shear wall type of core and the framed-tube should be considered.

3. Stiff girders or trusses are sometimes introduced in the framed-tube and bundled-tube structures at the top and also at intermediate levels. The influence of the presence of these elements in reducing the effects of shear lag in the structure should be investigated.

4. The diagonal truss tube system described in Chapter 1, is an extremely efficient system for very tall buildings. It will be interesting to enquire into the possibility of replacing the panels consisting of closely spaced diagonals by an equivalent uniform orthotropic plate, to form a substitute closed-tube structure. This will lead to an analysis of the structure similar to the one discussed in this thesis.

5. Mazzeo and De Fries[11] have described the design of a framed-tube building in which the corner columns were omitted. For such a structure it would be desirable to investigate the nature of shear transfer through the spandrel beams near the corners.

6. In the analysis discussed in this thesis it was assumed that the panels were subjected to in-plane deformations only. Any tendency for the panels to deform out of plane was considered to be restricted by the high in-plane stiffness of the floor slabs. Studies to include these secondary effects are desirable.

7. It would be desirable to consider the influence of warping of the floor slabs on the distribution of vertical stresses in the various panels.

8. It is a common practice with high-rise buildings to provide a deep beam at the first floor level which is supported on widely spaced columns. This will provide large unobstructed open spaces at the ground floor level. The problem of stress diffusion from a large number of columns at the upper levels to a few at ground level through this beam has to be tackled for the design of the beam.

9. The problem of differential heating of the opposite faces of the structure and its likely effect on the stress distribution should be examined.

10. The problem of the dynamics of framed-tube and bundled-tube structures should be investigated. Formulating the problem in terms of displacement variables, a free vibration study to give the dynamic characteristics of the structure may be made.

9.3 CONCLUSIONS

Simplified procedures have been presented for the analyses of framed-tube structures with a rigid base subjected to lateral forces and torsional moments. By replacing the discrete structure by an equivalent orthotropic tube, and making simplifying assumptions regarding the stress distributions in the structure, simple closed solutions have been obtained. Design curves have been presented for three standard load cases

in order to simplify the numerical computations and to allow a rapid assessment of the stress levels and degree of shear lag which occur in any particular configuration. It is found that the same design curves may be used both for bending and torsional actions.

Although three standard load cases have been considered, it is a straightforward matter to extend the solutions to any other load cases since the second order governing equation has been expressed in terms of the applied moment M or torque T.

The effects of variable corner column stiffness and the ratio of column width to spandrel beam thickness on the optimisation of framed-tube structures have been considered.

In the particular cases of uniformly distributed load and torque formulae have been derived to evaluate the maximum drift and rotation at the top of the structure. The same procedures may be used for other standard load cases.

The structural behaviour of a framed-tube structure with an elastic base and with different stiffness regions has been considered. The governing differential equation in each case remains the same; only the boundary conditions are found to differ.

Investigations of the distribution of vertical stresses in the framed-tube structure subjected to vertical forces have been carried out. On the basis of numerical examples with spandrel beams of different stiffnesses it

has been found that the flexibility of spandrel beams has little effect on the distribution of stresses in the panels.

A more general analysis of framed-tube structure subjected to lateral forces has also been presented. This has resulted in simultaneous differential equations of the second order which have been solved for the different load cases.

A theoretical study of the bundled-tube structure subjected to lateral loads has been made. Both simple and more general analyses have been presented for bundled-tube structure consisting of two and nine modular tubes. In the latter case a simple procedure based on a iterative method has been suggested. The governing differential equations are similar to the framed-tube structures.

An experimental investigation of the structural behaviour of framed-tube and bundled-tube structures has been carried out and the results of the investigation included in the thesis. Reasonable agreement between theory and experiment has been found.

REFERENCES

1. A.C.I. COMMITTEE REPORT 442 — "Response of Buildings to Lateral Forces" Jnl. A.C.I., Feb. 1971, pp.81-106.

2. IYENGAR, S.H. — "Bundled-tube structure for Sears Tower" Civil Engineering, A.S.C.E., Nov. 1972, pp.71-75.

3. IYENGAR, S.H. KHAN, F.R. and ZILS, Z.Z. — "The Sears Tower (Chicago): World's Tallest Building" Acier-Stahl-Steel, 7-8/1973, pp.308-313.

4. IYENGAR, S.H. AMIN, N. and CARPENTER, L. — "Computerized Design of World's Tallest Building" Computers and Structures, Vol. 2, pp.771-783.

5. KHAN, F.R. — "Recent Structural Systems in Steel for High-Rise Buildings" Conf. on Steel in Architecture, B.C.S.A., Nov. 24th-26th, 1969.

6. COULL, A. and SUBEDI, N.K. — "Framed-Tube Structures for High-Rise Buildings" Jnl. of the Struct. Div., Proc. A.S.C.E., Vol. 97, No. ST 8, Aug. 1971, pp.2097-2105.

7. RUTENBERG, A. — Discussion of Ref. 6, Jnl. of the Struct. Div., Proc. A.S.C.E., Vol. 98, No. ST 4, April 1972, pp.942-943.

8. KHAN, F.R. and AMIN, N.R. — "Analysis and Design of Framed-Tube Structures for Tall Concrete

Buildings" The Structural Engineer, Vol. 51, No. 3, March 1973, pp.85-92.

9. SCHWAIGHOFER, J. and AST, P.F. "Tables for the Analysis of Framed-Tube Buildings" Publication 72-01, March 1972, Department of Civil Engineering, University of Toronto, Canada.

10. AST, P.F. and SCHWAIGHOFER, J. "Economical Analysis of Large Framed-Tube Structures" Building Science, Vol. 9, 1974, pp.73-77.

11. MAZZEO, L.A. and DE FRIES, A. "Perimetral Tube for 37-story Steel Building" Jnl. of the Struct. Div., Proc. A.S.C.E., Vol. 98, No. ST 6, June 1972, pp.1255-1272.

12. COULL, A. and SUBEDI, N.K. "Hull-Core Structures subjected to Bending and Torsion" 9th Congress, International Association for Bridge and Structural Engineering, Amsterdam, May 8-13, 1972, pp.613-622.

13. RUTENBERG, A. "Analysis of Tube Structures using Plane Frame Programs" Regional Conf. on Tall Buildings, Bangkok, Jan. 1974, pp.397-413.

14. COULL, A. and BOSE, B. "Simplified Analysis of Framed-Tube Structures" Jnl. of the Struct.

Div., Proc. A.S.C.E., Vol. 101, No. ST 11, Nov. 1975, pp.2223-2240.

15. KUHN, P. "Stresses in Aircraft and Shell Structures" McGraw Hill Book Company, Inc., 1956.

16. WILLIAMS, D. "An introduction to the Theory of Aircraft Structures" Edward Arnold (Publishers) Ltd., London, 1960.

17. REISSNER, E. "Least Work Solutions of Shear Lag Problems" Jnl. of the Aeronautical Sciences, Vol. 8, 1941, pp.284-291.

18. REISSNER, E. "Analysis of Shear Lag in Box Beams by the principle of Minimum Potential Energy" Quarterly of Applied Mathematics, Vol. IV, No.3, 1946, pp.268-278.

19. A.C.I. COMMITTEE 435 "Allowable Deflections" Jnl. A.C.I., June 1968, pp.433-444.

20. GRINTER, L.E. "Numerical methods of Analysis in Engineering" The Macmillan Company, New York, 1949.

21. TIMOSHENKO, S. and WOINOWSKY-KRIEGER, S. "Theory of Plates and Shells" 2nd Edition, McGraw Hill Book Company, Inc., New York, 1959.

22. SCHECHTER, R.S. "The Variational method in Engineering" McGraw Hill Book Company, New York, 1967.

23. ROLL, F. "Materials for Structural Models" Jnl. of the Struct. Div., Proc. A.S.C.E., Vol. 94, No. ST 6, June 1968, pp.1353-1381.

24. BREEN, J.E. "Fabrication and Tests of Structural models" Jnl. of the Struct. Div., Proc. A.S.C.E., Vol. 94, No. ST 6, June 1968, pp. 1339-1352.

25. FIALHO, J.F.L. "The use of Plastics for making Structural Models" Bulletin RILEM No. 8, Sept. 1960, pp.65-74.

26. I.C.I. TECHNICAL SERVICE NOTE PX 122 "Perspex Acrylic Sheet: Properties" Second Edition, Imperial Chemical Industries Ltd., Sept. 1975.

27. I.C.I. TECHNICAL SERVICE NOTE PX 120 "Perspex Acrylic Sheet: Cementing-techniques and general information" Revised edition, Imperial Chemical Industries Ltd., July, 1973.